From Bone to Breath: How hematopoietic aging shapes macrophage fate, function and lung fibrosis

Doctoral thesis at the Medical University of Vienna
for obtaining the academic degree

Doctor of Philosophy

Submitted by

Asma Farhat, MSc

Supervisor:

Univ. Prof. Sylvia Knapp, MD, PhD

Co-supervisor:

Dr Riem Gawish, PhD

Department of Medicine I, Research Division Infection Biology,
Medical University of Vienna

Research Center for Molecular Medicine (CeMM) of the
Austrian Academy of Sciences, Vienna

Vienna, 02/2025

"*As you set out for Ithaka,*
hope your road is a long one,
full of adventure, full of discovery."

— C.P. Cavafy, *Ithaka*

Declaration

I, Asma Farhat, hereby declare that I have authored this doctoral thesis, entitled "*From Bone to Breath:* How hematopoietic aging shapes macrophage fate, function and lung fibrosis". I substantially conceptualized, designed, and executed the presented work. I have conducted my doctoral studies under the supervision of Prof. Sylvia Knapp, MD, PhD and co-supervised by Dr Riem Gawish, PhD at the Medical University of Vienna (MUW), Austria and at the Research Center for Molecular Medicine (CeMM) of the Austrian Academy of Sciences, Vienna, Austria.

This thesis is presented in cumulative form with the experimental work of my PhD studies presented in the manuscript "*An aging bone marrow exacerbates lung fibrosis by fueling profibrotic macrophage persistence*" (accepted for publication in *Science Immunology*) and is embedded and substantially discussed in this thesis. Individual contributions are listed below. The experiments were all conducted in Vienna (MUW & CeMM). All additional parts of the thesis were solely written by me, with input and feedback from Prof. Sylvia Knapp, MD, PhD.

DeepL was used to translate the thesis abstract into German 'Zusammenfassung'. No other AI tools were used to generate any text or rephrase text in this thesis. Given the academic, scientific context of the text, I acknowledge that several sentences in this thesis can be flagged as AI-generated text. I attest that to my knowledge, no text in this thesis was generated by AI.

First author publication (accepted for publication in *Science Immunology*)

An aging bone marrow exacerbates lung fibrosis by fueling profibrotic macrophage persistence.

Asma Farhat[1,2], Mariem Radhouani[1,2], Florian Deckert[1,2], Sophie Zahalka[1,2], Lisabeth Pimenov[1], Alina Fokina[1], Anna Hakobyan[2,3,4], Felicitas Oberndorfer[5], Jessica Brösamlen[1], Anastasiya Hladik[1], Karin Lakovits[1], Fanzhe Meng[1], Federica Quattrone[1,2], Louis Boon[6], Cornelia Vesely[7], Philipp Starkl[1], Nicole Boucheron[8], Jörg Menche[2,3,4,9,10], Joris van der Veeken[11], Wilfried Ellmeier[8], Anna-Dorothea Gorki[1], Clarissa Campbell[2], Riem Gawish[1†], Sylvia Knapp[1,12 †*].

† equal contribution.

Individual contributions:

Study conceptualization and design : AF, RG, SK; Investigation (experimental): AF, MR, SZ, LP, AFo, AH, KL, JB, FM, FO, FQ, PS, ADG, RG; Investigation (bioinformatics): FD, AHa, JM; Funding acquisition: RG, SK; Project administration: SK; Resources: LB, CV, NB, WE, JvdV, CC; Supervision: RG, SK; Writing – original draft: AF, RG, SK; Writing – review & editing: input from all authors.

Table of contents

List of Figures

Thesis Figures

Publication Figures:

Main Figures

Supplementary Figures:

Abstract

Repair and regeneration are essential for maintaining tissue integrity and organ function throughout life. However, with age, these fundamental processes falter, leading to a breakdown in homeostasis and impaired tissue repair. Today, with an ever-increasing aging population, the need to understand the mechanisms driving age-associated disease susceptibility, chronic inflammation, and tissue fibrosis is a pressing public health challenge. Idiopathic pulmonary fibrosis (IPF) is a prototypic age-associated fibrotic disorder, characterized by progressive scarring of lung tissue, which ultimately results in respiratory failure. While epithelial senescence and fibroblast hyperactivation are prime drivers of IPF, fibrosis progression is fundamentally influenced by the crosstalk with the immune system. In the lungs, embryonically derived tissue-resident alveolar macrophages (TR-AMs) play a crucial role in maintaining lung integrity. However, a lifetime of environmental perturbations leads to the gradual remodeling of the lung macrophage compartment. Upon lung injury, TR-AMs are depleted, leading to an influx of bone marrow-derived monocyte-derived alveolar macrophages (Mo-AMs). These Mo-AMs initially recruited in to regulate acute inflammation, when persistently activated, can perpetuate fibrosis through sustained inflammatory and profibrotic signaling. Although aging is recognized as a key driver of fibrosis, research has largely focused on effects of aging within the lung tissue. However, age-related changes simultaneously manifest in all cellular compartments – immune and non-immune. Aging is associated with chronic inflammation or 'inflammaging' and alterations at the hematopoietic stem cell level, leading to a myeloid-biased shift in hematopoiesis. Yet if and how hematopoietic aging influences the progression of lung fibrosis has remained largely unexplored. In our study, we aimed to determine whether an aged bone marrow and immune system influences fibrosis progression, independent of lung tissue age. Using heterochronic bone marrow transplant models, we found that an aged bone marrow autonomously exacerbated fibrosis, irrespective of the age of the lung tissue. This was associated with a heightened accumulation of inflammatory and profibrotic Mo-AMs. Once in the lungs, Mo-AMs from an aged bone marrow failed to transition into a tissue-resident homeostatic phenotype. Our findings indicate that cell-intrinsic aging increased Mo-AM numbers, while extrinsic lung immune signals shaped their phenotypic fate. Hematopoietic aging drove a pro-inflammatory milieu in the lungs post injury and limited the availability of a key anti-inflammatory cytokine, interleukin-10 (IL-10). Mechanistically, we found that regulatory T cells (Tregs), were a key source of IL-10 in the lung post injury, and the lack of Treg-derived IL-10 led to impaired Mo-AM maturation and worsened fibrosis. Our results establish a critical link between hematopoietic aging and fibrosis progression and uncover a Treg-mediated repair pathway gone awry with age.

Zusammenfassung

Reparatur und Regeneration sind für die Aufrechterhaltung der Unversehrtheit des Gewebes und der Organfunktionen unerlässlich. Mit zunehmendem Alter geraten diese grundlegenden Prozesse jedoch ins Stocken, was zu einem Zusammenbruch der Homöostase und einer Beeinträchtigung der Gewebereparatur führt. Angesichts einer immer älter werdenden Bevölkerung ist das Verständnis der Mechanismen, die der altersbedingten Krankheitsanfälligkeit, chronischen Entzündungen und Gewebefibrose zugrunde liegen, eine dringende Herausforderung für die öffentliche Gesundheit. Die idiopathische Lungenfibrose (IPF) ist ein prototypisches Beispiel für eine altersassoziierte fibrotische Erkrankung, die durch eine fortschreitende Vernarbung des Lungengewebes gekennzeichnet ist und schließlich zu Lungenversagen führt. Während mehrere Faktoren zur Pathogenese der IPF beitragen, darunter die epitheliale Seneszenz und die Hyperaktivierung von Fibroblasten, hat die Rolle des Immunsystems bei der Fibroseprogression zunehmend an Aufmerksamkeit gewonnen. In der Lunge spielen embryonal entstandene, gewebeeigene Alveolarmakrophagen (AMs) eine entscheidende Rolle bei der Aufrechterhaltung der Lungenintegrität. Allerdings führen lebenslange Umweltbelastungen zu einem allmählichen Umbau des Makrophagenkompartiments der Lunge. Nach einer Lungenverletzung werden die TR-AMs dezimiert, was zu einem Zustrom von aus dem Knochenmark stammenden Monozyten-Makrophagen (Mo-AMs) führt. Diese Mo-AMs werden zunächst rekrutiert, um akute Entzündungen zu regulieren, können aber bei anhaltender Aktivierung die Fibrose durch anhaltende entzündliche und profibrotische Signalübertragung aufrechterhalten. Der rechtzeitige Übergang von Mo-AMs in einen homöostatischen, gewebsresidenten Phänotyp ist daher vermutlich ein entscheidender Faktor für die Heilung von Verletzungen oder das Fortschreiten von dysregulierter Reparatur und Fibrose. Die Alterung des Lungengewebes wird seit langem als Hauptursache für die Fibrose angesehen, wobei man sich auf die epitheliale Dysfunktion und die Fibroblastenaktivierung konzentriert. Altersbedingte Veränderungen treten jedoch gleichzeitig in allen Gewebekompartimenten - immun und nicht-immun - auf. Die Alterung geht mit einem Zustand chronischer, geringgradiger Entzündungen („inflammaging“) und Veränderungen auf der Ebene der hämatopoetischen Stammzellen im Knochenmark einher, was zu einer myeloiden Verschiebung der Hämatopoese führt. Ob und wie die hämatopoetische Alterung das Fortschreiten der Lungenfibrose in anderen entfernten Organen wie der Lunge beeinflusst, ist jedoch noch weitgehend unerforscht.

In unserer Studie wollten wir herausfinden, ob ein gealtertes Knochenmark und Immunsystem unabhängig vom Alter des Lungengewebes direkt zur Fibroseprogression beiträgt. Anhand von heterochronen Knochenmarktransplantationsmodellen fanden wir heraus, dass ein gealtertes Knochenmark unabhängig vom Alter des Lungengewebes eine verstärkte Fibrose

auslöst. Dies ging mit einer verstärkten Anhäufung von entzündlichen und profibrotischen Mo-AMs einher. Einmal in der Lunge angekommen, gelang es den Mo-AMs aus gealtertem Knochenmark nicht, in einen gewebsresidenten homöostatischen Phänotyp überzugehen. Unsere Ergebnisse deuten darauf hin, dass die zelleigene Alterung und das Alter des Knochenmarks die Anzahl der Mo-AMs erhöht, während extrinsische Signale des Lungenimmunsystems ihr phänotypisches Schicksal bestimmen. Die hämatopoetische Alterung führte zu einem pro-inflammatorischen Milieu in der Lunge nach der Verletzung und schränkte die Verfügbarkeit eines wichtigen entzündungshemmenden Zytokins, IL-10, ein. Wir fanden heraus, dass regulatorische T-Zellen (Tregs) eine wichtige Quelle für IL-10 in der Lunge nach der Verletzung sind, und dass der Mangel an IL-10 aus Tregs zu einer gestörten Mo-AM-Reifung und einer Verschlechterung der Fibrose führt. Unsere Ergebnisse stellen eine kritische Verbindung zwischen hämatopoetischer Alterung und Fibroseprogression her und decken einen Treg-vermittelten Reparaturweg auf, der im Alter aus dem Ruder läuft.

Publications arising from this thesis

An aging bone marrow exacerbates lung fibrosis by fueling profibrotic macrophage persistence.

Asma Farhat[1,2], Mariem Radhouani[1,2], Florian Deckert[1,2], Sophie Zahalka[1,2], Lisabeth Pimenov[1], Alina Fokina[1], Anna Hakobyan[2,3,4], Felicitas Oberndorfer[5], Jessica Brösamlen[1], Anastasiya Hladik[1], Karin Lakovits[1], Fanzhe Meng[1], Federica Quattrone[1,2], Louis Boon[6], Cornelia Vesely[7], Philipp Starkl[1], Nicole Boucheron[8], Jörg Menche[2,3,4,9,10], Joris van der Veeken[11], Wilfried Ellmeier[8], Anna-Dorothea Gorki[1], Clarissa Campbell[2], Riem Gawish[1†], Sylvia Knapp[1,12 †*].

† equal contribution.

(Accepted, *Science Immunology*)

Abbreviations

Abbreviation	Full Form
ALI	acute lung injury
AMs	tissue-resident alveolar macrophages
AEPs	alveolar epithelial progenitors
ADI	alveolar differentiation intermediates
ARDS	acute respiratory distress syndrome
Arg1	arginase-1
AT1	alveolar type 1
AT2	alveolar type 2
BM-Mos	bone-marrow derived monocytes
CCL2	C-C motif chemokine ligand 2
CCR2	C-C motif chemokine receptor 2
C/EBPβ	CCAAT/enhancer-binding protein beta
CHIP	clonal hematopoiesis of indeterminate potential
CLPs	common lymphocyte progenitors
CMPs	common myeloid progenitors
COPD	chronic obstructive pulmonary disease
CRP	C reactive protein
CXCL1	C-X-C motif chemokine ligand 1
CTLA-4	cytotoxic T-lymphocyte-associated protein 4
DAMPs	damage-associated molecular patterns
DATP	damage-associated transient progenitors
ECM	extracellular matrix
EMP	erythro-myeloid precursors

Abbreviation	Full Form
EMT	epithelial-mesenchymal transition
EndMT	endothelial-mesenchymal transition
FDA	Food and Drug Administration
FL-Mos	fetal liver monocytes
FPF	familial pulmonary fibrosis
Foxp3	forkhead box P3
GM-CSF	granulocyte-macrophage colony-stimulating factor
GMPs	granulocyte-macrophage progenitors
HIF-1α	hypoxia-inducible factor-1α
HSC	hematopoietic stem cell
HSCs	hematopoietic stem cells
HRCT	high-resolution computed tomography
IGF-1	insulin-like growth factor 1
IL-10	interleukin-10
ILC2s	innate lymphoid cells
ILCs	innate-lymphoid cells
IPEX	immunodysregulation, polyendocrinopathy, enteropathy, X-linked
IPF	idiopathic pulmonary fibrosis
LAP	latency-associated protein
LT-HSCs	long-term hematopoietic stem cells
M-CSF	macrophage colony-stimulating factor
MEPs	megakaryocyte/erythroid progenitors
Mfge8	milk fat globule epidermal growth factor 8
MMPs	matrix metalloproteinases

Abbreviation	Full Form
Mo-AMs	monocyte-derived alveolar macrophages
MUC5B	mucin 5B
MPPs	multipotent progenitors
NF-κB	nuclear factor kappa-light-chain-enhancer of activated B cells
NLRs	NOD-like receptors
NO	nitric oxide
PAMPs	pathogen-associated molecular patterns
PD-1	programmed cell death protein 1
PDGF	platelet-derived growth factor
PPAR-γ	peroxisome proliferator-activated receptor gamma
PRRs	pattern-recognition receptors
ROS	reactive oxygen species
SAMacs	scar-associated macrophages
SARS-CoV-2	severe acute respiratory syndrome coronavirus 2
SatMs	segregated-nucleus-containing atypical monocytes
SASP	senescence-associated secretory phenotype
SP-A	surfactant protein A
SP-D	surfactant protein D
STAT1	signal transducer and activator of transcription 1
TGF-β	transforming growth factor-β
TERC	telomerase RNA component
TERT	telomerase reverse transcriptase
Tfh	T follicular helper
TLRs	Toll-like receptors

Abbreviation	Full Form
TNF-α	tumor necrosis factor-α
Tregs	regulatory T cells
TR-AMs	tissue-resident alveolar macrophages
UIP	usual interstitial pneumonia
VEGF	vascular endothelial growth factor
VEGF-α	vascular endothelial growth factor α
WISP-1	WNT1-inducible signaling pathway protein 1
WNT	wingless-related integration site
YS-Macs	yolk-sac derived macrophages
α-SMA	α-smooth muscle actin

Acknowledgements

As my PhD, draws to an end and I look back over the years, I am deeply grateful—for this incredible experience, the work I had the opportunity to do, the lab and community I was part of, and, most importantly, for all the wonderful people who made this journey possible.

I would like to thank my PhD supervisor, Sylvia Knapp, for her unwavering support, scientific guidance, and mentorship throughout. Sylvia, thank you for allowing me to be me, for pushing me to reach for more always, for giving me the freedom to explore ideas and trusting them, and for teaching me to advocate for myself. You understood what I needed and gave me the perfect balance of freedom and supervision. For all the 'plus 24 hours', for listening patiently to my unfinished sentences, for making my first paper such an enjoyable experience and for being a mentor I could go to for anything - I am truly grateful for you. I know this is not the end of our journey and I will turn to you for advice in the years to come.

Thank you, Riem, for being a fantastic co-supervisor and for always bringing enthusiasm, positivity and keeping the spirits high. Your energy made science and this PhD feel fun and creative, and I truly enjoyed brainstorming with and learning from you.

Thank you to all our wonderful collaborators and my thesis committee members who gave me scientific advice, resources, and support. I am incredibly privileged to be a part of CeMM, in all its spirited collaborations and community. Thank you, Giulio and Anita, for inspiring an environment of science, art, passion and enthusiasm. Thank you, Matthew, for your constant support. To all the talented and kind CeMMies I was fortunate enough to work with, learn from and be inspired by – thank you for the beer-hours, the Halloween parties, the CeMM outings, the Friday seminars and the fantastic science!

To all the members of the Knapp Lab – working with all of you has been incredible. You were the kindest and most fun lab mates I could have ever asked for. Thank you Knappsies for all the input, the discussions, the lab meetings, the coffee-breaks, the no-questions asked help and for the constant support. I loved coming to work every day and my PhD would not have been possible without every one of you! Thank you, Philipp and Stefanie, for always being there for advice, meetings and scientific input, I learnt a lot from you. Thea, for teaching me everything in the first year and passing on your love for AMs. Federica, Martin, and Sophie—for being incredible senior PhDs who shared their knowledge and were always there to help. Thank you, Nina, Karin, Anastasiya and Florian.M for all the administrative, experimental, and technical support, I truly appreciate it. Thank you for the cakes, for making the phone calls, and being there when things did not work. Anastasiya, I loved being the dream-team with you, your patience in teaching me, our bleo sessions and morning harvests, thank you!

To the current students – I really enjoyed being in the office with all of you, Jessi, Fanzhe,Jiaqi, Bihua – thank you for bringing your energy, fresh perspectives and fun to the lab, Florian.D for all the bioinformatics work and life advice!
Lisa, thank you for the discussions, the late-night company, the ramen, for being my sorting buddy and all the laughs. Alina, thank you for the coffee-breaks, our never-ending conversations, for us always getting lost together. Both of you were my cheerleaders, my friends and the best desk buddies to have on either side.
Maryem, I could not have asked for a better partner-in-(lab)-crime and I am so lucky I got to share this entire journey with you right from the first day. This thesis holds all our endless ELISAs and Legendplex, the calculations, the crazy experiment plans, the long harvest days, the many tip-box towers. Beyond the lab, through the countless laughs, the many (many) tears, the good, the bad, and the chaotic, I am so grateful to have had someone as kind, talented, inspiring, and fun as you as my friend for it all. Your constant support made all the difference, and I truly could not have done this PhD without you. What a ride it has been, I am so proud and happy of where this took us, I hope this is only the beginning and we get to work together again.

I want to thank my amazing friends, Anna, Sarada, Sumedh, who supported me along the way. Darren, thank you for being my rock through it all. I will always be grateful for your humour, support, patience, love and everything in between that carried me on through the long years. To my family—all my grandparents and the incredible generation of matriarchs before me who set the benchmark high, I hope I could do you proud.

My sister, Anjum, thank you for being both fierce and whimsical, for showing me what hard work really means, you taught me everything I know, and I will always look up to you.
And my mother, a thank you pales. You filled my world with books and birds, song and stories, plants and paper, history and wonder, a life of learning and exploring. If there is anything I do in science, it is because of you. Both of you are the reason I am who and where I am today, and for that, I am endlessly grateful.

Amidst baroque, cobblestone and vineyards – to the beautiful city of Vienna for being my home for the past six years, to the orange of the AKH that I have come to love, and to all the wonderful experiences, memories, lessons and people that shaped me—in science and beyond—*Danke schön!*

Chapter 1

Introduction

The following introduction aims to provide a detailed overview of the key concepts that will set the scene for the study '*An aging bone marrow exacerbates lung fibrosis by fueling profibrotic macrophage persistence*' presented in the second section, Results.

The introduction is divided into three sections:

1. Mechanisms of tissue repair and fibrosis
2. Lung macrophages through life: Fate, function and fibrosis
3. Mechanisms of aging

1.1 Mechanisms of tissue repair and fibrosis

1.1.1 What happens upon tissue injury?

When tissues are injured due to infection, toxic exposure, or mechanical damage, the body initiates a highly orchestrated wound healing process, in four phases **(Thesis Figure 1)** – hemostasis, inflammation, proliferation and remodeling to facilitate repair (Boothby *et al*, 2020; Wilkinson & Hardman, 2020). Upon acute **injury**, **hemostasis** occurs as blood vessels constrict and platelets aggregate at the site of injury, forming a clot to prevent further blood loss (Velnar *et al*, 2009). This clot not only stops bleeding but also provides a temporary matrix (Zaidi & Green, 2019), releasing growth factors that stimulate the healing process. At the same time, platelets secrete signals that increase blood vessel permeability, allowing immune cells to access the wound site (Chambers, 2003; Wynn, 2008). Damage to epithelial and endothelial cells or the initial recognition of an infectious pathogen by tissue resident macrophages or mast cells triggers the release of inflammatory mediators such as cytokines, chemokines and vasoactive amines, that causes the **inflammatory phase** to ensue, activating an anti-fibrinolytic coagulation cascade (Chambers, 2003). This leads to the formation of a provisional extracellular matrix (ECM), which exposes platelets to its components, promoting their aggregation and reinforcing the blood clot. As the clot solidifies, myofibroblasts, along with epithelial and endothelial cells, produce matrix metalloproteinases (MMPs), enzymes that degrade the basement membrane (McKeown *et al*, 2009). This degradation along with the release of inflammatory mediators allows immune cells, which are not normally present in the extravascular tissue, such as neutrophils and monocytes to infiltrate into the site of injury (Wynn, 2008). In parallel, the damage also initiates the release of damage-associated molecular patterns (DAMPs) and pathogen-associated molecular patterns (PAMPs) from dying cells and pathogens, which are recognized by the immune system (Zhang *et al*, 2010) . These molecular signals trigger a complex inflammatory response that recruits a variety of hematopoietic and non-hematopoietic cells, including monocytes, macrophages, neutrophils, natural killer cells, fibroblasts, epithelial cells, and stem cells, to the wound (Vestweber, 2015). Neutrophils and macrophages are particularly crucial, as they help clear debris, dead cells, and pathogens (Brinkmann *et al*, 2004; Kolaczkowska & Kubes, 2013). Macrophages play a dual role, transitioning from a pro-inflammatory to an anti-inflammatory or pro-resolution phenotype, which facilitates the resolution of inflammation and promotes tissue repair (Wynn & Vannella, 2016). Cytokines and chemokines released by these immune cells amplify the inflammatory response, and subsequently activate the adaptive immune system to the injury site, further attracting additional immune cells and enhancing the overall healing process (Keyes *et al*, 2016; Nosbaum *et al*, 2016) . As the tissue begins to heal, a **proliferation phase**

follows initiating the formation of new tissue (Wilkinson & Hardman, 2020). Fibroblasts proliferate and produce ECM components, including collagen, to provide structural support for the wound and essentially ‘plug the wound’. Simultaneously, growth factors such as vascular endothelial growth factor (VEGF) promote angiogenesis, ensuring an adequate blood supply to the healing tissue. Epithelial and endothelial cells migrate over the wound site, restoring the damaged tissue. Activated fibroblasts transition into myofibroblasts, which play a crucial role in wound contraction by pulling the edges of the wound closer together. The final stage of healing, known as the **remodeling phase**, involves the maturation and reorganization of the ECM. Collagen fibers are realigned, and the ECM is strengthened, improving the tensile strength of the healed tissue. This phase can extend over weeks or even years, depending on the severity of the injury and the individual's overall health. As the tissue structure stabilizes and returns to its normal state, the wound healing process is completed, resulting in restored function and integrity of the tissue.

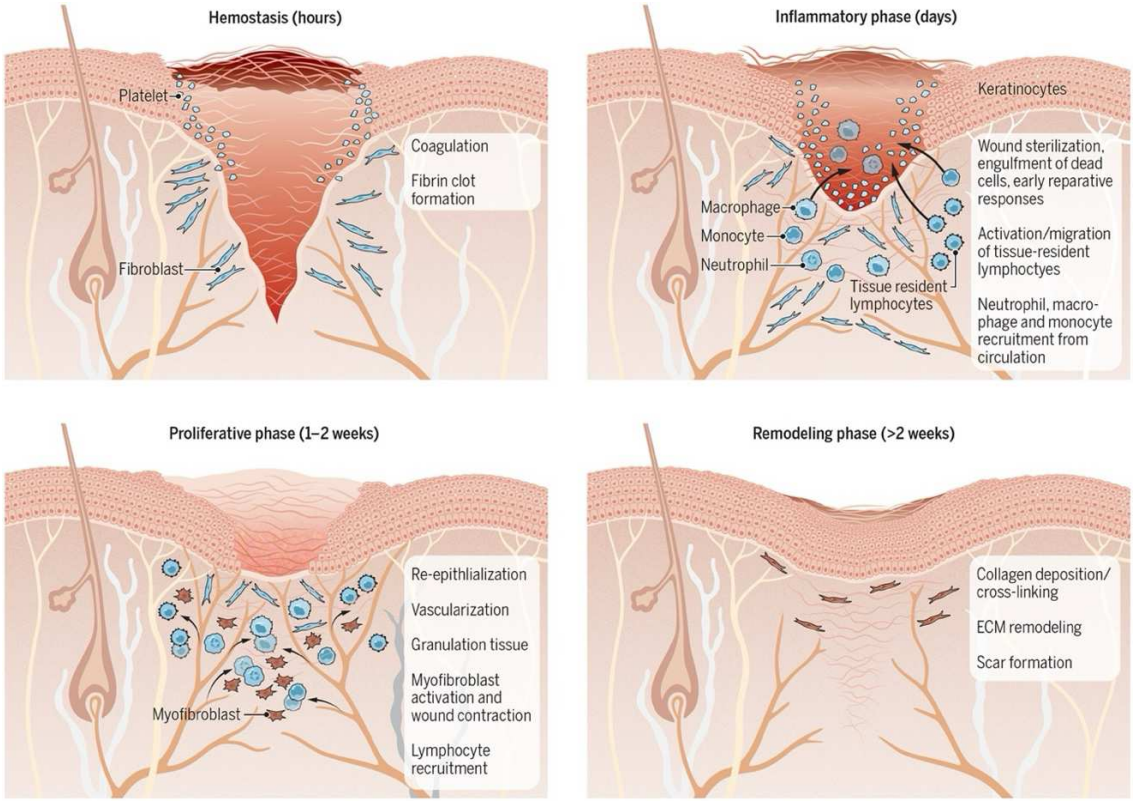

Thesis Figure 1: Phases of wound healing
Upon acute injury, wound healing is initiated in four general phases across tissues (skin injury depicted here) – hemostasis, inflammatory, proliferative and remodeling - *Illustration from (Boothby et al., 2020)*

1.1.2 Dysregulated wound healing leads to pathological fibrosis

When events in this tightly regulated, multi-factorial wound healing process becomes dysregulated, perturbed, or chronic—either due to the immune system's failure to adequately resolve the inflammatory response or because the injury is severe or repetitive—it can result in a chronic wound healing state. This prolonged dysfunction can ultimately lead to ***tissue fibrosis***, characterized by excessive scar tissue formation and impaired tissue function (Henderson *et al*, 2020). Fibrosis, a pathological consequence of a chronic wound healing response is defined by the excessive deposition of ECM components such as collagen and fibronectin around the injured tissue (Wynn & Ramalingam, 2012). This excessive ECM accumulation can lead to the formation of scar tissue that disrupts tissue architecture, ultimately impairing organ function and leading to end-stage conditions such as idiopathic pulmonary fibrosis, hepatic fibrosis and liver failure and heart failure. Fibrosis is a significant pathological outcome of many chronic inflammatory and autoimmune diseases such as scleroderma, rheumatoid arthritis, Crohn's disease, myelofibrosis (Bhattacharya & Ramachandran, 2023). It also plays a role in tumor progression and chronic graft rejection. Fibrosis can be initiated by several underlying triggers, including genetic mutations, persistent infections, repeated toxin exposure, chronic autoimmune inflammation, and increased inflammation with advanced age (Henderson *et al.*, 2020). A common feature across fibrotic diseases is the hyperactivation of fibroblasts, transforming them into myofibroblasts, cells which are responsible for producing excess ECM components, depositing collagen, and driving aberrant tissue remodeling along with the activation of profibrotic macrophages **(Thesis Figure 2)**. In the past decades, research has increasingly focused on understanding the molecular and immune mechanisms that trigger the activation of fibroblasts and transform them into myofibroblasts, aiming to develop therapeutic approaches to halt or reverse fibrosis progression.

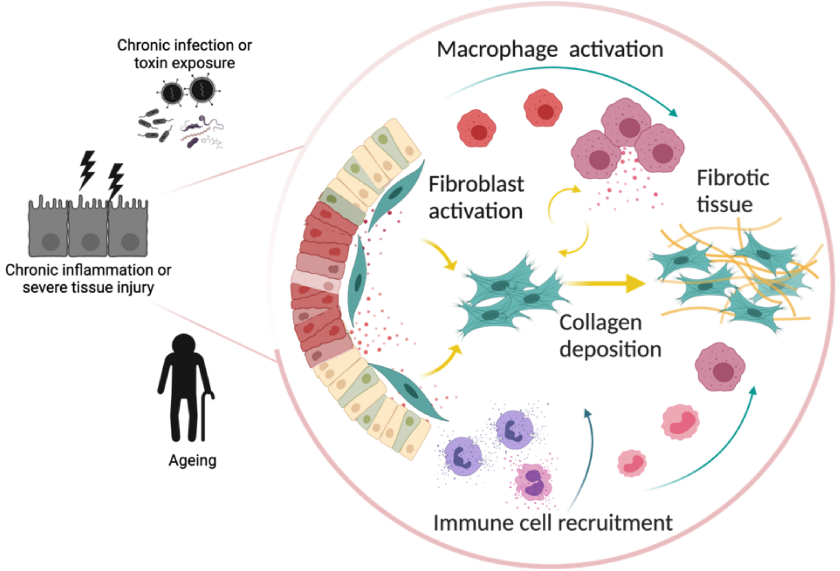

Thesis Figure 2: Aberrant tissue repair causes fibrosis
Chronic inflammation repetitive injury, advanced age can lead to dysregulated wound healing. Activated fibroblasts in concert with immune cells, especially macrophages produce excessive collagen ultimately leading to fibrotic and scar tissue formation.

1.1.3 Fibroblasts: central drivers of fibrosis

Fibroblasts are mesenchymal cells found in connective tissues throughout the body where they maintain the structural integrity of tissues by producing and remodeling the extracellular matrix (Plikus *et al*, 2021).They are widespread and reside in both dense connective tissues, such as tendons and ligaments, and loose connective tissues, such as the dermis, organ capsules, and beneath epithelial linings (Movat & Fernando, 1962). Their primary function is the production of ECM components, including collagen, glycoproteins, and proteoglycans, which provide structural support and mediate cell signaling in the tissue (Cialdai *et al*, 2022; Lendahl *et al*, 2022). They are also involved in paracrine signaling, providing cues for the differentiation of neighboring cells during organ development and repair. In wound healing, fibroblasts are indispensable during all three phases of the process: inflammation, proliferation, and remodeling (Knoedler *et al*, 2023). During the inflammatory phase, fibroblasts are activated by cytokines such as tumor-necrosis factor (TNF)-α, IL-1, and IL-6, which are released by platelets and immune cells (Correa-Gallegos *et al*, 2021). They secrete chemokines like C-C motif chemokine ligand 2 (CCL2) and C-X-C motif chemokine ligand 1 (CXCL1) to recruit additional immune cells to the injury site and produce matrix metalloproteinases to remodel the wound stroma, facilitating cell migration. In the proliferative phase, fibroblasts migrate into the fibrin clot and produce ECM proteins such as fibronectin, hyaluronic acid, and collagen. They also release pro-angiogenic factors like VEGF and FGF to support new blood vessel formation (Thulabandu *et al*, 2018). Stimulated by growth factors such as transforming growth factor- β (TGF-β), fibroblasts differentiate into myofibroblasts which are essential for wound closure. In the remodeling phase, myofibroblasts regulate ECM turnover, replacing type III collagen with type I collagen to restore tensile strength and contract the wound, a process mediated by α-smooth muscle actin (α-SMA) (Desmoulière *et al*, 2005).

In pathological conditions like fibrosis, fibroblasts and myofibroblasts play a central role as they secrete excessive ECM components, leading to abnormal tissue remodeling, scar formation and loss of tissue function in many organs such as the lung, liver, kidney, and heart (Lendahl *et al.*, 2022). Fibroblasts respond to tissue injury by differentiating into myofibroblasts, which propogate and persist in the fibrotic microenvironment. They also become resistant to apoptosis, resulting in sustained ECM production. Fibroblast activation can be driven by immune cells, epithelial-mesenchymal transition (EMT), or endothelial-mesenchymal transition (EndMT), further amplifying their fibrogenic activity (Zeisberg *et al*, 2007). In lung fibrosis, mesenchymal progenitor cells differentiate into various fibroblast subtypes, including myofibroblasts and matrix fibroblasts, contributing to the fibrotic ECM (Xie *et al*, 2018). In liver fibrosis, hepatic stellate cells act as the primary fibroblast-like cells, and

are activated by inflammatory signals from apoptotic hepatocytes and macrophages, leading to ECM accumulation and structural remodeling (Seki & Schwabe, 2015). Single-cell transcriptomics have revealed the heterogeneity of fibroblasts and their dynamic differentiation into myofibroblasts in different fibrotic contexts (Lendahl *et al.*, 2022) . Controlling the growth and activation of myofibroblasts has been a major challenge in fibrosis treatment. While fibroblasts are critical for normal wound healing, their dysregulated activation and resistance to programmed cell death underpin the pathogenesis of fibrosis (Kato *et al*, 2020). Fibroblasts are therefore a central target for therapeutic interventions to mitigate fibrosis, control ECM production and promote appropriate tissue repair (Zhao *et al*, 2022).

1.1.4 Immune dysregulation during fibrosis

Acute and persistent inflammation are central drivers of fibrosis, with severe injury triggering epithelial cell apoptosis in the lungs or hepatocyte necrosis in the liver, that initiate an inflammatory response which activates the deposition of ECM to seal the wound and restore tissue architecture (Chen & Stubbe, 2005; Fujii *et al*, 2010). Low level, chronic inflammation induces a continuous state of inflammation the drives repeated loops of the wound healing response, that often culminates in fibrosis. While removing the inflammatory trigger in these instances can halt the progression of tissue remodeling and fibrosis, in many cases of fibrosis, the exact cause of tissue damage is not clear or cannot be removed easily (Wynn & Ramalingam, 2012). This has led researchers to explore how immune system pathways might be targeted to help slow down or prevent fibrosis. Both the innate and adaptive immune systems are now recognized as critical components of the fibrotic pathway, making them attractive therapeutic targets (Wynn & Ramalingam, 2012). The initial nature of the injury often shapes the ensuing inflammatory response. Infection and injury caused by external stimuli such as pathogen-associated molecular patterns (PAMPs), activate pattern-recognition receptors (PRRs) on innate immune cells to initiate an inflammatory response (Li & Wu, 2021). Numerous cytokines (described below) contribute to the processes of wound healing and fibrosis, with specific gene groups being activated in different conditions (Henderson *et al.*, 2020).

1.1.5 Innate immunity in fibrosis

It is dysregulation of innate immune (that initiate wound healing) processes that often triggers the onset of fibrosis. The coagulation cascade that initiates tissue repair after injury itself can act as an initial trigger for fibrosis. When platelets are activated, they also produce growth factors that stimulate ECM production by fibroblasts and prolonged coagulation can lead to fibrosis. Patients with IPF show increased levels of X-box-binding protein-1, a factor that

promotes platelet differentiation, in the lung tissue, epithelial cells and lavage fluid as compared to healthy individuals (Korfei *et al*, 2008) .Thrombin – a key enzyme that converts fibrinogen to fibrin is also detected in the lungs and alveolar spaces, indicating an overactivation of the coagulation pathway in IPF. Thrombin further stimulates fibroblasts to proliferate and induces their activation into myofibroblasts (Hernández-Rodríguez *et al*, 1995). Additionally, injured alveolar pneumocytes in the airway epithelium can trigger an anti-fibrinolytic response (Kuwano *et al*, 1999), leading to fluid accumulation between tissues (interstitial edema), acute inflammation, and detachment of the epithelium from the basement membrane (Wilson & Wynn, 2009). Chemokines released by platelets or damaged cells, mechanical stress or increased reactive oxygen species (ROS) and nitric oxide (NO) production leads to the recruitment of infiltrating innate immune cells, including neutrophils and monocytes which can also differentiate into macrophages that then clear debris and remove pathogens (Wick *et al*, 2010). However, if these inflammatory cells remain for too long and are not cleared once they resolve the acute threat, they can build up in the tissue, leading to exacerbated tissue damage, scarring and fibrosis. Early removal of macrophages has been shown to mitigate liver fibrosis in mice (Duffield *et al*, 2005). Similarly, neutrophils can have an adverse impact in lung fibrosis as seen in bleomycin and hypersensitivity pneumonitis mouse models, while in the liver, dendritic cells can activate hepatic stellate cells, promoting fibrosis (Connolly *et al*, 2009; Pardo *et al*, 2000). The NLRP3 inflammasome which is activated by damage signals, regulates macrophage-mediated ECM turnover and the release of inflammatory cytokines (Martinon *et al*, 2009). Pattern recognition receptors (PRRs), such as Toll-like receptors (TLRs) and NOD-like receptors (NLRs) also play dual roles in lung fibrosis. While recognition of PAMPs and DAMPs trigger inflammation and pro-inflammatory cytokine production, ECM components such as fibronectin can also bind to TLRs, such as TLR4 and propel the inflammatory response further (Kelsh *et al*, 2014). Other myeloid cells such as mast cells, eosinophils and basophils also contribute to fibrosis. Mast cells have been shown to drive fibrosis during systemic sclerosis, kidney fibrosis and cardiac fibrosis by further recruiting inflammatory cells and producing pro-fibrotic factors (Levick *et al*, 2009). Eosinophils can produce pro-fibrotic mediators such as TGF-B and IL-13, with eosinophilia also being a biomarker for progressive pulmonary fibrosis (Humbles *et al*, 2004; Minshall *et al*, 1997). Similarly, while the exact role of basophils in fibrosis is yet unknown, an increase in basophils has been found in patients with interstitial lung diseases.

1.1.6 Monocytes and macrophages in tissue injury, repair and fibrosis

First identified by Elie Metchnikoff and aptly named ‘big eaters’ (Macrophage – Greek), macrophages are perhaps the most prominent cell type of the innate immune system. As research over time has shown, they wear many functional hats, the most primary being their

ability to phagocytose and clear cellular debris, damaged cells, and harmful pathogens. During an inflammatory response they often act as first responders and produce cytokines and chemokines, which then activates and recruits other immune cells (Varol *et al*, 2015). Tissue-resident macrophages are located in almost all tissues where maintain tissue homeostasis, often having distinct roles in different tissues (Ginhoux & Guilliams, 2016). In this section, a general overview of the role of macrophages in tissue injury and fibrosis is outlined. The development and functions of tissue-resident macrophages and recruited monocytes and macrophages in the context of the lung will be further explored in ***section 1.2***.

Monocytes and macrophages are key orchestrators of the wound healing process– playing distinct roles in regulating both the initiation and resolution of repair post injury and govern if appropriate resolution ensues or advances into pathological fibrosis (Murray & Wynn, 2011; Wynn & Vannella, 2016). Monocytes and macrophages exhibit remarkable plasticity, adopting different functional phenotypes – **pro-inflammatory**, **anti-inflammatory**, **pro-repair** and **pro-fibrotic** that depend on cues they receive from the environment and their surrounding niche – **Thesis Figure 3** (Wynn & Vannella, 2016).

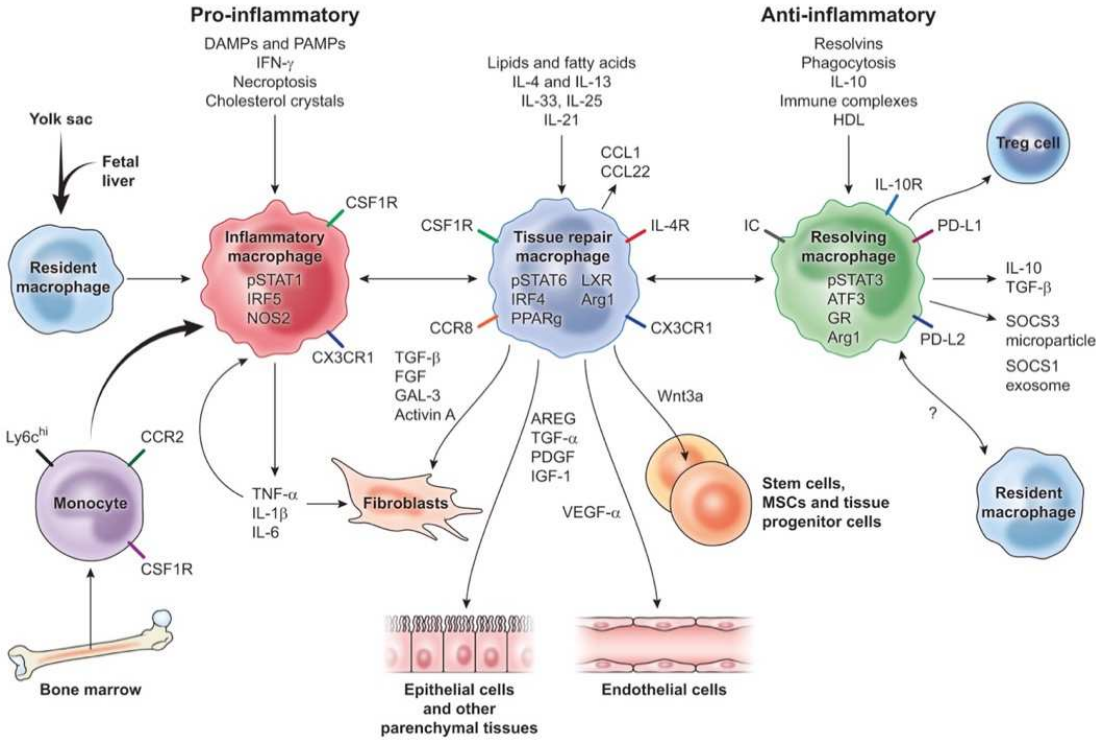

Thesis Figure 3: The many facets of macrophages
At every stage of the tissue repair process, macrophages adopt distinct phenotypes and play specific roles – inflammatory, reparative, anti-inflammatory and profibrotic. *Illustration from (Wynn & Vannella, 2016)*

Macrophages – critical orchestrators in tissue repair

The role of macrophages in wound healing was initially attributed to their function as scavenger cells – responsible for clearing cellular debris and apoptotic cells and phagocytosing pathogens after tissue injury (Peiser *et al*, 2002). Following injury, tissue-resident macrophages secrete chemokines, matrix metalloproteases and inflammatory cytokines that initiate the inflammatory response. Upon severe tissue damage, inflammatory monocytes ($Ly6C^+$) are recruited from the periphery, predominantly via their expression of C-C motif chemokine receptor 2 (CCR2) (in response to the chemokine CCL2) from the bone-marrow and differentiate into macrophages in the tissue (Epelman *et al*, 2014; Lechner *et al*, 2017). At this stage, these macrophages are pro-inflammatory (traditionally referred to as classically activated) (Murray *et al*, 2014), a state often initiated by IFN-y or activation of Toll-like receptors. This then further activates nuclear factor kappa-light-chain-enhancer of activated B cells (NF-κB) and signal transducer and activator of transcription 1 (STAT1) signaling pathways, which induces their production of reactive oxygen and nitrogen species, and secretion of pro-inflammatory cytokines like TNF-α, IL-1, and IL-6. These macrophages further produce cytokines such as IL-12 and IL-23, which can activate the adaptive immune response and triggers the differentiation of T helper cell subsets. While the induction of these inflammatory factors and cell types enables efficient neutralization and clearance of the pathogen, it can also cause tissue damage and become pathogenic, therefore controlling the inflammatory response of macrophages is critical to ensure wound healing and repair. While depleting monocytes and macrophages during the early inflammatory stage often blunts the inflammatory response, this depletion has also been shown to lead to inefficient wound healing and repair. Their sustained activation or prolonged recruitment can exacerbate damage and delay repair processes. (Duffield *et al.*, 2005; Gibbons *et al*, 2011). When macrophages are exposed to epithelial derived alarmins or type 2 cytokines such as IL-4 and IL-13, they take on an 'alternatively activated phenotype' which can be associated with repair and a return to homeostasis or if pathological, exacerbation of allergies and fibrosis (Borthwick *et al*, 2016; Bosurgi *et al*, 2017).

Macrophages also play a key role in regulating and suppressing the inflammatory response. These **anti-inflammatory macrophages** play a key role in immunoregulation, expressing proteins like arginase-1 (Arg1), Retnla, Pdl2, which help reduce the inflammatory response and restore homeostasis (Wynn & Vannella, 2016). Type-2 cytokines such as IL-4 and IL-13 are key drivers of this regulatory macrophage phenotype along with binding of Fc gamma receptors, apoptotic cells and prostaglandins. Once the inflammatory phase is under control, macrophages differentiate into a wound healing **reparative phenotype**, producing growth factors to initiate repair and cell proliferation, including platelet-derived growth factor (PDGF),

TGF-β1, insulin-like growth factor 1 (IGF-1), and vascular endothelial growth factor α (VEGF-α) (Wynn & Vannella, 2016). At this stage, macrophages can activate local and recruited fibroblasts, further promoting their differentiation into myofibroblasts, increasing collagen deposition and other ECM components to promote wound closure. Macrophages additionally regulate the proliferation of other parenchymal and stromal cells, and in the cases of severe injury, stimulate stem and progenitor cells to initiate tissue repair.

Macrophage during fibrosis

Macrophages are often always found near collagen-producing myofibroblasts in wounded tissue (**Thesis Figure 4**). These fibroblasts, as described above, produce chemokines and macrophage colony-stimulating factor (M-CSF) to attract and activate macrophages. In turn, macrophages, primed by factors such as IL-13, secrete key profibrotic molecules such as TGF-β1 and platelet-derived growth factor (PDGF), which are central to fibrotic progression (Murray *et al*, 2011). While other cell types also produce TGF-β1 and PDGF, macrophages have been identified as a significant source of these profibrotic factors that act upon adjacent fibroblasts, activating them and promoting collagen synthesis indicating that the physical proximity between macrophages and fibroblasts is essential for their communication and sustains the fibrotic process. Co-culture of macrophages and fibroblasts has demonstrated that an indespenible paracrine signaling axis exists between macrophages and fibroblasts that dictates their numbers and proliferation within fibrotic tissues (Zhou *et al*, 2018). The nature of these interactions can change based on the type and duration of tissue injury. Acute injury leads to a transient accumulation of macrophages that temporarily support fibroblast activity, whereas repeated or chronic injury results in persistent macrophage and fibroblast cell-circuits, driving sustained ECM deposition and a continuous and stable fibrotic state. Eventually fibroblasts can even lose the need for activation by macrophages, sustaining themselves through an aberrant autocrine loop. This has led to the classification of fibrosis as either 'hot,' characterized by active macrophage-fibroblast interactions, or 'cold,' dominated by autocrine fibroblast circuits (Adler *et al*, 2020).

Phagocytosis by macrophages, which is their most basic function itself can also either exacerbate or mitigate fibrotic processes depending on the context (Peiser *et al.*, 2002). When tissue injury leads to cell death, macrophages clear the resulting dead cells. The type of cell death—apoptotic or necrotic—determines the subsequent inflammatory response (Hotchkiss *et al*, 2009). Phagocytosis of apoptotic cells generally suppresses inflammation and can promote the resolution of fibrosis by removing stimuli that drive TGF-β1 and other profibrotic factors (Fadok *et al*, 1998). In contrast, engulfing necrotic cells triggers an inflammatory response that can be profibrotic by attracting additional immune cells and stimulating fibroblast activity. This however can also facilitate the cleanup of cellular debris that resolves

inflammation. Phagocytosis of erythrocytes, particularly by Kupffer cells in the liver, can induce fibrosis through oxidative stress and iron deposition (Otogawa *et al*, 2007). However, in models of liver injury, macrophages have been shown to promote tissue repair also by phagocytosing apoptotic cells, thereby reducing inflammation, and limiting fibrosis progression (Iredale, 2007; Iredale *et al*, 1998). Similarly, macrophages that express milk fat globule epidermal growth factor 8 (Mfge8) are able to clear apoptotic myofibroblasts and degrade excess collagen, resulting in the resolution of ongoing fibrosis (Atabai *et al*, 2009). Thus, the impact of macrophage phagocytosis on fibrosis, is quite divergent and influences both its development and resolution. Fibrosis is also associated with disrupted angiogenesis and prolonged hypoxia in the tissue (Wynn & Vannella, 2016). The transcription factor hypoxia-inducible factor-1α (HIF-1α) plays a significant role in TGF-β1-driven as silencing HIF-1α in alveolar macrophages has been shown to reduce their TGF-β1 production and mitigate bleomycin-induced fibrosis (Ueno *et al*, 2011). In type 2 cytokine dependent diseases including helminthic infections caused by *S.Mansoni* or in house-dust mite induced allergic asthma, chronic tissue remodeling can also eventually result in fibrosis. Here, fibrosis has shown to be TGF-B1 independent and is mainly driven by the type 2 cytokine IL-13. Although macrophages are not key producers of IL-13 themselves (Wynn, 2004), depleting CD11b+ monocytes and macrophages in IL-13 dependent mouse models of fibrosis prevents chronic type 2 driven inflammation and fibrosis. Borthwick et al, 2016 show that in contrast to other models of fibrosis, where macrophages adopt and switch between different phenotypes through the course of disease, in IL-13 mediated inflammation, macrophages remain in a pro-fibrotic state continuously, thereby their complete depletion at any stage serves to improve fibrosis. Here macrophages function to recruit CD4+ T helper 2 cells, by producing chemokines such as CCL1 and CCL22, furthering the type 2 response (Borthwick *et al.*, 2016).

A distinct macrophage population, segregated-nucleus-containing atypical monocytes (SatMs), which originate from Ly6C- progenitors, have been identified to drive lung fibrogenesis in mouse modelsa and are regulated by the transcription factor CCAAT/enhancer-binding protein beta (C/EBPβ). In mice that lack C/EBPβ, fibrosis is reduced while inflammation remains unchanged, whereas transferring these cells back into Cebpb−/− mice leads to fibrosis (Satoh *et al*, 2017). While recent research has also demonstrated the heterogeneity in the various macrophage populations or phenotypes that regulate fibrosis and tissue remodeling, the monocyte-derived profibrotic macrophage appears to be a conserved player, central to fibrosis across organs, in mouse and man (Bhattacharya & Ramachandran, 2023; Fabre *et al*, 2023). In human fibrotic tissues, a conserved population of monocyte-derived ‘scar-associated macrophages (SAMacs)’ has been identified as central drivers of fibrosis. These SAMacs share a similar gene expression profile across various organs, such as the liver and lung, and are characterized by the expression of TREM2, CD9, and SPP1

(Ramachandran *et al*, 2019). Sustained by factors like granulocyte-macrophage colony-stimulating factor (GM-CSF), TGF-β, and IL-17A, SAMacs closely interact with ECM-producing fibroblasts, forming a fibrotic niche wherein signaling molecules that they secrete like IL-1β, amphiregulin (AREG), and PDGF activate fibroblasts (Bhattacharya & Ramachandran, 2023; Henderson *et al.*, 2020).

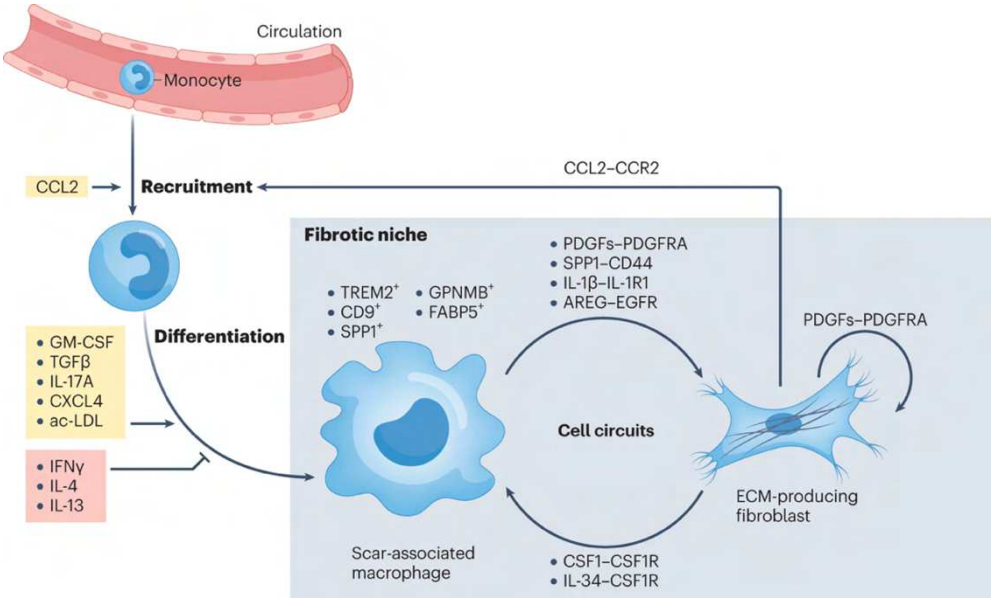

Thesis Figure 4: Macrophages and fibroblasts form a fibrotic niche
Macrophage-fibroblast cell circuits are conserved feature of fibrosis across organs and species. Illustration from (Bhattacharya & Ramachandran, 2023)

1.1.7 Adaptive immunity and fibrosis

In addition to key innate immune cells, cells of the adaptive immune system play a vast plethora of roles in tissue injury, repair and fibrosis and this section will only summarize the role of CD4+ helper T cells. The adaptive immune system is responsible for targeted immune responses through specialized cell types, primarily T cells and B cells. CD4+ helper T cells play an important role and can differentiate into various subsets such as Th1, Th2, Th17, and T follicular helper (Tfh) cells in response to specific cytokine environments and antigenic stimulation (Walker & McKenzie, 2018). Each subset is defined by unique transcription factors—T-bet for Th1 (Szabo *et al*, 2000), GATA3 for Th2 (Zheng & Flavell, 1997), RORγt for Th17 (Ivanov *et al*, 2006), and Bcl6 for Tfh cells (Johnston *et al*, 2009)—and secretes distinct cytokines to coordinate immune defense. Th1 cells produce IFN-γ, enhancing the immune response against intracellular pathogens; Th2 cells secrete IL-4, IL-5, and IL-13, essential in parasitic infections and mediating allergic responses; Th17 cells release IL-17 and IL-22, key for defense against extracellular bacteria and fungi (Miossec *et al*, 2009); and Tfh cells promote B cell maturation and antibody production through IL-4 and IL-21 (Zhang *et al*, 2023). While having specific markers and functions, the different Th subsets also exhibit considerable

plasticity and play distinct roles in fibrosis where they can contribute variably to its progression or inhibition (Wynn & Ramalingam, 2012). Th2 cells have been shown to drive fibrosis, specifically as they produce cytokines such as IL-4 and IL-13, which directly stimulate fibroblasts to synthesize collagen. This response, evolutionarily tailored for defense against helminth infections and facilitates tissue repair in response to tissue damage but can also lead to pathological fibrosis in conditions like chronic liver disease and lung fibrosis which can result, especially driven by IL-13 (Richard *et al*, 2016). Th2 cytokines can also promote the differentiation of alternatively activated macrophages, which express arginase-1 and chitinase proteins that support collagen synthesis and while they limit inflammation in acute settings, they can also exacerbate fibrosis. Th17 cells, defined by IL-17A secretion, contribute to inflammation-driven fibrosis, as seen in conditions like pulmonary and myocardial fibrosis (Feng et al, 2009). IL-17A drives neutrophil recruitment and tissue damage and can directly activate fibroblasts by inducing matrix metalloproteinases. The IL-1β–IL-17A–TGF-β1 axis underscores the pathway's role in fibrosis, emphasizing how upstream cytokines such as IL-1β and IL-23 drive profibrotic Th17 responses (Gasse *et al*, 2007; Wilson *et al*, 2010). Th1 cells on the other hand have also been associated with limiting fibrosis (Gurujeyalakshmi & Giri, 1995). IFN-γ, a key Th1 cytokine, inhibits TGF-β1 signaling by blocking Smad3 phosphorylation and promoting Smad7 expression, which attenuates downstream profibrotic gene activation along with suppressing fibroblast proliferation and collagen synthesis (Ulloa *et al*, 1999). Therefore, the roles of Th2, Th17, and Th1 cells in fibrosis is highly dynamic and can drive context-dependent pro- and antifibrotic mechanisms that are mediated by cytokines and macrophage subsets, shaping tissue repair and fibrotic outcomes (Wynn & Ramalingam, 2012).

Regulatory T cells (Tregs) in tissue repair and fibrosis

The adaptive immune system provides highly specific immunity and memory against pathogens. In this process, it needs to maintain self-tolerance i.e not react to self-antigens encountered to prevent autoimmune reactions. This regulation takes places via two mechanisms – central and peripheral tolerance (Mathis & Benoist, 2004; Xing & Hogquist, 2012). Central tolerance, occurs during development where self-reactive lymphocytes, in the case of T cells in the thymus or B cells in the bone marrow, are programmed to die through negative selection or their self-reactive antigen receptors are edited to non-reactive ones (Ohashi, 2003). Those T cells which recognize self-antigens with moderate affinity develop into regulatory T cells (Tregs) through the expression of a transcription factor forkhead box P3 (*Foxp3*) (Fontenot et al, 2003; Sakaguchi et al, 2008*)*. Tregs can also develop in the periphery from naïve CD4+ T cells that begin expressing *Foxp3* (pTregs) (Chen *et al*, 2003). Since not all self-reactive antigens are present in the thymus during development and some self-reactive

T cells might escape and exit the thymus, a second regulatory mechanism, known as peripheral tolerance exists to protect against autoimmunity (Walker & Abbas, 2002). Peripheral tolerance is crucial and regulates lymphocytes that first encounter their specific-self antigen outside of the thymus due to commensal bacteria, dietary antigens or antigens encountered during chronic infections, thus preventing autoimmune flares to innocuous environmental encounters (Brown & Rudensky, 2023). One main mechanism through which peripheral tolerance works is through the function of Tregs which exert a regulatory role in reigning in and actively restricting this self-reactive immune response in peripheral organs (Vignali *et al*, 2008). Tregs are therefore a distinct subset of CD4+ T cells that are mainly responsible for maintaining immune homeostasis and preventing autoimmune diseases by suppressing excessive immune responses and ensuring tolerance to self-antigens (Sakaguchi *et al.*, 2008). At barrier interfaces, such as the skin, gut and lung, Tregs are essential for ensuring immune tolerance given the constant encounter with environmental and commensal stimuli (Campbell *et al*, 2018; Muñoz-Rojas & Mathis, 2021). They are identified by the expression of CD4, CD25 (IL-2Rα), and the transcription factor *Foxp3*, which is indispensable for their development and suppressive function (Fontenot *et al.*, 2003; Hori *et al*, 2003). Mice completely lacking Tregs (Scurfy mice) or those experimentally ablated of Tregs, have exacerbated inflammation and develop severe autoimmunity which eventually leads to excessive tissue damage and death (Brunkow *et al*, 2001; Kim *et al*, 2007; Lahl *et al*, 2007), with a similar phenomenon observed in humans with a loss of function mutation in the *Foxp3* gene that causes Immunodysregulation, Polyendocrinopathy, Enteropathy, X-linked (IPEX) syndrome (Gambineri *et al*, 2003). Dysfunctional Tregs have also been observed in many autoimmune diseases including inflammatory bowel disease, type 1 diabetes, rheumatoid arthritis and lupus (Franz *et al*, 2007; Maul *et al*, 2005; Simone *et al*, 2021).

Tregs exert their suppressive effects through various mechanisms, including cell-contact-dependent inhibition, through the secretion of inhibitory cytokines like IL-10 and TGF-β (Tang & Bluestone, 2008; Vignali *et al.*, 2008), expression of inhibitory receptors such as cytotoxic T-lymphocyte-associated protein 4 (CTLA-4) and programmed cell death protein 1 (PD-1), and adenosine production via CD39 and CD73 (Deaglio *et al*, 2007; Jain *et al*, 2010). Treg-derived IL-10 has been shown to control inflammation and regulate the immune response in numerous contexts, including infections, allergy models, and autoimmune diseases (Rubtsov *et al*, 2008). For example, Tregs can reduce inflammation in allergy and asthma models by stimulating IL-10 production by effector T cells, a process that can be reversed by blocking IL-10 signaling (Joetham *et al*, 2007; Kearley *et al*, 2005). Similarly, TGF-β is crucial for the development of induced Treg cells and may directly suppress effector T cells in some settings. The dual role of TGF-β in promoting fibrosis and maintaining immune tolerance further complicates its function in disease (Hawrylowicz & O'Garra, 2005; Wan & Flavell, 2007).

Beyond their homeostatic role of regulating the immune response and self-tolerance, more recently, 'tissue-protective' or 'pro-repair' Tregs have also emerged to be active facilitators of tissue repair and regeneration (Arpaia *et al*, 2015; Boothby *et al.*, 2020; Burzyn *et al*, 2013; Loffredo *et al*, 2024). Tregs have been shown to protect stem cell niches during inflammatory activation (Fujisaki *et al*, 2011). In a model of acute lung injury (ALI), Tregs restrained excessive inflammation by increasing the availability of TGF-β and neutrophil apoptosis in the lung and during LPS-induced lung injury or peritonitis facilitated apoptotic clearance by macrophages (D'Alessio *et al*, 2009; Proto *et al*, 2018). In the heart, Treg-derived IL-10, IL-13 and TGF-β1 is essential for preventing scar formation post myocardial infarction. Similarly, during kidney injury, IL-10 production by Tregs was necessary for limiting a pro-inflammatory milieu as IL-10 deficient Tregs failed to restore kidney function (Kinsey *et al*, 2009).

In the context of fibrosis, Treg cells exhibit complex and often contradictory roles (Wang *et al*, 2020). Studies in idiopathic pulmonary fibrosis (IPF) have revealed significant impairments in Treg function, both systemically and locally within the lungs. These dysfunctions correlate with disease severity and may contribute to the dysregulated immune responses observed in IPF patients (Moore & Herzog, 2016). For instance, certain aberrant Treg subtypes, such as Sema7a^{+} Tregs, promote fibrosis through TGF-β1-mediated mechanisms (Reilkoff *et al*, 2013). Interestingly, Treg cells can also exhibit antifibrotic properties, as seen in models where enhancing Treg activity or altering their markers like CCR7 reduces fibrosis severity (Trujillo *et al*, 2010). The role of Tregs in fibrosis is further influenced by disease stage. In murine models of lung fibrosis, Tregs have been shown to contribute to TGF-β1 production and collagen accumulation during the injury phase, yet they may ameliorate fibrosis during later stages (Kotsianidis *et al*, 2009). Tregs also suppress Th2-driven inflammation, which is commonly associated with fibrosis and suppress fibrosis in the skin, but an imbalance in Treg subtypes and their skewed activation can exacerbate disease (Kalekar *et al*, 2019). These findings underscore the dual nature of Tregs in fibrotic diseases, where their suppressive functions can both mitigate and exacerbate pathology depending on the context.

1.1.8 Cytokines, chemokines, and growth factors involved in fibrosis

Fibrosis is driven by a complex network of cytokines, chemokines, and cellular interactions that promote fibroblast recruitment, proliferation, and excessive extracellular matrix (ECM) deposition (Henderson *et al.*, 2020) (**Thesis Figure 5**). TGF-β, a key pro-fibrotic cytokine is produced by a number of cells including T cells, macrophages, eosinophils and neutrophils and is the most widely studied factor for its role in fibrosis in most organs. TGF-β is maintained in an inactive state by the latency-associated protein (LAP). When triggered by proteases, integrins and MMPs, LAP is disrupted and releases active TGF-β. Activated TGF-β then promotes fibroblast proliferation, extracellular matrix (ECM) synthesis, myofibroblast

differentiation, recruits inflammatory cells via chemokines like MCP-1, and suppresses T-cell activity (Munger *et al*, 1999). On the other hand, can also reduce inflammation and trigger cell death. Its role seems to largely depend on the cell type producing it— TGF-β1 from macrophages is usually pro-fibrotic, while TGF-β1 from regulatory T cells can have anti-inflammatory effects (Kitani *et al*, 2003; Wynn & Ramalingam, 2012). Interestingly, in the next paragraph while other cytokines will be touched upon, they show a central theme of largely synergizing with TGF-β in their fibrotic roles (Henderson *et al.*, 2020). While TGF-β is the most studied and dominant cytokine in fibrogenesis, other cytokines are also involved depending on the experimental model and initiating source of injury and fibrosis (sterile, helminth, viral) (Wilson *et al.*, 2010). **TNF-**a, a key inflammatory factor, present early post-acute injury drives trans-endothelial migration and recruitment of inflammatory immune cells to the wound site. It has been shown to drive T cell mediated alveolitis and subsequent fibrosis and TNF-a knockout mice are protected from silica or bleomycin-induced lung fibrosis (Miyazaki *et al*, 1995; Piguet *et al*, 1989). Interestingly, the fibrosis-inducing macrophage subset SatMs (see section above), are key sources of TNF-a too in a bleomycin-induced fibrosis model (Satoh *et al.*, 2017). Similarly, mice deficient in **IL-1B**, another early inflammatory mediator also fail to develop severe fibrosis across organs such as the lung, liver, kidney, and heart (Gasse *et al.*, 2007; Wilson *et al.*, 2010). IL-1B can activate fibroblasts via epithelial to mesenchymal transition (EMT) and acts upstream of TGF-β to induce myofibroblast differentiation (Fan *et al*, 2001). **IL-17A**, produced by γδ T cells, CD4+ T cells, neutrophils, and mast cells, is another key cytokine that has been shown to drive fibrosis across multiple organs, including the lung, liver, and skin. In the bleomycin model of lung fibrosis, IL-17A which is secreted by CD4+ T cells exacerbates inflammation, neutrophil recruitment, and neutrophil-induced tissue injury, and TGF-β production (Wilson *et al.*, 2010). TGF-β1, when produced in a pro-inflammatory environment amplifies IL-17A production. In turn, IL-17A directly acts on fibroblasts where it maintains their expression of TGF-BR hence increasing downstream TGF-β sensing and continued activation of collagen-producing fibroblasts. **IL-4** and **IL-13**, that were introduced earlier in the context of macrophage activation, are significantly involved in the progression of fibrosis. Their induction shifts the inflammatory response from one that is more neutrophilic and dominated by proinflammatory macrophages (induced by cytokines such as IL-1, IL-17 etc) to one with increased eosinophils and alternatively activated macrophages (Gieseck *et al*, 2018). In addition to its role in activating macrophages (see previous section), IL-13 also induces fibroblast activation by directly stimulating collagen-producing fibroblasts and other stromal, parenchymal, and epithelial cell populations. Mouse models deficient in IL-13, IL-4R or IL-13RB1, along with studies that used neutralizing antibodies against them have shown to reduce fibrosis in various tissues, highlighting their involvement in fibrogenesis (Chiaramonte *et al*, 1999; Hart *et al*, 2017; Singh *et al*, 2017). Moreover, alarmins including IL-25, IL-33 and

thymic stromal lymphopoietin (TSLP) act as the first stimulators, inducing the production of IL-4 and IL-13 by innate lymphoid cells, eosinophils, and T cells, further amplifying type 2-driven fibrosis (Vannella *et al*, 2016). In both mouse and human lung fibrosis, an increase in IL-25 is observed and mechanistically, IL-25 was shown to then stimulate the production of IL-13 from ILC2s which increased collagen deposition in the lungs (Hams *et al*, 2014). **IL-11**, in a more recent finding was shown to amplify fibroblast activation with both IL-17 and IL-4/IL-13 signals converging to induce it (Ng *et al*, 2019; Schafer *et al*, 2017). Whether tissue fibrosis occurs through the IL-1-IL-17 driven axis or is IL-4/IL-13 mediated depends on the injury and tissue. Acute experimental models often see an IL-17 mediated activation of TGF-β1, whereas chronic or repetitive models lead to a type 2 response being activated (Wilson *et al.*, 2010). However, in cases where either one pathway was therapeutically targeted, it led to the induction of the other, highlighting an overlapping or converging role of different cytokines during fibrosis, which further complicates therapeutic strategies (Henderson *et al.*, 2020).

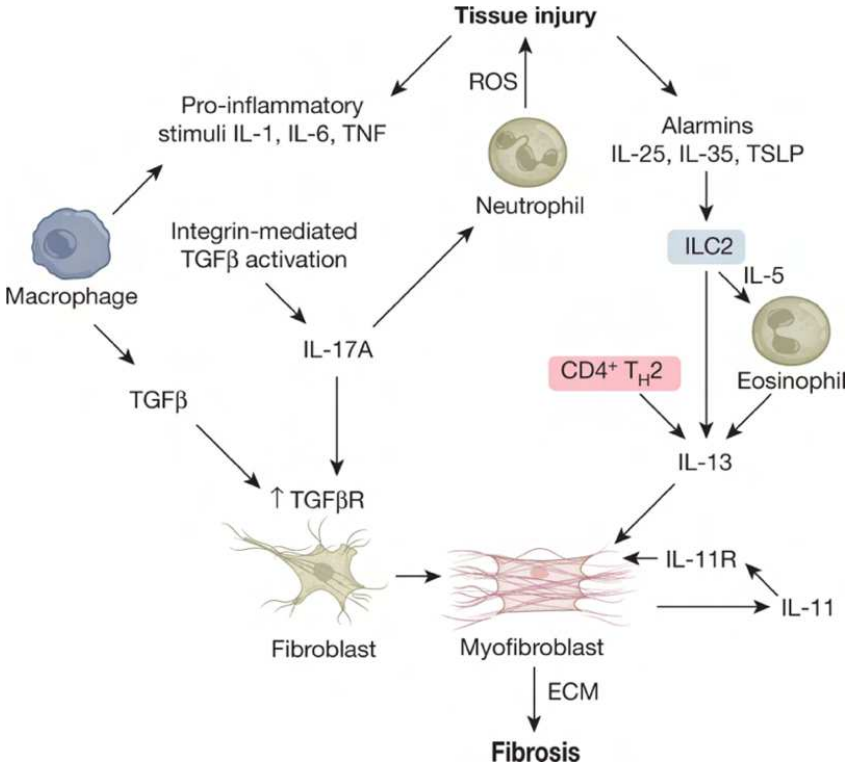

Thesis Figure 5: Cytokine networks in fibrosis
A complex network of multiple cytokines are central to many fibrotic diseases. Illustration from (Henderson *et al.*, 2020)

1.1.9 Idiopathic pulmonary fibrosis (IPF)

Description and Clinical Manifestations

Interstitial lung diseases (ILD) are a group of over 200 diseases that cause severe inflammation and scarring of the lungs which all ultimately impair gas exchange. While there are some non-fibrotic diseases, most ILDs are characterized by progressive fibrosis of the lungs (Wijsenbeek *et al.*, 2022). Amongst this idiopathic pulmonary fibrosis (IPF) is the most common form of fibrotic ILDs. IPF is a chronic, progressive, and fatal disease. Given its idiopathic nature it usually has an unknown etiology and poor prognosis (Selvarajah *et al*, 2023). The clinical symptoms of IPF include progressive dyspnea, reduced lung compliance, and an onset of symptoms such as shortness of breath and bibasilar crackles (King *et al.*, 2011). High-resolution computed tomography (HRCT) often shows that there is subpleural fibrosis and honeycombing in the lungs, while histopathology shows usual interstitial pneumonia (UIP) where there are fibroblastic foci interspersed with normal lung tissue. Key characteristic fibrotic changes in the lung include remodeling of the interstitium, distal airways, and alveolar spaces, often with hyperplastic epithelial cells, honeycomb cysts, and bronchiolization. These features contribute to irreversible lung dysfunction and architectural distortion (Raghu *et al*, 2018).

Prevalence and Epidemiology

IPF has a median survival of 2.5–3.5 years post-diagnosis (Ley *et al*, 2011) (**Thesis Figure 6**). Epidemiological studies have reported that there is an incidence of 3–9 cases per 100,000 people annually in North America and Europe. Globally, IPF incidence ranges between 0.09 and 1.30 per 10,000 individuals, with the highest rates in the U.S., South Korea, and Canada (Hutchinson *et al*, 2015). The disease primarily affects older males, with studies showing that 85% of patients over 70 (in a U.K population study) at diagnosis (Navaratnam *et al*, 2011). Despite the overall mortality rate declining from 2004 to 2017—likely due to reduced tobacco use, less reliance on immunosuppressants, and new antifibrotic treatments, IPF remains a significant health challenge (Fernandez Perez *et al*, 2010; Raghu *et al.*, 2006).

Risk Factors for Idiopathic Pulmonary Fibrosis (IPF)

Environmental Factors

Environmental exposures play a key role in IPF development by causing chronic alveolar epithelial injury (Abramson *et al*, 2020; Sack & Raghu, 2019) . Tobacco smoke is one of the most significant risk factors, with smokers—particularly those with familial IPF—at significantly higher risk of disease. Occupational exposures, such as metal and wood dust, livestock handling, and industrial fumes, have also been consistently linked to IPF (Abramson *et al.*,

2020; Gandhi *et al*, 2024). Studies show higher incidence rates in industrialized areas, with men being more affected in the past due to occupational roles (Gandhi *et al.*, 2024). Additionally, domestic exposures, such as mold, bird antigens, and poorly maintained ventilation systems, may contribute to disease risk, though the exact impact on disease progression remains unclear (De Sadeleer *et al*, 2018; Winterbottom *et al*, 2018). Air pollution and other particulate matter further exacerbate epithelial damage, particularly in individuals with underlying genetic predisposition (Johannson *et al*, 2014) .

Genetic Factors

Genetic predisposition significantly influences IPF susceptibility. Familial pulmonary fibrosis (FPF) is defined by cases where two or more family members are affected. This accounts for up to 20% of IPF cases (Adegunsoye *et al*, 2024). In sporadic IPF genetic mutations or variants in telomere-related genes (e.g., telomerase reverse transcriptase (TERT), and telomerase RNA component (TERC)) and cell-adhesion genes (e.g., DSP) are associated with disease risk (Sack & Raghu, 2019) . In IPF, the mucin 5B (MUC5B) promoter variant is the most common genetic alteration that is found to be present in 38% of patients and homozygous carriers have a 21-fold risk for developing disease. This impairs mucociliary clearance which then promotes epithelial injury and fibrosis (Yang *et al*, 2015a). However, known genetic variants explain only a fraction of disease cause, highlighting the complexity and idiopathic nature of IPF pathogenesis.

Aging

Aging is the most consistent and significant non-modifiable risk factor for IPF. The prevalence of IPF doubles every decade after the age of 50 (Gulati & Thannickal, 2019) (**Thesis Figure 6**). Cellular hallmarks of aging, such as telomere shortening, DNA damage, mitochondrial dysfunction, and dysregulated proteostasis all influence disease development (López-Otín *et al*, 2023). Senescence and loss of function of alveolar type 2 (AT2) cells is particularly important, as these cells exhibit impaired repair capacity and contribute to a profibrotic environment (Yao *et al*, 2021). Mitochondrial dysfunction and oxidative stress exacerbate DNA damage, further promoting cellular senescence. Telomere attrition is a key feature of aging in IPF, with genetic mutations in telomere maintenance genes driving fibrosis. Additionally, endoplasmic reticulum (ER) stress and the accumulation of misfolded proteins in AT2 cells lead to apoptosis, senescence, and fibrosis, further linking aging processes to IPF pathology (Korfei *et al.*, 2008).

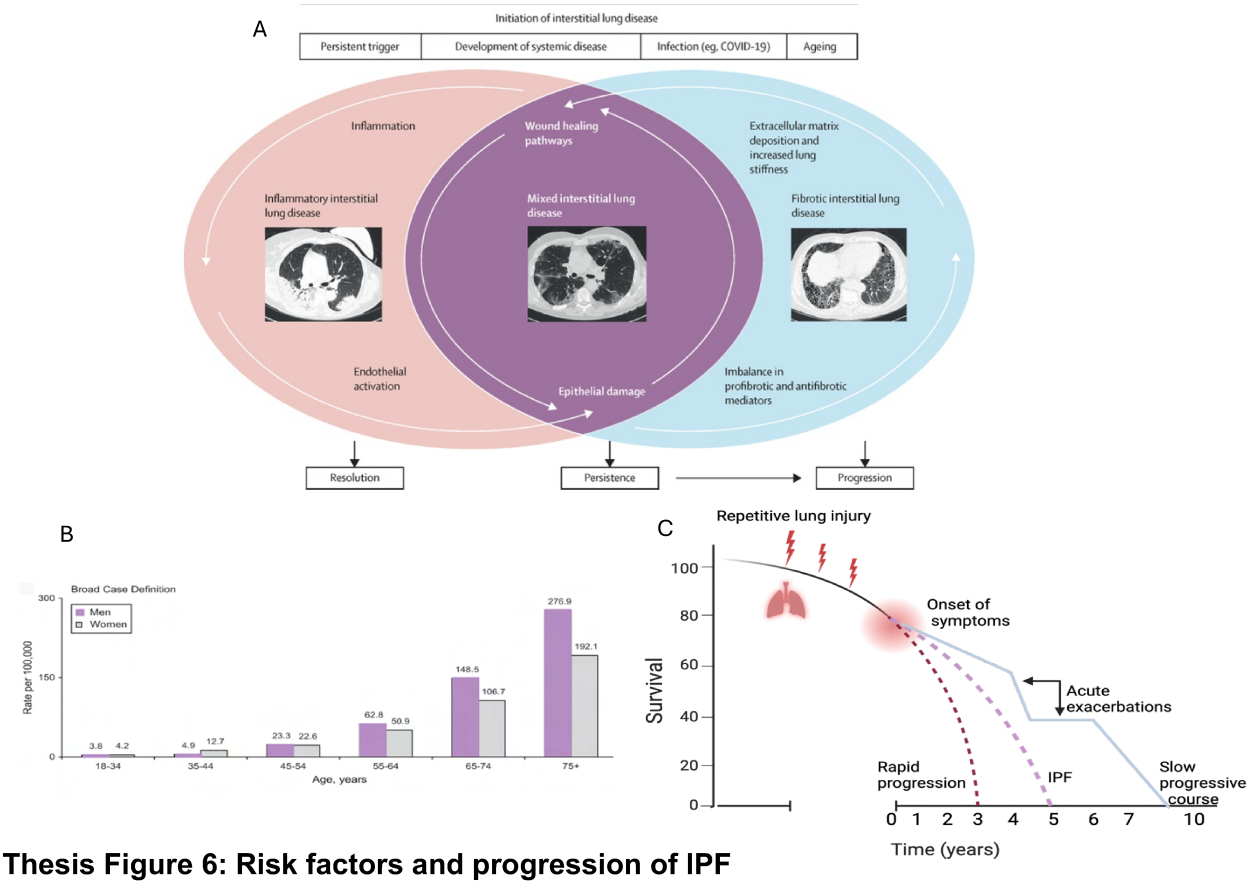

Thesis Figure 6: Risk factors and progression of IPF

(A) Inflammation, aberrant wound healing, epithelial damage are intricately linked to many ILDs leading to pulmonary fibrosis and impaired lung function. Illustration from (Wijsenbeek *et al*, 2022) (B) Advanced age is the highest risk factor for IPF. Graph from (Raghu *et al*, 2006).(C) A lifetime of lung injuries precedes symptom onset, with a short median survival (2.5–3.5 years). Patients with slow progression may remain stable for years but risk acute exacerbations that accelerate decline. Illustration modified from (King *et al*, 2011)

Experimental models of lung fibrosis

Lung fibrosis manifests due to repetitive lung injury to the alveolar epithelium followed by inflammation, myofibroblast hyperplasia, excessive collagen deposition and scar formation. This leads to disruption of the lung structure and impairs gas exchange. Acute exacerbations which involve severe lung injury or infection can also occur and lead to a high mortality in patients with a slow-progressive fibrosis (Wijsenbeek *et al.*, 2022). By the time patients seek treatment, the disease is at an advanced stage preventing the exact pathogenesis leading to lung fibrosis to be known. This also complicates the study of the mechanisms of fibrosis in humans and animal models have been used to study this; while they do not fully recapitulate every feature of IPF, they've helped understand the initiation, early inflammation, and how fibrosis develops over time (Moore & Hogaboam, 2008). Most animal (rodent) models involve exposure to particulates or drugs including asbestos, silica, and bleomycin (B. Moore *et al*, 2013). Amongst these bleomycin-induced lung injury has been the gold standard (Della Latta *et al*, 2015). Bleomycin is an antibiotic from *Streptomyces verticillatus* that was used as a

chemotherapeutic drug for human lung cancers but one of its major side-effects was lung fibrosis (Chen & Stubbe, 2005; Umezawa *et al*, 1967). It causes direct DNA damage to cells in organs such as the lung which have low levels of the bleomycin-inactivating enzyme bleomycin hydrolase (Chaudhary *et al*, 2006). In mice, when bleomycin is instilled intratracheally it induces damage to the lung epithelium causing severe epithelial injury that triggers an inflammatory response peaking around day 7 post injury, with immune cell infiltration and macrophage activation. Fibrosis begins to accumulate by day 14, with peak collagen deposition and extracellular matrix buildup around 21–28 days (*section 1.2*); however, in many mouse models this response eventually resolves, so repetitive instillations are often employed to study persistent, end-stage fibrosis (Della Latta *et al.*, 2015).

Current treatments for IPF

IPF is irreversible and fatal. The therapeutic landscape of IPF is spotted with decades of research and clinical trials, yet with no cure (Kam *et al*, 2022). A breakthrough came with the approval of two Food and Drug Administration (FDA)-approved drugs, Pirfenidone and Nintedanib, that both work to slow down the progression of the disease, by decelerating the decline of lung function (Somogyi *et al*, 2019). Pirefenidone targets the TGF-B pathway and has some anti-inflammatory effects, although the exact mechanisms of this are unclear, to slow fibrosis progression (King *et al*, 2014; Noble *et al*, 2011). Nintedanib, which is a tyrosine kinase inhibitors blocks PDGF and VEGF signaling which work to reduce the proliferation of fibroblasts and slows down the rate of lung scarring and respiratory failure, helping increase the median survival and manage symptoms (Richeldi *et al*, 2011; Richeldi *et al*, 2014) . Despite this, they only represent management of fibrosis and currently there are no therapies available to stop or reverse fibrosis completely in the (Selvarajah *et al.*, 2023). Several trials targeting different pathways are ongoing (Zhao *et al.*, 2022). These include senolytics, aimed at clearing age-related senescent cells and many cytokine and immune modulating inhibitors. Chemotherapy drugs like dasatinib and quercetin, have shown potential in reducing fibrosis by targeting senescent fibroblasts and epithelial cells (Somogyi *et al.*, 2019). Biologic drugs targeting fibrosis-driving pathways, such as pentraxin-2, which is a circulating glycoprotein that regulates monocyte-derived macrophage activation and galectin-3 inhibitors, which interfere with cell adhesion and fibrosis-related signaling, are currently in advanced clinical trials (Hirani *et al*, 2021; Van Den Blink *et al*, 2016). However, for patients with advanced fibrosis, lung transplantation still remains the only treatment option for prolonged survival (Kapnadak & Raghu, 2021). Given the vast mechanisms that regulate fibrosis as described above, the need for understanding both immune and tissue contributions is pressing (Somogyi *et al.*, 2019).

1.2 Lung Macrophages Through Life: Fate, Function, and Fibrosis

As a barrier organ constantly exposed to environmental insults, the lung has a unique environment that directly interfaces with the outside world. To maintain function and homeostasis, it relies on effective repair mechanisms (Planer & Morrisey, 2023). The lung macrophage compartment, regarded as a key regulator of tissue repair, plays a central role in this process. In this section, we will explore how different unique lung macrophage populations respond to inflammation, mediate repair, drive fibrosis, and evolve to adapt to the changing demands across the lifespan (Morales-Nebreda *et al*, 2015).

1.2.1 The structure of the lung

The lungs are our primary organs of respiration. They are responsible for a vital life process - the exchange of oxygen and carbon dioxide between the external environment and the bloodstream. Gas exchange occurs in the alveoli, that are located deep within the lung where a network of delicate tubes leads to a thin alveolar epithelial barrier. (Hsia *et al*, 2016). The alveolar epithelium directly lines with a dense capillary network to facilitate efficient gas exchange (Knudsen & Ochs, 2018). On average, the lungs process around 10,000 liters of air every day. This exposes them to both harmless particles and potentially harmful toxins or pathogens from the air (Schneider *et al*, 2021). To protect against these threats, the lungs have a number of different defense mechanisms, with the epithelium serving as the first protective layer, coupled with the innate immune system. The epithelium forms a mucosal barrier, ensuring that inhaled pathogens, particulates, and foreign materials do not compromise the lungs' structural or functional integrity over time (Basil *et al*, 2020). The upper airways are made up of pseudostratified epithelium with many cell types, including ciliated cells, goblet cells, club cells, basal progenitor cells, neuroendocrine cells, ionocytes and tuft cells. The lower airways end in respiratory bronchioles, alveolar ducts, and alveolar sacs, where gas exchange takes place through closely connected capillary networks. The lung alveolus is composed of epithelial, endothelial, mesenchymal, and immune cells, including alveolar and interstitial macrophages and dendritic cells (Travaglini *et al*, 2020; Vieira Braga *et al*, 2019). In a healthy state, the alveolar niche remains largely inactive, with slow cell turnover. However, due to its constant exposure to the external environment, the alveoli are frequently subjected to injury, requiring coordinated repair mechanisms to maintain lung function. Various cell types contribute to homeostasis, tissue regeneration, and immune regulation. When these processes become dysregulated, they can lead to ineffective repair, persistent inflammation, or fibrosis, ultimately impairing lung function (Basil *et al.*, 2020).

1.2.2 The respiratory epithelium – the injured soldiers

The alveolar epithelium is lined by two main cell types: alveolar type 1 (AT1) and alveolar type 2 (AT2) cells (Weibel, 2015). AT1 cells are flat, squamous cells that make up more than 95% of the alveolar surface area. They have a thin, flat, expansive structure in close proximity with endothelial cells and the lung's vasculature. The main function of AT1 cells is to facilitate efficient gas exchange between the alveoli and the bloodstream (Williams, 2003; Yang *et al*, 2015b). AT2 cells are cuboidal cells that reside at the corners of the alveoli. Although the number of AT2 cells is almost twice as many as AT1 cells, they cover less than 5% of the alveolar surface. They are primary producers of surfactant, a substance that reduces surface tension in the alveoli, ensuring they remain open for gas exchange (Chen *et al*, 2006). In addition, AT2 cells help regulate fluid balance, transport ions, modulate immune responses in the lung, and importantly function as progenitor cells that can differentiate into AT1 cells when needed for repair. Organs such as the lung which have a slow cell turnover, especially in the epithelium, rely on bifunctional stem cells. While early during postnatal development, both AT1 and AT2 cells are specified (Rawlins *et al*, 2009), during adulthood AT2 cells demonstrate stem-cell-like behavior and can give rise to new AT1 cells (Barkauskas *et al*, 2013). Clonal analysis studies showed that while most AT2 cells remain in a quiescent state, a small subset retained continuous stem cell activity during homeostasis. It was observed that an active AT2 cell had the ability to proliferate and repeatedly produce new AT1 cells, while nearby AT2 cells remained inactive. This resulted in clusters of AT1 cells that could be traced back to the single active AT2 cell lineage (Desai *et al*, 2014). Given its constant exposure to external perturbations, while remaining relatively quiescent, the alveolar epithelium exhibits a high need for regeneration. This can occur because of acute perturbations (ARDS, acute infection) as well as chronic damage from repetitive environmental exposures (Basil *et al.*, 2020; Planer & Morrisey, 2023). When the epithelial barrier is injured, without complete destruction, the numbers of AT2 cells rapidly increases. Repair and regeneration of the alveolar epithelium relies heavily on the progenitor capacity of AT2 cells and their ability to transition and form new AT1 cells (Zacharias *et al*, 2018). Within the AT2 population, a subset of cells expressing Axin2, a Wnt responsive gene, were identified as the population serving as progenitors, termed alveolar epithelial progenitors (AEPs). Wnt signaling therefore activates Axin2+ AEPs, promoting AT2 self-renewal (Nabhan *et al*, 2018).

Stem-cell AT2 to AT1 transition is not a direct, one-step process. Rather, AT2 cells transition through various intermediate states. These states are characterized by the expression of specific markers such as Krt8 and Cldn4 and across studies various terms such as Krt8+ alveolar differentiation intermediates (ADI) and damage-associated transient progenitors (DATP) have been used to define them (Jiang *et al*, 2020; Kobayashi *et al*, 2020; Strunz *et al*,

2020). Inflammation, particularly through signals like IL-1β that are secreted by interstitial macrophages, can push a subset of AT2 cells expressing IL1r1 into these transitional states to facilitate AT1 cell repopulation post injury therefore linking inflammation to the regulation of repair mechanisms (Choi *et al*, 2020). These transitional states are often associated with TGF-β signaling, p53 activation, cellular senescence, and inflammation (Bhandary *et al*, 2013). The presence of these intermediate cell populations suggests that AT2 cells display significant heterogeneity after injury, reflecting their various roles in regeneration or dysfunction (Olajuyin *et al*, 2019; Pooja *et al*, 2011).

In cases of IPF, AT2s are impaired and lose their progenitor capability, creating a gap in effective lung repair. The wingless-related integration site (WNT) Wnt–β-catenin pathway, important for tissue self-renewal, is persistently active in AT2 cells in pulmonary fibrosis (Chilosi *et al*, 2003). Its activation via WNT1-inducible signaling pathway protein 1 (WISP-1) promotes AT2 cell proliferation, epithelial-to-mesenchymal transition (EMT), and extracellular matrix (ECM) production by lung fibroblasts. Blocking WISP-1 reduces fibrosis in bleomycin-treated mice, highlighting its role in disease progression (Königshoff *et al*, 2009). Factors such as hypoxia and Notch signaling can drive these progenitor cells toward an airway phenotype rather than proper AT2 or AT1 differentiation, contributing to the formation of dysplastic structures and cysts characteristic of fibrotic lungs (Shiraishi *et al*, 2024). The failure of transitional cells to properly mature into fully functional AT1 cells under certain disease conditions could contribute to the lack of effective regeneration observed in lung fibrosis (Choi *et al.*, 2020) (**Thesis Figure 7**).

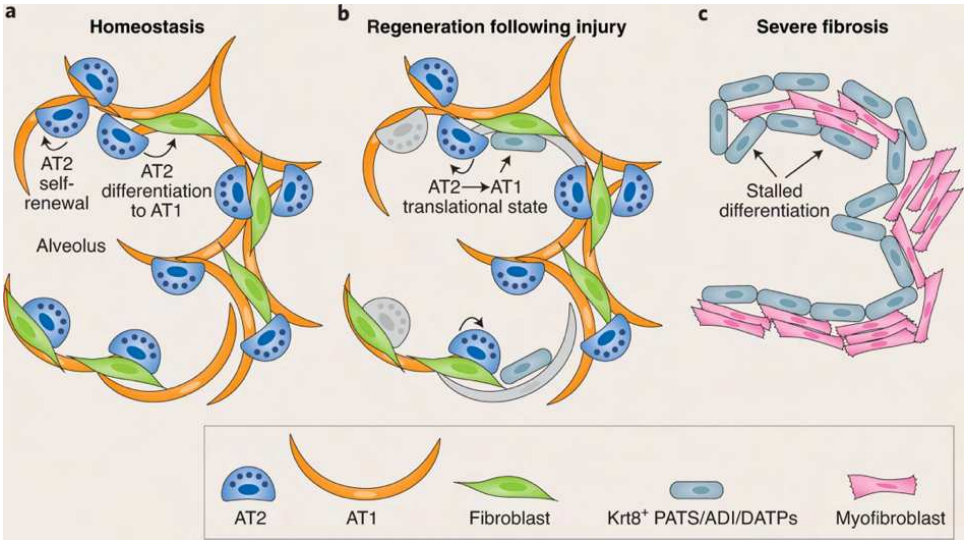

Thesis Figure 7: Alveolar Epithelial Repair and Fibrosis

(a) Injury-induced loss of AT1 and AT2 cells triggers AT2 proliferation and differentiation into AT1 cells for repair. (b) Transitional cell states emerge, differentiating into AT1 cells. (c) In fibrosis, transitional cells increase but fail to fully differentiate, contributing to impaired repair. Illustration from (Verheyden & Sun, 2020)

1.2.3 Pulmonary macrophage heterogeneity and function under steady state

Deep within the intricate network of alveoli and the adjacent intestitium or parenchyma reside the tissue-resident macrophages of the lung. At steady state, almost 95% of the cellular makeup in the alveoli is comprised of tissue-resident alveolar macrophages (TR-AMs) (Kopf *et al*, 2015). They are found on the luminal side of the alveoli within a specialized niche comprised epithelial cells (AT1 and AT2), capillary endothelial cells, and alveolar interstitial fibroblasts, that provide instructive signals that maintain their tissue-resident like identity (Westphalen *et al*, 2014). As the lung is constantly exposed to a barrage of environmental perturbations, situated at the interface of the airways and outside world, TR-AMs form the frontline defense of the lungs (Aegerter *et al*, 2022). Their key roles in maintaining tissue homeostasis and integrity in the lungs are to clear cellular debris and excess surfactant produced by the surrounding epithelial cells (Hussell & Bell, 2014b). Along with TR-AMs, in the interstitium/parenchyma, a small population called interstitial macrophages (IMs) exists at steady state. They are thought to support the stroma, nerves, and blood vessels and are phenotypically distinct from alveolar macrophages (AMs) (Liegeois *et al*, 2018) (**Thesis Figure 8)**.

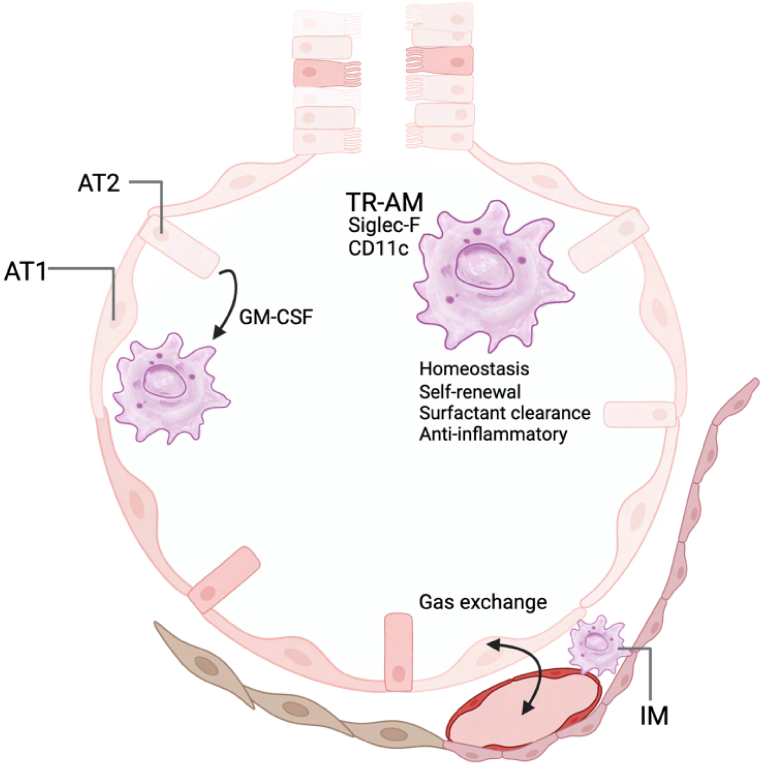

Thesis Figure 8: Tissue-resident alveolar macrophages at steady-state.
Tissue-resident alveolar macrophages in the alveoli and interstitial macrophages in the parenchyma populate the lungs at steady-state where they are they guardians of maintaining tissue homeostasis, a low-reactive environment, clearing surfactant and supporting vasculature and nerves. Based on(Aegerter *et al.*, 2022).

1.2.4 The ontogeny of tissue-resident alveolar macrophages

The ontogeny of tissue-resident macrophages was initially based on van Furth's model of the 'mononuclear phagocyte system (Van Furth & Cohn, 1968) where it was believed that tissue-resident macrophages are constantly replenished by circulating monocytes in the blood, derived from adult hematopoietic stem cell (HSC) progenitors in the bone marrow. This was substantiated by experiments in which tissue-resident macrophages of irradiation chimeras were replenished by those derived from donor bone marrow cells (Tarling & Coggle, 1982) . For decades to follow, this foundational paradigm was further supported by findings that uncovered a common multipotent monocyte progenitor that had the ability to give rise to macrophages and dendritic cells in-vivo upon adoptive transfer of bone marrow precursors into irradiated hosts (Fogg *et al*, 2006) . Furthermore, in-vitro studies of bone-marrow derived monocytes and adoptive transfer experiments of circulating monocytes conclusively demonstrated their ability to differentiate into macrophages (Sallusto & Lanzavecchia, 1994). While these studies, limited by the techniques available at the time, seemed to confirm van Furth's dogma and indeed showed that monocytes had the ability to differentiate into tissue-resident macrophages, these conclusions were drawn from experiments in which tissue-resident niches were depleted by irradiation thus compelling bone marrow precursors and monocytes to repopulate the niche (Maus *et al*, 2006). As a result, they did not clarify how tissue-resident macrophage populations were maintained and replenished under normal, steady-state conditions. In the early 2000s, an important breakthrough study showed that this prevailing concept did not uniformly apply to all tissues, as Langerhans cells (epidermal tissue-resident macrophage population) appeared to be radioresistant and repopulated from host cells post bone-marrow transplantation. This contrasted with circulating monocytes, which were of donor origin and only populated the tissue upon inflammatory injury to the skin that resulted in the loss of Langerhans cells (Merad *et al*, 2002). Similar findings followed, showing that microglia, tissue-resident macrophages in the brain, remained of host origin despite lethal irradiation (Ginhoux *et al*, 2010). In experiments where the lung was shielded from irradiation thus protecting the resident alveolar macrophage population from ablation, bone marrow derived monocytes did not replace the existing pool (Murphy *et al*, 2008). To investigate macrophage turnover without disruption of the host resident populations, parabiosis experiments, in which the circulatory systems of congenially marked mice were joined, revealed that under steady-state conditions macrophages in the lungs and brain remained solely derived from the host. On the other hand, macrophage populations in tissues such as the gut, dermis, and heart were seen to be repopulated from both host and donor origins (Hashimoto *et al*, 2013). Fate mapping studies (Yona *et al*, 2013) have now established that each tissue displays its own turn-over rate under steady state conditions, with the involvement

of circulating monocytes in maintaining macrophage populations during homeostasis confined to specific tissues. Instead, tissue-resident macrophages, such as microglia, alveolar macrophages in the lungs, Kupffer cells in the liver and splenic macrophages originate from embryonic precursors, which are seeded in these tissues before birth and continue to self-renew locally throughout adulthood, without significant input from bone-marrow derived precursors under steady-state conditions (Ginhoux *et al*, 2016).

Tissue-resident macrophages derive from three distinct precursors, namely yolk-sac derived macrophages (YS-Macs), fetal liver monocytes (FL-Mos) and bone-marrow derived monocytes (BM-Mos) (Ginhoux & Guilliams, 2016). Immune cells, including macrophages, are produced and seeded in three consecutive developmental waves of hematopoiesis (Bertrand *et al*, 2005). The first wave of primitive hematopoiesis emerges from blood islands of the extra-embryonic yolk sac around the embryonic age of E7.0 in mice (equivalent to 3 weeks of gestation in humans) (Palis & Yoder, 2001). This gives rise to erythroid, megakaryocyte and macrophage progenitors (Palis *et al*, 1999). These macrophage progenitors directly develop into YS-Macs, without a monocytic intermediate. Once the blood circulation is established at E8.5-9.0 (Gomez Perdiguero *et al*, 2015), YS-Macs are released from their entrapment in the blood islands and begin migrating to tissues by E8.5-10.0, forming the direct precursors for microglia in the brain (Ginhoux *et al.*, 2010; Kierdorf *et al*, 2013). At the same time, a second wave of hematopoiesis occurs (transient definitive wave) giving rise to erythro-myeloid precursors (EMP) that migrate into the fetal liver, where they expand and proliferate, giving rise to cells of multiple lineages including fetal liver monocytes from E12.5 onwards (Hoeffel *et al*, 2015). This intermediatory stage in the fetal liver is essential as studies have shown that EMPs do not have the capacity to establish tissue-resident macrophages when they are directly transplanted into immune-compromised mice (Ginhoux & Guilliams, 2016; Palis & Yoder, 2001). Fetal liver monocytes are released into the blood around day E13.5 and colonize most tissues, except for the brain (Ginhoux *et al.*, 2010), by E14.5, replacing tissue macrophages seeded during the primitive wave. The third, definitive hematopoiesis' wave produces the first hematopoietic stem cell (HSC) and colonizes the fetal liver, which becomes the primary site of embryonic hematopoiesis by E12.5. These precursors then seed the fetal bone marrow by E17.5, ultimately leading to the formation of adult hematopoietic stem cells in the bone marrow that give rise to the various cells of the adult immune system, including adult bone marrow derived monocytes, that will replenish the macrophage pool over life (Ginhoux & Guilliams, 2016; Hoeffel & Ginhoux, 2018; Hoeffel *et al*, 2012).

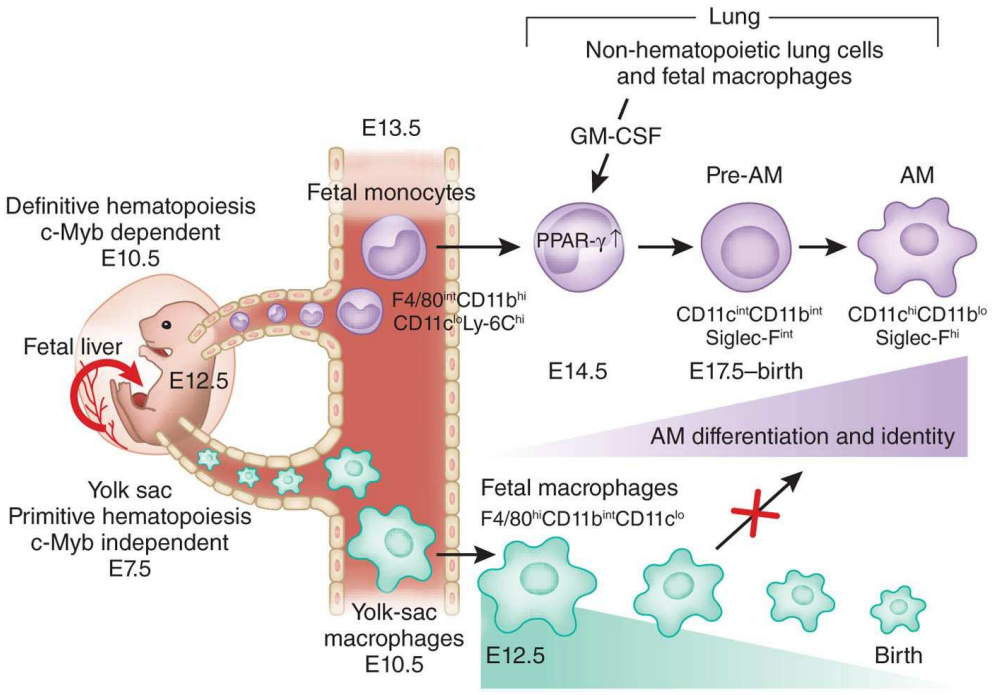

Thesis Figure 9: Development of alveolar macrophages - Fetal liver-derived monocytes colonize the lungs by E13.5–E14.5 and differentiate into alveolar macrophages via GM-CSF-induced PPAR-γ expression. Illustration from (Ginhoux, 2014)

Alveolar macrophages develop from fetal liver monocytes that initially seed the lungs around E14.5 and expand into a pre-AM state by E17.5 and migrate into the alveolar niche at P0 (Ginhoux & Jung, 2014; van de Laar *et al*, 2016), the day of birth through critical cues instructed by granulocyte-macrophage colony-stimulating factor (GM-CSF) secreted by alveolar epithelial cells (Gschwend *et al*, 2021a; Guilliams *et al*, 2013). The absence of AMs in GM-CSF or GM-CSF receptor-deficient mice underscores the importance of this signaling, while mice lacking macrophage colony-stimulating factor (M-CSF) still develop AMs. This differentiation is supported by autocrine TGF-β signaling, facilitated by the interaction between TGF-β and lung epithelial integrins. Together, these cues induce the expression of the transcription factor peroxisome proliferator-activated receptor gamma (PPAR-γ), activating the development and maturation of AMs (Schneider *et al*, 2014). Alongside PPAR-γ, other key transcription factors such as Bach2, Egr2, and Bhlhe40 further reinforce the unique identity of AMs and sustain their self-renewal, in addition to core macrophage defining transcription factors such as C/EBPB and PU.1 (Aegerter *et al.*, 2022; Daniel *et al*, 2020; Gorki *et al*, 2022; Mass *et al*, 2016; Rauschmeier *et al*, 2019; Shibata *et al*, 2001). Only by day 3 post birth (P3), AMs start to mature (Guilliams *et al.*, 2013) and express high levels of key surface markers including sialic acid-binding immunoglobulin-like lectin F (Siglec-F) and CD11c, which are characteristic of their identity (Ginhoux & Jung, 2014; Misharin *et al*, 2013; van de Laar *et al.*, 2016). (**Thesis Figure 9**). AMs continue to mature over the first weeks of life, reaching a stable homeostatic adult phenotype around P14-P21. This progressive maturation occurs in an

environment of dramatic tissue organization, cell turnover, exposure to the first breath and varying environmental stimuli from the external world. Our lab has shown that early in life, developing AMs spontaneously release inflammatory cytokines and eventually 'calm down' upon reaching maturity, achieving a low-reactive identity characteristic of mature homeostatic AMs (Saluzzo *et al*, 2017).

1.2.5 Environmental cues regulate TR-AM identity and function

The unique environment of TR-AMs, within the alveoli shapes their identity and function allowing them to act as both frontline defenders and mainstays of tissue homeostasis, while averting unwarranted inflammation in response to every ambient stimulus (Hussell & Bell, 2014b). TR-AMs function primarily to clear debris, inhaled particles and cellular waste via an immunologically silent process known as efferocytosis (Gheibi Hayat *et al*, 2019; Schneider *et al.*, 2014) .TR-AMs need to control immune responses without endangering the fragile alveolar tissue integrity. Therefore, tightly regulated environmental processes are needed to direct TR-AM function in maintaining tissue preservation and effective immune surveillance (Bain & Macdonald, 2022). The alveolar microenvironment plays a defining role in shaping the identity and function of AMs. Given their location, surrounded by a niche of epithelial cells, the cues and interactions with AT2 cells are essential for maintaining AMs. As mentioned above, GM-CSF produced by AT2 cells is indispensable for the development, function, and maintenance of AMs (Gschwend *et al*, 2021b; Guilliams *et al.*, 2013; Shibata *et al.*, 2001). Lung environments that lack GM-CSF (or GM-CSFR on AMs) where AMs fail to develop or are functionally impaired and unable to clear surfactant, lead to the onset of a rare disorder called pulmonary alveolar proteinosis (PAP), caused due to a buildup of excess surfactant that compromises efficient gas exchange and lung function. (Trapnell & Whitsett, 2002; Trapnell *et al*, 2003), During early life, neonatal lung environments display a skewing towards a type 2 environment. IL-33 and GM-CSF produced by epithelial cells cooperates with IL-13 producing type 2 innate lymphoid cells (ILC2s) (Saluzzo *et al.*, 2017) and basophils to imprint the identity of developing TR-AMs (Cohen *et al*, 2018) While not essential during fetal development, ILCs are another source of GM-CSF at steady state, supporting the maintenance of adult TR-AMs (Gschwend *et al.*, 2021a).

At steady-state i.e in the absence of infection, TR-AMs are kept in an immunosedated or low-reactive state by several inhibitory regulators to prevent inflammatory exacerbation in response to the constant environmental antigens they are presented with (Hussell & Bell, 2014b; Kulikauskaite & Wack, 2020). While a prime function of TR-AMs is to recycle and clear away excess surfactant, **pulmonary surfactants** themselves are critical regulators of AM function (Hussell & Bell, 2014b). A key function of TR-AMs is to surveil the airways (Neupane *et al*, 2020), which they perform by crawling along the luminal surface, directed by the actin

cytoskeleton. This function is regulated by surfactant protein A (SP-A) along with the complement C5a (Janssen *et al*, 2008; Neupane *et al.*, 2020), which directs the migration of TR-AMs through the pores of Kohn, permitting them to move between alveoli. Furthermore, SP-A and surfactant protein D (SP-D), bind to TR-AMs and regulate their immune activity by blocking the activation of Toll-like receptors (TLRs) on AMs at steady-state, which are responsible for detecting pathogen-associated molecular patterns (PAMPs) and initiating inflammatory responses (Gardai *et al*, 2003; Janssen *et al.*, 2008; Yamada *et al*, 2006). By inhibiting TLR signaling, these surfactant proteins ensure that AMs do not become hyper-activated in response to non-threatening stimuli, preserving the delicate balance of immune tolerance within the lungs (Gardai *et al.*, 2003; Haczku, 2008). Several cytokines and regulatory proteins fine-tune AM function and identity, helping maintain the low-reactive state and preventing excess inflammation (Hussell & Bell, 2014b). , TGF-β a potent immunoregulatory factor present in mouse and human lungs during homeostasis (Coker *et al*, 1996) and activated by αvβ6 integrin expressed by alveolar epithelial cells, ensures the maintenance of lung integrity (Meliopoulos *et al*, 2016). Loss of activated TGF-B as observed in studies where Itgb6 (gene encoding integrin B6) is deleted, resulting in the excess production matrix metalloproteinase-12 (MMP12) by dysfunctional AMs leading to lung emphysema and local inflammation, which can be corrected by over expression of TGF-β (Morris *et al*, 2003). TGF-β is crucial for the development and function of alveolar macrophages (AMs) through both autocrine and paracrine mechanisms involving TGF-β receptor (TGF-βR) expression and signaling on tissue-resident alveolar macrophages (TR-AMs). In mice, research has demonstrated that removing TGF-βR on AMs interferes with their proper development (Yu *et al*, 2017). Disruption in TGF-BR signaling also hinders GMCSFR expression, thereby further impacting AM maturation, however the precise interaction of these pathways remains unclear. TGF-β also appears to regulate the expression of **CD200R1**, an inhibitory receptor expressed on TR-AMs, that is essential for maintaining the activation threshold of AMs (Snelgrove *et al*, 2008). Consistent with this, the loss of TGF-β has also been shown to cause spontaneous production of pro-inflammatory cytokines by TR-AMs (Morris *et al.*, 2003). Similarly, **Interleukin-10 (IL-10)**, a key anti-inflammatory cytokine, regulates TR-AM responses via IL-10R which is expressed on both mouse and human alveolar macrophages (Fernandez *et al*, 2004; Lim *et al*, 2004). IL-10 binding on IL-10R activates the Janus kinase 1 (JAK1)-signal transducer and activator of transcription 3 (STAT3) pathway. This in turn activates key downstream genes including suppressor of cytokine signaling 3 (SOCS3), which plays a critical role in blocking pro-inflammatory signaling. SOCS3 inhibits cytokine receptors and dampens TLR signaling, preventing the release of pro-inflammatory mediators such as TNF and IL-6, ensuring that AMs remain in a low-reactive state during homeostasis, preventing chronic inflammation in the lungs (Fernandez *et al.*, 2004; Murray,

2006). Alveolar macrophages are carefully controlled by various environmental signals and pathways to keep their immune activity balanced. Molecules like TREM2, MARCO, CD200R, IL-10, SOCS3, GM-CSF, PPARγ and TGF-β work together to prevent unnecessary inflammation and maintain lung health (Branchett *et al*, 2021; Gao *et al*, 2013; Ghosh *et al*, 2011; Gschwend *et al.*, 2021a; Rooijen *et al*, 2019). These mechanisms allow macrophages to clear pathogens and debris without overreacting and damaging lung tissue. Understanding how these pathways regulate immune tolerance is vital for developing treatments for lung diseases where this balance is disrupted (Bain & Macdonald, 2022; Hussell & Bell, 2014b).

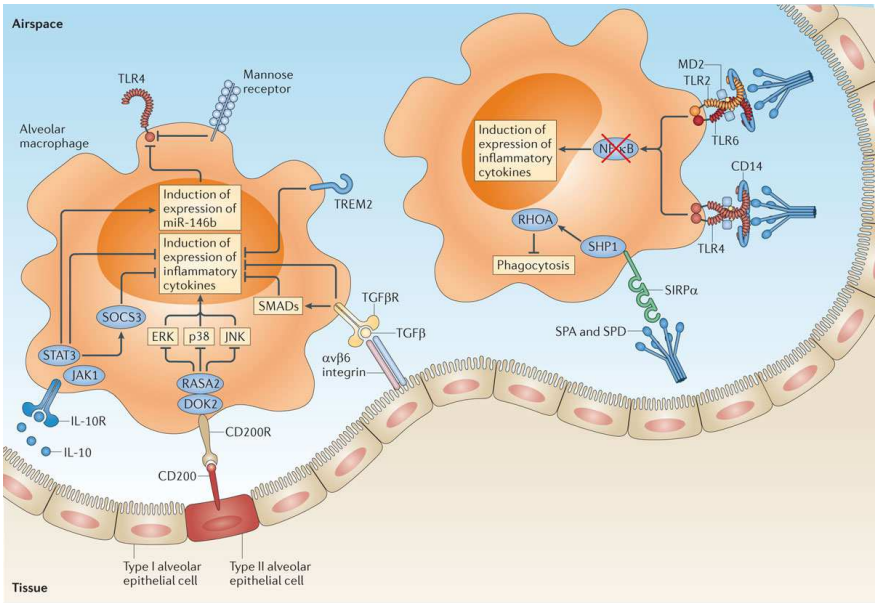

Thesis Figure 10: Regulation of alveolar macrophage identity and function
Regulation of alveolar macrophages by IL-10, TGFβ, TREM2, mannose receptor, CD200R, and surfactant proteins. Illustration from (Hussell & Bell, 2014b)

1.2.6 Alveolar macrophages during inflammation

Upon inflammation, TR-AMs can rapidly switch from their homeostatic role to an activated state, becoming essential orchestrators of the lung's innate immune defense (Ghosh *et al.*, 2011; Kopf *et al.*, 2015). They identify pathogen-associated molecular patterns (PAMPs) through pattern recognition receptors (PRRs), triggering an immediate and robust inflammatory response. Upon activation, AMs release a myriad of pro-inflammatory cytokines such as TNF-α, IL-1β, and type I interferons (IFNs) (Cakarova *et al*, 2009; Kumagai *et al*, 2007; Zahalka *et al*, 2022). This leads to the activation and recruitment of other immune cells like neutrophils, monocytes, and dendritic cells (DCs), T cells to the infection site, thereby amplifying the inflammatory response (Branchett *et al*, 2020; Grant *et al*, 2021; Westphalen *et al.*, 2014). TR-AMs are especially important during bacterial infections, such as pneumococcal pneumonia, where they coordinate the innate immune response to contain and clear the pathogen effectively. When the pathogen load is moderate, AMs can clear the pathogen, as

seen with low doses of *Streptococcus* pneumoniae (Knapp *et al*, 2003). When the pathogen burden exceeds their phagocytic capacity, they further upregulate chemokine production to further mobilize other immune cells (Aberdein *et al*, 2013). Once the inflammatory phase is under control, AMs transition into a resolutory phenotype, releasing anti-inflammatory agents like TGF-β, IL-1 receptor antagonist (IL-1RA), and prostaglandins to help calm the immune response (Hussell & Bell, 2014b). This shift helps restore lung homeostasis, preventing chronic inflammation. However, disruptions in regulatory signals can cause AMs to maintain a pro-inflammatory state, leading to excessive or prolonged immune responses and tissue damage.

1.2.6 Inflammation drives remodeling and repopulation of lung macrophages

While TR-AMs arise from embryonic derived precursors, studies have shown that bone-marrow derived monocytes can differentiate into bona-fide alveolar macrophages when provided with the required niche factors (van de Laar *et al.*, 2016). Therefore, while TR-AMs are long-lived cells, capable of self-renewing at steady state in the lungs with minimal contribution from monocytes, acute inflammation and severe injury or infection, leads to the loss of TR-AMs, a phenomenon referred to as the 'macrophage disappearance reaction' (Aegerter *et al.*, 2022; Barth *et al*, 1995). The cause of this depletion of TR-AMs remains elusive with several potential mechanisms proposed. TR-AMs may either become directly infected and undergo cell death, encounter pro-apoptotic signals from other dying immune cells or lose critical survival signals from injured epithelial cells that are needed for their maintenance in the alveoli or airway. Alternatively, damage to epithelial cells could also cause TR-AMs to become detached and cleared away. One theory in the field proposes that given their efferocytotic role and pro-repair propensity to promote a low-reactive anti-inflammatory state in the lungs, TR-AM may hinder the initial inflammatory response necessary to control an acute infection, making this disappearance an evolutionary feature that allows acute inflammation and effective pathogen clearance to ensue (Aegerter *et al.*, 2022; Bain & Macdonald, 2022; Malainou *et al*, 2023). A similar pattern is observed in human infections, including severe acute respiratory syndrome coronavirus 2 (SARS-CoV-2), where a marked reduction of TR-AMs is observed – although the exact trigger – direct infection or disruption of epithelial-TR-AM signals- remains unclear (Bailey *et al*, 2024; Chen *et al*, 2022b). Given this loss of TR-AMs, the lungs must quickly restore the alveolar macrophage population to ensure efficient gas exchange and maintain tissue integrity and function. Repopulation of the TR-AM population occurs through either local proliferation of the remaining TR-AMs (Jenkins *et al*, 2011; Minutti *et al*, 2017) or by the recruitment of monocytes that differentiate into macrophages to replace the lost population (Aegerter *et al*, 2020; Misharin *et al*, 2017) . When the injury is mild, as in the case of low dose LPS exposure, TR-AMs replenish themselves

through local proliferation during the recovery phase (Liu *et al*, 2019; Zahalka *et al.*, 2022). However, in the case of severe injury or infection – such as those caused by bleomycin-Induced lung injury and viral infections such as influenza, SARS-CoV-2 and gamma herpesvirus, bone-marrow derived monocytes, are recruited into the lungs to help aid the immune response, where they can differentiate into **monocyte-derived alveolar macrophages (Mo-AMs).** These recruited cells may take up residence in the tissue and add to the pool of long-term tissue resident macrophages (Thesis Figure 11). (Aegerter *et al.*, 2020; Li *et al*, 2022; Machiels *et al*, 2017; Misharin *et al.*, 2017; Wendisch *et al*, 2021).

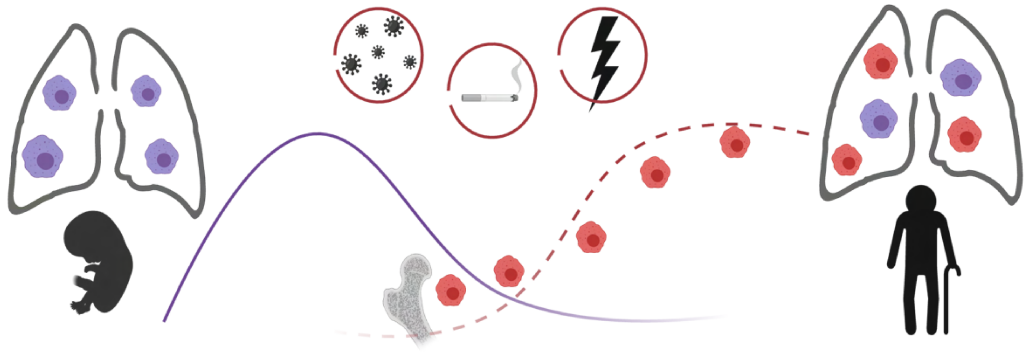

Thesis Figure 11: Inflammation drives remodeling of the lung macrophages compartment
Fetal-derived macrophages seed he lung early in life and self-renew. External perturbations remodel the macrophage composition and monocytes from the bone marrow become monocyte-derived alveolar macrophages and contribute the lung macrophage composition which becomes of heterogenous ontogeny over time and age. Based on (Morales-Nebreda *et al.*, 2015)

Recruited monocytes differentiate into macrophages in the lung

Monocytes develop in the bone marrow from common myeloid progenitors (CMPs) and are released into the bloodstream, poised to respond to tissue signals at steady state and upon inflammation (Guilliams *et al*, 2018; Van Furth & Cohn, 1968). They are subdivided into two broad subsets – classical monocytes ($Ly6C^{hi}$ CX_3CR1^{lo} in mice; CD14+ CD16- in humans) and non-classical monocytes ($Ly6C^{lo}$ CX_3CR1^{hi} ; CD14- CD16+) (Geissmann *et al*, 2003; Ziegler-Heitbrock, 2007). Classical monocytes contribute to the macrophage pool at steady state and are rapidly mobilized to tissues during the early phases of inflammation, whereas non-classical monocytes patrol blood vessels and help maintain tissue integrity (Auffray *et al*, 2007). Monocytes are present in the lung even under steady-state conditions. The majority of these consist of intravascular monocytes travelling through the pulmonary blood vessels, however some monocytes have been found to actively traverse the lung tissue without differentiating into macrophages. Monocytes are essential for transporting antigen to lymph nodes,

producing pro-inflammatory cytokines and anti-microbial compounds as well as serving as precursors that can differentiate into macrophages (Shi & Pamer, 2011). While macrophages in some tissues such as the gut are continuously replenished by monocytes at steady-state, alveolar macrophages see minimal contribution (Bain *et al*, 2014; Hashimoto *et al.*, 2013). However, the interstitial macrophage pool is steadily replenished by monocyte-derived cells, with monocytes undergoing a proliferative phase as they differentiate into Ims (Vanneste *et al*, 2023). During lung injury or inflammation, monocyte recruitment is amplified and, in some pathologies, also triggers a condition called 'emergency monopoiesis' where there is a rapid increase in monocyte production in the bone-marrow which are then mobilized to the tissue (Swann *et al*, 2024). Upon lung inflammation, there is an increased production of chemokines such as CCL2, CCL7, CCL5 and CCL10 produced by a number of cell types at the site of injury including epithelial and stromal cells (Malainou *et al.*, 2023). These signal through the CCR2 receptor expressed on monocytes in the bone-marrow, which facilitates their egress from the bone-marrow (Tsou *et al*, 2007). Mice lacking CCR2 or CCL2 are unable to effectively control *Streptococcus pneumoniae*, *Klebsiella pneumoniae*, and *Mycobacterium tuberculosis* infections, leading to elevated viral or bacterial loads (Winter *et al*, 2007; Xiong *et al*, 2015; Xiong *et al*, 2016). In models of SARS-CoV-2 and RSV, CCR2 deficiency also results in increased viral burden (Vanderheiden *et al*, 2021). Conversely post influenza infection and in bleomycin-induced lung fibrosis, CCR2-deficient mice show reduced influenza-induced lung damage and lung fibrosis respectively, highlighting the differential role of CCR2+ monocytes in both immune defense and promoting excessive lung pathology, depending on the initial infection or injury (Gibbons *et al.*, 2011; Lin *et al*, 2008).

1.2.7 Function and fate of monocyte-derived alveolar macrophages

Monocyte-derived alveolar macrophages (Mo-AMs), also named as recruited alveolar macrophages (RecAMs) or transient macrophages (TransMacs) (Aegerter *et al.*, 2022; Li *et al.*, 2022), exhibit distinct transcriptional, epigenetic, and functional properties compared to fetal derived TR-AMs. Mo-AMs share surface markers such as CD11c and CD64 with TR-AMs but express slightly lower levels of SiglecF (Bain & Macdonald, 2022), adopting an increasingly similar TR-AM like profile over time **(Thesis Figure 12)**.

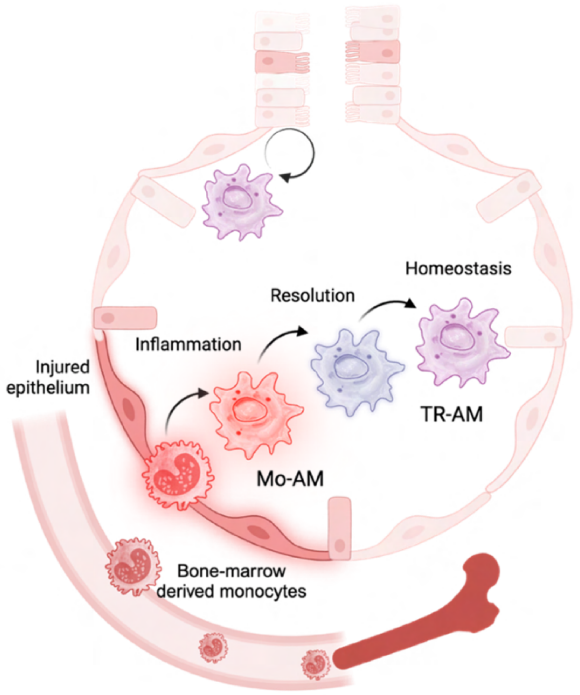

Thesis Figure 12: Monocyte to macrophage differentiation
Bone marrow-derived monocytes differentiate into Mo-AMs that eventually acquire a tissue-resident identity (TR-AM) in the lungs over time.

Function of Mo-AMs

Mo-AMs display a wide range of context dependent functions, which can have both protective and potentially detrimental outcomes, depending on the inflammatory setting. During viral infections such as influenza virus infection (IVI), Mo-AMs contribute significantly to the immune response by producing increased levels of pro-inflammatory cytokines, such as IL-6, to enhance resistance against *Streptococcus pneumoniae* and *Mycobacterium tuberculosis* (Aegerter *et al.*, 2020). They also express Arginase-1, enabling resistance to helminth infections (Chen *et al*, 2022a), and produce amphiregulin to promote tissue repair following injury (Minutti *et al*, 2019). In models of allergic asthma which are triggered by house dust mite exposure, Mo-AMs mitigate type 2 immune responses, thereby regulating inflammation and averting exacerbated responses (Machiels *et al.*, 2017). However, this pro-inflammatory nature of Mo-AMs can be detrimental, as demonstrated during severe COVID-19 infections, where the recruitment of Mo-AMs with a heightened inflammatory profile results in excessive cytokine production, including IL-1, IL-6, and TNF-α. This contributes to extensive lung damage and a ‘cytokine storm’, exacerbating disease severity (Grant *et al.*, 2021). As such, Mo-AMs have emerged as key players during lung injury, particularly in models such as bleomycin or asbestos induced injury. In these models, recruited Mo-AMs adopt a pro-fibrotic phenotype, driving the development of lung fibrosis (Misharin *et al.*, 2017). This pro-fibrotic

phenotype is also seen post severe COVID infection (Chen *et al.*, 2022b; Wendisch *et al.*, 2021). This illustrates that the differentiation and function of Mo-AMs are context-dependent, shaped by the local inflammatory and repair signals they receive upon recruitment (**Thesis Figure 13**).

Fate and differentiation of Mo-AMs

The differentiation and fate of Mo-AMs are determined by a complex interplay between their monocyte origin and the local microenvironment of the lung Mo-AMs have been shown to outcompete TR-AMs (remaining fetal-derived TR-AMs post insult) in repopulating the AM niche and display an increased responsiveness to the inflammatory lung environment (Li *et al.*, 2022). While macrophages are generally considered to exhibit phenotypic and functional plasticity, TR-AMs display limited plasticity in comparison to (van de Laar *et al.*, 2016), Mo-AMs derived from bone marrow precursors, which exhibit greater flexibility and immunoreactivity. This has been attributed to long-term residence in the lung microenvironment which constricts plasticity, conferring a homeostatic low-reactive phenotype instead to TR-AMs (Roquilly *et al*, 2020). Therefore, while Mo-AMs, due to their recent monocytic origin exhibit a high degree of immunoreactivity and adaptability of various functions and form in the lung, with time and residence in the lung, they too gradually adopt a low-reactive steady-state phenotype akin to TR-AMs (Kulikauskaite & Wack, 2020). This shows that while cell ontogeny determines initial reactivity and plasticity, tissue imprinting eventually shapes the long-term phenotype of Mo-AMs, with adoptive transfer experiments providing evidence that the tissue environment can imprint and determine the phenotype of macrophages from different precursors.

When infiltrating monocytes recruited during an inflammatory event differentiate into Mo-AMs, these Mo-AMs initially retain their monocyte-derived epigenetic profile, with open ‘ready-to-go’ chromatin states, which supports their enhanced sensitivity to environmental signals (Kulikauskaite & Wack, 2020). This allows Mo-AMs to rapidly respond to respiratory insults, contributing to their heightened pro-inflammatory capacity. For instance, in response to influenza-A virus, Mo-AMs produce higher levels of TNF-α, inducible nitric oxide synthase (iNOS)-derived NO, and IFN-β, which can promote alveolar damage (Herold *et al*, 2011; Herold *et al*, 2008). This heightened inflammatory state can shift over time; in low-grade sterile injury models, Mo-AMs may transition from a pro-inflammatory to an anti-inflammatory phenotype within days, supporting cell proliferation and tissue repair and adopt a more tissue-resident like phenotype (Pervizaj-Oruqaj *et al*, 2024b). This transition is also seen in models of bleomycin-induced lung injury and house dust mite-induced asthma, where Mo-AMs begin to adopt a phenotype similar to homeostatic TR-AMs as they settle into the lung environment

if resolution occurs, or often become pro-fibrotic if inflammation persists and appropriate resolution does not ensue (Loos *et al*, 2023; McQuattie-Pimentel *et al*, 2021; Misharin *et al.*, 2017) – Thesis Figure 13. The microenvironment plays a critical role in driving this functional trajectory of Mo-AMs. Signals from the alveolar epithelium, cytokines, and damage-associated molecular patterns (DAMPs) influence Mo-AM differentiation and activity, particularly during and post inflammation (Joshi *et al*, 2020; Loos *et al.*, 2023; Watanabe *et al*, 2021). Metabolic factors further shape Mo-AM function (Pervizaj-Oruqaj *et al*, 2024a); glycolysis, a key metabolic pathway, has been shown to influence macrophage polarization. Lactate, a byproduct of glycolysis, can modify histone proteins through lactylation, impacting gene expression and promoting a shift from pro-inflammatory to homeostatic functions over time (Zhang *et al*, 2019). This "lactate clock" mechanism ensures that macrophages eventually adopt a tissue-resolving phenotype, aligning with the low-glucose conditions found in the recovering lung (Woods *et al*, 2020). During acute inflammation, such as influenza infection or lung injury, Mo-AMs initially benefit from increased glucose availability, which supports glycolysis and sustained histone lactylation. This metabolic state facilitates a robust pro-inflammatory response but is gradually downregulated as glucose availability becomes scarce during recovery (Ogger & Byrne, 2021). The reduction of glycolysis and the cessation of glycolysis-driven histone modifications may contribute to the establishment of a less reactive, long-term homeostatic phenotype (Svedberg *et al*, 2019; Wculek *et al*, 2023). These metabolism-driven epigenetic modifications may be crucial for the functional adaptation of Mo-AMs as they transition to TR-AM-like cells (Pervizaj-Oruqaj *et al.*, 2024a). Therefore, while the origin of macrophages plays a role in defining their initial responsiveness, the signals encountered during differentiation, including metabolic cues, cytokines, cell-cell interactions and environmental factors significantly shape the long-term function of Mo-AMs. Determining the extent to which both ontogeny and cell intrinsic mechanisms and the extrinsic tissue imprinting of the microenvironment determine phenotype and function of lung macrophages in different respiratory pathologies remains an important area of research (Pervizaj-Oruqaj *et al.*, 2024a).

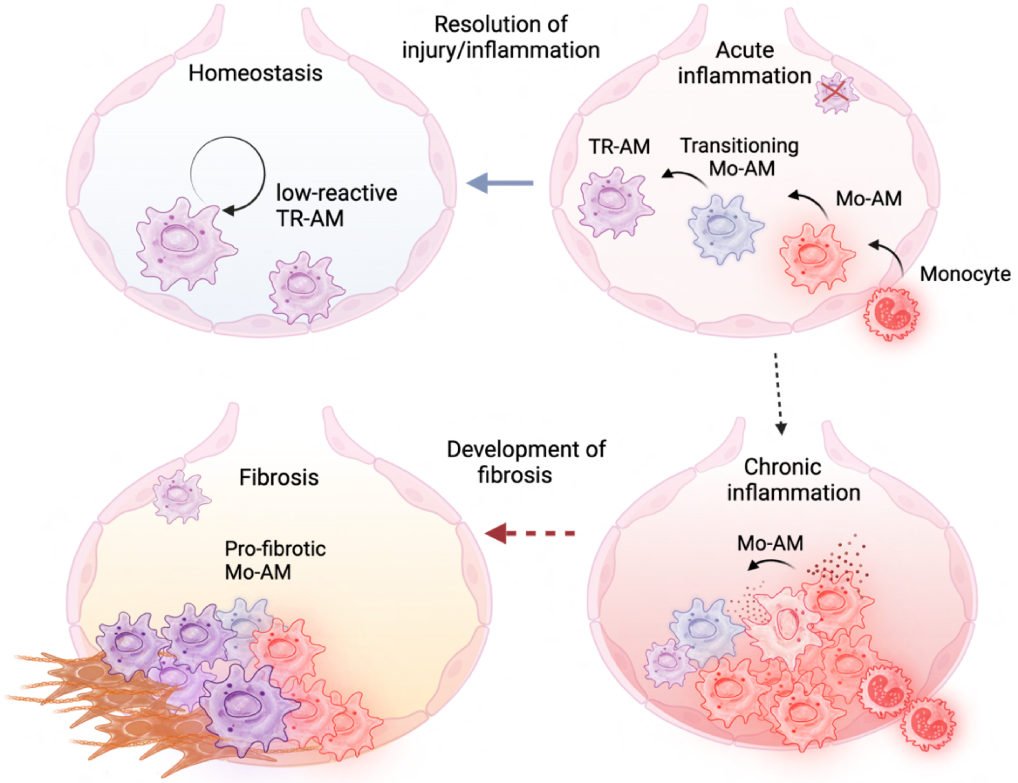

Thesis Figure 13: Mo-AM fate in inflammation and fibrosis

At baseline, low-reactive TR-AMs self-renew. During inflammation, monocytes differentiate into Mo-AMs. If resolution is effective, Mo-AMs transition into homeostatic TR-AMs, restoring homeostasis. In severe or prolonged inflammation, inflammatory Mo-AMs persist and can become pro-fibrotic.

1.2.8 Monocyte-derived macrophages are key profibrotic drivers in lung fibrosis

In section 1, the general roles of macrophages were described. Here, we will look at the role of lung macrophages, including AMs, IMs and Mo-AMs and their response to lung injury and fibrosis (Chakarov *et al*, 2019; Minutti *et al.*, 2017; Misharin *et al.*, 2017; Ogger *et al*, 2020; Sabatel *et al*, 2017). AMs being the first line of defense, rapidly respond to injury by releasing cytokines and growth factors to initiate repair and maintain alveolar integrity. During acute lung injury, AMs secrete factors such as PDGF, VEGF, and fibroblast growth factor (FGF), insulin-like growth factor (IGF)-1 to promote the proliferation and repair of alveolar epithelial cells (AECs) (Minutti *et al.*, 2019; Mu *et al*, 2020). Additionally, amphiregulin and epiregulin, produced by AMs, are crucial for tissue regeneration by activating epithelial growth factor receptors (EGFR) on AECs, ensuring the maintenance of the epithelial barrier (Meng *et al*, 2020; Minutti *et al.*, 2019). CCR2+ monocytes and differentiated Mo-AMs which are recruited during injury a exhibit metabolic and transcriptional profile that supports tissue repair (Lechner *et al.*, 2017). Their differentiation is influenced by signals such as IL-4 and IL-13 from innate lymphoid cells (ILC2s), which act through IL4Rα on macrophages to promote an anti-

inflammatory, pro-repair phenotype (Loos *et al.*, 2023; Minutti *et al.*, 2017). IL-33 receptor positive (ST2+) Mo-AMs, respond to IL-33 which is derived from epithelial cells and adopt an alternatively activated state. IL-13 then further drives Mo-AM maturation, promoting tissue regeneration (Dagher *et al*, 2020). A key feature of macrophage-mediated repair is their ability to interact with epithelial cells to coordinate wound healing. Early pro-inflammatory signals, such as TNF-α from recruited macrophages, can induce AECs to produce GM-CSF, reinforcing epithelial proliferation (Cakarova *et al.*, 2009). Mo-AMs also transition to pro-repair phenotypes marked by the production of growth factors essential for restoring vascular and epithelial integrity (Pervizaj-Oruqaj *et al.*, 2024a). In the context of severe lung injuries, such as those caused by viral infections, the IFN-dependent TRAIL pathway can induce apoptosis of infected and bystander AT1s, complicating the repair process (Herold *et al.*, 2008). However, macrophages can counteract these effects by expressing amphiregulin, which then induces TGF-β activation in pericytes to support vascular repair (Minutti *et al.*, 2019). Mo-AMs initially recruited during acute inflammation often display a pro-inflammatory profile, producing cytokines such as TNF-α and IL-1β. However, these cells gradually shift to a reparative state through metabolic and epigenetic modifications, such as lactate-driven histone acetylation which then induces the expression of genes promoting tissue homeostasis (Herold *et al.*, 2011). In human acute lung injury, this shift helps achieve resolution without fibrosis, as macrophages facilitate the timely clearance of apoptotic cells and secrete anti-inflammatory cytokines like IL-10 (Chung *et al*, 2007; Grabiec & Hussell, 2016).

When lung injury leads to prolonged or dysregulated repair, this can result in the development of fibrosis (Wynn & Vannella, 2016). Lung macrophages, particularly Mo-AMs, play a pivotal role in driving fibrosis (Joshi *et al.*, 2020; Misharin *et al.*, 2017) and activating fibroblasts. These recruited macrophages often differentiate into profibrotic phenotypes under the influence of local signals such as TGF-β, IL-4, IL-13, and IL-33, IL-17 as well as chemokines like CCL2 and CXCL12. CCR2+ monocytes are typically the precursors of profibrotic Mo-AMs, which then differentiate into and are maintained as Mo-AMs, through signaling pathways involving M-CSF and GM-CSF (Fabre *et al.*, 2023; Gibbons *et al.*, 2011; Joshi *et al.*, 2020). In both animal models and human fibrosis studies, including idiopathic pulmonary fibrosis (IPF) and COVID-19-associated lung injury, these macrophages have been identified as key players in this fibrotic process. (Aran *et al*, 2019; Bailey *et al.*, 2024; Bhattacharyya *et al*, 2022; Chen *et al.*, 2022b; Fabre *et al.*, 2023). Furthermore, a macrophage subset, expressing CX3CR1 and moderate levels SiglecF, indicating a transitional state between Mo-AM and bona fide TR-AMs was found to localize around fibrotic niches and promotes fibrosis (Aran *et al.*, 2019). Human studies have confirmed that these transitional macrophages show upregulated gene expression in idiopathic pulmonary fibrosis (IPF) and share conserved features across organs

(Fabre *et al.*, 2023). Interstitial macrophage subsets which have been identified across tissues such as the lung, fat, heart, and skin include LYVE1^{lo}MHCII^{hi}CX3CR1^{hi} and LYVE1^{hi}MHCII^{lo}CX3CR1^{lo} populations. The LYVE1^{hi}MHCII^{lo}CX3CR1^{hl} subset has been shown to have a protective role by mitigating fibrosis progression in mouse models (Chakarov *et al.*, 2019). In COVID-19, pro-fibrotic Mo-AMs in bronchoalveolar lavage (BAL) fluid expressed markers such as CD163, CD206, Lyve1 which are also associated with IMs and fibrosis-associated genes like TGF-β and legumain, suggesting the possibility of monocytes differentiating into an IM-like state before entering the alveoli and becoming pro-fibrotic macrophages (Wendisch *et al.*, 2021).

Fibrosis-associated AMs and Mo-AMs express high levels of profibrotic mediators such as TGF-β, PDGF, osteopontin (SPP1), and YKL-40 (CHI3L1), which can activate myofibroblasts and promote collagen production, a signature also found in human studies (Reyfman *et al*, 2019). The presence of macrophages producing osteopontin (SPP1) and MMP9 has been observed in the lungs of IPF patients, indicating their direct involvement in the remodeling of lung tissue (Morse *et al*, 2019). These cells fuel a fibrotic environment by interacting with transitional AECs (alveolar differentiation intermediates) that express high levels of keratin 8 (KRT8) and CCL2, forming a feedback loop that in turn recruits and activates more Mo-AMs (Strunz *et al.*, 2020) and preventing effective lung regeneration. Fibrosis is further exacerbated by macrophages' metabolic adaptations. Increased glycolysis in Mo-AMs supports ROS production and enhances their fibrotic potential via the IL-1β–HIF-1α axis, whereas blockade of HIF1-a in alveolar macrophages prevents fibrosis formation by decreasing levels TGF-B1 secretion (Ueno *et al.*, 2011). In contrast, defects in the itaconate pathway, which has been shown to have antifibrotic properties in lung macrophages, can exacerbate fibrogenesis (Ogger *et al.*, 2020). The regulation of these metabolic pathways underscores the complex nature of macrophage-mediated fibrosis, where both pro-resolving and pro-fibrotic roles coexist depending on the context and the balance of local lung signals (Ogger & Byrne, 2021). Genetic studies have highlighted the role of transcription factors such as C/EBPβ and EGR2 in the differentiation and function of profibrotic Mo-AMs. For example, deletion of C/EBPβ reduced bleomycin-induced fibrosis in mice by limiting monocyte-to-macrophage differentiation (Satoh *et al.*, 2017).Conversely, EGR2 was shown to be essential for the transition of recruited Mo-AMs to a pro-resolution phenotype during fibrosis regression (McCowan *et al*, 2021). The loss of these transcriptional regulators can shift the macrophage response from fibrotic to reparative, illustrating potential therapeutic targets for modulating macrophage behavior in fibrotic lung diseases. Human data also point to the therapeutic potential of targeting macrophage-associated pathways. For instance, inhibition of M-CSF signaling, and the use of TGF-β1-siRNA encapsulated in mannosylated nanoparticles have

shown promise in reducing fibrosis severity (Singh *et al*, 2022). Additionally, folate-linked TLR7 agonists have been developed to reprogram pro-fibrotic macrophages into anti-fibrotic phenotypes, effectively reducing pro-fibrotic cytokine production and collagen deposition in mouse models (Zhang *et al*, 2020). In conclusion, while lung macrophages play essential roles in injury repair, their maladaptive responses can drive fibrotic processes when repair mechanisms become chronic or dysregulated. The intricate balance between pro-repair and pro-fibrotic activities highlights the need for targeted therapies that modulate macrophage behavior to promote resolution and prevent fibrosis (Wynn & Vannella, 2016).

1.2.9 The alveolar macrophage compartment evolves over time and age

Fetal derived alveolar macrophages seed the lung early during embryonic development and self-renew under homeostatic conditions. However, aging profoundly impacts their phenotype and function. Studies in aged mice have shown that aging AMs display an inflammatory profile, with upregulated expression of pro-inflammatory cytokines such as IL-6, IL-1β, and TNF-α (Boe *et al*, 2022; McQuattie-Pimentel *et al.*, 2021). These changes often coincide with downregulated PPARγ signaling, contributing to an altered, inflammation-prone environment (Angelidis *et al*, 2019). Aged AM's display a reduced phagocytic and efferocytic capacity which then contributes to furthering this inflammatory state, resulting in a diminished ability to clear apoptotic cells and mitigate inflammation effectively (Wong *et al*, 2017). In aged mouse lungs, AMs exhibit significant transcriptional changes, including reduced expression of cell cycle genes and markers of proliferation, such as Ki67 (McQuattie-Pimentel *et al.*, 2021). Similar age-related changes in have also been observed in humans, with AMs derived from elderly individuals also showing reduced expression of cell adhesion and proliferation markers and a pro-inflammatory shift, characterized by increased production of TNF-α and IL-6 (Duong *et al*, 2021).These findings suggest that, with age, AMs become less effective in their regulatory and reparative functions, contributing to an increased susceptibility to respiratory infections and chronic lung conditions. The aging pulmonary environment has a significant impact on the function and phenotype of lung macrophages. When aged AMs were transferred into young mice, they displayed a young phenotype. In-vivo intratracheal GM-CSF administration to young and aged mice resulted in an increased AM proliferation in young mice and this response was absent in aged mice, and aged AMs did not upregulate cell-cycle genes (McQuattie-Pimentel *et al.*, 2021). However, they found no differences in GM-CSFR or signaling in aged AMs in comparison to young AMs. Instead, they found that aged lungs had increased levels of hyaluronan in the alveolar lining fluid, which then contributed to reduced proliferation of bone marrow-derived macrophages in response to GM-CSF when cultured on extracellular matrix proteins (McQuattie-Pimentel *et al.*, 2021). As the lung experiences repeated environmental challenges—such as viral infections, pollution, and cigarette smoke—

over a lifespan, the balance between tissue-resident AMs and recruited Mo-AMs shifts (Morales-Nebreda *et al.*, 2015). Studies using genetic lineage tracing in Ms4a3Cre-RosaTdT mice have shown that while blood monocytes are efficiently labeled from birth, tissue-resident macrophages (RTMs), including AMs, gradually show increased tdTomato labeling with age, indicating a shift towards bone marrow-derived cell replacement. By 36 months, AMs in the lungs are largely replaced by monocyte-derived alveolar macrophages (Mo-AMs) from the bone marrow, demonstrating a notable shift in the composition of the macrophage population over time (Liu *et al.*, 2019) (**Thesis Figure 14**).

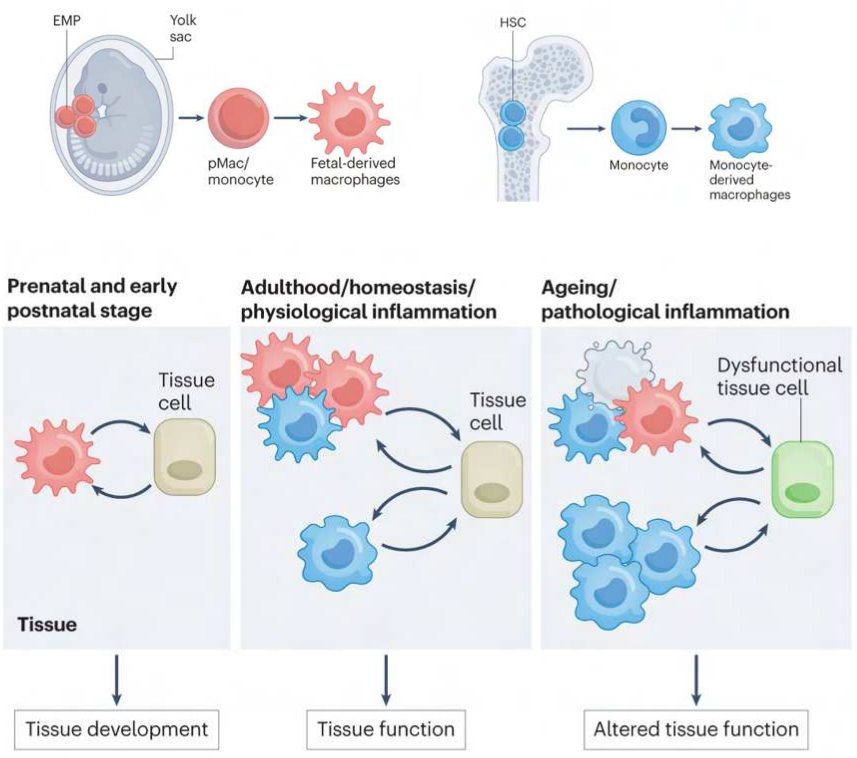

Thesis Figure 14: The ontogeny of lung macrophages over life.
Fetal derived macrophages seed the lungs early in life and maintain homeostasis. With every inflammatory exacerbation, Mo-AMs from the bone marrow infilitrate leading to a heterogenous ontogeny in the lungs. With age, there is increasing replacement and dysfunction in the alveolar macrophage compartment. Illustration modified from (Mass *et al*, 2023)

As lung macrophages evolve over time and with age, many open questions remain about how these changes influence repair and lung fibrosis. In humans, acute and chronic lung diseases such COVID-19 and IPF disproportionately affect older individuals and are associated with the progressive recruitment and persistence of monocyte-derived alveolar macrophages (Mo-AMs) with pro-inflammatory and fibrotic profiles (Bailey *et al.*, 2024). Studies suggest that the continual replacement of tissue-resident AMs by Mo-AMs may contribute to age-related changes in lung health, highlighting the role of macrophage ontogeny and the reshaping of the

lung macrophage compartment during lung health and aging (Aegerter *et al.*, 2022; Guilliams *et al*, 2020).

Age is the strongest risk factor for lung fibrosis, yet the mechanisms driving this susceptibility remain incompletely understood. Aging affects multiple biological processes and in the final section of the introduction, we will explore some of these fundamental aspects of aging biology and provide an overview of what is currently known about the role of aging in lung fibrosis.

1.3 Mechanisms of aging

Homeostatic regeneration and repair are fundamental biological processes crucial for sustaining life and ensuring the maintenance of tissue integrity (McKinley *et al*, 2023). Aging represents a significant breakdown in these vital processes, ultimately compromising organ function (López-Otín *et al.*, 2023). Aging stands as the dominant risk factor for the development of many chronic diseases associated with mortality in adults. By 2050, the global demographic is projected to shift, with adults over the age of 65 accounting for 20% of the population, i.e over 2 billion individuals -a three-fold increase (Dzau *et al*, 2019). Given that aging is associated with increased vulnerability to conditions such as cancer, cardiovascular disease, respiratory illnesses, and dementia, this population shift calls for pressing healthcare and socioeconomic solutions (Kennedy *et al*, 2014).

1.3.1 Hallmarks of aging

Aging can be defined (at least in a mechanistic sense) as a progressive decline of physiological processes over time, that occurs at the organ, tissue, cellular and molecular levels. This decline leads to the loss of tissue integrity and function, resulting in a breakdown of homeostasis and health, ultimately culminating in an increased vulnerability to death (Kinzina *et al*, 2019; López-Otín *et al*, 2013). In the past decade, a significant effort has been made to identify and categorize the molecular and cellular changes that drive aging, which are now recognized as the '**hallmarks of aging'**, first defined by López-Otin in 2013 and updated in 2023 (López-Otín *et al.*, 2013, 2023) (**Thesis Figure 15).** These hallmarks of aging are identified based on their progressive development with time and age, their capacity to intensify aging when exacerbated experimentally, and their potential to be slowed down, stopped, or reversed through targeted therapeutic interventions. The hallmarks of aging encompass molecular, cellular, and systemic features: genomic instability, telomere shortening, epigenetic changes, impaired proteostasis, disrupted macroautophagy, alterations in nutrient-sensing, mitochondrial dysfunction, cellular aging (senescence), stem cell dysfunction, altered cell-to-cell communication, **chronic inflammation (inflammaging**) (Franceschi *et al*, 2000), and dysbiosis. Each hallmark influences the other further, highlighting the complex and systemic nature of the aging process.(López-Otín *et al.*, 2013, 2023).

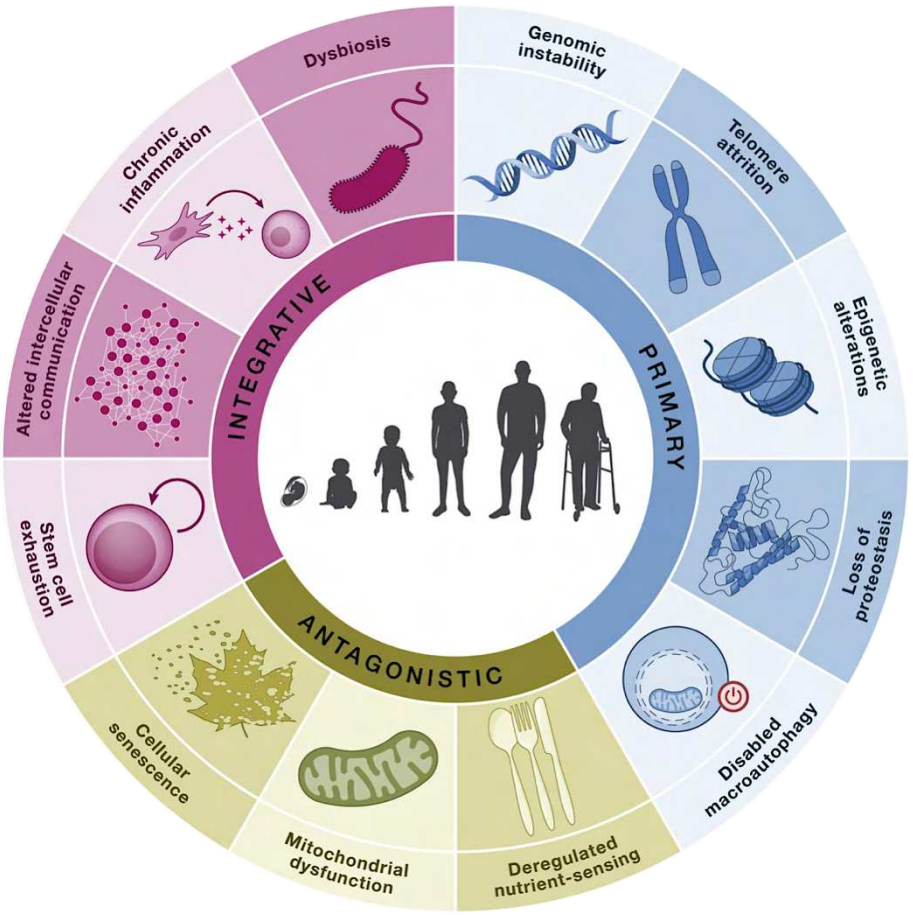

Thesis Figure 15: Hallmarks of aging
Aging manifests because of 12 key processes that have been categorized as the hallmarks of aging. Illustration from (López-Otín *et al.*, 2023)

1.3.2 Chronic inflammation and inflammaging

With age there is a systemic elevation of low-grade, unresolved inflammation that occurs in the absence of pathogens or acute injury, a phenomenon known as **inflammaging** (Franceschi *et al.*, 2000). Inflammaging is characterized by a marked increase in the levels of pro-inflammatory cytokines and factors such as IL-1β, IL-6, IL-8, and TNF-α, C reactive protein (CRP), serum amyloid A and fibrinogen and the chronic activation of the innate immune system (Bruunsgaard *et al*, 2003; Cesari *et al*, 2004; Cohen *et al*, 1997; Ferrucci *et al*, 2010; Gerli *et al*, 2001; Newman *et al*, 2016) (**Thesis Figure 16**). This elevated production of pro-inflammatory factors found in the blood and tissues is a biomarker of advancing age and is a strong predictor of chronic disease, cognitive decline, frailty and death (Dugan *et al*, 2023; Ferrucci & Fabbri, 2018). Inflammaging therefore is a key hallmark of human aging (López-Otín *et al.*, 2023) and determines how effectively the immune system can respond to infections and vaccinations (Mogilenko *et al*, 2021). Although inflammatory activity is heightened, the

immune response itself becomes ineffective and has a suppressed capacity of mounting an effective immune response to pathogens and newly encountered antigens (Ferrucci & Fabbri, 2018; Mittelbrunn & Kroemer, 2021). Due to its systemic impact, inflammaging, is often associated with multimorbidity in elderly individuals, influencing and potentiating the onset of a number of diseases including cardiovascular diseases, cancer, osteoporosis, dementia etc. (Furman *et al*, 2019). Inflammaging derives from the cellular and molecular damage from all the **other hallmarks** that cumulatively typify aging (López-Otín *et al.*, 2023). For instance, *genomic instability* induces inflammatory responses as nuclear and mitochondrial DNA enter the cytosol and activate DNA sensors. Subsequently when autophagy fails to clear this misplaced DNA effectively, it further exacerbates inflammation (Miller *et al*, 2021). Genomic instability also contributes to *clonal hematopoiesis of indeterminate* potential (CHIP), an age-associated expansion of hematopoietic stem cell clones, particularly myeloid cells with pro-inflammatory profile (Jaiswal *et al*, 2017). Increased *cellular senescence*, another key feature of aging is the accumulation of non-dividing cells in tissues as they age, particularly affecting fibroblasts and immune cells (Gorgoulis *et al*, 2019). It is often triggered by DNA damage, telomere shortening, oxidative stress, and infections (Blasco, 2005; Xu *et al*, 2022) and is a cardinal signature of chronic damage. Additionally, secondary or paracrine senescence can be induced by external inflammatory and fibrotic mediators such as CCL2, IL-1β, IL-6, IL-8, and TGF-β. Clearing of senescent cells has been shown to extend both the health and lifespan in experimental models (murine, zebrafish) and current research is focused on exploring the therapeutic potential of senolytics in humans (Chaib *et al*, 2022). Under homeostatic conditions cellular senescence is an essential part of normal tissue repair mechanisms as well as serving as an evolutionary protective mechanism against cancer. It involves two main processes: initiating the senescent state and recruiting immune cells to clear these cells, aiding tissue regeneration. However, when these processes falter, as is observed with aging, the risk of disease development increases (Vicente *et al*, 2016). Cellular senescence is not merely a halt in cell proliferation; it is marked by the development of a complex and multifaceted phenotype known as the senescence-associated secretory phenotype (SASP) (Coppé *et al*, 2010) (Campisi & D'Adda Di Fagagna, 2007). A defining feature of SASP is the increased secretion of pro-inflammatory molecules, including cytokines, chemokines, proteases, and growth factors. This secretory profile contributes to inflammation within the tissue microenvironment and can have profound effects on both the cells themselves and the surrounding tissues (Suryadevara *et al*, 2024). SASP is considered to be a form of molecular inflammation that not only sustains the senescent state but also promotes paracrine senescence, immune modulation, and creates a pro-tumorigenic environment (Campisi, 2013; Coppé *et al.*, 2010). While the immune system plays a crucial role in identifying and clearing senescent cells, it can be adversely affected by prolonged exposure to SASP itself (Ovadya *et al*, 2018). This results

in immunosenescence, a state in which immune function is impaired thereby diminishing the body's ability to respond effectively to infections and diseases (Fulop *et al*, 2018). The accumulation of senescent cells and the persistent secretion of SASP promote a cycle of inflammation and tissue damage, which in turn accelerates aging and the progression of age-related disorders (Ovadya *et al.*, 2018). Overall, SASP is a key feature of inflammaging and its impact on immune function, tissue health, and systemic inflammation underscore its role in driving age-related pathologies (Franceschi & Campisi, 2014; Furman *et al.*, 2019). Therefore mitigating the detrimental effects of SASP is said to be a critical therapeutic avenue aimed at reducing chronic inflammation and improving health in older adults (Campisi *et al*, 2019). At a macro-level, a lifetime of exposure to antigenic challenges, oxidative stress, imbalances in gut microbiota, onslaught of injuries and infection -compounded with varying lifestyle factors such as high-fat diets, increased central adipose accumulation etc – cumulatively contribute to increased systemic inflammation (López-Otín *et al.*, 2023). Within tissues, over time, foreign pathogens, the accumulation of cellular debris, and damage-associated molecular patterns (DAMPs) from dying further increase the pro-inflammatory milieu. This leads to sustained recognition by and activation of TLRs leading to heightened inflammatory responses, innate immune memory, or trained immunity of innate immune cells eventually culminating in aberrant and heightened responses to subsequent insult over time. With age there is an increase in hyperinflammatory monocytes that release excess amounts of TNFα, IL-1β, and IL-6 under basal conditions, a decrease in the number of NK cells as well as an accumulation of differentiated memory T cells that secrete various pro-inflammatory cytokines (Krishnarajah *et al*, 2021; Mittelbrunn & Kroemer, 2021). The aging of hematopoietic stem cells (HSCs) is central to the process of immunosenescence, where the immune system's efficiency diminishes over time. As HSCs age, they produce increasingly dysfunctional immune cells, driving the progression of Immunosenescence (Nogalska *et al*, 2024). This process is further accelerated by chronic inflammation, which reduces the self-renewal capacity of HSCs and hastens their decline. Studies in mice have shown that exposure to inflammatory signals during early and mid-life can lead to age-associated changes in hematopoiesis. These include reduced blood cell counts, bone marrow cytopenia, and the accumulation of adipocytes in the bone marrow—key features of aging-related hematopoietic decline (Bogeska *et al*, 2022).

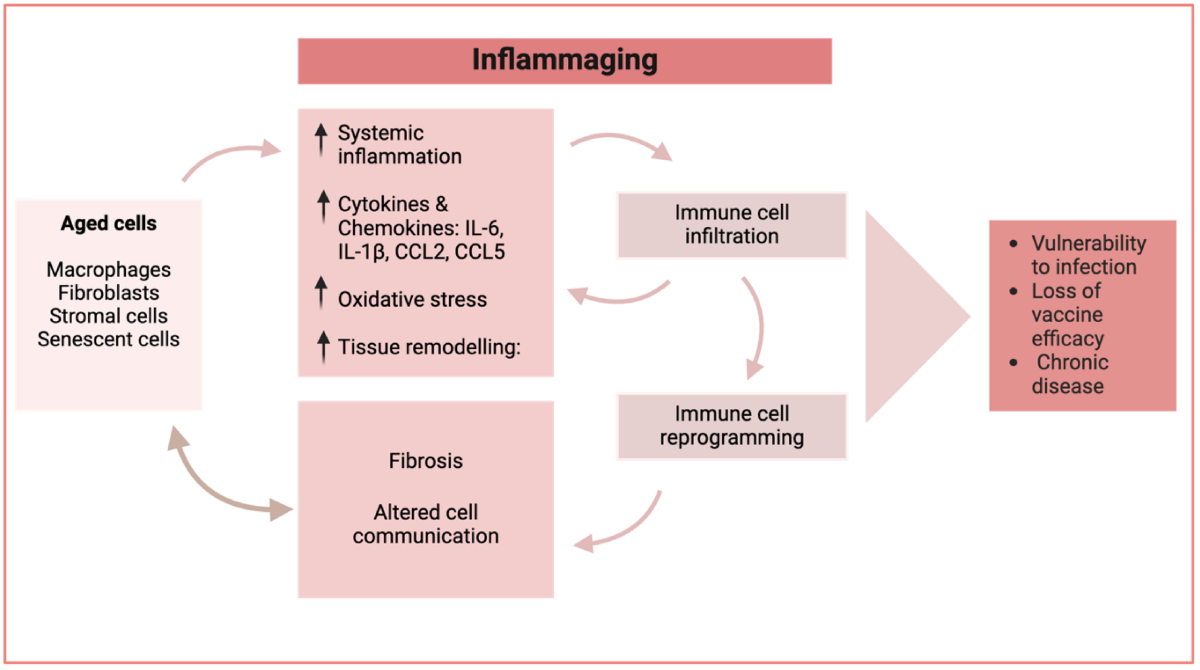

Thesis Figure 16: Inflammaging is a cardinal feature of aging.
Aging cells and senescent cells (immune and non-immune) produce increasing amounts of inflammatory mediators with age, leading to increased inflammaging that sets a cycle of altered cell-communication, fibrosis, chronic inflammation ultimately leading to increased vulnerability to disease and a maladaptive immune response. Illustration based on (Mogilenko et al, 2022)

1.3.3 The aging hematopoietic system

Hematopoiesis – basic concepts

Hematopoiesis is the continuous process through which all blood and immune cells throughout development, adulthood, and aging are continuously generated (Orkin & Zon, 2008). Hematopoietic stem cells (HSCs), which serve as the source, are mainly located in the bone marrow of adult mammals and give rise to all blood cell and immune lineages that then support tissue repair and immune function. HSCs are rare, self-renewing cells, and are capable of both long-term self-renewal and multilineage differentiation into the multitude of mature immune cells that populate all tissues (Orkin, 2000). HSCs produce multipotent and lineage-restricted progenitor cells, which serve as short-lived intermediates that eventually mature into fully functional immune cells (Orkin, 2000; Weissman, 2000). During development, hematopoietic stem cells (HSCs) rapidly establish the adult immune system. In adulthood, they support health and immunity by remaining in a state of quiescence and can be activated and produce immune cells as needed With aging, however, HSCs become dysfunctional, largely due to chronic inflammation and a deteriorated bone marrow environment leading to skewed differentiation, reduced regeneration and cell-intrinsic mutations (Kasbekar *et al*, 2023). Hematopoiesis begins during early embryonic development in both humans and murine models. It progresses

through distinct waves that transition from primitive to definitive hematopoiesis (Cumano & Godin, 2007) The initial wave or primitive hematopoiesis is a transient phase that takes place in the yolk sac and produces blood cells that are needed for early embryonic development and tissue oxygenation (Palis & Yoder, 2001). This is then followed by a subsequent wave, known as definitive hematopoiesis which takes place in the aorta–gonad–mesonephros (AGM) region (an area surrounding the dorsal aorta). It is during definitive hematopoiesis where the long-term pool of HSCs that persist throughout life is established. Here, adult-like hematopoietic stem cells (HSCs) emerge from the hemogenic endothelium of the AGM (Medvinsky & Dzierzak, 1996). These HSC then migrate to the fetal liver (FL), where they expand and mature before finally homing to the bone marrow (BM) (Cumano & Godin, 2007; Johnson & Moore, 1975). The bone marrow then becomes the primary residence of HSC in postnatal life and adulthood from where all blood and mature immune cells that are needed by all organ systems are produced throughout life (Orkin & Zon, 2008). Each of these waves of development are facilitated by distinct microenvironments or niches that provide cues guiding HSC development, proliferation, migration and multi-lineage differentiation (Dzierzak & Speck, 2008).

HSCs sit atop the hematopoietic hierarchy and generate all blood cell lineages which include the erythroid lineage which gives rise to erythrocytes (red blood cells), the megakaryocytic lineage (megakaryocytes and platelets) and the myeloid and lymphoid lineages which differentiate into all other immune cells of the innate and adaptive immune systems (Orkin & Zon, 2008) (**Thesis Figure 17).** In the bone marrow niche, most HSCs remain in a quiescent state and periodically divide to self-renew and produce multipotent and lineage restricted progenitors (MPPs) which act as an intermediate stage before producing lineage-committed mature cells (Wilson *et al*, 2008). The HSC compartment is identified by cells that express the Lin^{neg} Sca-1^{+} c-Kit^{+} (LSK) markers (Morrison & Weissman, 1994). The most primitive - the long-term HSCs (LT-HSCs), which possess robust self-renewal, totipotent and long-term reconstitution abilities, are identified within subsets expressing $CD34^{-}$,(as well as $CD38^{+}$ in humans), or low levels of Thy1.1 (Morita *et al*, 2010; Osawa *et al*, 1996). Short-term HSCs (ST-HSCs) and multipotent progenitors (MPPs), distinguished by $CD34^{+}$ (and $CD38^{-}$ in humans) markers, are capable of only transient reconstitution (Yang *et al*, 2005). The exact demarcations between ST-HSCs and MPPs are less distinct (Purton, 2022). Although MPPs maintain multipotency, they do exhibit lineage biases with transcriptional signatures similar to those of their progeny. MPP2 cells are biased toward megakaryocyte–erythroid differentiation, MPP3 toward myeloid differentiation, and MPP4 toward lymphoid differentiation (Eric *et al*, 2015; Eric M. Pietras, 2015; Swann *et al.*, 2024). LT-HSCs differentiate through a series of progenitor stages, each step narrowing their multipotency until they give rise to functional

mature blood cell types (Dzierzak & Speck, 2008). HSCs in mice give rise to two main types of lineage-restricted progenitors: common myeloid progenitors (CMPs) (Akashi *et al*, 2000) and common lymphocyte progenitors (CLPs) (Kondo *et al*, 1997). CMPs further develop into specialized progenitors including granulocyte-macrophage progenitors (GMPs) and megakaryocyte/erythroid progenitors (MEPs) (Iwasaki & Akashi, 2007). MEPs contribute to the production of cells essential for critical physiological functions such as oxygen transport (erythrocytes) and blood clotting (platelets from megakaryocytes) (Sanada *et al*, 2016). GMPs give rise to various myeloid cells such as neutrophils, monocytes, eosinophils, basophils, and dendritic cells. The myeloid lineage plays a vital role in maintaining fundamental physiological processes and responding quickly to pathogens to initiate immune defenses and promotes tissue repair (Hoeffel *et al.*, 2015; Iwasaki & Akashi, 2007). CLPs give rise to lymphoid cells, including T cells, B cells, natural killer (NK) cells and innate-lymphoid cells (ILCs) ensures a targeted immune response, offering long-term protection against specific pathogens (Karsunky *et al*, 2008; Kondo *et al.*, 1997).

Age-associated alterations in hematopoiesis

Aging of the hematopoietic system is closely tied to reduced immune system function, a higher prevalence of anemia, an increased proportion of myeloid cells, and a greater risk of hematological disorders (Montecino-Rodriguez *et al*, 2013).

Expansion of HSC Numbers with a Reduced Regenerative capacity with age: Aging leads to many notable changes in the HSCs themselves (Dorshkind *et al*, 2020). With age there is an exponential expansion in the numbers of HSCs from two to almost ten-fold as compared to young individuals. However, these HSCs display a significantly reduced long-term-renewal capacity (Dykstra *et al*, 2011). This suggests that although there is a dramatic increase in numbers, the reduced function and quality ultimately leads to a reduction in regenerative potential and function of the hematopoietic system over time (Rossi *et al*, 2005) While the exact mechanisms behind this age-related increase in HSCs numbers are still unclear, cell-intrinsic changes such as altered symmetrical or clonal self-renewal, reduced response to extrinsic cues and an altered bone-marrow niche and microenvironment all likely contribute (Kuribayashi *et al*, 2021; Latchney & Calvi, 2017) .

Skewed Differentiation and Myeloid Bias: The composition of the HSC pool also shifts with age (**Thesis Figure 17**). There is an increased number of myeloid-biased HSC clones, while balanced and lymphoid-biased HSCs become less prevalent (Nishi *et al*, 2019). One of the most pronounced characteristics of aging HSCs is the shift in their differentiation potential, leading to a myeloid bias i.e an increased production of myeloid lineage cells while the output of lymphoid and erythroid cells declines (Pang *et al*, 2011). Such changes in lineage

specification begin at early stages of hematopoiesis, where aged HSCs show a greater tendency to generate common myeloid progenitors (CMPs) over common lymphoid progenitors (CLPs) (Muller-Sieburg *et al*, 2004). Clonal analyses reveal that aged myeloid-biased HSCs not only increase in number but also exhibit reduced proliferative capacity and compromised functional quality (Yamamoto & Nakauchi, 2020; Yamamoto *et al*, 2018). Studies have demonstrated that aged HSCs upregulate myeloid-specific genes, such as *RUNX1*, and downregulate lymphoid-specific genes, reinforcing their tendency toward myeloid lineage commitment (Rossi *et al.*, 2005). This imbalance impacts the immune system, as the diminished production of lymphoid cells compromises adaptive immunity, contributing to immunosenescence. Elderly individuals consequently experience a higher susceptibility to infections, reduced vaccine efficacy, and a greater risk of myeloid malignancies (Hou *et al*, 2024; Krishnarajah *et al.*, 2021). Additionally, aged HSCs often express higher levels of pro-inflammatory molecules and interaction markers such as P-selectin and ICAM1, indicating a shift toward a pro-inflammatory state that supports myeloid differentiation (Chambers *et al*, 2007).

HSCs accumulate mutations over time, which can result in a significant proportion of blood cells originating from a single dominant HSC lineage. This phenomenon, known as clonal hematopoiesis, is linked to a higher risk of developing hematologic cancers and cardiovascular diseases (Jaiswal & Ebert, 2019; Jaiswal *et al.*, 2017). The reduced function of aged HSCs is influenced by several intrinsic changes, including accumulated DNA damage, impaired DNA repair mechanisms, increased reactive oxygen species, and altered cell polarity (Mejia-Ramirez & Florian, 2020). Epigenetic alterations are a hallmark of aging HSCs, characterized by hypermethylation of differentiation-associated genes and hypomethylation at loci related to self-renewal, along with changes in histone marks. These molecular modifications contribute to both diminished regenerative capacity and altered differentiation patterns (Beerman *et al*, 2013; Sun *et al*, 2014). While intrinsic mechanisms are central to HSC aging, extrinsic factors, such as changes in the bone marrow niche and systemic signaling, also play significant roles. Studies have shown that the aging process impacts HSC–niche interactions, with aged niches potentially supporting myeloid-skewed hematopoiesis due to altered signaling and structural changes (Latchney & Calvi, 2017; Sanmiguel *et al*, 2020). Chronic low-grade inflammation, continuous exposure to immune challenges such as lipopolysaccharides, and altered chemokine profiles (e.g., CCL5) influence HSC behavior and may reinforce the age-associated myeloid bias (Kovtonyuk *et al*, 2016). Understanding these age-associated changes in HSCs and their impact on the hematopoietic and immune systems is crucial for developing therapeutic strategies aimed at maintaining or restoring HSC function and mitigating the consequences of aging on immune health.

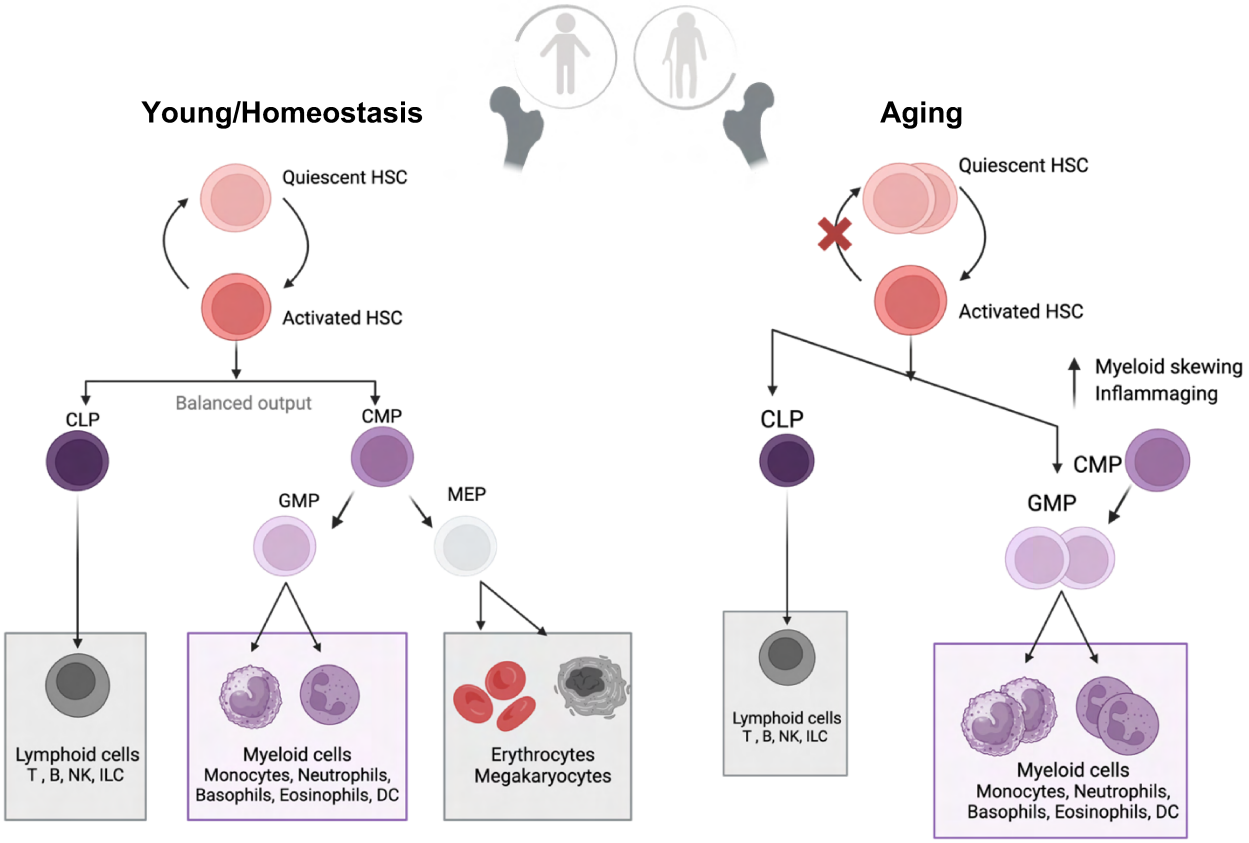

Thesis Figure 17: The hematopoietic tree
In healthy, young individuals during homeostasis there is a balanced output of lymphoid and myeloid progenitors and mature cells, whereas with age there is myeloid-biased skewing in the bone-marrow. Based on (Swann *et al.*, 2024).

1.3.4 The aging lung

Functional, structural, and physiological changes in the aging lung

Aging leads to a deterioration in pulmonary function even without the presence of direct disease-related changes (Han *et al*, 2023). In humans, the developing lung continues to mature post birth, reaching its maximum developmental and functional capacity between 18-25 years of age, after which it stays relatively stable until the age of 35 (Sharma & Goodwin, 2006). After this point, lung function begins to gradually decline – a process characterized by a reduction of alveolar surface, increased formation of alveolar dead space, altered elasticity of the lung parenchyma and diminished capacity to clear mucus (Schneider *et al.*, 2021) (**Thesis Figure 18**). With advanced age, the lung barrier integrity is compromised. This, along with a weakened immune response, pathogen resistance and increased inflammatory levels renders the lung susceptible to respiratory infections as evidenced by the COVID-19 pandemic as well as an increased risk for chronic diseases such as lung cancer, chronic obstructive pulmonary disease (COPD), IPF, pneumonia and acute respiratory distress syndrome (ARDS)

(Van Der Poll & Opal, 2009; Williamson *et al*, 2020). Alveoli, the key structures required for gas exchange in the lung, while remaining stable during adulthood, gradually begin to alter over time. With age, there is a decrease in alveolar density and total alveolar surface area, declining by 2.5m^2 every decade (Miller, 2010). This is accompanied by an expansion of alveolar and duct size which alters the alveolar-capillary surface area (Quirk *et al*, 2016), leading to decreased surface tension and elastic recoil in the lungs. Consequently, this along with the loss of elastic fibers that support the alveoli, results in an increase in end-expiratory lung volume, i.e the amount of air left in the lungs after exhalation (Babb & Rodarte, 2000) and an increase in functional residual capacity .

Thesis Figure 18: The aging lung

Over time there are key structural and physiological changes that change the lung tissue that

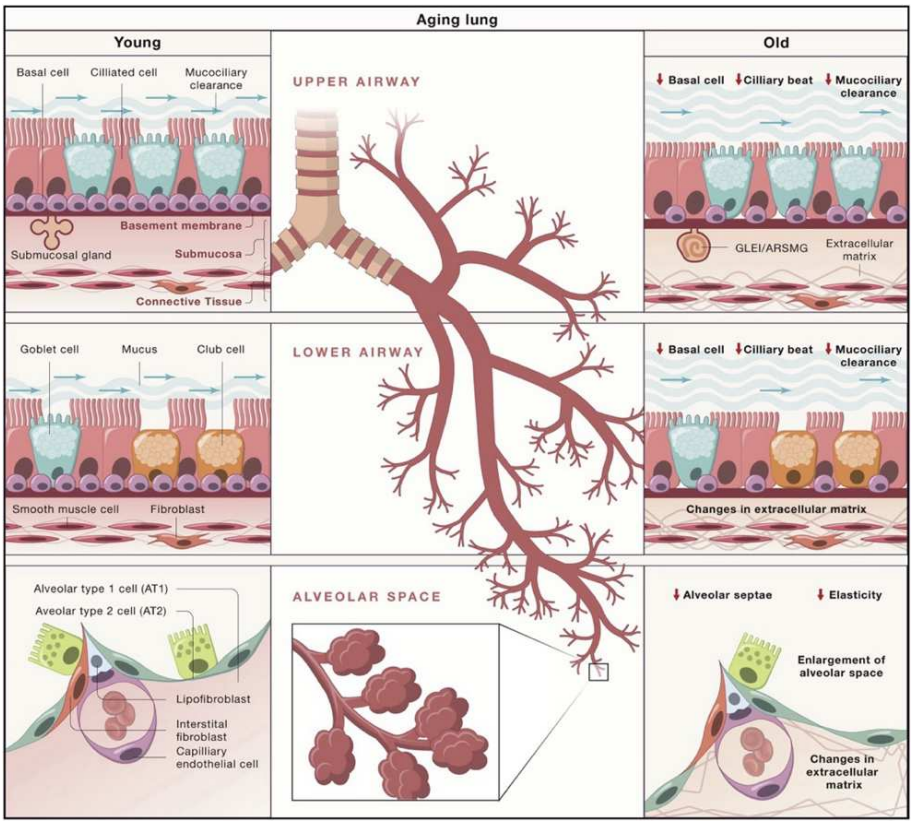

result in loss of elasticity, mucosal clearance and alveolar space. Illustration from (Schneider *et al.*, 2021)

Failed repair and increasing fibrosis in the aging lung

Age is a key factor in the failure of alveolar repair and susceptibility to fibrosis in the lungs (Han *et al.*, 2023). Aged mice show impaired regenerative responses compared to their younger counterparts and after bleomycin-induced injury, older mice develop more severe and persistent fibrosis (Watanabe *et al.*, 2021). Similarly, there is increased mortality and they fail

to completely repair lung tissue following influenza-induced damage (Yin *et al*, 2014). Young After pneumonectomy (unilateral) young mice have the ability to regenerate lung tissue but this is lost with age and AT2 cells from older mice exhibit diminished regenerative capacity, forming fewer and smaller alveolar organoids in vitro compared to those from younger mice, emphasizing the decline in alveolar repair efficiency with age (Chen *et al*, 2021). Polyploidy, an intrinsic mechanism observed in differentiating AT2 cells, increases cell size by scaling with DNA content. While this may provide short-term benefits during acute injury by preserving barrier integrity, it reduces the proliferative potential of AT2 cells (Selmecki *et al*, 2015; Weng *et al*, 2022). Telomere shortening has been documented in healthy aged human lungs, though the specific cell types responsible remain unclear (Alder *et al*, 2015). Reduced mucociliary clearance in both the upper and lower airways compromises the lung's defense mechanisms, contributing to chronic injury and repair deficits (Proença De Oliveira-Maul *et al*, 2013). Aged AT2 cells and fibroblasts show enhanced expression of genes associated with cholesterol biosynthesis, leading to lipid accumulation in epithelial cells and fibroblasts (Hecker *et al*, 2014; Kato *et al.*, 2020). Moreover, the proportion of ciliated cells in the airway increases with age, altering the club-to-ciliated cell ratio, which may affect epithelial homeostasis and repair. Aging leads to a decline in lung stem cell function, with basal and club cells decreasing in number and AT2 cells showing reduced regenerative capacity despite stable numbers (Schneider *et al.*, 2021). Factors such as oxidative stress, mitochondrial dysfunction, telomere shortening, and epigenetic changes contribute to this decline, impairing lung repair and promoting diseases like fibrosis and emphysema (Han *et al.*, 2023). The exact interactions between epithelial, mesenchymal, and immune cells in aging remains unclear.

Lung aging is also associated with aging of the immune cells in the lung, although their specific roles in lung fibrosis and how they impact disease progression remain less known (Schneider *et al.*, 2021). With age, the lung immune system also undergoes several changes that impair its ability to respond to injury and infection. As described before, alveolar macrophages, show reduced efficiency in clearing pathogens and apoptotic cells (Boe *et al.*, 2022), Neutrophils exhibit delayed apoptosis and prolonged tissue presence, leading to excessive tissue damage (Hazeldine *et al*, 2014; Kulkarni *et al*, 2019). Dendritic cells become less effective at antigen presentation, weakening adaptive immune responses and reducing the ability to mount effective immune defenses (Zhao *et al*, 2011). Aging also disrupts lymphocyte function—naïve T cell numbers decline, while memory T cells accumulate and adopt a more pro-inflammatory phenotype, contributing to chronic low-grade inflammation in the lungs (Jiang *et al*, 2011; Messaoudi *et al*, 2004). B cells show reduced diversity, limiting effective antibody responses, which further weakens immune surveillance (Frasca & Blomberg, 2009). Given these

widespread immune alterations, it is crucial to understand how aging shapes immune cell function in the context of chronic lung disease.

While aging is the greatest risk factor for lung fibrosis, research so far has primarily focused on structural changes in the lung as the primary driver, whereas the impact of immune aging on fibrosis remains less understood and often considered a downstream response of tissue aging. Macrophages are key orchestrators of fibrosis, as we have described in this introduction (*section 1*), especially in the lungs, where monocyte-derived macrophages—replenished from the bone marrow—drive pathology *(section 2).* With each inflammatory event over time, these bone marrow-derived macrophages replace the resident population and contribute to fibrosis progression. However, if and how an aging bone marrow and hematopoietic system impacts lung macrophage fate, function and ultimately lung fibrosis remains unknown. Understanding whether age-related changes in the bone marrow contribute to macrophage-driven fibrosis will be critical to uncovering new mechanisms of disease progression **(Thesis Figure 19).**

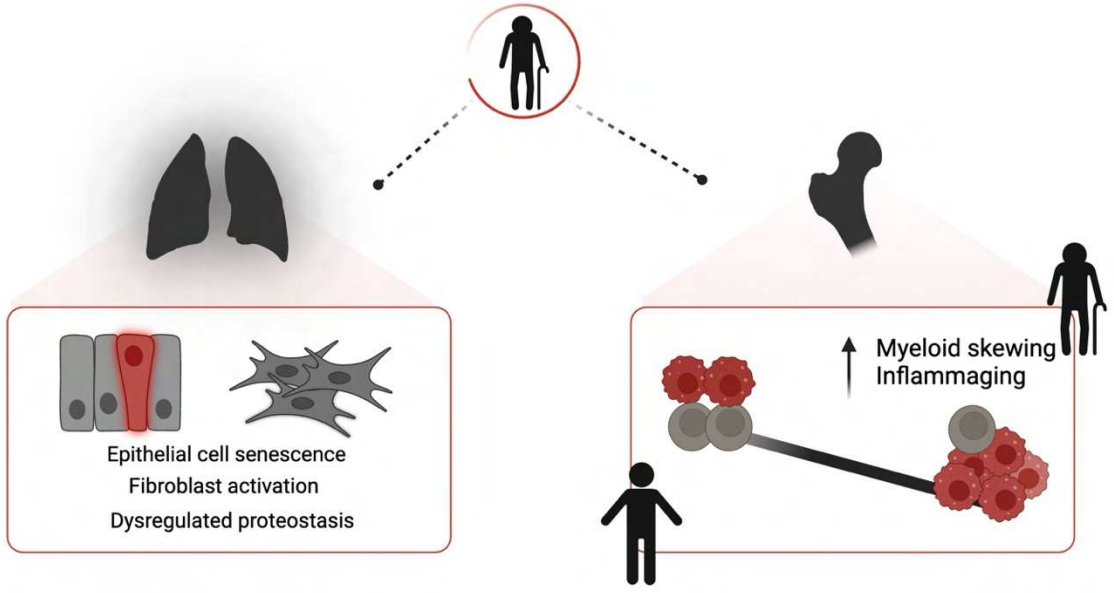

Thesis Figure 19: Aging in the lung tissue and hematopoietic system
Age-associated changes in the lung tissue including epithelial dysfunction and fibroblast activation are known drivers of lung fibrosis. At the same time hematopoietic aging leads to myeloid skewing and a state of inflammaging.

Aims of the thesis

The progressive decline of homeostatic processes and the increasing chronicity of disease with age has become evident. Fibrosis, which worsens with age, is widely recognized as a consequence of dysregulated immune-tissue interactions. While both immune and non-immune compartments contribute to fibrosis, their specific roles in disease progression remain unclear. In lung fibrosis, age-related changes in the lung tissue (non-immune compartment) are considered primary drivers of disease. Simultaneously, monocyte-derived alveolar macrophages (Mo-AMs) from the bone marrow have also emerged as key profibrotic players in the pathogenesis of lung fibrosis. Yet, how aging of the bone marrow and immune system directly contributes to chronic diseases such as lung fibrosis remains poorly understood. We therefore hypothesized that an aging bone marrow could be a primary driver of fibrosis severity with advanced age, independent of structural tissue aging.

This thesis therefore aims to determine the impact of hematopoietic aging on fibrosis progression and macrophage fate and function in the lungs.

I aimed to investigate:

1) If an aging bone marrow drives fibrosis severity independent of lung tissue age.
2) Whether hematopoietic myeloid bias with age alters the lung immune cell landscape.
3) How hematopoietic aging influences Mo-AM phenotype, function, and acquisition of tissue residency and to what extent this is governed by intrinsic versus extrinsic factors.
4) Identify potential immune or repair pathways that could be dysregulated by hematopoietic aging which could be targeted to promote efficient repair post injury.

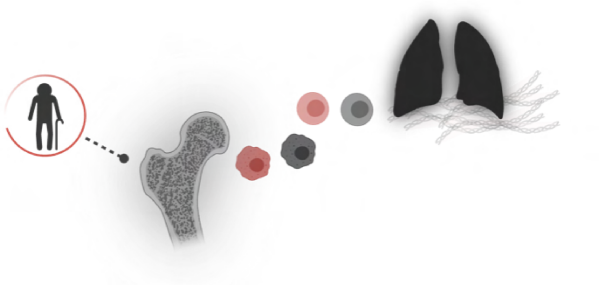

Chapter 2

Results

In the following study, we investigated if an aging bone marrow independently influenced lung fibrosis. To study this, we set up a heterochronic bone marrow transplant model. Here we transplanted bone marrow cells from either young or aged donor mice into irradiated young recipient mice. Therefore, the recipients had a similar young lung tissue and structural cell compartment but either young or aged immune cells. We then used intratracheal bleomycin administration to induce severe lung injury and subsequent fibrosis in recipient mice. We assessed the development of fibrosis and disease progression between the groups. We then dissected the mechanisms of monocyte-derive alveolar macrophage (Mo-AM) fate and phenotype in the lungs. In this study we found that the age of the bone marrow was sufficient to drive exacerbated lung fibrosis. Moreover, we found that aged Mo-AMs displayed an enhanced profibrotic and prolonged inflammatory profile in the lungs. Over time, they failed to transition into a homeostatic tissue-resident phenotype. Mechanistically, we found that hematopoietic aging led to a hampered resolution axis between Tregs and Mo-AMs in the lungs, leading to delayed Mo-AM maturation and exacerbated lung fibrosis.

Accepted on 19.02.2025, ***Science Immunology***

An aging bone marrow exacerbates lung fibrosis by fueling profibrotic macrophage persistence.

Asma Farhat[1,2], Mariem Radhouani[1,2], Florian Deckert[1,2], Sophie Zahalka[1,2], Lisabeth Pimenov[1], Alina Fokina[1], Anna Hakobyan[2,3,4], Felicitas Oberndorfer[5], Jessica Brösamlen[1], Anastasiya Hladik[1], Karin Lakovits[1], Fanzhe Meng[1], Federica Quattrone[1,2], Louis Boon[6], Cornelia Vesely[7], Philipp Starkl[1], Nicole Boucheron[8], Jörg Menche[2,3,4,9,10], Joris van der Veeken[11], Wilfried Ellmeier[8], Anna-Dorothea Gorki[1], Clarissa Campbell[2], Riem Gawish[1†], Sylvia Knapp[1,12 †*].

[†] equal contribution

An aging bone marrow exacerbates lung fibrosis by fueling profibrotic macrophage persistence.

Asma Farhat[1,2], Mariem Radhouani[1,2], Florian Deckert[1,2], Sophie Zahalka[1,2], Lisabeth Pimenov[1], Alina Fokina[1], Anna Hakobyan[2,3,4], Felicitas Oberndorfer[5], Jessica Brösamlen[1], Anastasiya Hladik[1], Karin Lakovits[1], Fanzhe Meng[1], Federica Quattrone[1,2], Louis Boon[6], Cornelia Vesely[7], Philipp Starkl[1], Nicole Boucheron[8], Jörg Menche[2,3,4,9,10], Joris van der Veeken[11], Wilfried Ellmeier[8], Anna-Dorothea Gorki[1], Clarissa Campbell[2], Riem Gawish[1†], Sylvia Knapp[1,12 †*].

[1] Medical University of Vienna, Department of Medicine I, Research Division of Infection Biology, Vienna, Austria.

[2] CeMM, Research Center for Molecular Medicine of the Austrian Academy of Sciences, Vienna, Austria.

[3] Max Perutz Labs, Vienna Biocenter Campus (VBC), Vienna Austria

[4] Department of Structural and Computational Biology, University of Vienna, Vienna Austria.

[5] Medical University of Vienna, Department of Pathology, Vienna, Austria.

[6] JJP Biologics, Warsaw, Poland

[7] Medical University of Vienna, Center for Anatomy and Cell Biology, Vienna, Austria.

[8] Medical University of Vienna, Center for Pathophysiology, Infectiology and Immunology, Institute of Immunology, Vienna, Austria.

[9] Faculty of Mathematics, University of Vienna, Vienna, Austria

[10] Ludwig Boltzmann Institute for Network Medicine at the University of Vienna, Vienna, Austria

[11] Research Institute of Molecular Pathology (IMP), Vienna, Austria.

[12] Ignaz Semmelweis Institute, Interuniversity Institute for Infection Research, Vienna, Austria

[†] These authors contributed equally to this work

* Correspondence: sylvia.knapp@meduniwien.ac.at (S. Knapp)

ABSTRACT:

Pulmonary fibrosis is an incurable disease that manifests with advanced age. Yet, how hematopoietic aging influences immune responses and fibrosis progression remains unclear. Using heterochronic bone marrow transplant mouse models, we found that an aged bone marrow exacerbates lung fibrosis irrespective of lung tissue age. Upon lung injury, there was an increased accumulation of monocyte-derived alveolar macrophages (Mo-AMs) driven by cell-intrinsic hematopoietic aging. These Mo-AMs exhibited an enhanced profibrotic profile and stalled maturation into a homeostatic, tissue-resident phenotype. This delay was shaped by cell-extrinsic environmental signals such as reduced pulmonary IL-10, perpetuating a profibrotic macrophage state. We identified regulatory T cells (Tregs) as critical providers of IL-10 upon lung injury that promote Mo-AM maturation and attenuate fibrosis progression. Our study highlights the impact of an aging bone marrow on lung immune regulation and identifies Treg-mediated IL-10 signaling as a promising target to mitigate fibrosis and promote tissue repair.

One Sentence Summary:

Hematopoietic aging drives lung fibrosis and profibrotic macrophage influx, stalling their maturation via reduced Treg-derived IL-10.

INTRODUCTION

With rising life expectancies and a growing aging population, understanding how advanced age leads to increased disease morbidity is an imminent public health concern (*1*). Aging is associated with enhanced vulnerability to chronic respiratory pathologies including Idiopathic Pulmonary Fibrosis (IPF) (*2, 3*). IPF is characterized by progressive and severe scarring of the lung tissue, ultimately leading to lung failure (*4*). While genetic predisposition and environmental triggers contribute to its etiology, advanced age is by far the most prevalent risk factor for onset of the disease (*5*). Age-related cellular senescence, aberrant epithelial activation, mitochondrial dysfunction, and impairments in immunity influence IPF disease progression (*6-8*). Repair and regeneration are vital for maintaining tissue integrity (*9*), with tissue-resident (TR-) alveolar macrophages (AMs) playing a key role in preserving lung homeostasis during early life. Homeostatic TR-AMs self-renew with minimal contribution from circulating monocytes (*10, 11*). Damage to the alveolar epithelium during severe lung inflammation, such as that caused by bleomycin injury, depletes TR-AMs and leads to monocyte recruitment from the bone marrow, which then differentiate into monocyte-derived AMs (Mo-AMs) (*12-14*). While Mo-AMs are beneficial during acute infections (*12*), their chronic presence contributes to pathologies like lung fibrosis (*15-17*) as they secrete profibrotic factors

which activate fibroblasts and sustain the fibrotic process (*18, 19*). In the lungs, Mo-AMs undergo marked phenotypic and functional changes, eventually acquiring a phenotype similar to that of TR-AMs (*20-22*). The speed at which activated Mo-AMs transition into a less reactive TR-AM state contributes to disease outcome and the likelihood of restored lung homeostasis (*23*).

While previous studies have comprehensively addressed the role of aging lung tissue (*24*) and shown that an increased susceptibility to lung fibrosis with age is associated with elevated Mo-AMs, these effects have been primarily attributed to impairments in epithelial cell proteostasis and differentiation (*20, 25*). How the aging bone marrow and derived hematopoietic immune cells (i.e., Mo-AMs) impact disease when recruited into a distant organ remains incompletely understood. An aging immune system is characterized by a state of low-grade, systemic inflammation, termed inflammaging (*26*). Although aged hematopoietic stem cells display a reduced regenerative capacity, intrinsic changes in their differentiation potential and a higher propensity for myelopoiesis leads to an expansion of myeloid progenitors and mature cells at the expense of lymphopoiesis (*27-30*). This skewing contributes to an increase in myeloid-based malignancies with age, which coincides with impaired adaptive immunity. Such changes impair the immune system's inability to mount an appropriate immune response or promote tissue integrity and repair (*31*). In this study, we asked whether immune cells derived from an aged bone marrow could influence inflammation and fibrosis in the lungs. We found that an aged bone marrow autonomously produced more profibrotic Mo-AMs, which propagated fibrosis development independent of pulmonary tissue age. In the lungs, these Mo-AMs were slower to adopt a homeostatic tissue-resident phenotype due to reduced availability of regulatory T cell (Treg)-derived IL-10, resulting in exacerbated lung fibrosis.

RESULTS

An aged bone marrow exacerbates bleomycin-induced lung fibrosis in mice.

Age is a major risk factor for lung fibrosis, as seen in both humans and mice (*2, 25*). While dysregulation of the aging epithelia has been described as a prime driver of fibrosis severity, the potential contribution of an aged hematopoietic system remains unclear (*25*). We challenged young-adult (8-week-old) and aged (70-week-old) mice intratracheally (i.t) with bleomycin to induce fibrosis (**Fig. 1A**). Aged mice exhibited greater disease severity with sustained body weight loss, (**Fig. 1B**), enhanced collagen deposition (**Fig. S1A**), and increased pulmonary infiltration of myeloid cells, including monocyte-derived alveolar macrophages (Mo-AMs, SiglecF^{lo} CD11b^{hi}) (**Fig. 1C and S1B, gating strategy S1C**). Given this elevated influx of bone marrow-derived Mo-AMs in aged mice, we asked if this was driven by changes in the abundance of bone marrow progenitors, considering the age-associated myeloid bias that occurs in the hematopoietic progenitor niche (30). At baseline, aged mice

had elevated granulocyte-monocyte progenitors (GMPs), reduced common lymphoid progenitors (CLPs) in the bone marrow (**Fig. S1D-G**), and lower T and B cells in the blood (**Fig. S1H**). By day 7 post-bleomycin, aged mice exhibited a pronounced myeloid shift in the bone marrow, (**Fig. 1D, S1I-J**) and increased neutrophils and monocytes in the blood (**Fig. S1K**). We thus hypothesized that this myeloid skewing in the bone marrow of aged mice could contribute to enhanced recruitment of myeloid cells to the lung and influence the severity of lung fibrosis.

To study the impact of an aging bone marrow independently of structural tissue age, we performed heterochronic bone marrow transplants in which young adult (8-week-old) recipient mice received bone marrow cells from either aged (70-week-old) mice or young adult (8-week-old) controls (**Fig. 1E**). Two months post-transplantation, we treated mice with bleomycin and analyzed the lungs at seven days (D7, inflammatory phase) and 14 or 21 days (D14/D21, fibrotic phase) (*15*) post-challenge (**Fig. 1E**). Young recipient mice transplanted with aged bone marrow showed increased lethality at a dose of 1.5U/Kg (**Fig. 1F**) and consistently lost more body weight when treated with a lower bleomycin dose (1U/Kg) to ensure survival (**Fig. 1G**) as compared to control mice that received bone marrow from young donors. Despite both groups having similar, young structural cells in the lungs, including collagen producing fibroblasts (*32*), reconstitution with aged bone marrow increased fibrotic burden. This was evidenced by increased lung collagen deposition (**Fig. 1H**) and elevated alpha-smooth muscle actin (α-SMA) expression, indicating enhanced myofibroblast activation (*33*) following bleomycin treatment (**Fig. 1I**). Exacerbated fibrosis in recipients of aged bone marrow was verified by histological scoring (Ashcroft score) and increased hydroxyproline levels in the lung tissue at D21 (peak fibrosis) (**Fig. 1J, 1K**) and was already evident by D14 (**Fig. S2A, S2B**). Pulmonary TGF-β levels (**Fig. 1L**) and fibrotic genes such as *Actb*, *Arg1*, *Vegf* and *Col1a1* were elevated by D21 (**Fig. 1M**). To test whether hematopoietic aging promoted fibrosis by enhancing lung injury in the early inflammatory phase post-bleomycin challenge (D7), we assessed the total protein concentration in the BALF (**Fig. S2C**) and the number of apoptotic lung cells ($TUNEL^+$) but found no differences between the two recipient groups (**Fig. S2D, S2E**). Together, our data show that an aged bone marrow is sufficient to exacerbate the development of lung fibrosis, without altering the degree of bleomycin-induced lung injury.

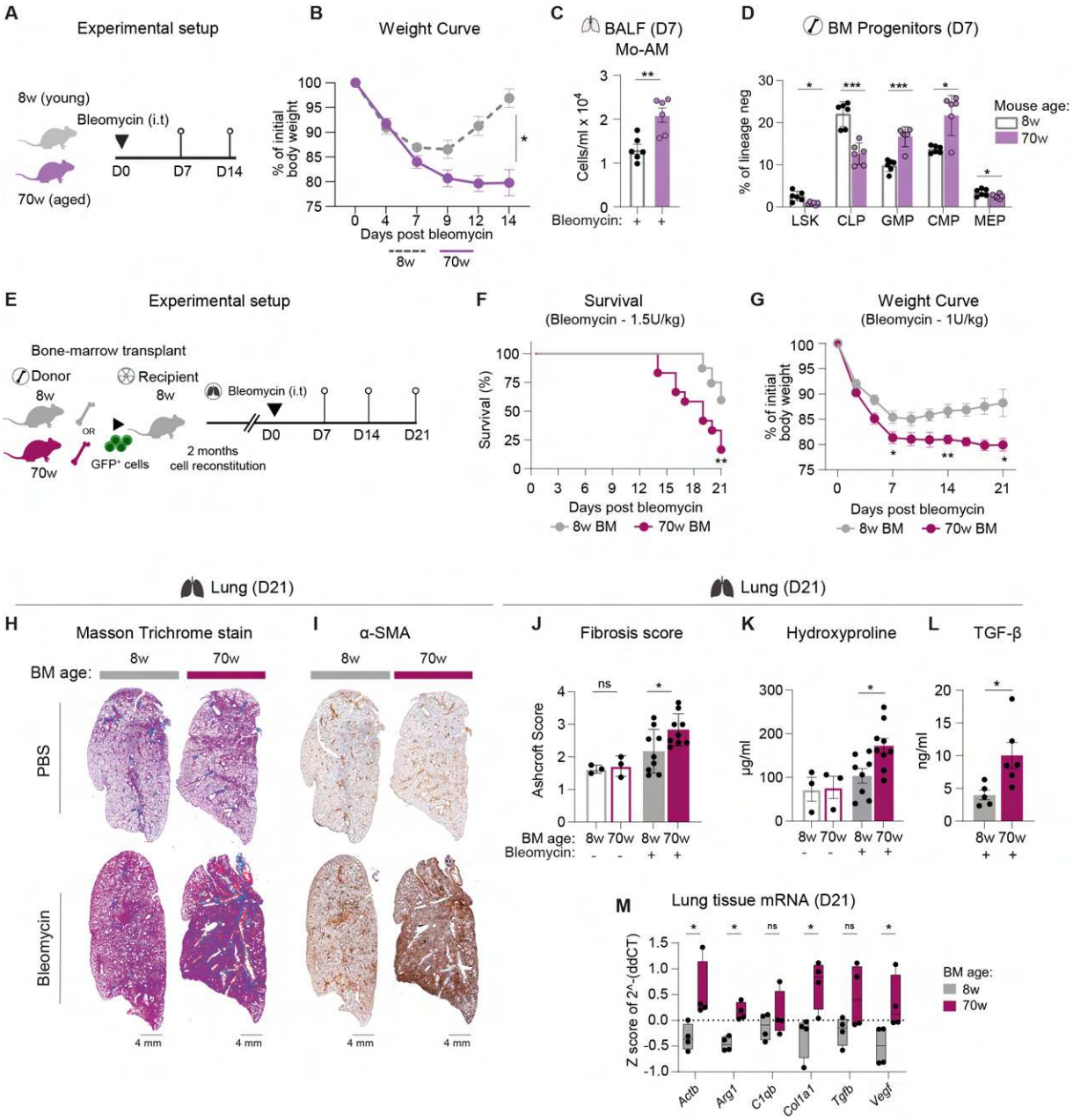

Fig. 1. An aged bone marrow exacerbates lung fibrosis.

(A) Experimental setup. (**B to D**): Bleomycin (1U/kg) was given to 8-week-old (8w) or 70-week-old (70w) C57BL/6J WT mice with end points taken seven (D7) or 14 days (D14) post challenge. (*n = 5- 7* per group per time point; i.t – intratracheal). **(B)** Body weight curve showing percentage loss of initial body weight post bleomycin challenge. **(C)** Absolute numbers of monocyte-derived alveolar macrophages (Mo-AM) from the bronchoalveolar lavage fluid (BALF) on D7 post bleomycin challenge. Mo-AMs gated as SiglecF^{lo} CD11b^{hi} from CD64^{+} MerTK^{+} cells. **(D)** Hematopoietic stem cell progenitors in the bone marrow expressed as percentage of lineage-negative cells (lineage see Fig. S1D; (LSK – Sca1^{+} cKit^{+} cells; CLP – common lymphoid progenitor; GMP – granulocyte-monocyte progenitor; CMP- common myeloid progenitor; MEP – megakaryocyte-erythroid progenitor). **(E)** Experimental set up. (**F to M)**: young (8w) C57BL/6J WT recipient mice were lethally irradiated and transplanted with bone marrow cells from young (8w) or aged (70w) donor mice (GFP^{+} bone marrow cells). 2 months post reconstitution, recipients were given bleomycin i.t.. (*n* = 5–10 per time point). **(F)** Survival curve until D21 post challenge (1.5 U/kg - high bleomycin dose). **(G)** Body weight curve until D21 (1 U/kg - low bleomycin dose). **(H–I)** Histological sections of left lung lobe (D21) post bleomycin/PBS. **(H)** Masson Trichrome staining for collagen deposition. **(I)** Alpha-smooth muscle actin (α-SMA) staining for activated

myofibroblasts. **(J)** Fibrosis quantified by a modified Ashcroft score of lung histology (D21). **(K)** Hydroxyproline quantification from lung tissue (D21). **(L)** ELISA of lung activated TGF-β (D21). **(M)** Gene expression analyzed by real-time qPCR from lung homogenates. CT values relative to *Gapdh* (2^-ddCT), shown as z-score per gene across both groups (*n* = 4 per group). Data are representative of two or three independent experiments. Symbols on bar graphs represent individual mice. For (B, G, J, K) two-way analysis of variance (ANOVA) with Tukey's multiple comparison test was used, Student's two tailed t test (C, L), multiple unpaired t-tests with Welch correction followed by Holm-Šídák test (D), survival curve (F) a Log-rank (Mantel-Cox) test, multiple-unpaired t-tests (M) was used. Error bars represent SEM or SD. *P ≤ 0.05; **P < 0.01; ***P < 0.001; ns: not significant.

An aged bone marrow autonomously promotes enhanced monocyte-derived alveolar macrophage influx upon lung injury.

Given the profibrotic role of bone marrow-derived Mo-AMs in the lungs (*15*), we assessed whether an aging bone marrow could impact Mo-AM accumulation upon bleomycin injury in mice. Although baseline levels remained similar (**Fig. S3A**), young recipients of aged bone marrow had increased myeloid progenitors (GMPs) and mature myeloid cells (monocytes and neutrophils) in the bone marrow after bleomycin challenge (**Fig. 2A, S3B, S3C**). This was accompanied by elevated numbers of Mo-AMs, monocytes (**Fig. 2B**), neutrophils and dendritic cells (**Fig. S3D**) in the bronchoalveolar lavage fluid (BALF) post-bleomycin, mirroring naturally aged animals. While most lung cell populations were efficiently reconstituted in both groups after transplantation (**Fig. S3E, S3F**), recipients of aged bone marrow had decreased numbers of TR-AMs (SiglecF^{hi} CD11b^{lo}) in the BALF and lung at baseline (**Fig. 2C, S3F**).

To determine if the increased Mo-AM influx in recipients of aged bone marrow resulted from enhanced availability of AM niche space, we shielded the thorax of young recipient mice during irradiation and transplanted GFP$^+$ bone marrow cells from young or aged mice (**Fig. 2D**). There was minimal contribution of GFP$^+$ donor cells in the lungs prior to fibrosis induction (**Fig. S3G**) and GFP$^+$ SiglecF^{lo} Mo-AMs infiltrated the lungs only once bleomycin was given (**Fig. S3H**). Shielded mice that received aged bone marrow still experienced greater body weight loss during the course of bleomycin challenge (**Fig. 2E**). Despite bearing lung-tissue resident immune cells of young host origin (GFP$^-$) and displaying no deficit in the number of SiglecF^{hi} TR-AMs at baseline (**Fig. 2F, 2G**), we observed an increased influx of GFP$^+$ Mo-AMs (**Fig. 2F, 2H**) and neutrophils (**Fig. S3I**) upon bleomycin challenge. We then investigated if young bone marrow could reduce Mo-AM influx in aged mice by transplanting young or aged bone marrow into irradiated aged mice (**Fig. 2I**). Despite the presence of aged lung tissue, young bone marrow protected aged mice from bleomycin-induced weight loss (**Fig. 2J**) and reduced Mo-AM (**Fig. 2K**), monocyte and neutrophil (**Fig. S3J**) numbers to levels comparable to young mice with young bone marrow at D7. Together, these data demonstrate that an aged bone marrow autonomously drives Mo-AM influx and is a key determinant of disease severity, irrespective of the age of the lung tissue or lung resident immune cells.

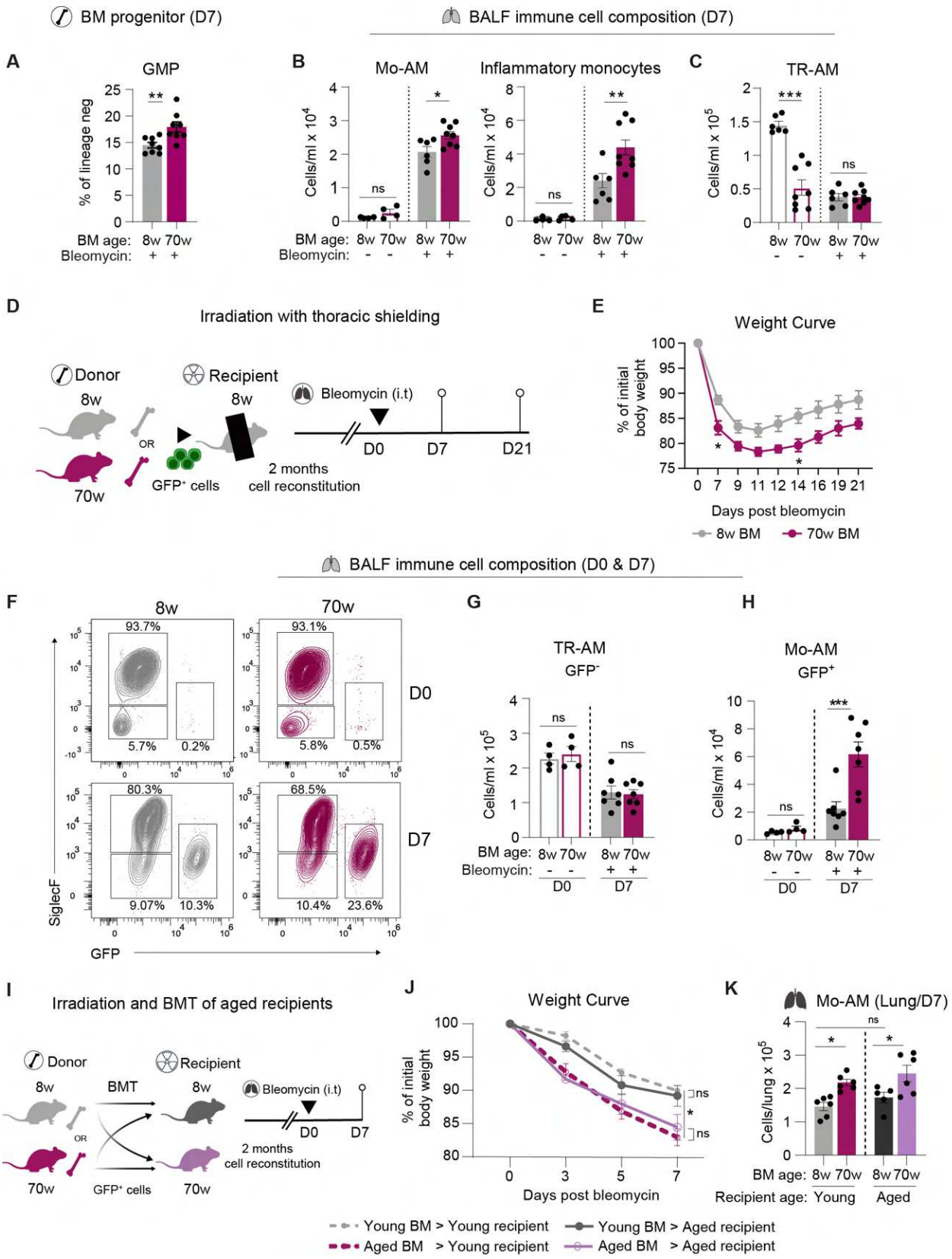

Fig. 2. An aged bone marrow autonomously promotes enhanced monocyte-derived alveolar macrophage influx upon lung injury.
(A to C) Whole body irradiation (8w-old recipients) and bone marrow transplant with 8w or 70w donor cells, PBS/Bleomycin (i.t.) administered two months post-reconstitution; parameters assessed at D7 (n = 4–9/group). **(A)** GMP from the bone marrow expressed as percentage of lineage-negative cells. **(B)**

Absolute numbers of cells showing Mo-AMs (SiglecF^{lo} CD11b^{hi}) and inflammatory monocytes (Ly6C^{hi} CD11b^{+}) from the BALF. **(C)** Absolute numbers of TR-AMs (SiglecF^{hi} CD11b^{lo}) from BALF. **(D)** Experimental set up **(E to H)**. Young (8w) C57BL/6 WT recipient mice were irradiated with a lead shield placed over the thoracic cavity and transplanted with bone marrow cells from 8w or 70w donor mice (GFP^{+}); 2 months post-reconstitution challenged with bleomycin. (*n* = 6–8/group with bleomycin; *n* = 4/group at D0/baseline). **(E)** Body weight curve until D21. **(F)** Flow cytometry plots showing GFP^{+} and GFP^{-} SiglecF^{hi} TR-AMs and SiglecF^{lo} MoAMs, respectively, in the BALF of 8w and 70w bone marrow recipients at D0 (baseline; top panel) and D7 (bottom panel). **(G)** Absolute numbers of TR-AMs (GFP^{-} cells) and **(H)** Mo-AMs (GFP^{+} cells) from the BALF on D0 (baseline) and D7 (post bleomycin challenge). **(I)** Experimental setup for **(J to K)**. Young (8-week-old) and aged (70-week-old) C57BL/6J WT recipient mice were irradiated and transplanted with 8w or 70w GFP^{+} bone marrow cells 2 months post-reconstitution, recipients were administered bleomycin (i.t) (*n* = 5–7/group). **(K)** Body weight curve until D7. **(L)** Absolute numbers of Mo-AMs from whole lung tissue at D7. Data representative of three independent experiments (A-C) or two independent experiments (D-L). Symbols on bar graphs represent individual mice. Flow cytometry plots and histological sections are representative of each group. For (A), Student's two tailed t test, (B-C, G-H) two-way ANOVA with post-hoc Šídák's multiple comparisons test, (E, J, K) two-way ANOVA with post-hoc Tukey's multiple comparisons test was used (mixed effect for E). Error bars represent SEM. *P ≤ 0.05; **P < 0.01; ***P < 0.001; ns: not significant.

Mo-AMs from aged bone marrow display a delayed transition into a homeostatic phenotype.

Once in the lungs, the phenotype acquired by Mo-AMs and the rate of transition into homeostatic macrophages in the tissue governs their functional outcome (*23*). We therefore analysed macrophage dynamics from the initial inflammatory phase (D7) to the development of fibrosis (D14) using flow cytometry and transcriptomic analysis. D14 served as the fibrotic endpoint as two distinct macrophage populations based on SiglecF expression can still be distinguished at this time (**Fig. 3A**). In both groups, there was an initial depletion of SiglecF^{hi} TR-AMs and influx of SiglecF^{lo} Mo-AMs on D7 after bleomycin (**Fig. 3B**). However, recipients of aged bone marrow showed slower SiglecF^{hi} TR-AM restoration and prolonged accumulation of SiglecF^{lo} Mo-AMs in the lung tissue (**Fig. 3B, 3C**). Mo-AMs initially express low levels of SiglecF, and gradually upregulate SiglecF as they become increasingly tissue-resident-like (*34*). While Mo-AMs from both young and aged bone marrow displayed comparably low SiglecF expression at D7, aged Mo-AMs failed to upregulate SiglecF at D14 (**Fig. 3D**), indicating delayed maturation. Using the thorax-shielded bone marrow chimera model (from **Fig. 2D**) to trace the transition of donor bone marrow-derived GFP^{+} SiglecF^{lo} Mo-AMs into SiglecF^{hi} TR-AMs over time, we found that no GFP^{+} macrophages expressed high SiglecF levels at D7 in both groups and most GFP^{+} Mo-AMs transitioned to a SiglecF^{hi} TR-AM state by D21 and D42 (**Fig. S4A**). However, the percentage of GFP^{+} Mo-AMs that co-expressed SiglecF from an aged bone marrow remained lower when compared to young bone marrow-derived cells, further highlighting delayed acquisition of a TR-AM phenotype (**Fig. S4A, S4B**). We next analyzed the transcriptome of Mo-AMs and TR-AMs at D7 and D14 post-bleomycin challenge (**Fig. 3A**). Principal component analysis revealed that the TR-AM population

became increasingly similar over time between the two groups (**Fig. 3E**) and showed signs of reconstitution by monocyte-derived cells by D14 (increased expression of *Ccr2, Ccr5, Csf1r* and *H2-Ab1)* (**Fig. S4C, Data file S1**). However, considerable differences persisted between young and aged bone marrow derived Mo-AMs at D14 (**Fig. 3F**), with distinctive gene expression patterns across this transitional phase between the two groups (**Fig. S4D, Data file S2**). At D7 post-bleomycin, Mo-AMs from aged bone marrow exhibited an early profibrotic profile (elevated expression of *Spp1, Col1a2, Col3a1,Timp3*), though inflammatory gene expression (*Il1b*, *Nfkb1*, *Cxcl2)* was lower compared to Mo-AMs from young bone marrow (**Fig. S4E, Data file S3**). While aged Mo-AMs upregulated *Ly-6c1, Ly-6a* and *Cd34,* a signature of their early monocytic legacy, expression of monocyte-to-macrophage differentiation markers (*Lgals3*, *Foxp1, Csf2rb*) was reduced (**Fig. S4E**) *(35, 36)*. In contrast, at D14, aged Mo-AMs displayed delayed but heightened expression of key pro-inflammatory mediators (*Nfkb1*, *Malt1*, *Jak2*), chemokines (*Ccl17, Ccl8*) and activation markers (*Cd80, Cd86*), whereas young Mo-AMs already downregulated most inflammatory genes (**Fig. 3G, Data file S4**). Aged Mo-AMs maintained a more pronounced profibrotic signature of collagenases *(Col1a1, Col1a2*), matrix metalloproteases (*Mmp12, Mmp13*), *Fnip2*, *Fgf13* and *Tgfb1*, with young Mo-AMs expressing only a specific subset of profibrotic genes *(Mmp14, Spp1, Fabp5*). By D14, young Mo-AMs had upregulated homeostatic TR-AM genes, including *Car4, Fth1, Lyz2, and CD68 (37)* along with metabolic regulators such as *Acod1* and *Mfge8,* known to mitigate the fibrotic response (*38, 39*). In contrast, Mo-AMs from recipients of aged bone marrow failed to do so (**Fig. 3G**). Together, these data show that Mo-AMs derived from an aged bone marrow experience a delayed transition towards a tissue-resident phenotype, coinciding with the slower return to homeostasis following lung injury.

Cell-intrinsic factors determine Mo-AM influx while environmental signals delay their transition with age.

To investigate the extent of cell-intrinsic and cell-extrinsic factors influencing Mo-AM phenotype, we exposed young and aged Mo-AMs/TR-AMs to identical lung microenvironments. Irradiated young recipient mice (CD45.2 background) were reconstituted with a 1:1 mix of young (GFP+) and aged (CD45.1) donor bone marrow cells (**Fig. 3H**). Post-transplant, young and aged bone marrow cells repopulated the bone marrow and lungs with a similar efficiency overall (**Fig. S5A**). However, repopulation by aged CD45.1^{+} bone marrow-derived cells was characterized by a strong skewing towards increased myeloid cells and decreased lymphoid cells in the bone marrow and lung at baseline (PBS-treated mice) (**Fig. S5B-E**). This skewed distribution persisted after bleomycin challenge (**Fig. S5F-I**). The ratio of aged Mo-AMs (and interstitial macrophages (IMs) in the PBS control mice/baseline) was

higher at D7 and D14 post-bleomycin (**Fig. 3I, 3J, S5J)**, indicating that the increased recruitment of aged Mo-AMs is due to an intrinsic myeloid bias in aged bone marrow or an increased cell-intrinsic proliferative capacity of aged monocytes/Mo-AMs. Conversely, PBS treated mice had a similar reconstitution of young and aged bone marrow-derived TR-AMs in the lungs (**Fig. 3K, 3L, S5K**), unlike the baseline TR-AM deficit observed following transplantation of aged bone marrow alone (**Fig. 2C**), with no difference in the absolute cell counts of TR-AMs at D7 and D14 post-bleomycin (**Fig. 3L**). Together, these findings suggests that, while cell-intrinsic factors determine absolute Mo-AM numbers, the presence of young hematopoietic cells may be sufficient to maintain TR-AM numbers or drive efficient Mo-AM to TR-AM transition.

Notably, lung hydroxyproline content (**Fig. 3M**) and collagen deposition in the lungs at D14 post-bleomycin was reduced in 1:1 mixed chimeric mice when compared to mice transplanted with aged cells alone (**Fig. S5L, S5M**), suggesting that young hematopoietic cells mitigate exacerbated fibrosis in spite of increased influx of aged Mo-AM. We thus speculated that fibrosis severity was not solely driven by initial Mo-AM numbers, but further determined by the immune microenvironment that shapes Mo-AM transcriptional states and transition. While Mo-AMs sorted from mice that received only aged bone marrow had upregulated key fibrotic and inflammatory genes (*Col1a1*, *Ccl17, Tgfb*) in comparison to young Mo-AMs, young and aged Mo-AMs isolated from 1:1 chimeric mice did not display these differences (**Fig. 3N)**. These findings indicate that the increased number of Mo-AMs is autonomously driven by an aged bone marrow and cell-intrinsic differences in aged monocytes/Mo-AMs. In contrast, the transcriptional phenotype acquired by Mo-AMs in the lungs, as well as their profibrotic features, seem to be regulated by extrinsic environmental factors derived from other hematopoietic cells.

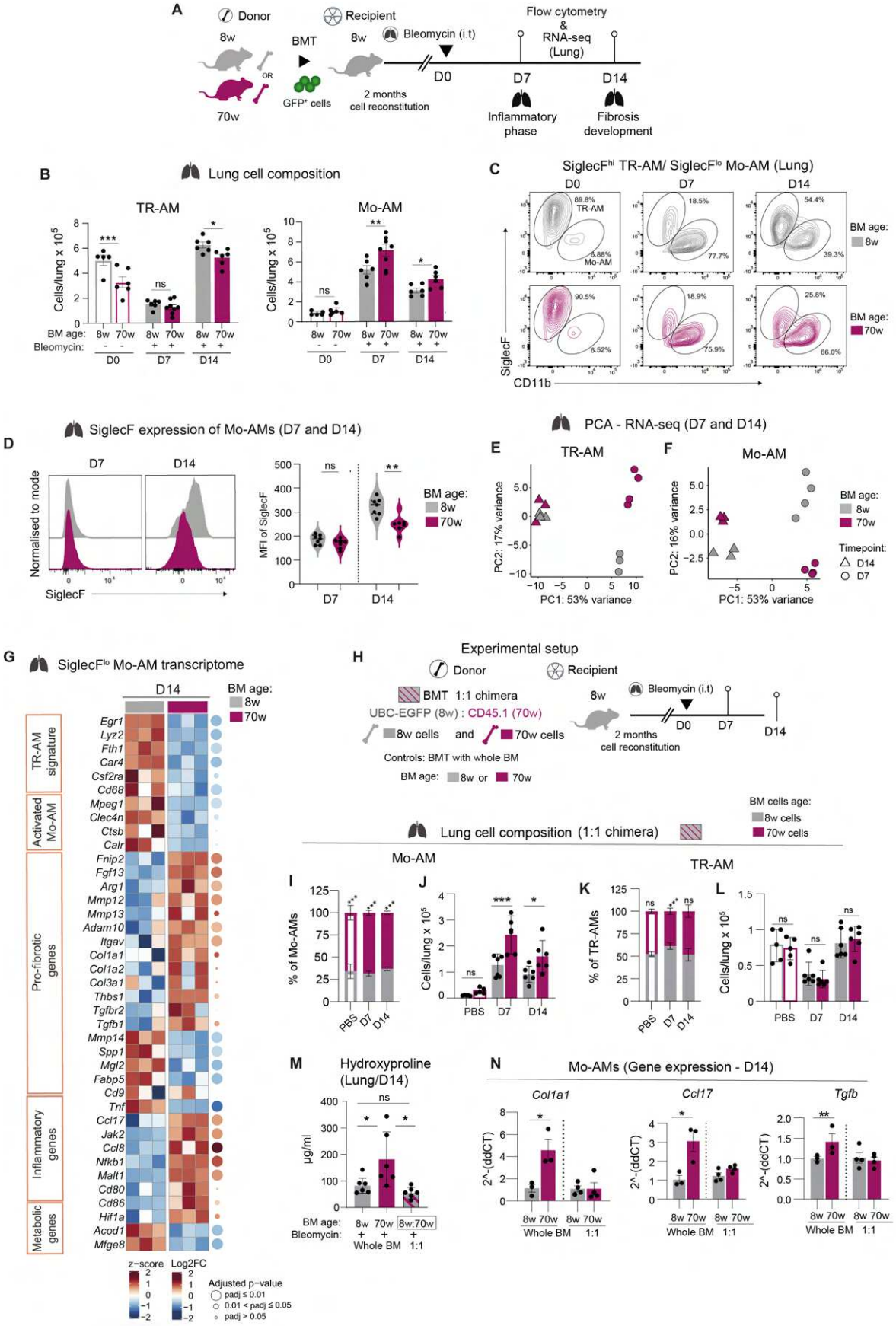

Fig. 3. Mo-AMs from aged bone marrow delay their transition into a homeostatic phenotype. **(A)** Experimental setup. **(B to G)** Lung TR-AMs and Mo-AMs from recipients of 8w or 70w bone marrow analyzed by flow cytometry and bulk RNA-seq (sorted cells,) at D7 (inflammatory phase) and D14

(fibrosis development) post bleomycin. **(B)** Absolute cell numbers of lung TR-AMs and Mo-AMs. **(C)** Representative flow cytometry plots at D0, D7, D14. **(D)** SiglecF expression on Mo-AMs at D7 and D14. Right panel-quantification of mean fluorescence intensity (MFI; a.u). **(E–F)** Principal component analysis (PCA) of sorted lung **(E)** TR-AMs and **(F)** Mo-AMs from recipients of 8w and 70w bone marrow (D7 and D14 (*n*= 4/D7 and *n*= 3/D14). **(G)** Heatmap of selected differentially expressed genes (DEGs) expressed by Mo-AMs (D14, *n*= 3/group) (*15, 16, 37, 38*). Heatmap color: z-score of normalized log(CPM) across both groups/gene; columns: individual samples; circle sizes: adjusted p-value; circle colors: log2 fold change of 70w vs 8w bone marrow recipient Mo-AMs. Extended gene list in **data file S4**. **(H)** Experimental setup for **(I to N)**. 8w recipient mice irradiated and transplanted with bone marrow cells from young (8w, GFP^+ bone marrow) and aged (70w, CD45.1 bone marrow) donor mice in a 1:1 ratio. PBS or D7, D14 post bleomycin **(I)** percentage of lung Mo-AMs within the total Mo-AM population and **(J)** absolute cell numbers of lung Mo-AMs from 8w (GFP^+) or 70w ($CD45.1^+$) cells. **(K)** Percentage of lung $SiglecF^{hi}$ TR-AMs within the total TR-AM population and **(L)** absolute cell counts of lung $SiglecF^{hi}$ TR-AMs from 8w (GFP^+) or 70w ($CD45.1^+$) cells. **(M)** Hydroxyproline quantification (lung tissue) of recipients reconstituted with 8w (grey bar), 70w bone marrow cells (purple bar) and (8w): 70w bone marrow chimera (1:1; grey and purple stripes bar) at D14 post bleomycin. **(N)** Gene expression (real-time qPCR) from lung Mo-AMs sorted from recipients of 8w or 70w whole bone marrow transplant (left panel) and 8w (GFP^+) and 70w ($CD45.1^+$) 1:1 chimeric recipient (right panel) at D14 post bleomycin. Data representative of three independent experiments (flow cytometry), *n* = 5–8 per group per time point (B-D) and n = *5-6* per time point of one independent experiment (H-N). For (B, D, I-L) a two-way ANOVA with post-hoc Tukey's multiple comparisons test, (M) one-way ANOVA and (N) two-way ANOVA with post-hoc Šídák's multiple comparisons test was used. Error bars represent SD.*P ≤ 0.05; **P < 0.01; ***P < 0.001; ns: not significant.

Hematopoietic aging decreases IL-10 availability and drives a pro-inflammatory milieu in the lung.

Given the delayed transition of aged Mo-AMs to a homeostatic TR-AM phenotype, we examined lung microenvironmental signals that might influence this process. By D7 post-bleomycin, mice reconstituted with aged bone marrow displayed an altered lung cytokine profile, with increased pro-inflammatory mediators such as IFN-γ, IL-6, CXCL1, and CCL17, but reduced IL-10 and IL-13 levels (**Fig. 4A, S6A**) with a corresponding transcriptional state in lung tissue (**Fig. S6B**). The most substantial difference between the groups post bleomycin-induced injury was the substantially lower IL-10 levels, which persisted through the inflammatory and fibrotic phases (**Fig. 4B**). As IL-10 is a key anti-inflammatory cytokine (*40*), we hypothesized that reduced IL-10 availability could impair timely resolution of bleomycin-induced lung injury. To test this, we treated young adult mice with a neutralizing IL-10 antibody intranasally between D0 and D7 (**Fig. 4C**). IL-10 neutralization strongly increased weight loss (**Fig. 4D**) and reduced predicted survival post D7 (**Fig. S6C**). By D7, anti-IL10 treated mice showed increased Mo-AM numbers, reduced TR-AMs, and the emergence of a $CD11c^{low}$ $CD11b^{hi}$ SiglecF+ (TR)-AM population (**Fig. 4E, S6D**), suggesting that IL-10 maintains homeostatic TR-AMs. To assess if IL-10 had an impact onMo-AM maturation, we neutralized IL-10 in the lungs from D7 to D14 post-bleomycin challenge (**Fig. 4C**). While body-weight loss was unaffected (**Fig. 4F**), IL-10 neutralization increased Mo-AM accumulation by D14 (**Fig. 4G, 4H**), with a decreased resolutory ($CD206^+$) (*41*) and increased activated ($CD86^+$) (*42*) Mo-

AM phenotype (**Fig. S6E**), indicating that IL-10 is necessary for efficient Mo-AM transition into a homeostatic state.

We next asked if Mo-AM differentiation or activation was influenced by IL-10 in the lung microenvironment. Single cell RNA sequencing (scRNA-seq) of immune cells from the BALF of young adult mice identified three populations of macrophages in the alveolar space during the inflammatory phase (D7) post bleomycin challenge: TR-AMs (cluster 0 *Lyz2*, *Ccl6*, *Ftl1* expression), cells of recent monocyte origin or early Mo-AMs (cluster 1, high *Ccr2*, *CD74*, *H2-A* expression) and profibrotic Mo-AMs (cluster 2 with high expression of *Mafb*, *Mmp14*, *Itgam*, *Cd36*) (**Fig. 4I, S6F, S6G**). Only cluster 2 profibrotic Mo-AMs expressed elevated levels of *Il10rb*, encoding the IL-10 receptor (**Fig. 4J, Data file S5**). Further transcriptomic analysis of Mo-AMs revealed that IL-10 signaling downstream targets, including *Tnip3, Etv3, Cd80, Cd86,* and *Stat3* (*43, 44*), were induced in young Mo-AMs at D7 and promptly downregulated by D14, while aged Mo-AMs showed a deferred expression of these genes by D14 (**Fig. 4K**).

To assess the direct effects of IL-10 on Mo-AM phenotype, we sorted Mo-AMs from young or aged mice on D7 post-bleomycin and stimulated them *ex-vivo* with IL-10 (**Fig. 4L**). At baseline (without stimulation), aged Mo-AMs showed increased IL-6, CXCL1 and CCL17 cytokine secretion and gene expression levels compared to young Mo-AMs (**Fig. 4M, S6H, S6I**). IL-10 stimulation efficiently suppressed this inflammatory signature in both groups (**Fig. 4M, S6H, S6I)**, demonstrating comparable responsiveness to IL-10. Conversely, GM-CSF, essential for TR-AM maintenance (39), had no impact on the inflammatory profile (**Fig. S6J**). These data highlight the importance of environmental IL-10 in determining the Mo-AM response at this early juncture and that suppressed IL-10 levels, such as during hematopoietic aging, sustains their inflammatory phenotype.

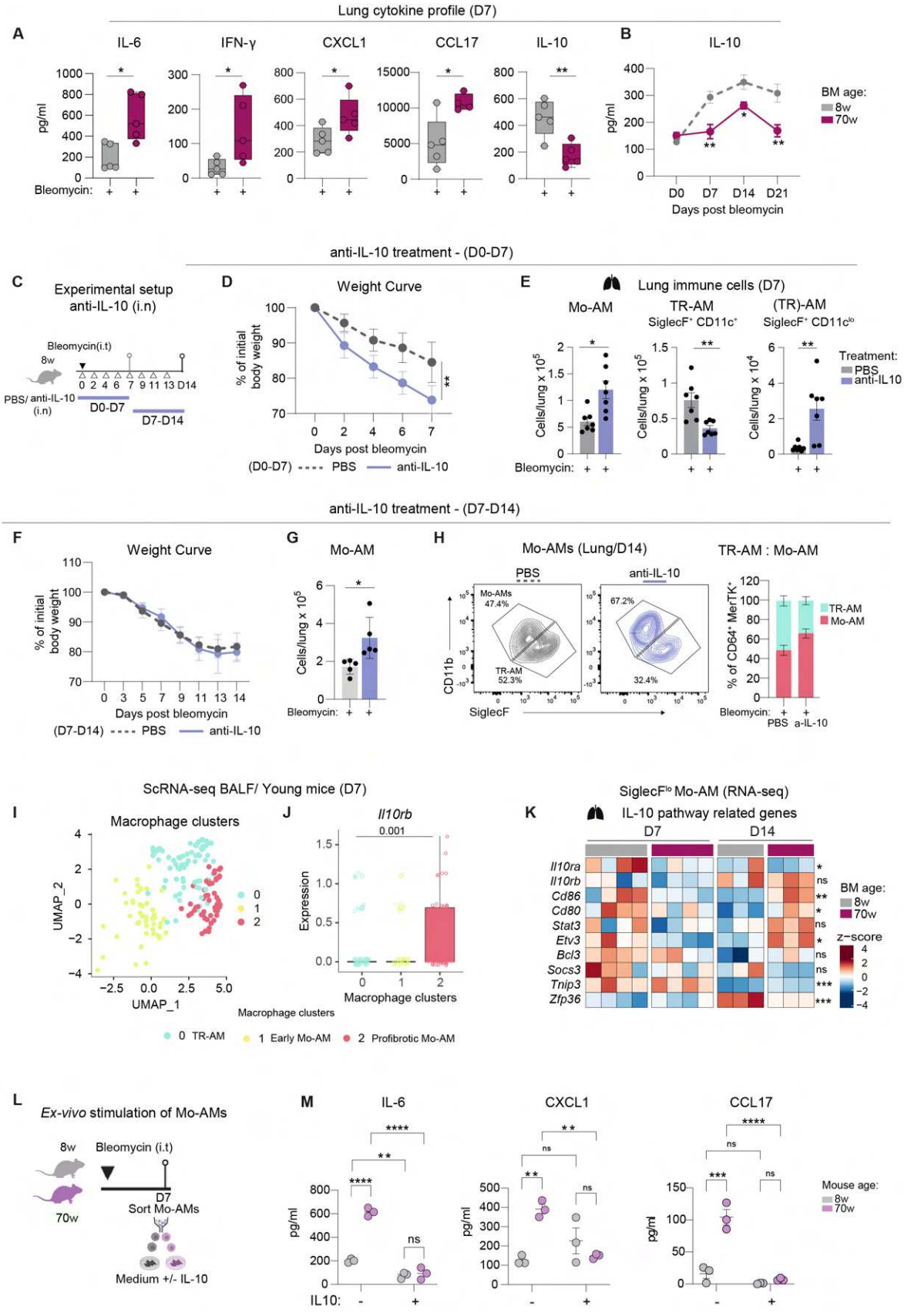

Fig. 4. Hematopoietic aging decreases IL-10 availability and drives a pro-inflammatory milieu in the lung.

(A) Cytokine analysis of lung homogenates from recipients of 8w and 70w bone marrow at D7 post bleomycin. **(B)** ELISA of IL-10 from lung homogenate at D0, D7, D14 and D21 post bleomycin. **(C)**

Experimental set up for **(D to I)**: 8-week-old C57BL/6J mice were given bleomycin (i.t) and intranasally (i.n) treated with anti-IL-10 antibody or PBS at the indicated time points (D0-D7) or (D7-D14) until an endpoint of D7 or D14. **(D)** Weight curve until D7. **(E)** Absolute numbers of lung myeloid cells (Mo-AMs, TR-AMs (SiglecF^{hi} CD11b^{lo} CD11c^{hi}), (TR)-AM-like cells (SiglecF^{hi} CD11b^{lo} CD11c^{lo})). **(F)** Weight curve until D14. **(G)** Absolute numbers of lung Mo-AMs -D14 **(H)** Representative flow cytometry plots and bar graphs showing percentage of TR-AMs and Mo-AMs expressed as a percentage of MerTK^{+} CD64^{+} cells. **(I)** Seurat clustering of three macrophage populations identified from ScRNA-seq from the BALF of 8-week-old mice at D7 post bleomycin (Cluster gene list in data file**S5**). **(J)** Expression of *Il10rb* on Clusters 0 (TR-AMs), 1 (early Mo-AMs) and 2 (profibrotic Mo-AMs). **(K**) Heatmaps of transcriptomic analysis of selected IL-10 related genes on sorted lung Mo-AMs from recipients of 8w and 70w bone marrow at D7 and D14 post bleomycin (n = 3–4 per group). Heatmap color represents z-score of log(CPM) normalized expression across all 4 groups (8w/D7; 70w/D7; 8w/D14; 70w/D14) per gene. Columns represent individual samples (gene expression data in data file **S3** and **S4** for D7 and D14, respectively). **(L)** Experimental set-up **(M to N).** Mo-AMs were sorted from 8w or 70wd WT mice at D7 after bleomycin and cultured ex-vivo for 24 hours in medium with or without IL-10 (n = 4 per group, cells sorted and pooled together in 3 technical replicates per group). **(M)** Cytokine secretion analysis 24 hours post-culture/stimulation (absolute values in pg/ml). For (F-G) BALF cells from six mice were pooled and sequenced. For (A, E, G, H) Student's two tailed unpaired t-test, (B) multiple unpaired t-test, (D,F) and (K, M) a two-way ANOVA with post-hoc Bonferroni and Tukey's multiple comparisons test, respectively (overall column factor for K, individual comparisons in data file S10) and (J) a Wilcoxon-Rank Sum test with Bonferroni correction (Seurat) was used. Error bars represent SEM or SD *P ≤ 0.05; **P < 0.01; ***P < 0.001; ns: not significant.

Hematopoietic aging restricts lung IL-10-producing Tregs upon lung injury.

To identify cellular sources of IL-10 in the lung environment affected by hematopoietic aging, we analyzed intracellular IL-10 in major lung immune cells post-bleomycin. Bone marrow age did not affect IL-10 levels in IL-10-producing innate immune cells, including neutrophils, TR-AMs, Mo-AMs, IMs, ILCs, and NK cells (**Fig. S7A**) (*45*). However, CD4^{+} T cells in young mice engrafted with aged bone marrow produced less IL-10 upon bleomycin challenge **(Fig. 5A)**. Specifically, CD25^{+} cells, and CD4^{+} CD25^{+} Foxp3^{+} regulatory T cells (Tregs) had lower IL-10 levels **(Fig. S7B, 5B).** Although the total number of CD4^{+} T cells post-bleomycin challenge was similar **(Fig. S7C)**, IL-10^{+} CD4^{+} T cell abundance was lower in recipients of aged bone marrow **(Fig. 5C;** gating strategy in **S7D)** with a reduced frequency of Foxp3^{+} Tregs amongst IL-10^{+} immune cells (**Fig. S7E**). While Tregs expanded upon bleomycin injury in both groups, an aged bone marrow curtailed Treg expansion (**Fig. 5D, 5E**) at both the inflammatory (D7) and fibrotic (D14) phases, with pronounced reductions of the IL-10^{+} subset **(Fig. 5F)**. In contrast, CD49b^{+} Lag3^{+} type 1 regulatory T (Tr1) cells, other known IL-10 producers (*46*), were unaffected by bone marrow age **(Fig. S7F).** The diminished Treg expansion was associated with increased Th1 (T-bet^{+}) and reduced Th17 (Rorγt^{+}) numbers (**Fig. S7G**).

While Tregs can be radioresistant (*47*), young host-derived Tregs in the lungs were minimal (**Fig. S7H**) and all IL-10^{+} Foxp3^{+} were donor-derived (**Fig. S7I**). A reduction in IL-10^{+} Tregs was also recapitulated in naturally aged mice post-bleomycin **(Fig. S7J, S7K**). Using the thoracic shielding model to distinguish between tissue-resident (GFP$^{–}$) and peripheral (GFP^{+})

Tregs, we found a specific reduction in lung GFP$^+$ Foxp3$^+$ and GFP$^+$ IL-10$^+$ Tregs (**Fig. 5G**) and IL-10 levels (**Fig. S7L**) in mice engrafted with aged bone marrow. Collectively, our results show that reduced IL-10 in the lungs of naturally aged mice and recipients of aged bone marrow display impaired recruitment of IL-10$^+$ Tregs following bleomycin challenge.

Transcriptomic analysis of CD25$^+$ CD4$^+$ T cells on D7 post-bleomycin revealed significant differences in the expression of key Treg markers (*48*), including *Ctla-4, Icos,* and *Tnfrsf18l* (**Fig. 5H, Data file S6**). In mice that received aged bone marrow, there was a notable reduction in the absolute numbers of ICOS$^+$ and GITR$^+$ Tregs (**Fig. S8A**) and a shift towards Th1-like Tregs (Tbet$^+$), while no differences were detected in Th17-like (Rorγt$^+$) or Th2-like Tregs (Gata3$^+$) (**Fig. S8B, S8C**), indicating that hematopoietic aging leads to both numerical and transcriptional alterations in lung Tregs.

To contextualize these findings, we integrated data from the Human Lung Cell Atlas (HLCA) (*49*), comparing transcriptional profiles from young and aged healthy individuals, IPF patients, and young and aged COVID-19 patients. We used COVID-19 samples to compare young and aged individuals post-acute lung injury, given that IPF data are predominantly derived from aged patients with end-stage disease (**Fig. S8D, Data file S7**). Tregs (**Fig. S8E**) from healthy aged individuals showed increased expression of *IFNG*, indicating a Th-1-like shift similar to our observations in mice, while the levels of *CTLA4, FOXP3,* and *IL2RA* tended to be lower (**Fig. 5I, Table S8**). Aged Tregs were also enriched for inflammation- and fibrosis-associated genes at baseline (**Fig. 5J, Data file S8**). Mo-AMs from IPF patients expressed canonical profibrotic genes (*SPP1, COL6A, FN1*) (*32, 49, 50*) (**Fig. S8F, Data file S9**). Similarly, aged COVID-19 Mo-AMs exhibited an activated, profibrotic phenotype with elevated *FCN1*, *CXCL8*, *CCL4* and *PDGFA* expression (*51*) (**Fig. S8F**). Together, these data show that hematopoietic aging hampers the Treg response, reducing Treg-derived IL-10 in mice, with aged-related Treg alterations also observed in aged human lung samples.

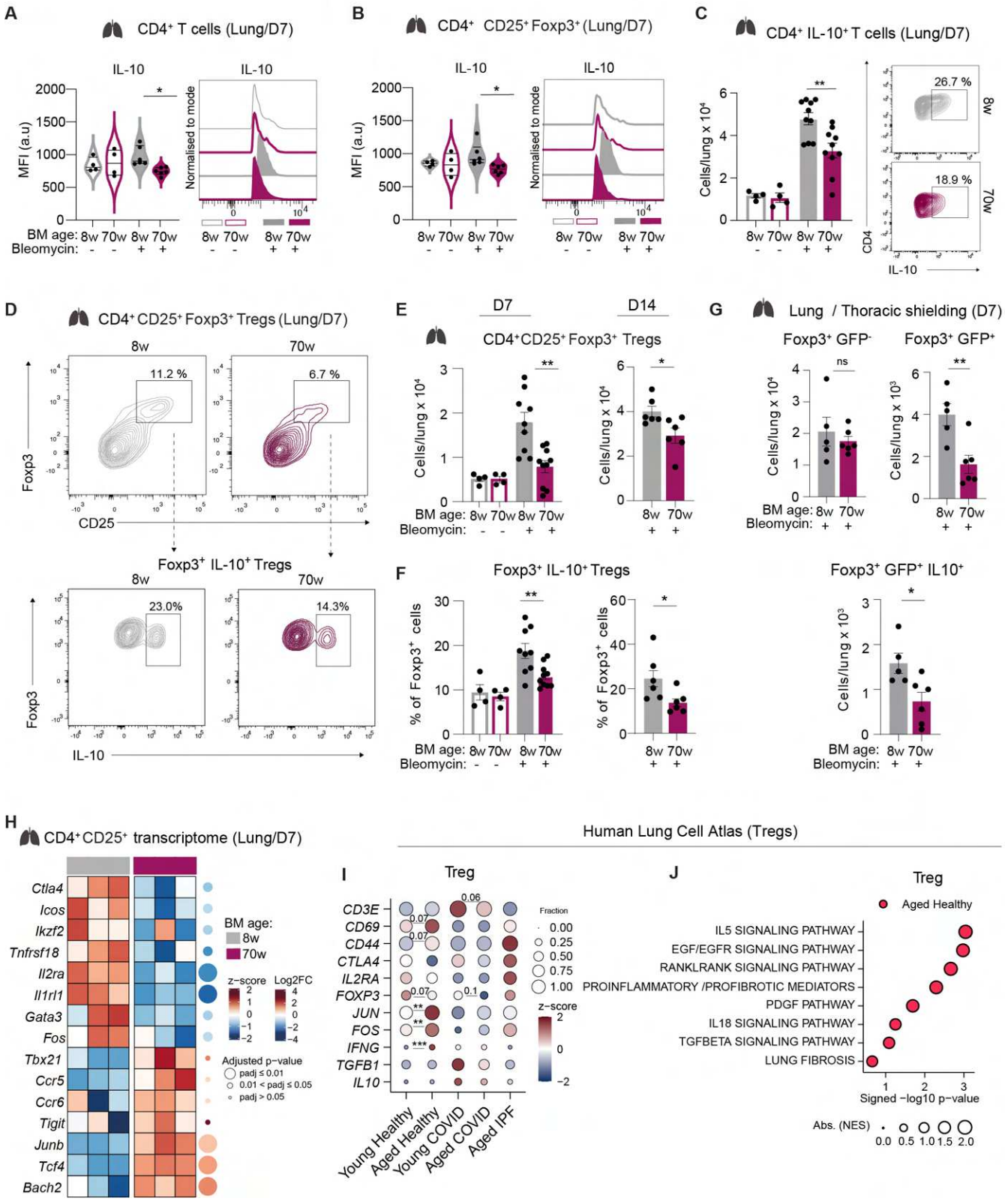

Fig. 5. Hematopoietic aging restricts lung IL-10-producing Tregs upon lung injury
(A) Histograms of intracellular IL-10 staining and MFI quantification of IL-10 by flow cytometry of lung CD4⁺ T cells from recipients of (8w) or (70w) bone marrow at D7 (PBS/bleomycin treatment). **(B)** Histograms of intracellular IL-10 staining of lung CD4⁺ CD25⁺ Foxp3⁺ cells and MFI quantification of IL-10. **(C)** Absolute cell numbers of lung CD4⁺ IL-10⁺ T cells, representative flow cytometry plots of

percentage of lung IL-10$^+$ CD4$^+$ T cells from recipients of (8w) and (70w) bone marrow at D7 post bleomycin. **(D)** Representative flow cytometry plots of (top panel) lung CD4$^+$ CD25$^+$ Foxp3$^+$ cells, (bottom panel) Foxp3$^+$ IL-10$^+$ cells D7 post bleomycin. **(E)** Absolute cell numbers of lung CD4$^+$ CD25$^+$ Foxp3$^+$ cells and **(F)** Percentage of Foxp3$^+$ cells expressing intracellular IL-10 of PBS-treated, D7 and D14 post bleomycin (*n* =4-10). **(G)** Absolute numbers of lung CD4$^+$ Foxp3$^+$ GFP$^-$ or GFP$^+$ and Foxp3$^+$ GFP$^+$ IL-10$^+$ cells from recipients of irradiation with thoracic shielding at D7 post bleomycin (*n* = 5–6). **(H)** Transcriptomic analysis of CD4$^+$ CD25$^+$ lung cells sorted at D7 post bleomycin from the lungs of recipients of 8w or 70w bone marrow. Heatmap depicting selection of DEGs (*n* = 3/group). **(I)** Transcriptomic analysis of Tregs from the Human Lung Cell Atlas. Heatmap showing selection of gene expression with a z-score per gene across all groups – Young Healthy, Aged Healthy, Young COVID, Aged COVID and Aged IPF (see methods). **(J)** Gene set enrichment analysis showing selected significantly enriched pathways in Tregs from Aged Healthy samples**.** Data representative of three independent experiments (A-F) or two independent experiments (G). Symbols on bar graphs represent individual mice. For (A, B,C,E (D7), F (D7)) a two-way ANOVA with post-hoc Tukey's multiple comparison, (E (D14), F (D14), G) a Student's two tailed unpaired t-test and was used. For (H, I, J) DEA by Limma was used (data file S8). Error bars represent SEM. *P ≤ 0.05; **P < 0.01; ***P < 0.001; ns: not significant.

IL-10-producing Tregs promote Mo-AM maturation and attenuate fibrosis.

To examine whether T-cell-derived IL-10 impacts Mo-AM responses and fibrosis development, we generated 1:1 mixed bone marrow chimeras using TCR-α$^{-/-}$ and IL-10$^{-/-}$ bone marrow (**Fig. S9A**), which lack IL-10-producing T cells but retain functional B and myeloid compartments. Controls included WT (8w:8w or 70w:70w), TCR-α KO:WT (8w), or IL-10 KO:WT (8w) chimeras (**Fig. S9A**). TCR-α KO:IL-10$^{-/-}$ chimeras exhibited increased disease severity post-bleomycin compared to controls (**Fig. S9B, S9C**) and reduced IL-10 levels, confirming T cells as a major IL-10 source in the lungs (**Fig. S9D**). While Mo-AM numbers were comparable to WT controls at D7 (**Fig. S9E**), they remained elevated by D14 (**Fig. S9F**), indicating persistent Mo-AM accumulation in the absence of T-cell-derived IL-10.

Transcriptomic and cellular interaction analysis among IL-10-expressing cell types (TR-AMs, Mo-AMs, monocytes, CD4$^+$CD25$^–$, and CD4$^+$CD25$^+$ cells) suggested that CD25$^+$ T cells were the primary IL-10 source interacting with IL-10R-expressing monocytes and Mo-AMs in young bone marrow recipients **(Fig. 6A**). This interaction was reduced in recipients of aged bone marrow (**Fig. 6B, S9G**). Moreover, intravenous (i.v.) labeling of CD45$^+$ cells at D7 post bleomycin challenge revealed that Tregs, like Mo-AMs, localized to the lung parenchyma (**Fig. S9H, S9I**) and immunohistology demonstrated that Foxp3$^+$ cells were in close proximity to F4/80$^+$ macrophages in bleomycin-challenged lungs (**Fig. S9J**).

We therefore asked how the reduction of these CD25$^+$ T cells observed upon hematopoietic aging impacted the disease course and Mo-AM response. Partial depletion of CD25$^+$ cells including Tregs, with an anti-CD25 antibody, during the inflammatory phase post-bleomycin (D(-2) to D7) (**Fig. S10A, S10B**), caused weight loss (**Fig. S10C**) and decreased lung IL-10 levels (**Fig. S10D**) but had no impact on Mo-AM numbers at D7 (**Fig. S10E**). In contrast,

depletion during the fibrotic phase (D7 to D14) (**Fig. S10F**) did not affect body weight (**Fig. S10G**) but increased Mo-AM accumulation by D14 (**Fig. S10H-J**). To model the age-related reduction in Tregs observed throughout the disease course (**Fig. 5E**), we used DEREG Foxp3-EGFP reporter mice and partially depleted Tregs via i.t. Diphtheria toxin (DT) administration between D(-2) and D14 (**Fig. 6C, Fig. S10K**). Both IL-10^{+} and IL-10^{-} Treg numbers were reduced, and this was further associated with an expansion of T-bet^{+} T-helper cells during fibrosis (**Fig. S10L**), thus resembling key features we had observed upon hematopoietic aging. Treg reduction led to a pronounced decrease in body weight (**Fig. 6D**), increased collagen deposition, higher Ashcroft score (**Fig. 6E, F**), lower lung IL-10 levels and elevated inflammatory cytokines (**Fig. 6G, S10M**) as compared to control mice. DEREG mice had elevated numbers of Mo-AMs at D14 with lower SiglecF expression levels (**Fig. 6H, 6I, 6J)**, indicating delayed Mo-AM maturation.

To verify if Treg depletion specifically during the fibrotic development phase impacted Mo-AM transition, we treated Foxp3-DTR mice (*52*), a model that allowed us to efficiently ablate Tregs over a shorter period of time, with DT administered only from D7 to D14 post-bleomycin (**Fig. 6K, S10N, S10O**). This resulted in increased weight loss (**Fig. S10P**), elevated lung hydroxyproline levels (**Fig. S10Q**), Mo-AM accumulation with lower SiglecF expression (**Fig. 6L, 6M, 6N**), a reduction in resolutory-like (CD206^{+}) Mo-AMs and an increase in activated Mo-AMs (CD86^{+}) (**Fig. S10R**) compared to control mice. This was confirmed in a bone marrow transplant model using Foxp3-DTR or Rosa26iDTR donors to compare DT treatment during the full course (D0-D14) versus the fibrotic phase (D7-D14) post-bleomycin challenge (**Fig. S10S, S10T**). Mice lacking Tregs exhibited weight loss and increased Mo-AM accumulation, while DT treatment alone caused no adverse effects in PBS-treated controls (D0-D14) (**Fig. S10U, S10V**).

Finally, to determine if Foxp3-Treg-derived IL-10 specifically reduces Mo-AM accumulation, independent of other Treg mechanisms, we generated 1:1 mixed bone marrow chimeras using Foxp3-DTR and IL-10$^{-/-}$ donors. This setup allowed assessment of IL-10's role in Mo-AM transition without fully depleting Tregs (**Fig. 6O**). Control groups were transplanted with a 1:1 ratio of Foxp3-DTR: Foxp3-DTR; Foxp3-DTR: 8w old WT; or Foxp3-DTR: 70w old WT bone marrow. Post reconstitution, all groups received DT treatment (D0-D14). Mixed chimeras of Foxp3-DTR with either aged bone marrow or IL-10$^{-/-}$ bone marrow exhibited pronounced weight loss, similar to mice completely lacking Tregs (reconstituted only with Foxp3-DTR) (**Fig. 6P**), and had elevated lung hydroxyproline levels (**Fig. S11A**) when compared to mice that received young bone marrow. Mice deficient in IL-10-producing Tregs had increased numbers of lung Mo-AMs at D14 (**Fig. 6Q**) that had low SiglecF expression (**Fig. 6R**), akin to those devoid of Tregs. This indicates that the absence of IL-10 from Tregs, even without a notable reduction in Treg numbers (**Fig. S11B**), is sufficient to cause Mo-AM accumulation,

supporting the critical role of Treg-derived IL-10 as a mediator that facilitates the efficient maturation of Mo-AMs. This parity between the depletion of IL-10-producing Tregs and their reduction due to hematopoietic aging underscores their essential regulatory role in shaping Mo-AM transition and lung fibrosis outcome post bleomycin challenge.

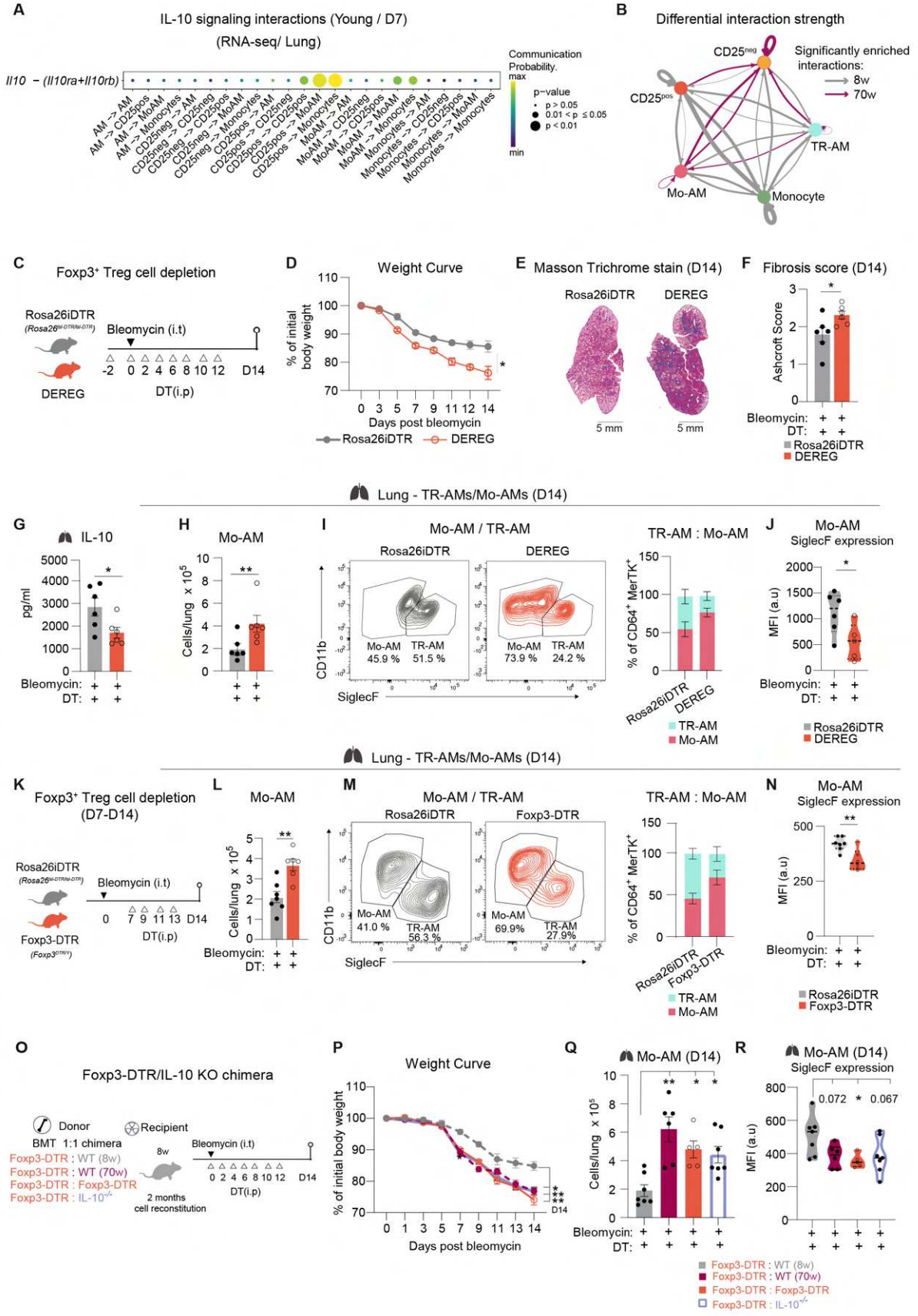

Fig. 6. IL-10-producing Tregs promote Mo-AM maturation and attenuate fibrosis.
(A-B) CellChat analysis from transcriptomic data of sorted lung cell populations: TR-AMs, Mo-AMs, monocytes, CD4+ CD25+ and CD4+ CD25− T cells from recipients of 8w or 70w bone marrow (D7/post

bleomycin). **(A)** Receptor-ligand interactions of IL-10 signaling pathway from recipients of 8w bone marrow. **(B)** Differential interaction strength between the given cell types. Enriched interactions: grey (8w) and purple (70w). Arrow direction: interaction flow, arrow weight: interaction strength. **(C)** Experimental set up for **(D-J)**. DEREG mice or Rosa26iDTR (*Rosa26$^{lsl\text{-}DTR/lsl\text{-}DTR}$*) controls were given Diphtheria-toxin (DT) intraperitoneally (i.p) and bleomycin (i.t) at specified time points (*n* = 6-7 per group). **(D)** Body weight curve until D14. **(E)** Histological lung sections -Masson Trichrome stain. **(F)** Modified Ashcroft fibrosis score of lung histology at D14 post bleomycin. **(G)** IL-10 levels from lung homogenates (ELISA). **(H)** Absolute numbers of lung Mo-AMs. **(I)** Representative flow cytometry plots and TR-AMs and Mo-AMs expressed as a percentage of MerTK$^+$ CD64$^+$ cells. **(J)** Mean fluorescence intensity of SiglecF expression on Mo-AMs. **(K)** Experimental set up for **(L-N)**. Foxp3-DTR (*Foxp3$^{DTR/Y}$*) or Rosa26iDTR (*Rosa26$^{lsl\text{-}DTR/lsl\text{-}DTR}$*) mice were given bleomycin (i.t; D0), and DT (i.p) from D7 until D14 (endpoint), every two days. **(L)** Absolute cell numbers of lung Mo-AMs. **(M)** Representative flow cytometry plots and TR-AMs and Mo-AMs expressed as a percentage of MerTK$^+$ CD64$^+$ cells. **(N)** Mean fluorescence intensity of SiglecF expression on Mo-AMs. **(O)** Experimental set up for **(P to R)**. 8-w-old mice were irradiated and transplanted a 1:1 ratio of bone marrow cells: (Foxp3-DTR : WT (8w)); (Foxp3-DTR : WT (70w)); (Foxp3-DTR:Foxp3-DTR); (Foxp3-DTR: IL-10$^{-/-}$), challenged with bleomycin (i.t; D0) 2 months post-transplant, and administered DT every 2 days from D0 until D14 (endpoint). **(P)** Body weight curve. **(Q)** Absolute cell counts of lung Mo-AMs (D14). **(R)** Mean fluorescence intensity of SiglecF expression on Mo-AMs. Data representative of one or two independent experiments. For (D,P) a two-way ANOVA post-hoc Tukey's multiple-comparison test, for (F-N) a Student's two tailed t test was used. For (Q-R) one-way ANOVA with post-hoc Dunnett's multiple comparisons to the Foxp3-DTR:WT (8w) group as the control was used. Error bars represent SEM. *P ≤ 0.05; **P < 0.01; ***P < 0.001; ns: not significant.

DISCUSSION

Tissue injury triggers a cascade of inflammatory events, recruiting and activating immune and non-immune cells to coordinate repair (*4*). With age, there is increasing aberration in these processes leading to chronicity of injury and tissue fibrosis. Despite significant research advances (*53, 54*), lung transplantation remains the only treatment for advanced disease (*53, 54*). Critical gaps persist in understanding the fine interplay between aging structural and immune cells that determine the fate of an injured lung. Here, we investigated the impact of hematopoietic age on lung fibrosis by decoupling it from the aging lung tissue. We found that, irrespective of the lung tissue or tissue-resident cell age, bone marrow age determines Mo-AM influx and fibrosis severity. Exacerbated fibrosis in recipients of aged bone marrow was not only associated with increased Mo-AM numbers but was fueled by a delayed transition of inflammatory, profibrotic Mo-AMs into a tissue-resident homeostatic state. We found that Treg-derived IL-10 was a key factor that dampens pro-inflammatory Mo-AMs upon lung injury and this axis was hampered with age.

Bone marrow-derived Mo-AMs are key drivers of lung fibrosis (*15, 16, 20, 55*), with Mo-AM-like, scar-associated macrophages of monocytic origin observed to cluster around fibrotic foci in the lungs of IPF patients (*56*). In models of bleomycin- and asbestos-induced fibrosis (*25*), the increased presence of Mo-AMs in fibrosis-susceptible, aged mice has been explained by age-related dysregulation of epithelial cell differentiation and increased epithelial barrier

permeability (*25*). However, this is based on studies conducted in naturally aged mice, where age-related aberrations in all cell compartments simultaneously manifest. Here, using heterochronic transplantation, we disentangled age-related effects of lung structural cells from those of bone marrow-derived immune cells. We observed that young mice receiving aged bone marrow exhibited an influx of Mo-AMs comparable to naturally aged mice upon bleomycin injury and this was reversed when aged mice received young bone marrow.

Similar to naturally aged mice (*20*), young recipients of aged bone marrow had fewer TR-AMs at baseline. Inadequate self-maintenance by aged resident macrophages could lead to their increased substitution by bone-marrow derived macrophages over time. This is supported by recent findings showing progressive replacement of fetal macrophages with bone marrow-derived macrophages during aging in naive mice (*13*). The macrophage-niche model underscores niche availability as a core pre-requisite for monocyte engraftment and differentiation to macrophages (*57*). Our findings using the thoracic shielding model indicate that while niche space may influence monocyte/Mo-AM turnover under homeostasis, its sole availability does not explain the heightened monocyte/Mo-AM infiltration observed in recipients of aged bone marrow after bleomycin injury given similar numbers of host-derived tissue resident macrophages. In 1:1 bone marrow chimeras, aged Mo-AMs outcompeted young cells, suggesting that the influx is driven by the output, differentiation, or homing potential of aged bone marrow progenitors, independent of the lung resident cell niche. While our study focuses on the transition phase of Mo-AM as they start adopting a TR-AM-like fate, the aged bone marrow could already have an impact on monocyte function and transition, which warrants further work.

Restoring barrier integrity post-injury is a critical step and involves the differentiation of alveolar type 2 (AT2) cells into alveolar type 1 (AT1) cells, which are crucial for gas exchange (*58*). We found that repopulation of the lung with aged immune cells, while inducing heightened inflammation and cell infiltration to bleomycin-induced lung injury, did not alter the degree of initial injury to the lung tissue in the readouts we tested. A previous study mechanistically showed that early inflammatory signals from monocyte-derived macrophages in the lung were needed to prime AT2 cells for differentiation (*59*). However, prolonged activation led to the formation of a dysregulated intermediate cell state, hampering barrier repair (*59, 60*). In line with this, we observed that young Mo-AMs exhibited an early inflammatory signature, which they promptly downregulated and began differentiating into homeostatic TR-AMs. Conversely, aged Mo-AMs retained and exacerbated an inflammatory and profibrotic profile over time. We speculate that the failure of aged Mo-AMs to efficiently transition out of this early activated state contributes to impaired epithelial restoration and increased fibrosis with age.

The infiltration and subsequent differentiation of Mo-AMs are governed by signals present in the microenvironment, influencing their function and phenotype. We observed a heightened inflammatory milieu with increased levels of IFN-γ and IL-6, but reduced IL-10 in the lungs of young mice engrafted with aged bone marrow, suggesting the lack of a key resolutory mediator. IL-10 has been shown to play a regulatory role in fibrosis by limiting IL-17A-driven fibrotic pathology and reducing profibrotic TGF-β activity (*61*). However, its effects can be context-dependent (*37*). In our model, IL-10 functioned as an early anti-inflammatory mediator, mitigating the initial inflammatory signature of Mo-AMs in young bone marrow recipients. IL-10R signaling on macrophages has previously been shown to be crucial for maintaining mucosal homeostasis in the gut and preventing colitis by promoting the maintenance of anti-inflammatory macrophages (*62, 63*), with IL-10R loss leading to the accumulation of immature inflammatory macrophages (*64*). Conversely, in the absence of immediate inflammation, the presence of IL-10 may push Mo-AMs into a state of repair overdrive and perpetuate the fibrotic response as previously reported (*65*). However, in line with our findings, IL-10RA was specifically expressed on profibrotic macrophages in the lungs of IPF patients, underscoring a role for IL-10-dependent modulation of macrophage function during lung fibrosis.

Our work showed that reduced IL-10 in recipients of aged bone marrow was due to its decreased production by Tregs. The absence of Treg-derived IL-10 or depletion of Tregs replicated the worsened fibrosis observed in young mice transplanted with aged bone marrow. Tregs modulate the immune environment by dampening inflammation and promoting tissue repair (*66*) and, similar to the impact of IL-10, can have a dual role in fibrogenesis. While Tregs can promote fibroblast stimulation under non-inflammatory conditions (*67*), they can be anti-fibrotic, restraining inflammation and subsequent fibrosis perpetuated by effector $CD4^+$ T cells as seen in *Aspergillus fumigatus* infection-induced fibrosis (*68*) or upon sterile silicon dioxide-induced lung injury (*67*). We found that Tregs and T cell-produced IL-10 shaped the myeloid cell response during bleomycin-induced fibrosis. Although IL-10 did not directly impact the early recruitment of Mo-AMs in the lungs, it did critically influence the maturation of profibrotic Mo-AMs into homeostatic tissue-resident like cells. Furthermore, depletion of Tregs specifically during the fibrotic development phase (D7-D14) was sufficient to hamper appropriate Mo-AM maturation into a TR-AM phenotype. Our findings distinguish the early lung injury phase (D0-D7) from the fibrotic development phase (D7-D21) in the bleomycin model. Importantly, while the loss of IL-10 or Tregs during the early injury phase heightens inflammation and impacts readouts such as body weight loss, reducing IL-10 or Tregs during the fibrotic development phase drives the delayed transition of Mo-AMs without obvious effects on early inflammation.

Tregs from aged bone marrow recipients exhibited transcriptional alterations and showed a Th-1 skewing. In line with this, prior work found that aging leads to cell-intrinsic dysfunction in Tregs, impairing their ability to facilitate tissue repair in the lungs following influenza infection (*69*). We found that loss of IL-10 from Tregs alone, without significant reduction in their numbers, was sufficient to exacerbate disease severity and Mo-AM accumulation, highlighting that the loss of efficient IL-10 production by Tregs during aging leads to a dysfunctional resolutory circuit in the lungs. While we focused on the role of Treg-derived IL-10, Mo-AM maturation at different stages can be influenced by signals from other cell types, namely ILC2s (*70, 71*) and basophils (*72*). Altogether, our study highlights the overarching influence that the age of the hematopoietic system has on exacerbating lung fibrosis by promoting influx of Mo-AMs upon injury. By showing that the combination of increased numbers and stalled transition of Mo-AMs into a homeostatic state contributes to a worsened fibrotic outcome, we emphasize their crucial role in governing the tissue response to injury. Moreover, the identified Treg-driven IL-10 axis, which we show hastens Mo-AM maturation and is suppressed by an aging bone marrow, provides a promising therapeutic avenue to accelerate tissue repair and prevent the development of fibrosis.

MATERIALS AND METHODS

Study Design

The aim of this study was to investigate the impact of an aging bone marrow on the development of lung fibrosis. In this study, we used bone marrow transplant models to generate chimeric mice in which young (8-week-old) mice were transplanted with cells from young (8-week-old) or aged (70-week-old) bone marrow, allowed to reconstitute for two months before intratracheal challenge with bleomycin to induce fibrosis. We explored the impact of the aging immune system on the course of lung fibrosis via bone marrow transplant, bone marrow chimeras, flow cytometry, lung histology, microscopy, ELISA/Legendplex analysis and readouts of weight loss and survival of the mice. We further studied the impact of IL-10 and interaction between cell types involved in an IL-10-mediated resolution axis via transcriptomic analysis and the use of transgenic mice. For most experiments, two to four independent replicate experiments, unless stated in the figure legends, were conducted, all of which yielded comparable results. Data shown in this study are representative of independent experiments as described in the individual figure legends. Sample sizes were in accordance with that specified in the study protocol for animal ethics; in most mouse experiments a sample size of 4-12 (per group/time point/treatment) were determined to be needed to see a difference with a significance level of 5% and a statistical power of 0.8. The ROUT test (Q=1%) test was used to identify any outliers from the dataset. Additionally, any data points excluded due to obvious technical errors are documented in Data File S10. For most mouse experiments, a

minimum of 5-10 mice per group per experiment were used in bleomycin groups and 4- 6 mice in baseline (D0) or PBS control. Three mice per genotype were used as bone marrow donors per experiment and cells from all donors per genotype were pooled before transplant into recipients. Histopathological scoring of lung sections was conducted by an independent blinded pathologist or automated quantification. Allocation of animals into experimental groups was random at the start of the experiment. Recipient mice of different bone marrow genotypes were housed within the same cage. The number of mice, replicate experiments and statistical tests are provided in the respective figure legends.

Mice

All animal experiments performed in this study were carried out in accordance with current guidelines stipulated by the Ethical review committee of the Medical University of Vienna and the Austrian Ministry of Sciences (protocol ID BMBWF-66.009/0338-V/Jb/2019; 2022-0.726.852; VL: 2023-0.684.562;). Healthy age-matched 8–10-week-old male mice (classified as young adult mice) and 70–80-week-old male mice (aged mice) were used throughout the study. C57BL/6J mice were originally purchased from Janvier Labs and bred in-house at the Core Facility Laboratory Animal Breeding and Husbandry, Medical University of Vienna in a specific pathogen-free environment according to the Federation of European Laboratory Animal Science Associations (FELASA) guidelines. Only male mice were used throughout the study, both as recipients and bone marrow donors. All mice were matched for age and genetic background in individual experiments and fed a standard chow diet. Aged mice were housed in the same room as young mice. Within each bone marrow transplant experiment, each cage contained recipients from all groups/conditions of bone marrow donor cells to control for microbiome derived effects.

For further details on mouse strains, see Supplementary materials and methods.

Bleomycin administration

Mice were administered with Bleomycin Sulfate (Sigma Aldrich) resuspended in 30 µl of endotoxin free PBS (Sigma-Aldrich) at a dose of 1.5 U/kg (high dose, only used in Fig. 1F), or 1 U/kg (low dose, all other experiments) or with 30 µl PBS only (controls) at D0 and harvested at days 7, 14, 21 or 42 post challenge. Doses were calculated based on the average weight of the mice prior to the start of the experiment. Mice were anesthetized via intraperitoneal (i.p) injection of Ketasol (100 mg/kg; OGRIS Pharma) and Rompun (10 mg/kg; Bayer) and placed on a rodent intubation stand (BrainTree). The tongue was set aside with blunt ended forceps and 30 µl of PBS or Bleomycin Sulfate was administered intratracheally (i.t) using a 200 µl pipette. Animals were then placed on a heating pad and monitored until awake and ambulatory.

Bone marrow transplants

Whole body irradiation was performed at 6 Gy twice (2 x 6 Gy) with a 3-hour gap between irradiation rounds. For thoracic shielding, lead shields were placed over the chest during irradiation at a single dose of 9 Gy. Bone marrow cells (4 x 10^6 cells) were harvested from young (8–10 weeks) and aged (70–75 weeks) UBC-GFP, CD45.1 donors or 8–12-week-old TCR-α-/-, Foxp3-DTR, Rosa26DTR, and IL-10-/- mice, and injected retro-orbitally in 100 µl PBS, 4 hours post-irradiation. For 1:1 bone marrow chimera, 2 x 10^6 cells from each genotype were mixed before administration. Mice were housed for 2 months post-transplantation for reconstitution before experiments. For detailed protocol see supplementary methods.

In-vivo treatments

8–10-week-old WT (C57BL/6J) mice were administered 50 µl at a dose of 150 µg anti-IL-10 (clone JES5.2A5) intranasally under light isoflurane anesthesia (2% isoflurane 2 L/min O_2) (D0-D7 or D7-D14, every alternate day) or Anti-CD25 (Clone PC6) at a dose of 500 µg/mouse per time point in 200 µl PBS (D0-D7 or D7-D14, every alternate day). DEREG mice received 50 µg/kg Diphtheria Toxin (DT) i.p. on D-2, followed by 10 µg/kg every 2 days (D0–D14); Foxp3-DTR mice received 10 µg/kg DT i.p. every 2 days from D0–D14 or D7–D14. Rosa26-DTR mice were used as controls for all experiments. Further details in Supplementary materials and methods.

Cell isolation and organ processing

Bronchoalveolar lavage fluid (BALF), lungs, bone marrow, and blood were processed into single-cell suspensions for flow cytometry analysis, cell sorting, RNA-sequencing, or ex-vivo culture. For the detailed protocol on organ processing, see supplementary materials and methods.

Stimulation with PMA/Ionomycin for intracellular IL-10 detection

Cell suspensions were resuspended in 100 µl of PBS 1% BSA containing PMA (Sigma; 250 ng/mL) and Ionomycin (Sigma; 1 ug/mL) and incubated at 37°C for 4 hours. Brefeldin-A (BioLegend; 1:1000 dilution) was added in the last hour. Cells were washed in cold PBS 1% BSA, and extracellular and intracellular staining and fixing was conducted as described above.

Ex-vivo IL-10 stimulation

Mo-AMs (defined as Viable/$CD45^+$/$CD64^+$ $MerTK^+$/$SiglecF^{lo}$/$CD11b^+$ subset) were sorted from the lungs of young (8-week-old) and aged (70-week-old) mice, seven days post bleomycin treatment. Cells from four animals per groups/age were sorted and pooled together. From this

pool, 3 wells i.e technical replicates of each age group were seeded *ex-vivo* on a 96 well plate at 50,000 cells/well in RPMI 1640 containing 3% FCS and 1% penicillin-streptomycin (PS; Sigma) and stimulated with either murine IL-10 (eBioscience; 10 ng/ml) or GM-CSF (30 ng/ml, PeproTech) or control media for 24 hours. Supernatant was collected for cytokine measurement by ELISA/LEGENDPLEX, and cells were lysed in TRIzol Reagent (Invitrogen) for subsequent RNA isolation.

Histology

Lung tissue samples (the left lobe was taken from experiments without BAL collection) were fixed in 7.5 % formalin overnight, embedded in paraffin and sectioned (5 µm thickness). Sections were stained with Hematoxylin and Eosin (HE), Masson's Trichrome (Sigma-Aldrich), α-smooth muscle actin (Abcam), FoxP3 (D6O8R) rabbit mAb (Cell Signaling) followed by staining with DAB substrate (SignalStain® DAB Substrate Kit, Cell Signaling); F4/80 (D2S9R) XP® rabbit mAb (Cell Signaling) followed by staining with Vector® Red Substrate Kit, Alkaline Phosphatase (Vector Labs); Terminal deoxynucleotidyl transferase dUTP nick end labeling (TUNEL) (In Situ Cell Death Detection Kit, TMR Red, Roche) according to manufacturer's guidelines.

Microscopy

Whole section image scans were obtained using a Vectra Polaris microscope (PerkinElmer) or a TissueFAXS (TissueGnostics) at the Imaging Core Facility of the Medical University of Vienna. Images were assessed using QuPath software (Version 3.0), TissueQuest (Version 7.1) and HALO (Version 3.6.4) and assessment parameters applied to whole image scans and to all images within each experiment. For image quantification details see Supplementary materials and methods.

Ashcroft score

Evaluation of the severity of fibrosis was performed by a blinded pathologist and done using the Ashcroft scoring system (*73*). Both HE staining and Masson's Trichrome staining were utilized for evaluation purposes. Each lung section was examined microscopically using a 10x objective. Fibrosis was assessed using a score ranging from 0 to 8 for each microscopic field based on the Ashcroft criteria and the mean score was calculated.

Hydroxyproline measurement

Lungs tissue samples were weighed and snap-frozen prior to the hydroxyproline assay. The assay was conducted according to manufacturer's instructions (Sigma Aldrich, MAK463).

Cytokine and Chemokine analysis

Tissue and serum cytokines/ chemokines were measured using the LEGENDplex Mouse Macrophage/Microglia Panel (BioLegend), Mouse TH panel (BioLegend) and Mouse Inflammation panel (BioLegend). Samples were prepared according to the manufacturer's protocols and analysed by flow cytometry. Data analysis was performed using the LEGENDplex data analysis software. IL-10 (OPTeia mouse IL-10 ELISA, BD Biosciences) and TGF-β (Mouse TGF-beta 1 DuoSet ELISA, R&D Systems) were measured using ELISA following manufacturer's instructions.

RNA-isolation and qPCR

Messenger RNA was isolated with TRIzol Reagent (Invitrogen) or RNeasy Mini and Micro kits (Qiagen). For real-time PCR assays, cDNA synthesis was performed using the iScript cDNA Synthesis Kit (Biorad), according to manufacturer's protocol. Real-time PCR was performed with SYBR Green Master Mix reagents (Applied Biosystems) on a StepOnePlus Real-Time PCR System (Applied Biosystems). Transcript levels were normalized to *Gapdh*.

Bulk RNA-seq (Quant-seq)

Lung immune cells from recipients of young and aged bone marrow (7- and 14-days post-bleomycin) were sequenced using the QuantSeq 3' mRNA-Seq Library Prep Kit FWD for Illumina (Lexogen). Sequencing was performed on an Illumina NovaSeq 6000. RNA sequencing data were mapped to the GRCm39 (mm10) mouse genome using STAR v2.7.9a and analyzed for differential expression with limma-voom (limma v3.50.3). Normalized counts (log2(CPM)) were used for downstream analysis, including PCA, cell-cell interaction (CellChat), and quality control. Further details on library preparation/bioinformatics analysis are in the supplementary methods section.

Single cell RNA-seq

Single-cell RNA-seq was performed on BAL cells collected on day 7 post-bleomycin challenge from four male, 8-week-old mice. Cells were processed and sequenced using the Chromium Next GEM Single Cell 3' Reagent Kits v3.1 on an Illumina HiSeq 4000. Data were aligned and processed with the CellRanger pipeline and analyzed using Seurat v4.1.1 in R v4.2.0. For further details, see supplementary methods.

Analysis of data from Human Lung Cell Atlas

The Human Lung Cell Atlas (HLCA) v1.0 dataset was analyzed (*49*), using studies by Banovich and Kropski (2020), Kaminski (2020), Lafyatis Rojas (2019), Lambrechts (2021), Meyer (2019, 2021), Misharin Budinger (2018), Wunderlink (2021), and Zhang (2021).

Comparisons were made across lung conditions (healthy, COVID-19, IPF) and age groups (young ≤40 years, aged >40 years) for cell types: classical monocytes (cMo), non-classical monocytes (nMo), alveolar macrophages (AM), interstitial macrophages (iMac), AM proliferating, CD4 T cells (Th), and regulatory T cells (Treg). Further details are provided in the supplementary methods section.

Statistical analysis:

Data was analysed using Prism (GraphPad Prism 8.0-10.2.3; GraphPad Software Inc, San Diego, CA) and data is presented as mean ± SD or mean ± SEM (information for individual figures is in the corresponding figure legend). For comparisons between two groups, Student's two tailed t test, Mann-Whitney test or multiple t tests followed by Holm-Šídák test was used. For comparison between multiple groups, a one-way (one treatment condition) or two-way ANOVA (two treatment conditions/ different time points), followed by a Tukey's multiple comparison test, Dunnett's multiple comparison test, Šídák's multiple comparisons test, or a Bonferroni's multiple comparisons test (see Figure legends) with a single pooled variance. A log-rank (Mantel-Cox) test was used for survival curves. Statistical significance: ns, not significant; *P < 0.05, **P < 0.01, ***P < 0.001, and ****P < 0.0001. Statistical analysis for the RNA-seq analysis is presented in the respective methods section.

List of Supplementary Materials

Data file S6. Differentially expressed genes of lung TR-AM, Mo-AM, monocytes, $CD4^+$ CD25pos and $CD4^+$ CD25neg cells at D7 from recipients of 8w and 70w bone marrow.
Data file S7. Summary of studies and meta data used from the Human Lung Cell Atlas.
Data file S8. Differentially expressed genes and gene set enrichment of Tregs from the Human Lung Cell Atlas.
Data file S9. Differentially expressed genes of Mo-AMs from the Human Lung Cell Atlas.
Data file S10. Raw data file.

Supplementary table S1
Supplementary references: (*74*),(*16, 49, 52, 75-86*)

REFERENCES:

1. A. Bektas, S. H. Schurman, R. Sen, L. Ferrucci, Aging, inflammation and the environment. *Exp Gerontol* **105**, 10-18 (2018).
2. E. R. Fernandez Perez, C. E. Daniels, D. R. Schroeder, J. St Sauver, T. E. Hartman, B. J. Bartholmai, E. S. Yi, J. H. Ryu, Incidence, prevalence, and clinical course of idiopathic pulmonary fibrosis: a population-based study. *Chest* **137**, 129-137 (2010).
3. G. Raghu, D. Weycker, J. Edelsberg, W. Z. Bradford, G. Oster, Incidence and prevalence of idiopathic pulmonary fibrosis. *Am J Respir Crit Care Med* **174**, 810-816 (2006).
4. T. A. Wynn, T. R. Ramalingam, Mechanisms of fibrosis: therapeutic translation for fibrotic disease. *Nat Med* **18**, 1028-1040 (2012).
5. S. Meiners, O. Eickelberg, M. Königshoff, Hallmarks of the ageing lung BACK TO BASICS HALLMARKS OF THE AGEING LUNG. *Eur Respir J* **45**, 807-827 (2015).
6. S. Gulati, V. J. Thannickal, The Aging Lung and Idiopathic Pulmonary Fibrosis. *Am J Med Sci* **357**, 384-389 (2019).
7. J. M. Van Deursen, The role of senescent cells in ageing. *Nature 2014 509:7501* **509**, 439-446 (2014).
8. H. W. Stout-Delgado, S. J. Cho, S. G. Chu, D. N. Mitzel, J. Villalba, S. El-Chemaly, S. W. Ryter, A. M. K. Choi, I. O. Rosas, Age-Dependent Susceptibility to Pulmonary Fibrosis Is Associated with NLRP3 Inflammasome Activation. *Am. J. Respir. Cell Mol. Biol.* **55**, 252-263 (2016).
9. T. A. Wynn, K. M. Vannella, Macrophages in Tissue Repair, Regeneration, and Fibrosis. *Immunity* **44**, 450-462 (2016).
10. D. Hashimoto, A. Chow, C. Noizat, P. Teo, M. B. Beasley, M. Leboeuf, C. D. Becker, P. See, J. Price, D. Lucas, M. Greter, A. Mortha, S. W. Boyer, E. C. Forsberg, M. Tanaka, N. van Rooijen, A. Garcia-Sastre, E. R. Stanley, F. Ginhoux, P. S. Frenette, M. Merad, Tissue-resident macrophages self-maintain locally throughout adult life with minimal contribution from circulating monocytes. *Immunity* **38**, 792-804 (2013).
11. L. van de Laar, W. Saelens, S. De Prijck, L. Martens, C. L. Scott, G. Van Isterdael, E. Hoffmann, R. Beyaert, Y. Saeys, B. N. Lambrecht, M. Guilliams, Yolk Sac Macrophages, Fetal Liver, and Adult Monocytes Can Colonize an Empty Niche and Develop into Functional Tissue-Resident Macrophages. *Immunity* **44**, 755-768 (2016).
12. H. Aegerter, J. Kulikauskaite, S. Crotta, H. Patel, G. Kelly, E. M. Hessel, M. Mack, S. Beinke, A. Wack, Influenza-induced monocyte-derived alveolar macrophages confer prolonged antibacterial protection. *Nat Immunol* **21**, 145-157 (2020).
13. F. Li, F. Piattini, L. Pohlmeier, Q. Feng, H. Rehrauer, M. Kopf, Monocyte-derived alveolar macrophages autonomously determine severe outcome of respiratory viral infection. *Sci Immunol* **7**, eabj5761 (2022).
14. B. Machiels, M. Dourcy, X. Xiao, J. Javaux, C. Mesnil, C. Sabatel, D. Desmecht, F. Lallemand, P. Martinive, H. Hammad, M. Guilliams, B. Dewals, A. Vanderplasschen, B. N. Lambrecht, F. Bureau, L. Gillet, A gammaherpesvirus provides protection against allergic asthma by inducing the replacement of resident alveolar macrophages with regulatory monocytes. *Nat Immunol* **18**, 1310-1320 (2017).
15. A. V. Misharin, L. Morales-Nebreda, P. A. Reyfman, C. M. Cuda, J. M. Walter, A. C. McQuattie-Pimentel, C. I. Chen, K. R. Anekalla, N. Joshi, K. J. N. Williams, H. Abdala-Valencia, T. J. Yacoub, M. Chi, S. Chiu, F. J. Gonzalez-Gonzalez, K. Gates, A. P. Lam, T. T. Nicholson, P. J. Homan, S. Soberanes, S. Dominguez, V. K. Morgan, R. Saber, A. Shaffer, M. Hinchcliff, S. A. Marshall, A. Bharat, S. Berdnikovs, S. M. Bhorade, E. T. Bartom, R. I. Morimoto, W. E. Balch, J. I. Sznajder, N. S. Chandel, G. M. Mutlu, M. Jain, C. J. Gottardi, B. D. Singer, K. M. Ridge, N. Bagheri, A. Shilatifard, G. R. S. Budinger, H. Perlman, Monocyte-derived alveolar macrophages drive lung fibrosis and persist in the lung over the life span. *J Exp Med* **214**, 2387-2404 (2017).
16. N. Joshi, S. Watanabe, R. Verma, R. P. Jablonski, C. I. Chen, P. Cheresh, N. S. Markov, P. A. Reyfman, A. C. McQuattie-Pimentel, L. Sichizya, Z. Lu, R. Piseaux-Aillon, D. Kirchenbuechler, A. S. Flozak, C. J. Gottardi, C. M. Cuda, H. Perlman, M. Jain, D. W. Kamp, G. R. S. Budinger, A. V. Misharin, A spatially restricted fibrotic niche in pulmonary fibrosis is sustained by M-CSF/M-CSFR signalling in monocyte-derived alveolar macrophages. *Eur Respir J* **55**, 1900646 (2020).
17. A. J. Byrne, T. M. Maher, C. M. Lloyd, Pulmonary Macrophages: A New Therapeutic Pathway in Fibrosing Lung Disease? *Trends Mol Med* **22**, 303-316 (2016).
18. X. Zhou, R. A. Franklin, M. Adler, J. B. Jacox, W. Bailis, J. A. Shyer, R. A. Flavell, A. Mayo, U. Alon, R. Medzhitov, Circuit Design Features of a Stable Two-Cell System. *Cell* **172**, 744-757 e717 (2018).

19. D. Aran, A. P. Looney, L. Liu, E. Wu, V. Fong, A. Hsu, S. Chak, R. P. Naikawadi, P. J. Wolters, A. R. Abate, A. J. Butte, M. Bhattacharya, Reference-based analysis of lung single-cell sequencing reveals a transitional profibrotic macrophage. *Nat Immunol* **20**, 163-172 (2019).
20. A. C. McQuattie-Pimentel, Z. Ren, N. Joshi, S. Watanabe, T. Stoeger, M. Chi, Z. Lu, L. Sichizya, R. P. Aillon, C. I. Chen, S. Soberanes, Z. Chen, P. A. Reyfman, J. M. Walter, K. R. Anekalla, J. M. Davis, K. A. Helmin, C. E. Runyan, H. Abdala-Valencia, K. Nam, A. Y. Meliton, D. R. Winter, R. I. Morimoto, G. M. Mutlu, A. Bharat, H. Perlman, C. J. Gottardi, K. M. Ridge, N. S. Chandel, J. I. Sznajder, W. E. Balch, B. D. Singer, A. V. Misharin, G. R. S. Budinger, The lung microenvironment shapes a dysfunctional response of alveolar macrophages in aging. *J Clin Invest* **131** (4), e140299 (2021).
21. Y. Lavin, D. Winter, R. Blecher-Gonen, E. David, H. Keren-Shaul, M. Merad, S. Jung, I. Amit, Tissue-resident macrophage enhancer landscapes are shaped by the local microenvironment. *Cell* **159**, 1312-1326 (2014).
22. S. Yona, K. W. Kim, Y. Wolf, A. Mildner, D. Varol, M. Breker, D. Strauss-Ayali, S. Viukov, M. Guilliams, A. Misharin, D. A. Hume, H. Perlman, B. Malissen, E. Zelzer, S. Jung, Fate mapping reveals origins and dynamics of monocytes and tissue macrophages under homeostasis. *Immunity* **38**, 79-91 (2013).
23. J. Kulikauskaite, A. Wack, Teaching Old Dogs New Tricks? The Plasticity of Lung Alveolar Macrophage Subsets. *Trends Immunol* **41**, 864-877 (2020).
24. L. Plantier, B. Crestani, S. E. Wert, M. Dehoux, B. Zweytick, A. Guenther, J. A. Whitsett, Ectopic respiratory epithelial cell differentiation in bronchiolised distal airspaces in idiopathic pulmonary fibrosis. *Thorax* **66**, 651-657 (2011).
25. S. Watanabe, N. S. Markov, Z. Lu, R. Piseaux Aillon, S. Soberanes, C. E. Runyan, Z. Ren, R. A. Grant, M. Maciel, H. Abdala-Valencia, Y. Politanska, K. Nam, L. Sichizya, H. G. Kihshen, N. Joshi, A. C. McQuattie-Pimentel, K. A. Gruner, M. Jain, J. I. Sznajder, R. I. Morimoto, P. A. Reyfman, C. J. Gottardi, G. R. S. Budinger, A. V. Misharin, Resetting proteostasis with ISRIB promotes epithelial differentiation to attenuate pulmonary fibrosis. *Proc Natl Acad Sci U S A* **118**, (2021).
26. C. Franceschi, M. Bonafe, S. Valensin, F. Olivieri, M. De Luca, E. Ottaviani, G. De Benedictis, Inflamm-aging. An evolutionary perspective on immunosenescence. *Ann N Y Acad Sci* **908**, 244-254 (2000).
27. B. Dykstra, S. Olthof, J. Schreuder, M. Ritsema, G. de Haan, Clonal analysis reveals multiple functional defects of aged murine hematopoietic stem cells. *J Exp Med* **208**, 2691-2703 (2011).
28. M. S. Kowalczyk, I. Tirosh, D. Heckl, T. N. Rao, A. Dixit, B. J. Haas, R. K. Schneider, A. J. Wagers, B. L. Ebert, A. Regev, Single-cell RNA-seq reveals changes in cell cycle and differentiation programs upon aging of hematopoietic stem cells. *Genome Res* **25**, 1860-1872 (2015).
29. D. J. Rossi, D. Bryder, J. M. Zahn, H. Ahlenius, R. Sonu, A. J. Wagers, I. L. Weissman, Cell intrinsic alterations underlie hematopoietic stem cell aging. *Proc Natl Acad Sci U S A* **102**, 9194-9199 (2005).
30. M. Mann, A. Mehta, C. G. de Boer, M. S. Kowalczyk, K. Lee, P. Haldeman, N. Rogel, A. R. Knecht, D. Farouq, A. Regev, D. Baltimore, Heterogeneous Responses of Hematopoietic Stem Cells to Inflammatory Stimuli Are Altered with Age. *Cell Rep* **25**, 2992-3005 e2995 (2018).
31. K. Dorshkind, T. Hofer, E. Montecino-Rodriguez, P. D. Pioli, H. R. Rodewald, Do haematopoietic stem cells age? *Nat Rev Immunol* **20**, 196-202 (2020).
32. T. Tsukui, K. H. Sun, J. B. Wetter, J. R. Wilson-Kanamori, L. A. Hazelwood, N. C. Henderson, T. S. Adams, J. C. Schupp, S. D. Poli, I. O. Rosas, N. Kaminski, M. A. Matthay, P. J. Wolters, D. Sheppard, Collagen-producing lung cell atlas identifies multiple subsets with distinct localization and relevance to fibrosis. *Nat Commun* **11**, 1920 (2020).
33. S. L. Vyalov, G. Gabbiani, Y. Kapanci, Rat alveolar myofibroblasts acquire alpha-smooth muscle actin expression during bleomycin-induced pulmonary fibrosis. *Am J Pathol* **143**, 1754-1765 (1993).
34. E. L. Gautier, T. Shay, J. Miller, M. Greter, C. Jakubzick, S. Ivanov, J. Helft, A. Chow, K. G. Elpek, S. Gordonov, A. R. Mazloom, A. Ma'Ayan, W.-J. Chua, T. H. Hansen, S. J. Turley, M. Merad, G. J. Randolph, Gene-expression profiles and transcriptional regulatory pathways that underlie the identity and diversity of mouse tissue macrophages. *Nat. Immunol.* **13**, 1118-1128 (2012).
35. C. Shi, M. Sakuma, T. Mooroka, A. Liscoe, H. Gao, K. J. Croce, A. Sharma, D. Kaplan, D. R. Greaves, Y. Wang, D. I. Simon, Down-regulation of the forkhead transcription factor Foxp1 is required for monocyte differentiation and macrophage function. *Blood* **112**, 4699-4711 (2008).
36. J. Gschwend, S. P. M. Sherman, F. Ridder, X. Feng, H. E. Liang, R. M. Locksley, B. Becher, C. Schneider, Alveolar macrophages rely on GM-CSF from alveolar epithelial type 2 cells before and after birth. *J Exp Med* **218**, e20210745 (2021).
37. H. Aegerter, B. N. Lambrecht, C. V. Jakubzick, Biology of lung macrophages in health and disease. *Immunity* **55**, 1564-1580 (2022).

38. P. P. Ogger, G. J. Albers, R. J. Hewitt, B. J. O'Sullivan, J. E. Powell, E. Calamita, P. Ghai, S. A. Walker, P. McErlean, P. Saunders, S. Kingston, P. L. Molyneaux, J. M. Halket, R. Gray, D. C. Chambers, T. M. Maher, C. M. Lloyd, A. J. Byrne, Itaconate controls the severity of pulmonary fibrosis. *Sci Immunol* **5**, eabc1884 (2020).
39. K. Atabai, S. Jame, N. Azhar, A. Kuo, M. Lam, W. McKleroy, G. Dehart, S. Rahman, D. D. Xia, A. C. Melton, P. Wolters, C. L. Emson, S. M. Turner, Z. Werb, D. Sheppard, Mfge8 diminishes the severity of tissue fibrosis in mice by binding and targeting collagen for uptake by macrophages. *J Clin Invest* **119**, 3713-3722 (2009).
40. D. F. Fiorentino, A. Zlotnik, T. R. Mosmann, M. Howard, A. O'Garra, IL-10 inhibits cytokine production by activated macrophages. *J Immunol* **147**, 3815-3822 (1991).
41. E. Fraser, L. Denney, A. Antanaviciute, K. Blirando, C. Vuppusetty, Y. Zheng, E. Repapi, V. Iotchkova, S. Taylor, N. Ashley, V. St Noble, R. Benamore, R. Hoyles, C. Clelland, J. M. D. Rastrick, C. S. Hardman, N. K. Alham, R. E. Rigby, A. Simmons, J. Rehwinkel, L.-P. Ho, Multi-Modal Characterization of Monocytes in Idiopathic Pulmonary Fibrosis Reveals a Primed Type I Interferon Immune Phenotype. *Frontiers in Immunology* **12**, (2021).
42. A. V. Misharin, L. Morales-Nebreda, G. M. Mutlu, G. R. S. Budinger, H. Perlman, Flow Cytometric Analysis of Macrophages and Dendritic Cell Subsets in the Mouse Lung. *Am. J. Respir. Cell Mol. Biol.* **49**, 503-510 (2013).
43. B. K. Weaver, E. Bohn, B. A. Judd, M. P. Gil, R. D. Schreiber, ABIN-3: a molecular basis for species divergence in interleukin-10-induced anti-inflammatory actions. *Mol Cell Biol* **27**, 4603-4616 (2007).
44. A. P. Hutchins, S. Poulain, D. Miranda-Saavedra, Genome-wide analysis of STAT3 binding in vivo predicts effectors of the anti-inflammatory response in macrophages. *Blood* **119**, e110-119 (2012).
45. C. Sabatel, C. Radermecker, L. Fievez, G. Paulissen, S. Chakarov, C. Fernandes, S. Olivier, M. Toussaint, D. Pirottin, X. Xiao, P. Quatresooz, J. C. Sirard, D. Cataldo, L. Gillet, H. Bouabe, C. J. Desmet, F. Ginhoux, T. Marichal, F. Bureau, Exposure to Bacterial CpG DNA Protects from Airway Allergic Inflammation by Expanding Regulatory Lung Interstitial Macrophages. *Immunity* **46**, 457-473 (2017).
46. N. Gagliani, C. F. Magnani, S. Huber, M. E. Gianolini, M. Pala, P. Licona-Limon, B. Guo, D. B. R. Herbert, A. Bulfone, F. Trentini, C. Di Serio, R. Bacchetta, M. Andreani, L. Brockmann, S. Gregori, R. A. Flavell, M.-G. Roncarolo, Coexpression of CD49b and LAG-3 identifies human and mouse T regulatory type 1 cells. *Nat Med* **19**, 739-746 (2013).
47. N. Komatsu, S. Hori, Full restoration of peripheral Foxp3 ⁺ regulatory T cell pool by radioresistant host cells in scurfy bone marrow chimeras. *Proceedings of the National Academy of Sciences* **104**, 8959-8964 (2007).
48. A. Liston, D. H. D. Gray, Homeostatic control of regulatory T cell diversity. *Nature Rev. Immun.* **14**, 154-165 (2014).
49. L. Sikkema, C. Ramírez-Suástegui, D. C. Strobl, T. E. Gillett, L. Zappia, E. Madissoon, N. S. Markov, L.-E. Zaragosi, Y. Ji, M. Ansari, M.-J. Arguel, L. Apperloo, M. Banchero, C. Bécavin, M. Berg, E. Chichelnitskiy, M.-I. Chung, A. Collin, A. C. A. Gay, J. Gote-Schniering, B. Hooshiar Kashani, K. Inecik, M. Jain, T. S. Kapellos, T. M. Kole, S. Leroy, C. H. Mayr, A. J. Oliver, M. Von Papen, L. Peter, C. J. Taylor, T. Walzthoeni, C. Xu, L. T. Bui, C. De Donno, L. Dony, A. Faiz, M. Guo, A. J. Gutierrez, L. Heumos, N. Huang, I. L. Ibarra, N. D. Jackson, P. Kadur Lakshminarasimha Murthy, M. Lotfollahi, T. Tabib, C. Talavera-López, K. J. Travaglini, A. Wilbrey-Clark, K. B. Worlock, M. Yoshida, Y. Chen, J. S. Hagood, A. Agami, P. Horvath, J. Lundeberg, C.-H. Marquette, G. Pryhuber, C. Samakovlis, X. Sun, L. B. Ware, K. Zhang, M. Van Den Berge, Y. Bossé, T. J. Desai, O. Eickelberg, N. Kaminski, M. A. Krasnow, R. Lafyatis, M. Z. Nikolic, J. E. Powell, J. Rajagopal, M. Rojas, O. Rozenblatt-Rosen, M. A. Seibold, D. Sheppard, D. P. Shepherd, D. D. Sin, W. Timens, A. M. Tsankov, J. Whitsett, Y. Xu, N. E. Banovich, P. Barbry, T. E. Duong, C. S. Falk, K. B. Meyer, J. A. Kropski, D. Pe'Er, H. B. Schiller, P. R. Tata, J. L. Schultze, S. A. Teichmann, A. V. Misharin, M. C. Nawijn, M. D. Luecken, F. J. Theis, An integrated cell atlas of the lung in health and disease. *Nat Med* **29**, 1563-1577 (2023).
50. C. Morse, T. Tabib, J. Sembrat, K. L. Buschur, H. T. Bittar, E. Valenzi, Y. Jiang, D. J. Kass, K. Gibson, W. Chen, A. Mora, P. V. Benos, M. Rojas, R. Lafyatis, Proliferating SPP1/MERTK-expressing macrophages in idiopathic pulmonary fibrosis. *Eur. Respir. J.* **54**, 1802441 (2019).
51. D. Wendisch, O. Dietrich, T. Mari, S. Von Stillfried, I. L. Ibarra, M. Mittermaier, C. Mache, R. L. Chua, R. Knoll, S. Timm, S. Brumhard, T. Krammer, H. Zauber, A. L. Hiller, A. Pascual-Reguant, R. Mothes, R. D. Bülow, J. Schulze, A. M. Leipold, S. Djudjaj, F. Erhard, R. Geffers, F. Pott, J. Kazmierski, J. Radke, P. Pergantis, K. Baßler, C. Conrad, A. C. Aschenbrenner, B. Sawitzki, M. Landthaler, E. Wyler, D. Horst, S. Hippenstiel, A. Hocke, F. L. Heppner, A. Uhrig, C. Garcia, F. Machleidt, S. Herold, S. Elezkurtaj, C. Thibeault, M. Witzenrath, C. Cochain, N. Suttorp, C. Drosten,

C. Goffinet, F. Kurth, J. L. Schultze, H. Radbruch, M. Ochs, R. Eils, H. Müller-Redetzky, A. E. Hauser, M. D. Luecken, F. J. Theis, C. Conrad, T. Wolff, P. Boor, M. Selbach, A.-E. Saliba, L. E. Sander, SARS-CoV-2 infection triggers profibrotic macrophage responses and lung fibrosis. *Cell* **184**, 6243-6261.e6227 (2021).

52. J. M. Kim, J. P. Rasmussen, A. Y. Rudensky, Regulatory T cells prevent catastrophic autoimmunity throughout the lifespan of mice. *Nat Immunol* **8**, 191-197 (2007).
53. T. E. King, Jr., W. Z. Bradford, S. Castro-Bernardini, E. A. Fagan, I. Glaspole, M. K. Glassberg, E. Gorina, P. M. Hopkins, D. Kardatzke, L. Lancaster, D. J. Lederer, S. D. Nathan, C. A. Pereira, S. A. Sahn, R. Sussman, J. J. Swigris, P. W. Noble, A. S. Group, A phase 3 trial of pirfenidone in patients with idiopathic pulmonary fibrosis. *N Engl J Med* **370**, 2083-2092 (2014).
54. L. Richeldi, R. M. du Bois, G. Raghu, A. Azuma, K. K. Brown, U. Costabel, V. Cottin, K. R. Flaherty, D. M. Hansell, Y. Inoue, D. S. Kim, M. Kolb, A. G. Nicholson, P. W. Noble, M. Selman, H. Taniguchi, M. Brun, F. Le Maulf, M. Girard, S. Stowasser, R. Schlenker-Herceg, B. Disse, H. R. Collard, I. T. Investigators, Efficacy and safety of nintedanib in idiopathic pulmonary fibrosis. *N Engl J Med* **370**, 2071-2082 (2014).
55. L. Morales-Nebreda, A. V. Misharin, H. Perlman, G. R. Budinger, The heterogeneity of lung macrophages in the susceptibility to disease. *Eur Respir Rev* **24**, 505-509 (2015).
56. T. Fabre, A. M. S. Barron, S. M. Christensen, S. Asano, K. Bound, M. P. Lech, M. H. Wadsworth, 2nd, X. Chen, C. Wang, J. Wang, J. McMahon, F. Schlerman, A. White, K. M. Kravarik, A. J. Fisher, L. A. Borthwick, K. M. Hart, N. C. Henderson, T. A. Wynn, K. Dower, Identification of a broadly fibrogenic macrophage subset induced by type 3 inflammation. *Sci Immunol* **8**, eadd8945 (2023).
57. M. Guilliams, G. R. Thierry, J. Bonnardel, M. Bajenoff, Establishment and Maintenance of the Macrophage Niche. *Immunity* **52**, 434-451 (2020).
58. T. J. Desai, D. G. Brownfield, M. A. Krasnow, Alveolar progenitor and stem cells in lung development, renewal and cancer. *Nature* **507**, 190-194 (2014).
59. J. Choi, J. E. Park, G. Tsagkogeorga, M. Yanagita, B. K. Koo, N. Han, J. H. Lee, Inflammatory Signals Induce AT2 Cell-Derived Damage-Associated Transient Progenitors that Mediate Alveolar Regeneration. *Cell Stem Cell* **27**, 366-382 e367 (2020).
60. D. N. Kotton, E. E. Morrisey, Lung regeneration: mechanisms, applications and emerging stem cell populations. *Nat Med* **20**, 822-832 (2014).
61. M. S. Wilson, S. K. Madala, T. R. Ramalingam, B. R. Gochuico, I. O. Rosas, A. W. Cheever, T. A. Wynn, Bleomycin and IL-1beta-mediated pulmonary fibrosis is IL-17A dependent. *J Exp Med* **207**, 535-552 (2010).
62. Dror, A. Biswas, Jeremy, K. McCann, E. Conaway, Naresh, Ivan, Ziad, S. Lavoie, M. Ibourk, Deanna, Janneke, Johanna, R. Somech, B. Weiss, R. Beier, Laurie, Christen, Fernanda, Alexandre, M. Sherlock, Atul, W. Müller, J, Francisco, C. Klein, Aleixo, Bruce, Scott, Interleukin-10 Receptor Signaling in Innate Immune Cells Regulates Mucosal Immune Tolerance and Anti-Inflammatory Macrophage Function. *Immunity* **40**, 706-719 (2014).
63. E. Zigmond, B. Bernshtein, G. Friedlander, Catherine, S. Yona, K.-W. Kim, O. Brenner, R. Krauthgamer, C. Varol, W. Müller, S. Jung, Macrophage-Restricted Interleukin-10 Receptor Deficiency, but Not IL-10 Deficiency, Causes Severe Spontaneous Colitis. *Immunity* **40**, 720-733 (2014).
64. I. Patik, N. S. Redhu, A. Eran, B. Bao, A. Nandy, Y. Tang, S. El Sayed, Z. Shen, J. Glickman, J. G. Fox, S. B. Snapper, B. H. Horwitz, The IL-10 receptor inhibits cell extrinsic signals necessary for STAT1-dependent macrophage accumulation during colitis. *Mucosal Immunology* **16**, 233-249 (2023).
65. A. Bhattacharyya, K. Boostanpour, M. Bouzidi, L. Magee, T. Y. Chen, R. Wolters, P. Torre, S. K. Pillai, M. Bhattacharya, IL10 trains macrophage profibrotic function after lung injury. *Am J Physiol Lung Cell Mol Physiol* **322**, L495-L502 (2022).
66. N. Arpaia, J. A. Green, B. Moltedo, A. Arvey, S. Hemmers, S. Yuan, P. M. Treuting, A. Y. Rudensky, A Distinct Function of Regulatory T Cells in Tissue Protection. *Cell* **162**, 1078-1089 (2015).
67. S. Lo Re, M. Lecocq, F. Uwambayinema, Y. Yakoub, M. Delos, J. B. Demoulin, S. Lucas, T. Sparwasser, J. C. Renauld, D. Lison, F. Huaux, Platelet-derived growth factor-producing CD4+ Foxp3+ regulatory T lymphocytes promote lung fibrosis. *Am J Respir Crit Care Med* **184**, 1270-1281 (2011).
68. T. Ichikawa, K. Hirahara, K. Kokubo, M. Kiuchi, A. Aoki, Y. Morimoto, J. Kumagai, A. Onodera, N. Mato, D. J. Tumes, Y. Goto, K. Hagiwara, Y. Inagaki, T. Sparwasser, K. Tobe, T. Nakayama, CD103hi Treg cells constrain lung fibrosis induced by CD103lo tissue-resident pathogenic CD4 T cells. *Nat. Immunol.* **20**, 1469-1480 (2019).

69. L. Morales-Nebreda, K. A. Helmin, M. A. Torres Acosta, N. S. Markov, J. Y. S. Hu, A. M. Joudi, R. Piseaux-Aillon, H. Abdala-Valencia, Y. Politanska, B. D. Singer, Aging imparts cell-autonomous dysfunction to regulatory T cells during recovery from influenza pneumonia. *JCI Insight* **6**, (2021).
70. S. Saluzzo, A. D. Gorki, B. M. J. Rana, R. Martins, S. Scanlon, P. Starkl, K. Lakovits, A. Hladik, A. Korosec, O. Sharif, J. M. Warszawska, H. Jolin, I. Mesteri, A. N. J. McKenzie, S. Knapp, First-Breath-Induced Type 2 Pathways Shape the Lung Immune Environment. *Cell Rep* **18**, 1893-1905 (2017).
71. P. Loos, J. Baiwir, C. Maquet, J. Javaux, R. Sandor, F. Lallemand, T. Marichal, B. Machiels, L. Gillet, Dampening type 2 properties of group 2 innate lymphoid cells by a gammaherpesvirus infection reprograms alveolar macrophages. *Sci Immunol* **8**, eabl9041 (2023).
72. M. Cohen, A. Giladi, A. D. Gorki, D. G. Solodkin, M. Zada, A. Hladik, A. Miklosi, T. M. Salame, K. B. Halpern, E. David, S. Itzkovitz, T. Harkany, S. Knapp, I. Amit, Lung Single-Cell Signaling Interaction Map Reveals Basophil Role in Macrophage Imprinting. *Cell* **175**, 1031-1044 e1018 (2018).
73. T. Ashcroft, J. M. Simpson, V. Timbrell, Simple method of estimating severity of pulmonary fibrosis on a numerical scale. *J Clin Pathol* **41**, 467-470 (1988).
74. B. C. Schaefer, M. L. Schaefer, J. W. Kappler, P. Marrack, R. M. Kedl, Observation of antigen-dependent CD8+ T-cell/ dendritic cell interactions in vivo. *Cell Immunol* **214**, 110-122 (2001).
75. P. Mombaerts, A. R. Clarke, M. A. Rudnicki, J. Iacomini, S. Itohara, J. J. Lafaille, L. Wang, Y. Ichikawa, R. Jaenisch, M. L. Hooper, S. Tonegawa, Mutations in T-cell antigen receptor genes alpha and beta block thymocyte development at different stages. *Nature* **360**, 225-231 (1992).
76. R. Kühn, J. Löhler, D. Rennick, K. Rajewsky, W. Müller, Interleukin-10-deficient mice develop chronic enterocolitis. *Cell* **75**, 263-274 (1993).
77. K. Lahl, C. Loddenkemper, C. Drouin, J. Freyer, J. Arnason, G. Eberl, A. Hamann, H. Wagner, J. Huehn, T. Sparwasser, Selective depletion of Foxp3+ regulatory T cells induces a scurfy-like disease. *J Exp Med* **204**, 57-63 (2007).
78. T. Buch, F. L. Heppner, C. Tertilt, T. J. A. J. Heinen, M. Kremer, F. T. Wunderlich, S. Jung, A. Waisman, A Cre-inducible diphtheria toxin receptor mediates cell lineage ablation after toxin administration. *Nat Methods* **2**, 419-426 (2005).
79. S. Jin, C. F. Guerrero-Juarez, L. Zhang, I. Chang, R. Ramos, C. H. Kuan, P. Myung, M. V. Plikus, Q. Nie, Inference and analysis of cell-cell communication using CellChat. *Nat Commun* **12**, 1088 (2021).
80. Y. Hao, S. Hao, E. Andersen-Nissen, W. M. Mauck, S. Zheng, A. Butler, M. J. Lee, A. J. Wilk, C. Darby, M. Zager, P. Hoffman, M. Stoeckius, E. Papalexi, E. P. Mimitou, J. Jain, A. Srivastava, T. Stuart, L. M. Fleming, B. Yeung, A. J. Rogers, J. M. McElrath, C. A. Blish, R. Gottardo, P. Smibert, R. Satija, Integrated analysis of multimodal single-cell data. *Cell* **184**, 3573-3587.e3529 (2021).
81. C. Hafemeister, R. Satija, Normalization and variance stabilization of single-cell RNA-seq data using regularized negative binomial regression. *Genome Biol* **20**, 296 (2019).
82. C. S. McGinnis, L. M. Murrow, Z. J. Gartner, DoubletFinder: Doublet Detection in Single-Cell RNA Sequencing Data Using Artificial Nearest Neighbors. *Cell Systems* **8**, 329-337.e324 (2019).
83. C. Domínguez Conde, C. Xu, L. B. Jarvis, D. B. Rainbow, S. B. Wells, T. Gomes, S. K. Howlett, O. Suchanek, K. Polanski, H. W. King, L. Mamanova, N. Huang, P. A. Szabo, L. Richardson, L. Bolt, E. S. Fasouli, K. T. Mahbubani, M. Prete, L. Tuck, N. Richoz, Z. K. Tuong, L. Campos, H. S. Mousa, E. J. Needham, S. Pritchard, T. Li, R. Elmentaite, J. Park, E. Rahmani, D. Chen, D. K. Menon, O. A. Bayraktar, L. K. James, K. B. Meyer, N. Yosef, M. R. Clatworthy, P. A. Sims, D. L. Farber, K. Saeb-Parsy, J. L. Jones, S. A. Teichmann, Cross-tissue immune cell analysis reveals tissue-specific features in humans. *Science* **376**, (2022).
84. R. Lopez, J. Regier, M. B. Cole, M. I. Jordan, N. Yosef, Deep generative modeling for single-cell transcriptomics. *Nat Methods* **15**, 1053-1058 (2018).
85. M. D. Luecken, M. Büttner, K. Chaichoompu, A. Danese, M. Interlandi, M. F. Mueller, D. C. Strobl, L. Zappia, M. Dugas, M. Colomé-Tatché, F. J. Theis, Benchmarking atlas-level data integration in single-cell genomics. *Nat Methods* **19**, 41-50 (2022).
86. J. W. Squair, M. Gautier, C. Kathe, M. A. Anderson, N. D. James, T. H. Hutson, R. Hudelle, T. Qaiser, K. J. E. Matson, Q. Barraud, A. J. Levine, G. La Manno, M. A. Skinnider, G. Courtine, Confronting false discoveries in single-cell differential expression. *Nat Commun* **12**, (2021).

Acknowledgments:

We thank the Biomedical Sequencing Facility (CeMM and Medical University of Vienna), the Core Facilities Flow Cytometry and Imaging (Medical University of Vienna), and the staff of the Core Facility of Laboratory Animal Breeding and

Husbandry (Medical University of Vienna). We thank Peter Kuess for help with the thoracic shielding experiments.

Funding:

Austrian Science Fund SFB-F061(P04) (SK); Austrian Science Fund ZK 57-B and V 10 25-B (RG).

Author contributions:

Conceptualization: AF, RG, SK; Investigation (experimental): AF, MR, SZ, LP, AFo, AH, KL, JB, FM, FO, FQ, PS, ADG, RG; Investigation (bioinformatics): FD, AHa, JM; Funding acquisition: RG, SK; Project administration: SK; Resources: LB, CV, NB, WE, JvdV, CC; Supervision: RG, SK; Writing – original draft: AF, RG, SK; Writing – review & editing: all authors.

Competing interests: The authors declare no competing interests.

Data and materials availability: RNA sequencing data has been publicly deposited at the NCBI Gene Expression Omnibus (GEO) repository under accession numbers GSE274253 (Bulk RNA-Seq) and GSE277799 (ScRNA-seq). The subset of the human lung cell atlas (*49*))presented in this study was uploaded to Zenodo as Seurat and AnnData object. The CellTypist and consensus cell type annotation are stored in the respective metadata data slots - https://zenodo.org/records/14532104. No custom code generated for this work; standard code used as described in methods. Tabulated data underlying the figures is provided in data file S10. All other data are available in the main text or supplementary materials.

Supplementary materials and methods

Mice strains:

Ubiquitously green fluorescent protein (UBC-GFP) mice (UBC-GFP mice (C57BL/6-Tg(UBC-GFP)30Scha/J) (*74*) and B6 CD45.1 (B6.SJL-Ptprca Pepcb/BoyJ) were originally purchased from Jackson Laboratories (JAX stock #004353 and #002014) and bred in-house. TCR-α $^{-/-}$ (B6.129S2-*Tcra*^{tm1Mom}/J) (*75)* and IL-10 $^{-/-}$ (B6.129P2-*Il10*^{tm1Cgn}/J) (*76*) mice were backcrossed and bred with in-house C57BL/6J mice. DEREG (depletion of regulatory T cells) Foxp3-EGFP mice (C57BL/6-Tg (Foxp3-DTR/EGFP)23.2Spar/Mmjax) (*77*) and Foxp3-DTR mice (B6.129(Cg)-Foxp3tm3(Hbegf/GFP)Ayr/J) (*52*) were bred and housed at the Core Facility Laboratory Animal Breeding and Husbandry, Medical University of Vienna.

ROSA26iDTR mice (Rosa26Idtr Gt(ROSA)26Sor$^{tm1(HBEGF)Awai}$/J) (*78*), originally purchased from Jackson Laboratories and bred in-house, were used as controls for experiments with DEREG and Foxp3-DTR mice. Cage bedding was mixed between the cages for DEREG or Foxp3-DTR mice and Rosa26iDTR controls prior to and throughout the experiment to control for microbiome derived cage effects. DEREG mice were used to replicate partial depletion of Foxp3+ Tregs as seen with hematopoietic ageing (*77*). This incomplete depletion in DEREG mice is attributed to the BAC transgene's inability to fully replicate endogenous Foxp3 expression, allowing some Treg cells that do not express the BAC transgene to escape DT-mediated depletion.

Bone marrow transplant (whole body lethal irradiation and irradiation with thoracic shielding)

For whole body irradiation and bone marrow transplant, 7–9-week-old young mice (C57BL/6J) or 60–65-week-old, aged mice (C57BL/6J) were lethally irradiated at a dose of 6 Gy delivered twice (2 x 6 Gy) using a XYLON Maxishot (YXLON International GmbH), with a 3-hour gap between each dose. 4 x 10^6 bone marrow cells were injected retro-orbitally (r.o) in 100 µl PBS, 4 hours after the final irradiation with mice maintained under light isoflurane anesthesia (2% isoflurane 2 L/min O_2). Bone marrow cells were harvested from young (8–10 weeks old) or aged (70–75 weeks old) UBC-GFP mice and CD45.1 mice, TCR-α$^{-/-}$ mice, Foxp3-DTR mice (8-12 weeks old), Rosai26DTR mice (8-12 weeks old) and IL-10$^{-/-}$ mice (7–10 weeks old), from the femur and tibia. The epiphyses were cut, and bones were flushed through using a 1 ml syringe (with 27 g needles) pre-filled with RPMI-1640 (Gibco) medium passed through a 70 µm filter, counted and resuspended in 100 µl PBS prior to injection into recipient mice. For 1:1 bone marrow chimeras, 2 x 10^6 cells from each genotype were mixed before injection into recipients. Mice were housed for 2 months post irradiation and bone marrow transplant to allow for complete cell reconstitution before the start of the respective experiments. For irradiation with thoracic shielding, mice were anesthetized with Ketasol (100 mg/kg; OGRIS Pharma) and Rompun (10 mg/kg; Bayer) and placed dorsally with a lead shield (3 mm thickness, 25 mm x 25 mm in size; GoodFellow) covering the thoracic cavity during irradiation. Mice were irradiated once with a dose of 9 Gy (maximum irradiation dose that did not lead to baseline depletion of lung tissue resident alveolar macrophages with shielding), and 4 hours post irradiation injected retro-orbitally with bone marrow cells as described above while placed under light isoflurane anesthesia (2% isoflurane 2 L/min O_2).

Anti-IL-10 treatment

8–10-week-old WT (C57BL/6J) mice were treated with an anti-IL-10 antibody (clone JES5.2A5) administered intranasally under light isoflurane anesthesia (2% isoflurane 2 L/min O_2) in a total volume of 50 µl at a dose of 150 µg anti-IL-10 that was resuspended in endotoxin-free PBS or with 50 µl of PBS (controls) per timepoint. Anti-IL-10 was given at D0, D2, D4 and

D6 post bleomycin challenge and mice were harvested at D7 or at D7. D9, D11, D13 and harvested at D14 (independent experiments).

Anti-CD25 treatment

8–10-week-old WT (C57BL/6J) mice were administered i.p with anti-CD25 (Clone PC61) at a dose of 500 µg/mouse per timepoint in 200 µl PBS or injected with only PBS (control mice) on days -2, 0, 2, 4, 6 prior/post bleomycin challenge - D(-2) to D7) or from D7 to D14.

Diphtheria-Toxin administration

For DEREG mice given DT from D(-2) to D14): DEREG mice and Rosa26iDTR mice were administered (i.p) with 50 µg/kg Diphtheria Toxin (Calbiochem) resuspended in 200 µl endotoxin free PBS two days prior to bleomycin and with 10 µg/kg every 2 days starting at day 0 post bleomycin challenge until the end point at D14.

Foxp3-DTR mice and Rosa26iDTR mice, and recipients of the respective bone marrow (DT from D0 to D14 or D7 to D14): Mice were administered (i.p) with 10 µg/kg Diphtheria Toxin every 2 days starting at day 0 or day 7, respectively, post bleomycin challenge until the end point at D14. Cell depletion was confirmed by flow cytometry from lung tissue.

Intravascular staining of immune cells

Mice were placed in under light isoflurane anesthesia (2% isoflurane 2 L/min O_2) and 1µg of CD45 antibody in 100µl PBS was injected retro-orbitally (i.v). Mice were removed from isoflurane anesthesia and sacrificed for organ collection after 3 minutes.

Cell isolation and organ processing for single cell suspensions

Bronchoalveolar lavage (BAL), Lung, Bone marrow and Blood

For flow cytometry analysis, BAL fluid (BALF) was collected by making a midline incision of the trachea and the airways/lung were perfused with 1 ml of endotoxin free saline (NaCl) via an 18-gauge tracheal cannula (Venflon, BD) in 500 µl instillations. BALF collected from each mouse was weighed. BALF samples were centrifuged (300g, 4°C, 10 minutes) and cell pellets were resuspended in PBS 1% BSA (BSA; Carl Roth). BAL supernatant was collected and stored at -20°C until further analysis. Post lavage lungs or whole lungs (in experimental set ups without lavage) were weighed, and homogenized with a gentleMACS™ Tissue Dissociator (Miltenyi Biotec) following the manufacturer's protocol (program m_lung_01_02) followed by digestion in RPMI-1640 (Gibco) medium supplemented with 5% FCS (Sigma), collagenase I (160 U/mL; Gibco) and DNase I (12 U/mL; Sigma) for 35 minutes (37°C, 180 rpm agitation) on a shaker. Post a second homogenization (program m_lung_02_01), the lung tissue was filtered through a 70 µm strainer (Miltenyi Biotech), centrifuged for 5 minutes (4°C, 300 g) and the cell pellets were resuspended in ACK lysis buffer (150 mM NH_4Cl,10 mM $KHCO_3$, 0.1 mM Na_2EDTA, pH 7.2 – 7.4; chemicals from Sigma) for erythrocyte lysis and incubated on ice for 4 minutes. Erythrocyte lysis was stopped by the addition of 5 ml cold PBS 1% BSA, suspensions were filtered again over a 30 µm strainer, centrifuged and resuspended

in cold PBS 1% BSA for antibody cell staining and fixation. Bone marrow cells for flow cytometry were collected from the femur. Femurs were gently crushed using a mortar and pestle and resuspended in RPMI medium supplemented with 5% FCS. The cell suspension was passed over a 70 µm filter, centrifuged as above and resuspended in PBS 1% BSA for antibody cell staining and fixation. 500 µl of blood was drawn from the vena cava and collected in EDTA tubes (Greiner Bio-One). 100 µl of blood was resuspended with 5 ml of ACK Lysis buffer for the lysis of erythrocytes for 5 minutes at room temperature (RT) and the reaction was stopped with an additional 5 ml of PBS 1% BSA. The suspension was centrifuged, and the cell pellet was resuspended in PBS 1% BSA for antibody cell staining and fixation.

Flow cytometry.

Cell suspensions were incubated with anti-mouse CD16/32 (Biolegend) for 15 minutes at RT, followed by incubation with fluorescently labelled monoclonal antibodies and Fixable Viability Dye eFluor 780 (Thermofisher, 1:3000 dilution) diluted in PBS 1% BSA for 40 minutes at 4°C. Antibodies used are listed in Table S1 below.

Post staining, cells were washed with PBS and fixed for 20 minutes at RT with Fix&Perm Fixation Medium A (Nordic Mubio) or True-Nuclear Transcription Factor Buffer Set (Biolegend) for intracellular staining following manufacturer's protocol. For intracellular staining, following extracellular surface staining, cells were washed and fixed using the True-Nuclear Transcription Factor staining kit (BioLegend) as per manufacturer's protocol with minor modifications. Cells were fixed with 50 µl of True-Nuclear 1X Fix concentrate for 30 minutes at RT. Cells were washed and resuspended in 1X TrueNuclear Perm Buffer for a total of three times and were then resuspended in 50 µl of 1X TrueNuclear Perm Buffer containing the intracellular antibodies and stained at 4°C overnight. Stained and fixed cells were washed in PBS and resuspended in a final volume of 200 µl PBS in a 96 well plate and analysed via an LSRFortessa (BD Biosciences). Data was analysed using FlowJo software (FlowJo, LLC) up to version 10.7.2.

For cell sorting, cells were isolated from BALF or lung tissue suspensions and resuspended in and sorted into cold PBS 2% BSA on a FACSAria™ Fusion flow cytometer (BD). SSC-A and FSC-A discrimination was used to remove debris and FSC-A and FSC-H to exclude doublet cells. Dead cells and erythrocytes stained with Fixable Viability Dye (efluor 780; Bioscience) and anti-mouse TER-119 (APC/Cy7; Biolegend) were excluded. Gating strategies used for identifying sorted Mo-AMs and TR-AMs are shown in Fig. S1C.

Bulk RNA-seq (Quant-seq)

Lung immune cells from recipients of young and aged bone marrow (7- and 14-days post-bleomycin) were sequenced using the QuantSeq 3' mRNA-Seq Library Prep Kit FWD for

Illumina (Lexogen). Sequencing was performed on an Illumina NovaSeq 6000. RNA sequencing data were mapped to the GRCm39 (mm10) mouse genome using STAR v2.7.9a and analyzed for differential expression with limma-voom (limma v3.50.3). Normalized counts (log2(CPM)) were used for downstream analysis, including PCA, cell-cell interaction (CellChat), and quality control. Further details on library preparation and bioinformatics analysis are provided in the supplementary materials and methods section.

RNA-seq analysis was performed on lung immune cells from recipients of young and aged bone marrow, 7- and 14-days post bleomycin challenge. Cells (30,000-80,000) were sorted from the lungs into cold PBS 2% BSA, and the pellet resuspended in RLT Buffer (Qiagen). RNA was isolated using the RNeasy Micro kit (Qiagen). Post isolation, RNA was precipitated with ice cold absolute ethanol, 3 M Sodium Acetate (NaOAc pH 5.2; ThermoFischer) and Linear Polyacrlamide (LPA; Sigma Aldrich) overnight and resuspended in 10 µl of 10 mM Tris buffer (pH 8.0; Invitrogen). RNA concentration was measured by fluorometric (Qubit) analysis For Quant-seq, libraries were prepared using the QuantSeq 3' mRNA-Seq Library Prep Kit (FWD) for Illumina (Lexogen) in combination with the PCR Add-on Kit for Illumina (Lexogen) and the UMI Second Strand Synthesis Module for QuantSeq FWD (Lexogen), following the manufacturers' protocol (Low input protocol). Libraries were prepared with an input of 10 ng RNA and 12–18 amplification cycles. Sample quality was assessed on a Bioanalyzer 2100 (Agilent Technologies) and a Tapestation (Agilent Technologies). 75bp single-end sequencing was performed by the Biomedical Sequencing Facility (BSF, Center of Molecular Medicine and Medical University of Vienna) on a NovaSeq6000 (Illumina).

Demultiplexing raw BAM files were obtained from the Biomedical sequence facility (BSF) and converted to FASTQ files with *picard SamToFastq* (v.2.25.5). Adapter sequences (--fastqc –length 15) and polyA sequences (--length 15 --adapter A {20] –stringency 20 -e 0) were trimmed with Trimgalore (v.0.6.6). The mouse reference genome GRCm39 (mm10) was used as reference for read alignment. The reference indexing and read mapping (outFilterMismatchNoverLmax=0.1) was done with STAR (v.2.7.9a). The *featureCounts* function (countMultiMappingReads=FALSE GTF.featureType="gene") from the R *Rsubread* (v.2.8.2) package was used to generate gene-based count matrices. Gene names were converted from Ensemble to MGI symbol format with biomaRt (v.2.50.3) based custom scripts. The reference GTF file's biotype information was used to identify and remove rRNA genes. Count expression values were normalized to log2(CPM) using TMM normalized library sizes implemented with the *edgeR* package (v.3.36.0), specifically using the *calcNormFactors* and *cpm* functions. The library size, rRNA ratio, and the median log2(CPM) were computed to assess the overall quality of the samples. For identifying outlier samples, the data was split by cell type, and the *limma* package (v.3.50.3) was employed to compute the *voom* sample quality weight, considering the group variables (mouse age and sampling time point). Only the

four highest scoring samples were retained. Finally, the first two principal components were plotted, and outlier samples were visually identified based on both the principal component plot and the sample quality scores obtained previously.

For differential expression analysis count matrix and meta data were first subset by the respective sample groups. The genes of the log2(CPM) count matrix were then filtered to only retain genes whose expression was greater than the CPM threshold in at least two samples of a group. The CPM threshold was derived by dividing the value 5 by the mean normalized library size before scaling to one million. For differential expression analysis the *limma* (3.50.3) package with *voomWithQualityWeights* and default settings for the *lmFIt* and *eBayes* steps were used. For the model matrix, the formula ~0^{+}group was used for comparison with more than two groups and the *decideTes*t function was used with the method set to global to adjust for p-values for multiple group comparison. For variance stabilization the count data matrix was transformed with the rlog function from the DESeq2 (v.1.34.0) package prior PCA computation with the plotPCA function. The output was returned as data table and plotted with a custom ggplot2 script. For cell-cell interaction analysis we used the R package *CellChat* (v.1.6.0) with reticulate (v.1.28) for python (v.3.8.12) compatibility for machine learning tasks. As recommended by the authors (*79*) we used log (CPM^{+}1) values and set raw.use=TRUE in the *computeCommunProb* function. Otherwise, default settings were used except for adjusting the p value threshold of the *identifyOverExpressedGenes* function to 0.1. For Fig. S4D for better visual representation, we selected the largest clusters with a significant difference between any one comparison groups that contained genes of Mo-AM marker genes of activation, differentiation, pro-inflammatory and pro-fibrotic genes (annotated examples on graph), based on literature (*16*). All clusters and genes are listed in data file S2.

Single cell RNA-seq

For single cell RNA-seq, BAL was collected on day 7 post bleomycin challenge from four male, 8-week-old mice, cells were pooled and sorted into PBS with 0.02% BSA to exclude erythrocytes and dead cells. Cell quality was checked, and concentration was adjusted to 800 cells/µl and 10,000 cells were loaded onto the 10x Chromium controller. Library preparation was performed using the Chromium Next GEM Single Cell 3′ Reagent Kits v3.1 protocol. Libraries were sequenced on an Illumina HiSeq 4000 (86 million reads). Single-cell RNA-seq data were aligned and processed by the CellRanger pipeline followed by analysis using the Seurat package (v4.1.1) (*80*) in the R environment (v4.2.0) (R Core Team 2021). We performed cell and feature filtering using the following thresholds: nFeature_RNA > 200 & nFeature_RNA < 2500 & percent.mt < 25. We applied the scTransform method (*81*) implemented in Seurat for normalization and variance stabilization.

Analysis of data from Human Lung Cell Atlas

The full version of the integrated Human Lung Cell Atlas (HLCA) v1.0 (*49*) was downloaded from https://data.humancellatlas.org/hca-bio-networks/lung/atlases/lung-v1-0. The atlas was then subset with the following conditions: The lung condition must be associated with healthy, COVID-19, or IPF. The tissue source must be lung or lung parenchyma. The healthy control samples must have age or mean of age range annotated. To reduce technical bias, single-nucleus sequencing data and non-10x library protocols were excluded. This process resulted in samples from studies including Banovich and Kropski 2020, Kaminski 2020, Lafyatis Rojas 2019, Lambrechts 2021, Meyer 2019, Meyer 2021, Misharin Budinger 2018, Wunderlink 2021, and Zhang 2021.

Only the core data set was filtered based on quality matrices. For quality control, we only retained cells with at least 800 UMIs, more than 500 features, and less than 15% mitochondrial reads. We next split the atlas by donor id and ran doubletfinder from scDblFinder (v1.8.0) (*82*). Next, we used CellTypist (v1.1.0) (*83*). Immune_All_high.pkl and Immune_All_low.pkl for cell type classification without majority voting. The atlas was next subset by cell type using the ann_level_4 and transf_ann_level_4_label for the Core and Extended data sets respectively to only retain cells labeled as Classical monocytes (cMo), Non-classical monocytes (nMo), Alveolar macrophages (AM), Interstitial macrophages (iMac), and CD4 T cells (Th). Next, we removed all doublet cells, split the data by study, and filtered out cells by thresholding the number of detected features per cell to be higher than the lower 1% quantile of all cells within a study. Finally, samples with fewer than 50 cells after quality control were omitted. Since only samples from the core HLCA have full meta data we recovered the sex, smoking status, age or age range and tissue digestion protocol for the Extended HLCA samples. The categories of the lung condition were simplified to healthy, COVID, or IPF and the tissue sampling method categories to BALF or tissue. The samples were stratified by age into young (<=40 yrs) and aged (>40 yrs). The lung condition and age class categories were used to create a grouping variable (Young Healthy, Aged Healthy, Young COVID, Aged COVID, Aged IPF). The cell type labels from level 4 were adjusted as follows. The label interstitial macrophages were set to MoAM and cells that were annotated as interstitial Mph perivascular or alveolar Mph proliferating on annotation level 5 were set to iMac and AM proliferating, respectively. Cells that were classified as regulatory T cells by CellTypist were annotated as Treg. The adjusted labels from level 4 were used for all downstream tasks and are referred to as cell type labels. To reduce bias in the feature space due to the 3’ 10x and 5’ 10x library preparation protocols we subset the feature matrix to only retain protein coding genes and features that are detected at any level with both protocols. The procedure yielded 366.122 cells and 14.247 features.

For visualization tasks the data were integrated with SCVI (v1.1.2) (*84*). The study was used as batch key, the sample id as categorical covariant, and percentage MT reads as continuous covariant. The size factor key was set to the sequencing depth per cell prior feature filtering. The model was designed with default settings except that two layers were used and a negative binomial distribution for the gene likelihood (*85*). The model was trained for 25 epochs, and training evaluation was done by monitoring the reconstruction loss for the train and validation sets. We used scanpy (v1.9.6) to compute a neighborhood graph on the ten-dimensional latent space (n_neighbors=30) as basis for the UMAP embedding (min_dist=1) and leiden clustering (resolution=1, flavor=igraph).

For differential expression analysis between groups (combined age and disease label) we used pseudobatches (*86*) and the voomLmFit linear model implemented in edgeR (v3.36.0). Briefly, the data set was first split by cell type and processed as follows: a gene was deemed expressed in a single sample if at least three counts in three cells were detected. Only genes that were expressed in at least three samples within any group were kept. The gene expression profile of each sample was then summed to create cell type pseudobatches. The linear model was fitted with the group variable as fixed effect (~0^{+}group) and the study as mixed effect by the means of limma duplicate correlation and blocking. The test statistics from the model fit were computed with the limma (v3.50.3) eBayes function and results of specific group comparison were fetched with topTable. For gene set enrichment analysis, we used the same workflow as we did with the QuantSeq data.

Plotting and visualization

For plotting and visualization custom R scripts with ggplot2 (v.3.4.2) and ComplexHeatmap (v.2.10.0) were used (Bulk-seq), Seurat visualization tools and custom functions using the ggplot2 (v3.4.0) package (ScRNA-seq) and GraphPad Prism 8.0-9.0; GraphPad Software Inc, San Diego, CA).

Microscopy image analysis and quantification

For quantification of TUNEL+ cells, the algorithm Indica Labs - HighPlex FL.v4.2.14 (HALO Version 3.6.4) was used – nuclear detection for DAPI and TUNEL stain. For detection of $Foxp3^{+}$ and $F4/80^{+}$ cells, the algorithm Indica Labs – Multiplex IHC v3.4.9 (HALO Version 3.6.4) was used. F4/80 was detected as a cytoplasm stain and Foxp3 as a nuclear stain. Image shown (Fig. S9J) shows a colocalization mask of F4/80 (pink) and Foxp3 (yellow) staining (see methods – Histology). For image quantification of Masson Trichrome stained area, the algorithm Area Quantification v2.4.3 (HALO Version 3.6.4) was used.

Supplementary Figures and legends

Fig. S1

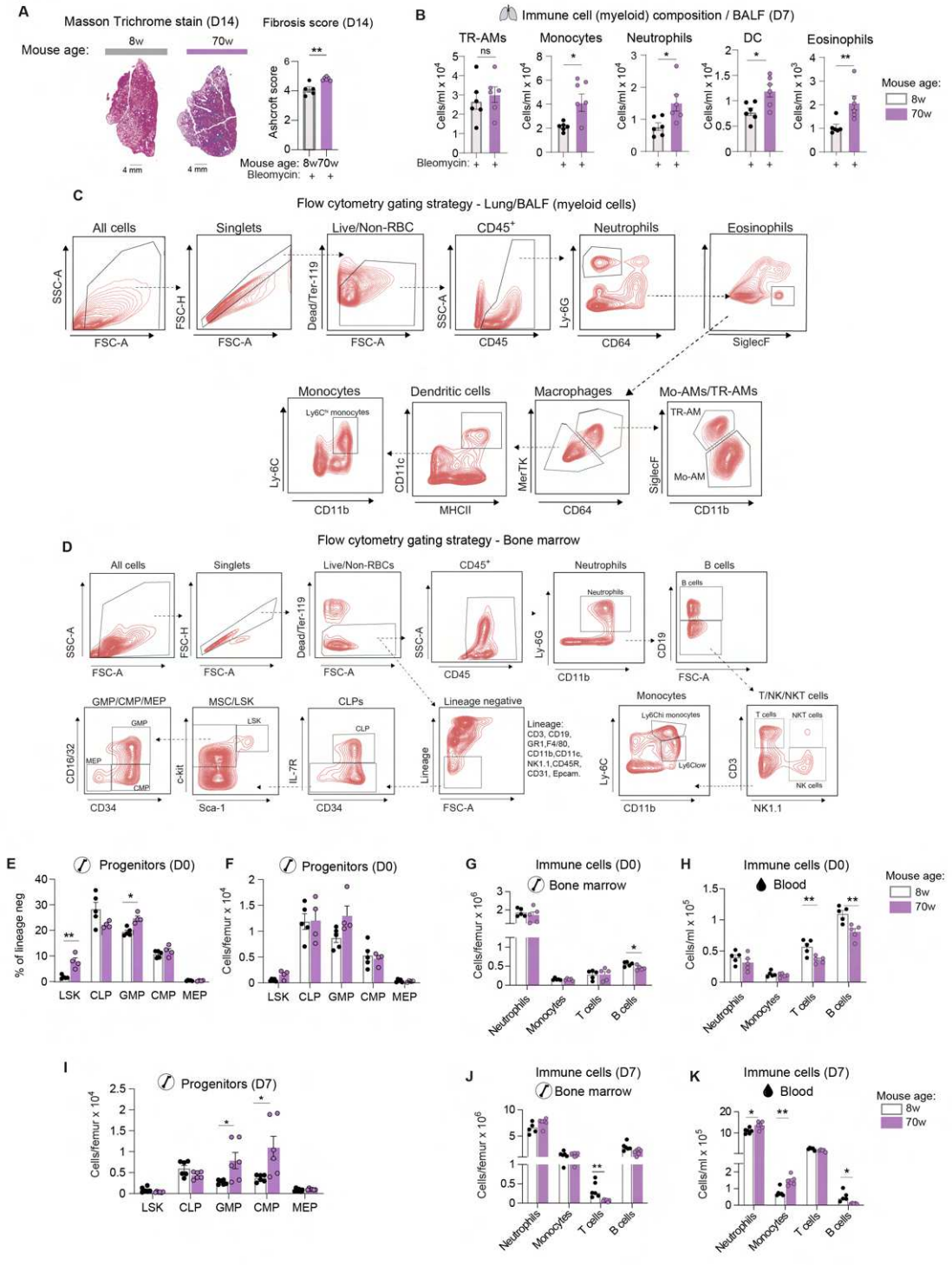

Fig. S1. Aged mice develop exacerbated lung fibrosis that is accompanied by an increased myeloid output at the hematopoietic stem cell level.
(A-G) Bleomycin (1U/kg) was given intratracheally to 8-week-old or 70-week-old C57BL/6 WT mice with end points taken seven (D7) or 14-days (D14) post challenge (n = 4–6) **(A)** Histological sections of left lung lobe taken at D14 post bleomycin challenge stained with Masson Trichrome stain for collagen deposition and scored with a modified Ashcroft score. **(B)** Absolute cell numbers per ml BALF (myeloid cell composition). **(C)** Flow cytometry gating strategy of myeloid cells from the BALF or lung tissue. **(D)** Flow cytometry gating strategy for bone marrow hematopoietic progenitors and mature CD45$^+$ immune

cells. **(E)** Percentage of hematopoietic stem cell progenitors at baseline (D0) in the bone marrow expressed as a percentage of lineage negative cells (lineage and gating see Fig. S1D) from young or aged mice. **(F)** Absolute cell numbers of hematopoietic stem cell progenitors at baseline (D0) in the bone marrow. **(G)** Absolute cell numbers of bone marrow immune cells at baseline (D0). **(H)** Absolute cell numbers of peripheral blood immune cells at baseline (D0). **(I)** Absolute cell numbers of hematopoietic stem cell progenitors at D7 post bleomycin in the bone marrow. **(J)** Absolute numbers of bone marrow immune cells at D7 post bleomycin challenge. **(K)** Absolute numbers of peripheral blood immune cells at D7 post bleomycin challenge. Data are representative of two independent experiments. Symbols on bar graphs represent individual mice. For (S1A,B) Student's two tailed unpaired t test, (S1E-F) multiple unpaired followed by Holm-Šídák test and (S1G-K) multiple unpaired t-test was used. Error bars represent SEM.*P<0.05, **P< 0.01, ***P<0.001.

Fig. S2

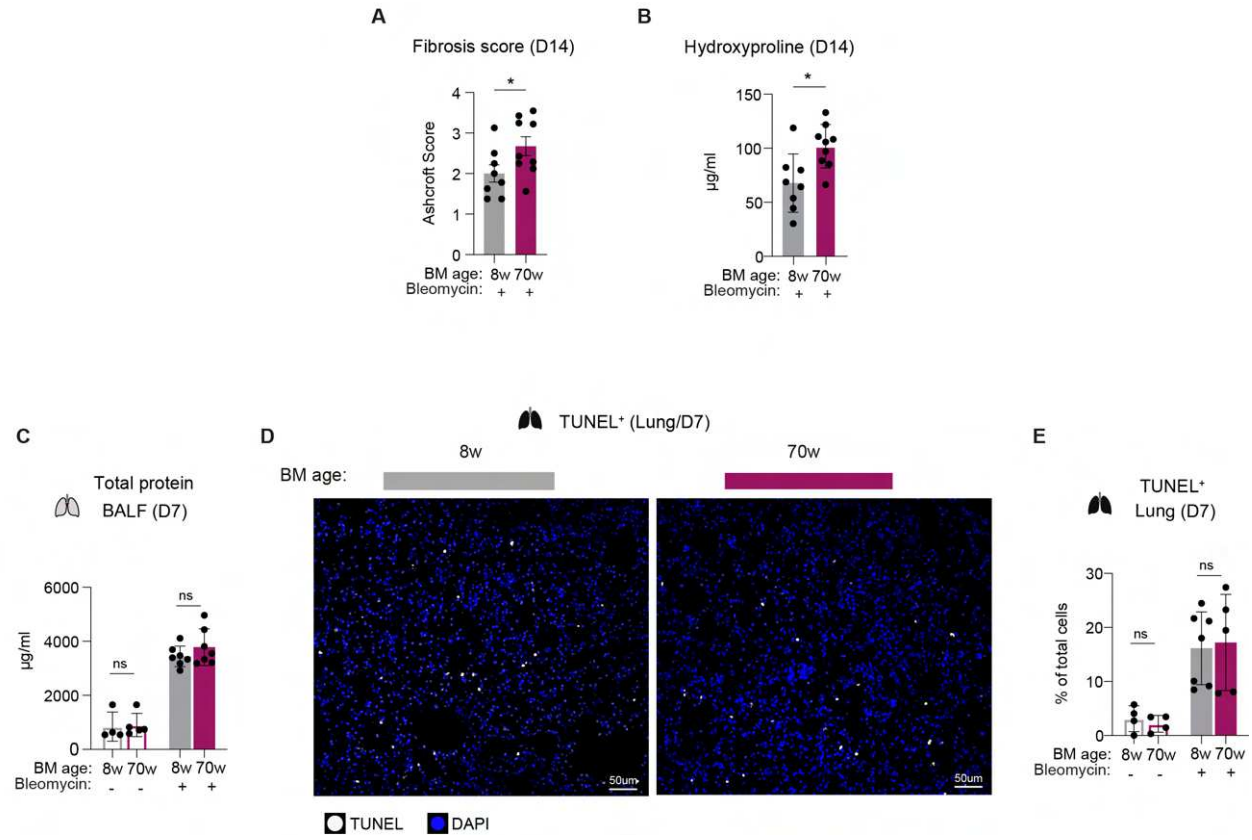

Fig. S2. Increased fibrosis at D14 but no difference in initial lung injury between recipients of young and aged bone marrow

(A) Lung fibrosis quantified by a modified Ashcroft score of lung histology (D14). **(B)** Hydroxyproline quantification from lung tissue (D14). **(C)** Total BAL protein (µg/ml) measured from supernatant of 1ml BALF collected from lungs of recipients of young or aged bone marrow at D7 post PBS or bleomycin treatment. **(D)** TUNEL staining of lung tissue sections of recipients of young or aged bone marrow at D7 post bleomycin treatment. **(E)** TUNEL score showing percentage of TUNEL⁺ cells in the whole left lobe lung section (quantified by number of TUNEL⁺ cells out of total cells in the whole lung section). Symbols on bar graphs represent individual mice. For (A, B) Mann-Whitney test was used (*n*=8-9). For (C,D) two-way analysis of variance (ANOVA) was used with Tukey's multiple comparisons test (*n*=4-7, C,D from independent experiments). Error bars represent SEM or SD. *P ≤ 0.05; **P < 0.01; ***P < 0.001; ns: not significant.

Fig. S3

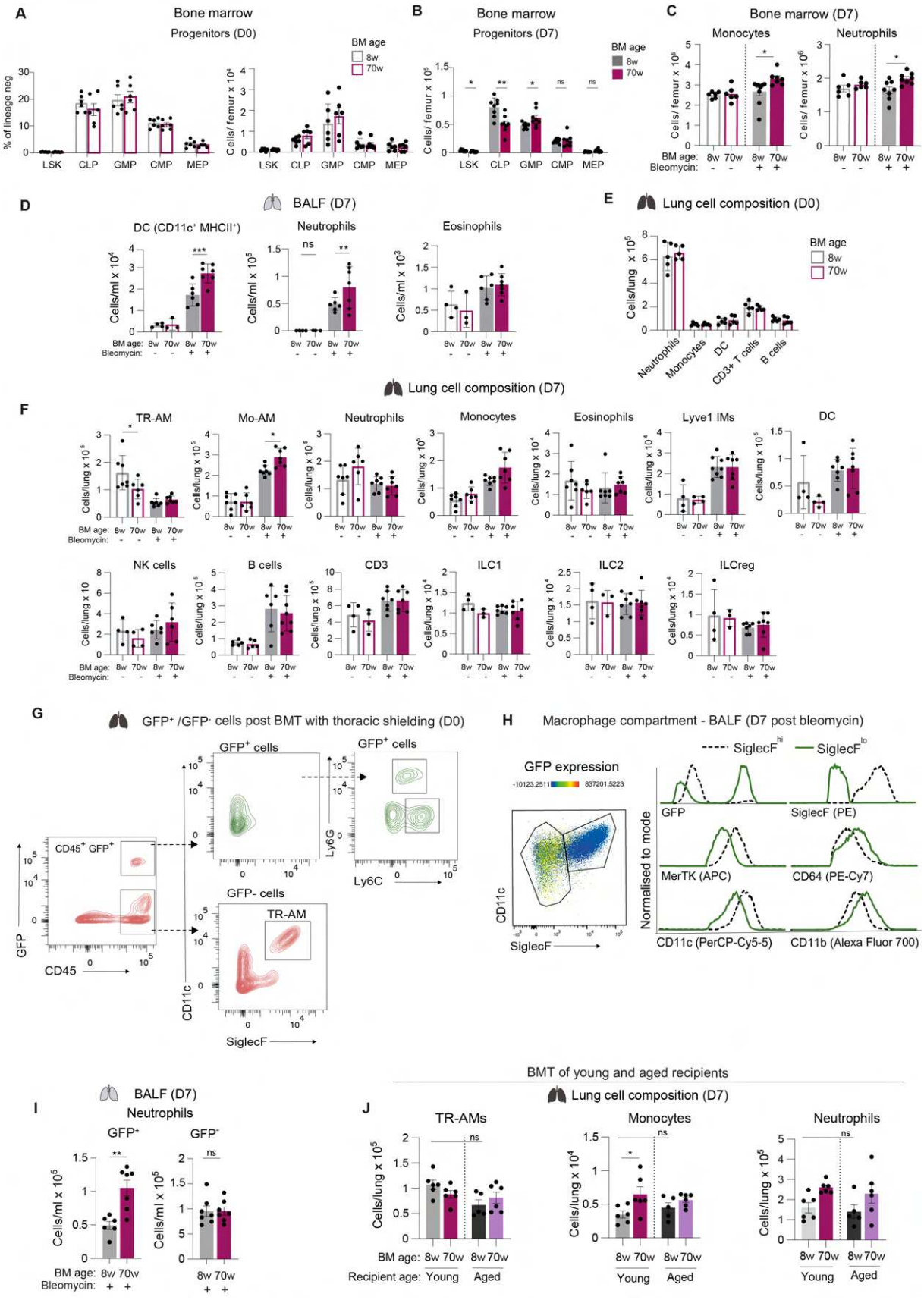
A
Bone marrow
Progenitors (D0)
BM age
8w
70w
% of lineage neg
Cells/ femur x 10⁴
LSK
CLP
GMP
CMP
MEP
B
Bone marrow
Progenitors (D7)
Cells/ femur x 10⁵
C
Bone marrow (D7)
Monocytes
Neutrophils
Cells/ femur x 10⁵
Cells/ femur x 10⁶
BM age:
Bleomycin:
D
BALF (D7)
DC (CD11c⁺ MHCII⁺)
Neutrophils
Eosinophils
Cells/ml x 10⁴
Cells/ml x 10⁵
Cells/ml x 10³
E
Lung cell composition (D0)
Cells/lung x 10⁵
Neutrophils
Monocytes
DC
CD3+ T cells
B cells
Lung cell composition (D7)
F
TR-AM
Mo-AM
Neutrophils
Monocytes
Eosinophils
Lyve1 IMs
DC
NK cells
B cells
CD3
ILC1
ILC2
ILCreg
Cells/lung x 10⁵
Cells/lung x 10⁴
Cells/lung x 10
G
GFP⁺ /GFP⁻ cells post BMT with thoracic shielding (D0)
GFP⁺ cells
GFP⁺ cells
CD45⁺ GFP⁺
GFP
CD45
Ly6G
Ly6C
GFP- cells
TR-AM
CD11c
SiglecF
H
Macrophage compartment - BALF (D7 post bleomycin)
GFP expression
SiglecF^hi
SiglecF^lo
CD11c
SiglecF
Normalised to mode
GFP
SiglecF (PE)
MerTK (APC)
CD64 (PE-Cy7)
CD11c (PerCP-Cy5-5)
CD11b (Alexa Fluor 700)
I
BALF (D7)
Neutrophils
GFP⁺
GFP⁻
Cells/ml x 10⁵
BM age:
Bleomycin:
BMT of young and aged recipients
J
Lung cell composition (D7)
TR-AMs
Monocytes
Neutrophils
Cells/lung x 10⁵
Cells/lung x 10⁴
BM age:
Recipient age:
Young
Aged

Fig. S3. Myeloid cell composition in the lungs post bone marrow transplant including irradiation with thoracic shielding.
(A-E) Two months post whole body irradiation and bone marrow transplant, recipients of young (8w) or aged (70w) bone marrow were given PBS or bleomycin (i.t) **(A)** Percentage of hematopoietic stem cell progenitors in the bone marrow 2 months after bone marrow transplant at baseline (D0); expressed as a percentage of lineage negative cells and absolute cell numbers (lineage and gating see Fig. S1D). **(B)** Absolute cell numbers per femur of hematopoietic stem cell progenitors and **(C)** Absolute cell numbers per femur of mature monocytes and neutrophils from the bone marrow at D7 post PBS or bleomycin treatment. **(D)** Absolute cell numbers per ml BALF (myeloid cell composition) **(E)** Absolute cell numbers of lung (post-lavage) immune cells at baseline, 2 months post reconstitution from recipients of young (8w) and aged (70w) bone marrow. **(F)** Absolute cell numbers of immune cells from the lung tissue (whole lung tissue) at D7 post PBS or bleomycin treatment. **(G-J)** Young (8-week-old) C57BL/6 WT recipient mice were irradiated with a lead shield placed over the thoracic cavity and then transplanted with bone marrow cells from young (8w) or aged (70w) donor mice (GFP^+ bone marrow cells) and two months post cell reconstitution were treated with bleomycin **(G)** Representative flow cytometry plots showing GFP positive and negative cells from the lungs of recipients with thoracic shielding at D0/baseline. **(H)** Flow cytometry plot (showing heatmap statistics of GFP expression) and histograms representing expression of macrophage markers (on x-axis) by $SiglecF^{hi}$ TR-AMs and $SiglecF^{lo}$ Mo-AMs from the BALF at D7 post bleomycin challenge. Flow cytometry histograms of marker expression are normalized to mode. **(I)** Absolute numbers of GFP positive and negative neutrophils from the BALF. **(J)** Young and aged recipients were transplanted with young or aged bone marrow cells – Absolute cell count numbers (myeloid) from the lung tissue at D7 post bleomycin treatment. Data are representative of two or three independent experiments. Symbols on bar graphs represent individual mice. For (S3A) multiple unpaired t test followed by Holm-Šídák test and (S3B) multiple unpaired t-test was used. For (S3C, S3D, S3F) a two-way ANOVA with post-hoc Šídák's multiple comparisons test and (S3J) with a post-hoc Tukey's multiple comparison test and (S3E, S3I) a Student's two tailed unpaired t-test was used. Error bars represent SEM. *P<0.05, **P< 0.01, ***P<0.001.

Fig. S4

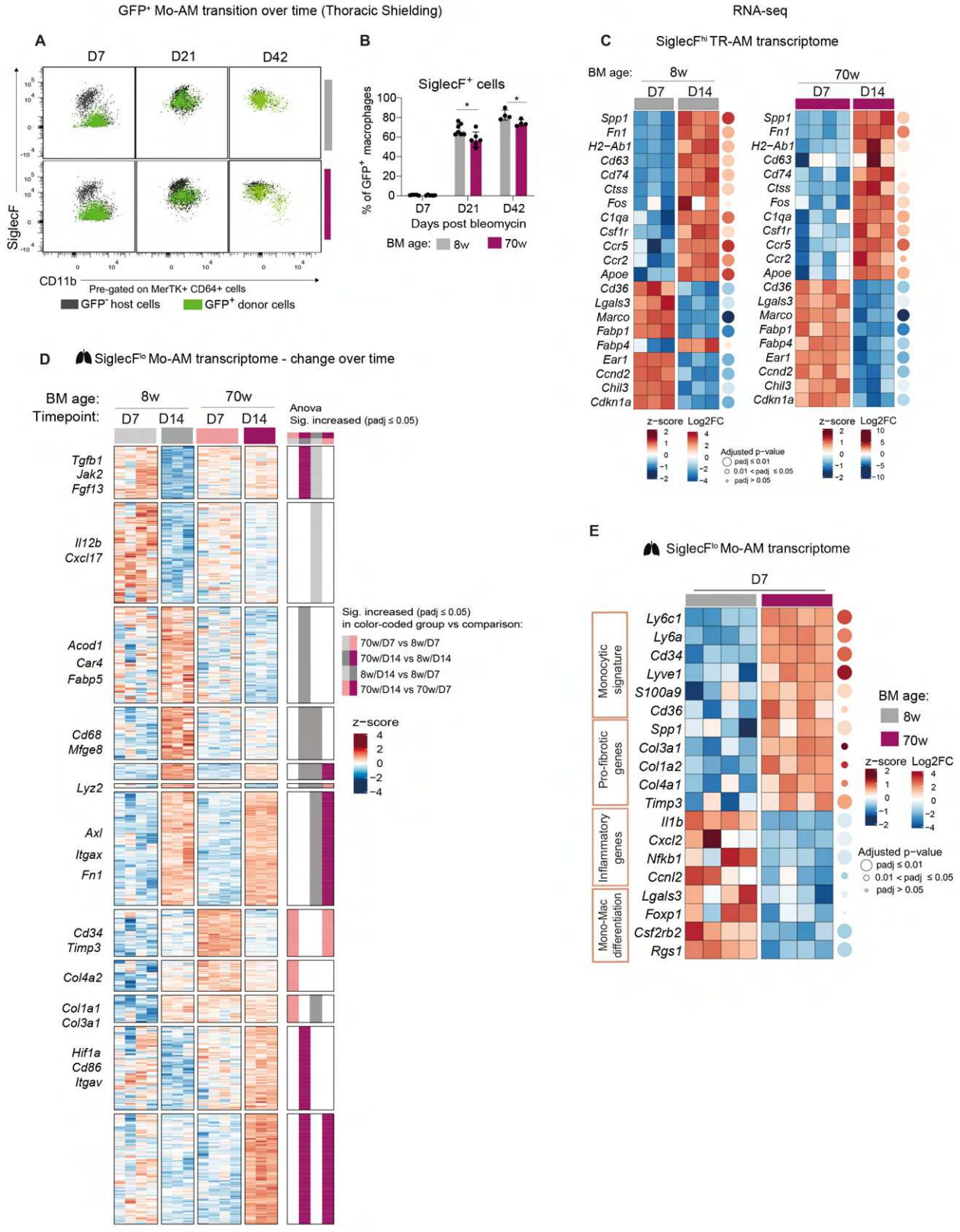

Fig. S4. Distinct transitional dynamics of lung Mo-AMs from young and aged bone marrow at D7 and D14 following bleomycin injury.

(A) Flow cytometry plots showing GFP^+ donor Mo-AMs (green colored population) over time at D7, D21 and D42 from the lungs of recipients of young (8w) and aged (70w) bone marrow with thoracic shielding. Black colored population represents GFP^- recipient cells. Plots were pre-gated on $MerTK^+$ $CD64^+$ and the subsequent GFP^+ and GFP^- populations overlaid on each other. **(B)** Percentage of GFP^+ macrophages that express SiglecF in the lungs of bone marrow recipients with thoracic shielding over time. **(C)** Heatmap showing a selection of significantly differentially expressed genes (DEGs) from $SiglecF^{hi}$ TR-AMs, sorted from the lungs at D7 and D14 post bleomycin challenge from recipients of young (8w) and aged (70w) bone marrow. Each heatmap shows z-score of log(CPM) normalized expression of DEG between D7 and D14 for 8w recipients (left panel) and 70w recipients (right panel). Column represents individual samples (n = 3–4). Circle sizes represent the adjusted p-value and circle colors indicate the log2 fold change expression at D14 vs D7. Gene list provided in **data file S1**. **(D)** Heatmap of selected clusters of DEG from lung Mo-AMs from recipients of young (8w) and aged (70w) bone marrow sorted at D7 and D14 post bleomycin. Clustering was done on all genes. The clustering done by finding all combinations of significant differential expression patterns between the groups. Cluster numbers were assigned based on cluster size in descending order. Only selected clusters are shown in the figure in the following order of clusters – 10, 6, 7, 11, 16, 28, 4, 13, 14,15, 8, 5. The extended cluster list with genes is provided in **data file S2**. **(E)** Heatmap depicting selection of DEGs (extended gene list in **data file. S3**) from lung Mo-AMs sorted at D7 post bleomycin challenge. Heatmap color represents z-score of log(CPM) normalized expression across both groups per gene. Columns represent individual samples. Circle sizes represent the adjusted p-value and circle colors indicate the log2 fold change expression of recipients of 70w vs recipients of 8w bone marrow. For (S4A) a two-way ANOVA with post-hoc Tukey's multiple comparison was used, (S4C,E) DEA using Limma and for (S4D) a two-way ANOVA using Limma was done. S4D – Colored statistical groups denote genes that are significantly upregulated in one group relative to the other specified in the legend. The color specifically highlights the group exhibiting the upregulation within the two comparison groups. *P ≤ 0.05; **P < 0.01; ***P < 0.001; ns: not significant. Error bars represent SEM.

Fig. S5

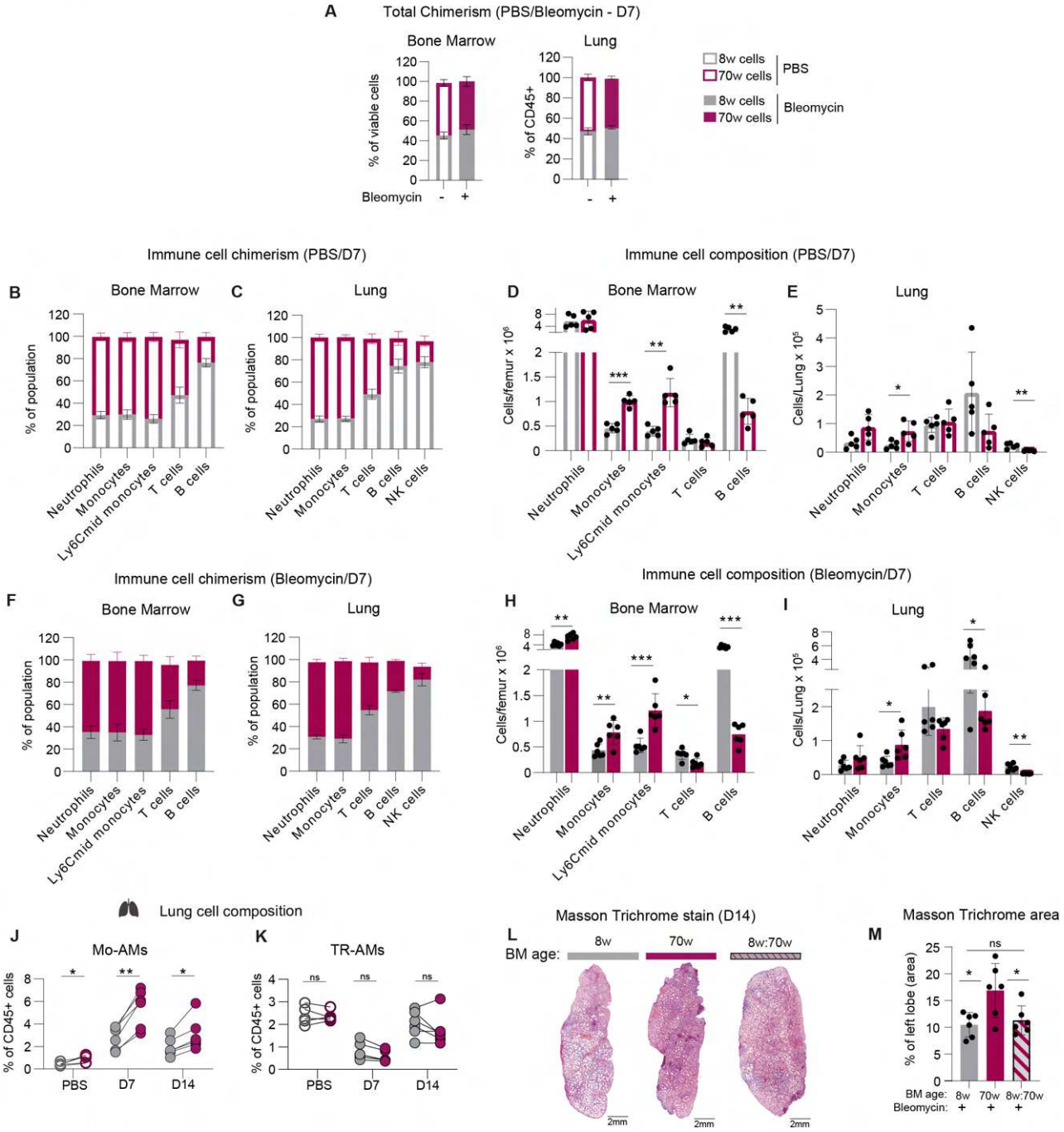

Fig. S5. Aged bone marrow derived monocytes/Mo-AMs outcompete young cells when transplanted in a 1:1 chimera.

(A-M) Young (8-week-old) C57BL/6J WT recipient mice were lethally irradiated and transplanted with bone marrow cells from young (8w, GFP$^+$ bone marrow) and aged (70w, CD45.1 bone marrow) donor mice in a 1:1 ratio to generate chimeric mice. 2 months post reconstitution, recipients were given PBS or bleomycin – endpoints at D7 or D14. **(A)** Total chimerism of young (8w, GFP$^+$) and aged (70w, CD45.1$^+$) cells in the bone marrow (percentage of total viable cells) and lung (percentage of total CD45$^+$ cells) after PBS or bleomycin treatment at D7. **(B)** Immune cell chimerism in the bone marrow in PBS mice – expressed as percentage of young (8w, GFP$^+$) and aged (70w, CD45.1$^+$) cells within each bone marrow immune cell population and **(C)** within each lung immune cell population. **(D)** Absolute cell numbers of 8w and 70w cells in bone marrow and **(E)** lung of PBS control mice. **(F)** Immune cell chimerism in the bone marrow at D7 post bleomycin challenge– expressed as percentage of young

(8w, GFP$^+$) and aged (70w, CD45.1$^+$) cells within each bone marrow immune cell population and **(G)** within each lung immune cell population. **(H)** Absolute cell numbers of 8w and 70w cells in bone marrow and **(I)** lung at D7 post bleomycin challenge. **(J)** Percentage of young (8w, GFP$^+$) and aged (70w, CD45.1$^+$) Mo-AMs expressed as a percentage of CD45$^+$ cells in the lungs**. (K)** Percentage of young (8w, GFP$^+$) and aged (70w, CD45.1$^+$) TR-AMs expressed as a percentage of CD45$^+$ cells in the lungs. **(L)** Lung histology (left lobe) sections stained with Masson Trichrome and **(M)** Quantification of Masson Trichrome stained area from lung histology sections (as a % of entire left lobe) at D14 post bleomycin challenge of recipients reconstituted with young (8w) bone marrow cells (grey bar), aged (70w) bone marrow cells (purple bar) and young (8w):aged (70w) bone marrow chimera (1:1). For (S5A) a paired two-tailed t-test ,(S5B-I) a Student's two tailed t test or multiple Student's t test with Welch correction, (S5J-K) a Wilcoxon matched-pairs signed rank test was used for each timepoint, (S5M) a one-way ANOVA with post-hoc Šídák's multiple comparisons test was used. Error bars represent SD or SEM. *P ≤ 0.05; **P < 0.01; ***P < 0.001; ns: not significant.

Fig. S6

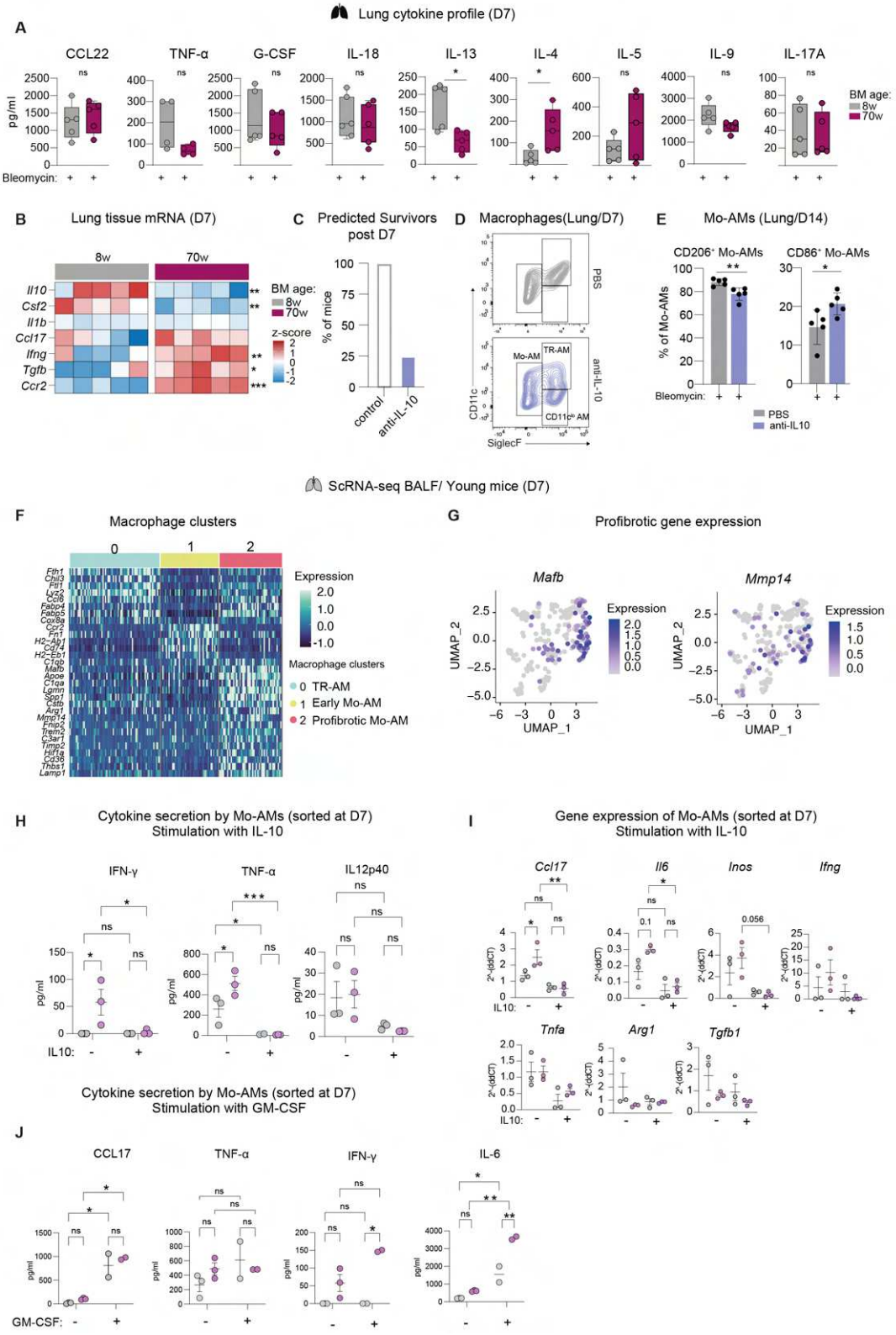
Lung cytokine profile (D7)
A
CCL22
TNF-α
G-CSF
IL-18
IL-13
IL-4
IL-5
IL-9
IL-17A
pg/ml
Bleomycin:
BM age:
8w
70w
B
Lung tissue mRNA (D7)
8w
70w
Il10
Csf2
Il1b
Ccl17
Ifng
Tgfb
Ccr2
z-score
C
Predicted Survivors post D7
% of mice
control
anti-IL-10
D
Macrophages(Lung/D7)
PBS
anti-IL-10
Mo-AM
TR-AM
CD11c
SiglecF
CD11c^hi AM
E
Mo-AMs (Lung/D14)
CD206⁺ Mo-AMs
CD86⁺ Mo-AMs
% of Mo-AMs
Bleomycin:
PBS
anti-IL10
ScRNA-seq BALF/ Young mice (D7)
F
Macrophage clusters
Expression
Macrophage clusters
0 TR-AM
1 Early Mo-AM
2 Profibrotic Mo-AM
G
Profibrotic gene expression
Mafb
Mmp14
UMAP_1
UMAP_2
H
Cytokine secretion by Mo-AMs (sorted at D7)
Stimulation with IL-10
IFN-γ
TNF-α
IL12p40
pg/ml
IL10:
I
Gene expression of Mo-AMs (sorted at D7)
Stimulation with IL-10
Ccl17
Il6
Inos
Ifng
Tnfa
Arg1
Tgfb1
2^-(ddCT)
IL10:
Cytokine secretion by Mo-AMs (sorted at D7)
Stimulation with GM-CSF
J
CCL17
TNF-α
IFN-γ
IL-6
pg/ml
GM-CSF:

Fig. S6. Decreased levels of *Il10* gene expression in the lung tissue of aged bone marrow recipients.
(A) Cytokine analysis from lung homogenates of recipients of young (8w) and aged (70w) bone marrow at D7 post bleomycin. **(B)** Expression of genes from the lung tissue homogenate analysed by real-time qPCR with CT values relative to *Gapdh*. Heatmap shows z-score of 2^-(ddCT) values calculated across both groups per gene (n=5/group). **(C-E)** 8-week-old C57BL/6J mice were given bleomycin and intranasally (i.n) treated with anti-IL10 antibody or PBS every second day (D0-D7 or D7-D14). **(C)** Predicted percentage of mice that would have survived post D7 according to body weight loss at D7. **(D)** Representative flow cytometry plots showing cells pre-gated on $MerTK^+$ $CD64^+$ in the lung **(E)** Percentage of lung Mo-AMs co-expressing CD206 or CD86. **(F–G)** Single cell RNA-seq analysis from the BALF of 8-week-old mice at D7 post bleomycin challenge. **(F)** Heatmap of genes expressed in Clusters 0, 1, 2. Each line represents a cell and each row the corresponding labelled gene. **(G)** Expression plot of *Mafb* and *Mmp14*. **(H)** Absolute values (pg/ml) of cytokine secretion analysis from supernatant of cultured Mo-AMs, 24 hours post seeding and stimulation with cell culture media alone or with IL-10. Symbols represent technical replicates. **(I)** Gene expression analysis (RT-qPCR) from cultured Mo-AMs, 24 hours stimulation with cell culture media or IL-10 expressed as 2^-(ddCT) relative to *Gapdh*. Symbols represent technical replicates. **(J)** Absolute values (pg/ml) of cytokine secretion analysis from supernatant of cultured Mo-AMs, 24 hours post seeding and stimulation with GM-CSF. For (S6A, S6E) Student's two tailed unpaired t test, (S6B) multiple unpaired t-tests, (S6H-J) a two-way ANOVA with post-hoc Tukey's multiple-comparison tests. Error bars represent SEM.*P ≤ 0.05; **P < 0.01; ***P < 0.001; ns: not significant.

Fig. S7

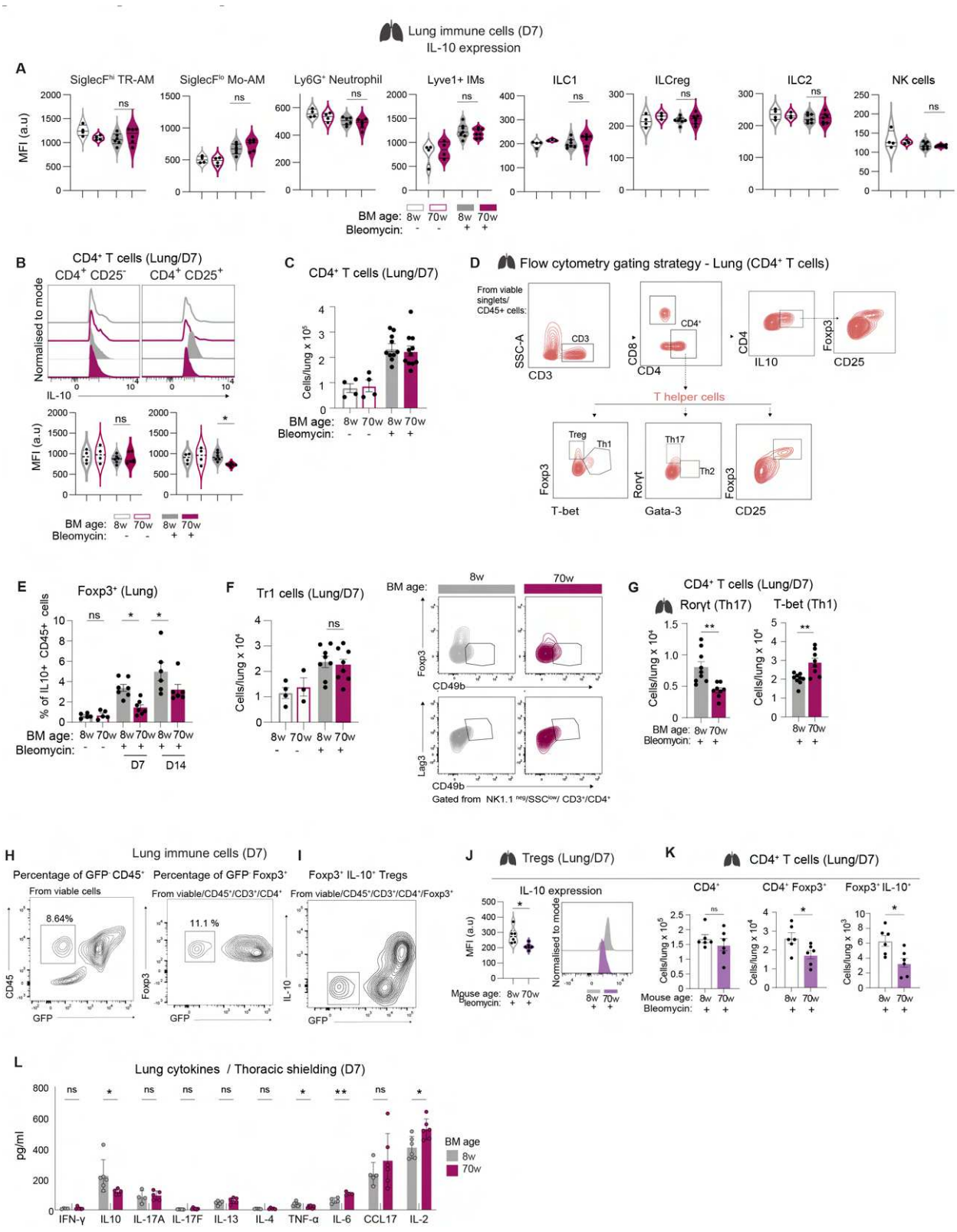

Fig. S7. The IL-10 producing CD4⁺ T cell composition in the lung is altered between recipients of young and aged bone marrow.
(A) Histograms of intracellular IL-10 staining of lung immune cells (SiglecF^{hi} TR-AMs, SiglecF^{lo} Mo-AMs, neutrophils, Lyve1^{+} interstitial macrophages, ILC1, ILCreg, ILC2 and NK cells) and MFI quantification of IL-10 by flow cytometry at D7 post PBS or bleomycin (*n* = 6–9). **(B)** Histograms of

intracellular IL-10 staining of $CD4^+$ $CD25^-$ and $CD4^+$ $CD25^+$ cells and MFI quantification of IL-10 at D7 post PBS or bleomycin. **(C)** Absolute number of $CD4^+$ T cells (PBS or bleomycin) at D7. **(D)** Gating strategy of $CD4^+$ T cells, $IL\text{-}10^+$ CD4 T cells and T helper cells. **(E)** Percentage of $CD4^+$ $Foxp3^+$ cells of total $IL\text{-}10^+$ immune ($CD45^+$) cells in the lungs. **(F)** Absolute cell numbers of Tr1 ($CD49b^+$ $Lag3^+$ cells in the lung at D7 post PBS or bleomycin treatment and representative flow cytometry plot. **(G)** Absolute numbers of lung $CD4^+$ $Ror\gamma t^+$ and $CD4^+$ $Tbet^+$ cells at D7 post bleomycin from recipients of 8w and 70w bone marrow. **(H)** Flow cytometry plots showing the average percentage of GFP^- (host-derived) radioresistant $CD45^+$ cells two months post-irradiation, the average percentage of GFP^- (host-derived) radioresistant $Foxp3^+$ cells (gated from $CD4^+$ $CD25^+$ $Foxp3^+$) two months post-irradiation and bleomycin treatment at D7 and **(I)** presence/absence of GFP^- (host-derived) radioresistant $Foxp3^+$ $IL10^+$ cells (pre-gated from total $CD4^+$ $CD25^+$ $Foxp3^+$ cells) two months post-irradiation and bleomycin treatment at D7 in recipients of young bone marrow. **(J)** Expression histograms of intracellular IL-10 staining of $CD4^+$ $CD25^+$ $Foxp3^+$ and MFI quantification of IL-10 by flow cytometry and **(K)** absolute numbers of indicated cells from naturally young and aged WT mice at D7 post bleomycin. **(L)** Absolute values (pg/ml) of lung cytokines (from lung homogenate) at D7 post bleomycin in lungs of recipients of 8w and 70w bone marrow that were irradiated with thoracic shielding. Data is representative of two or three independent experiments. Symbols on bar graphs represent individual mice. For (S7A-C, S7F) a two way ANOVA with post-hoc Tukey's multiple comparison ,(S7E) with post-hoc Šídák's multiple comparisons test, (S7G, J, K) Student's two tailed unpaired t test and (S7L) multiple unpaired t-tests were used. Error bars represent SEM.*$P \leq 0.05$; **$P < 0.01$; ***$P < 0.001$; ns: not significant.

Fig. S8

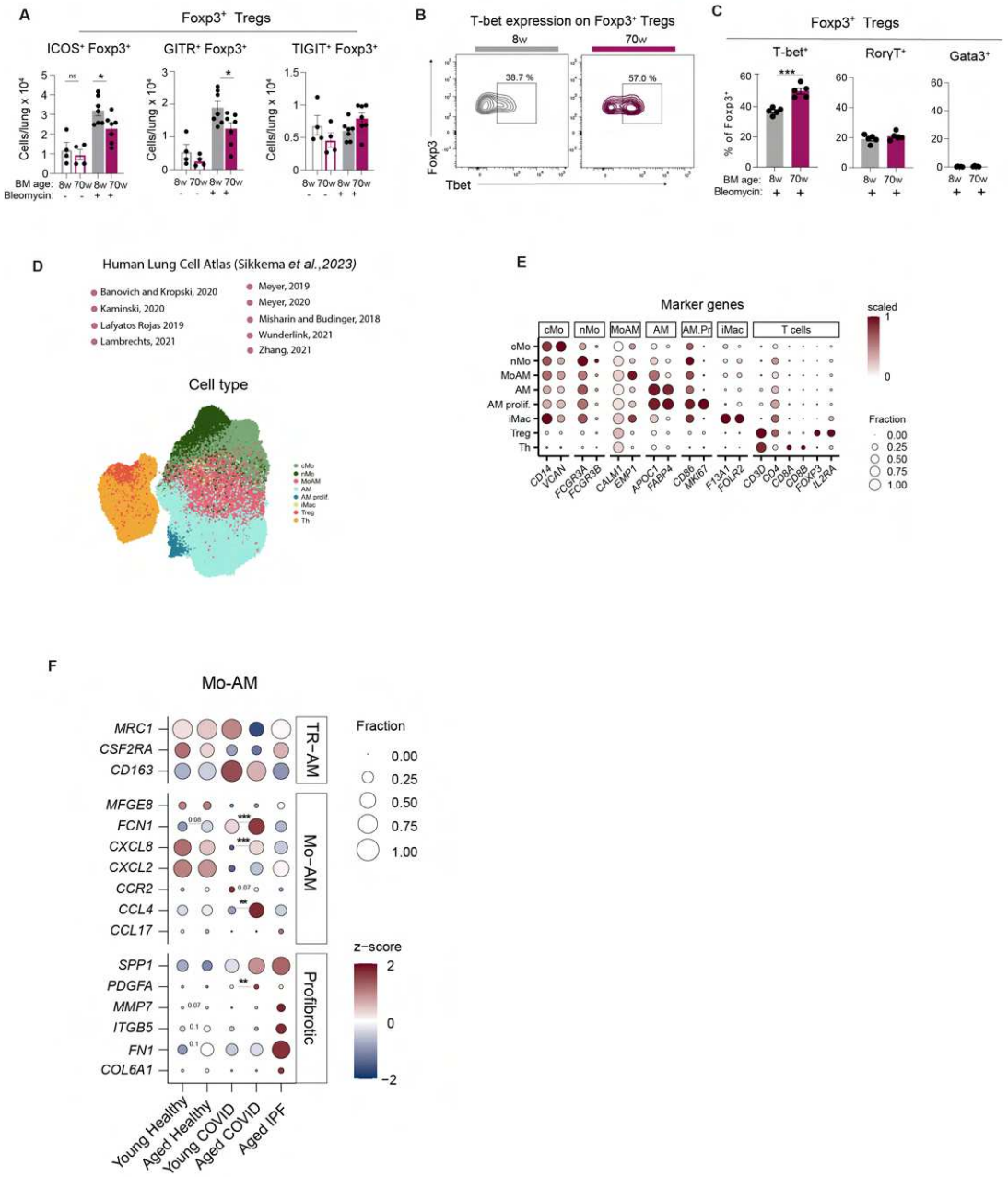

Fig. S8. Foxp3⁺ Treg subsets are altered with age/an ageing bone marrow in mice and humans. **(A-C**) Characterization of lung Foxp3⁺ cells from recipients of 8w and 70w bone marrow at D7 post PBS/ bleomycin challenge **(A)** Absolute cell numbers of CD4⁺ Foxp3⁺ cells co-expressing ICOS, GITR and TIGIT. **(B)** Flow cytometry plots of T-bet⁺ Foxp3⁺ cells. **(C)** Percentage of CD4⁺ Foxp3⁺ cells co-expressing Tbet, Rorγt or Gata3. **(D-F)** The Human Lung Cell Atlas (HLCA) was used to analyze samples from Young Healthy, Aged Healthy, Young COVID, Aged COVID and Aged IPF patient samples. **(D)** UMAP showing classical monocytes (cMo), non-classical monocytes (nMo), monocyte-derived alveolar macrophages (Mo-AMs), alveolar macrophages (AMs), proliferating AMs, interstitial macrophages (iMacs), Tregs and other CD4+ T cells (Th). **(E)** Marker genes used to verify cell annotations. **(F)** Heatmap showing expression of selected genes categorized as TR-AM-like, Mo-AM-like and profibrotic, with a z-score per gene across all groups. Data is representative of one or two independent experiments. Symbols on bar graphs represent individual mice. For (S8A) a two-way ANOVA with post-hoc Tukey's multiple-comparison tests and (S8C) a Student's two tailed t test, (S8F) DEA analysis p-values (*Limma*) between indicated groups are shown on graph (data file S9). *P ≤ 0.05; **P < 0.01; ***P < 0.001; ns: not significant. Error bars represent SEM.

Fig. S9

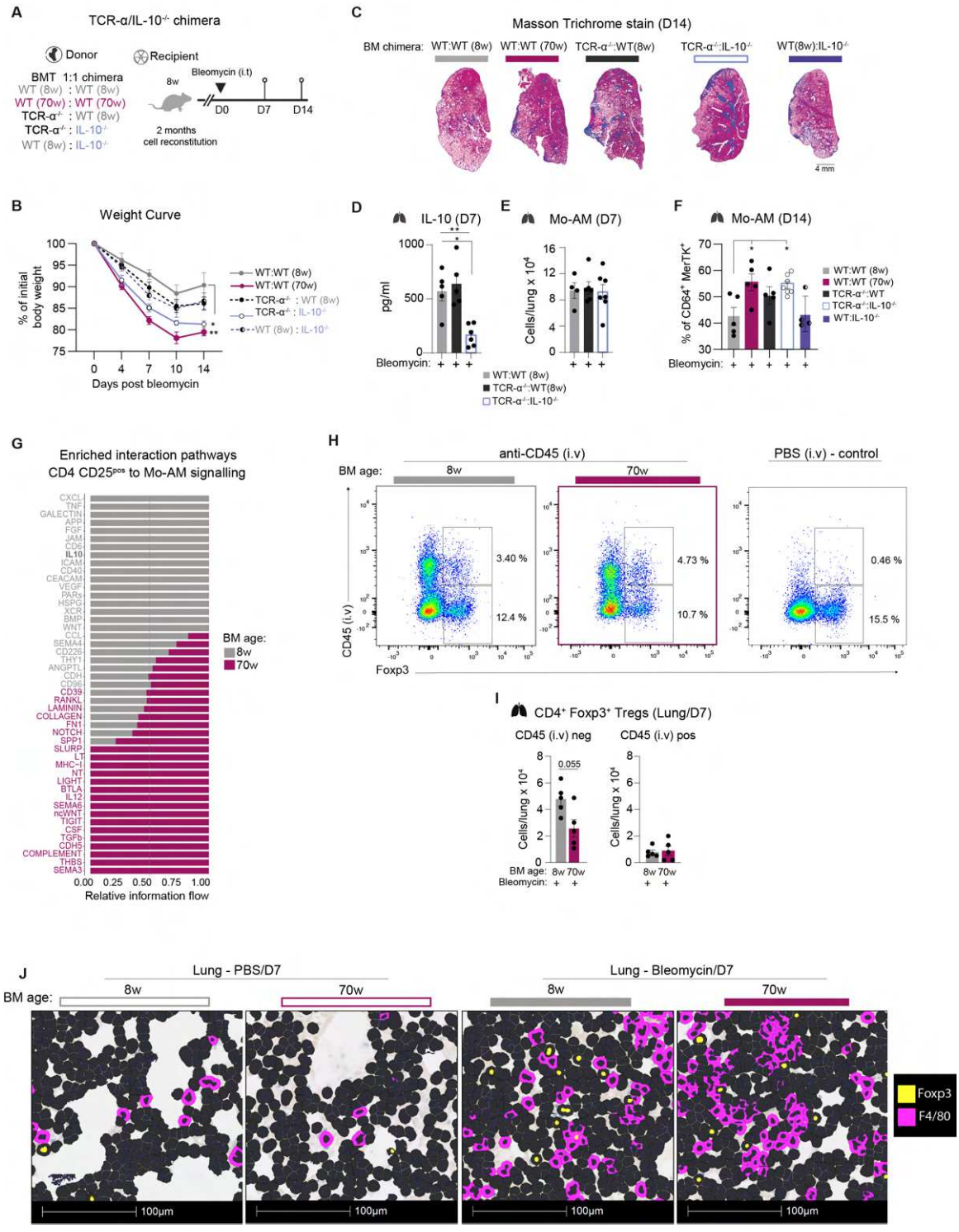

Fig. S9. Loss of T cell-mediated IL-10 promotes lung fibrosis.

(A) Experimental set up for **(A–F)** 8-week-old mice were irradiated and transplanted in a 1:1 ratio of bone marrow cells in the following groups: (WT (8w): WT (8w); (WT (70w): WT (70w); (TCR-α$^{-/-}$: young WT); (TCR-α-$^{-/-}$: IL-10$^{-/-}$) and (WT (8w): IL-10$^{-/-}$). TCR-α$^{-/-}$ and IL-10$^{-/-}$ mice were 8-weeks old. BM chimeras were challenged with bleomycin 2 months post-transplant (*n* = 5–7 per group). **(B)** Body weight curve until D14 post bleomycin challenge. **(C)** Histological sections of left lung lobe taken at D14

post bleomycin challenge stained with Masson Trichrome stain for collagen deposition. **(D)** ELISA of IL-10 from lung homogenates taken at D7 post bleomycin. **(E**) Absolute number of Mo-AMs from bone marrow chimeras at D7 post bleomycin. **(F)** Mo-AM numbers expressed as a percentage of $CD64^+$ $MerTK^+$ cells at D14. **(G)** CellChat analysis from transcriptomic data of sorted lung cell populations from recipients of young and aged bone marrow, showing relative information flow of significant signaling pathways between $CD4^+$ $CD25^+$ T cells (source) and Mo-AMs (target). **(H-I)** Fluorophore labelled anti-CD45 antibody was administered (i.v – intravenous) prior to organ collection at D7 post bleomycin challenge. **(H)** Flow cytometry plots showing $CD45^+$ (i.v) against $Foxp3^+$ expression in from lungs of recipients of young and aged bone marrow and control (no CD45 (i.v) administration) in the right panel. **(I)** Absolute cell numbers of CD45 (i.v) negative (intraparenchymal) and CD45 (i.v) positive $Foxp3^+$ cells (intravascular). **(J)** $F4/80^+$ (pink) and $Foxp3^+$ (yellow) staining of lung tissue sections of recipients of 8w or 70w bone marrow at D7 post PBS (left panel) and bleomycin (right panel) treatment. Stains shown are colocalization masks. For (S9B) a two-way ANOVA with post-hoc Dunnett's test, (S9D-F) a one-way ANOVA with post-hoc Dunnett's test and (S9I) Student's two tailed unpaired t-test was used. *P ≤ 0.05; **P < 0.01; ***P < 0.001; ns: not significant. Error bars represent SEM.

Fig. S10

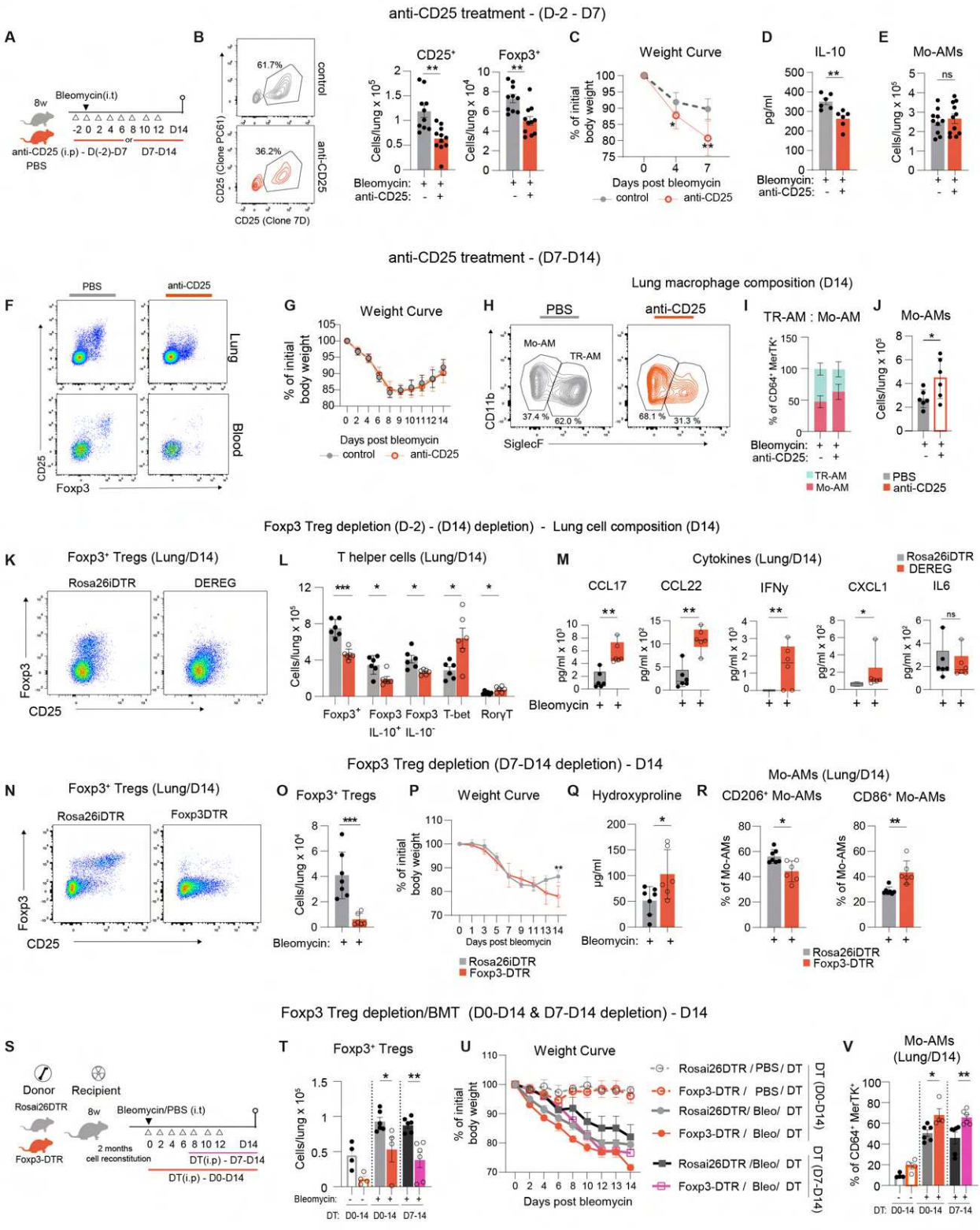

Fig. S10. Depletion of Tregs during the fibrotic development phase and/or loss of Treg -derived IL10 leads to Mo-AM accumulation.

Experimental set up for **(A-J)** 8-week-old C57BL/6J mice were treated i.p. with anti-CD25 mAb or PBS between (i) D-2 and D7 **(B-E),** with the end point at D7; or (ii) between D7 and D14 (**F-J)** with the end point at D14 post bleomycin challenge **(B)** Flow cytometry plots showing lung CD25⁺ CD4⁺ T cells from mice, which received anti-CD25 antibody or PBS, analyzed at D7 post bleomycin and absolute numbers

of CD25$^+$ and Foxp3$^+$ T cells on D7. **(C)** Body weight curve showing percentage of initial body weight loss until D7 post bleomycin. **(D)** ELISA of IL-10 from lung homogenates taken at D7 post bleomycin. **(E)** Absolute cell numbers of lung Mo-AMs at D7 post bleomycin and anti-CD25/PBS treatment. **(F)** Flow cytometry plots showing lung (top) and blood (bottom) CD25$^+$ T cells from mice, which received anti-CD25 antibody or PBS, analysed at D14 post bleomycin. **(G)** Body weight curve showing percentage of initial body weight loss from D0 to D14 post bleomycin. **(H)** Representative flow cytometry plots showing percentage of SiglecF and CD11b-expressing cells (Mo-AMs and TR-AM) pre-gated on MerTK$^+$ CD64$^+$ cells. **(I)** Percentage of TR-AMs and Mo-AMs expressed as a percentage of CD64$^+$ MerTK$^+$ lung cells. **(J)** Absolute cell numbers of lung Mo-AMs at D14 post bleomycin and anti-CD25/PBS treatment. **(K–M)** DEREG mice or Rosa26iDTR control were given bleomycin (i.t) and DT (i.p) every second day starting from D-2 to D14 pre/post bleomycin, data shown is from the lungs at D14 post bleomycin and DT-treatment. **(K)** Representative flow cytometry plots showing Foxp3$^+$ Tregs in the lungs. **(L)** Absolute cell numbers of lung Foxp3$^+$ IL-10$^+$ cells, Foxp3$^+$ IL10$^-$, T-bet$^+$ cells and Rorγt$^+$ cells. **(M)** Absolute values (pg/ml) of lung cytokines. **(N-R)** Foxp3-DTR or Rosa26iDTR controls were given bleomycin at D0, followed by DT (i.p) starting at D7 until the endpoint at D14, every two days, data shown is from the lungs/body-weight loss at D14 post bleomycin and DT-treatment. **(N)** Representative flow cytometry plots showing Foxp3$^+$ cells in the lungs of Rosai26DTR or Foxp3-DTR mice. **(O)** Absolute cell numbers of lung Foxp3$^+$ cells. **(P)** Body weight curve showing percentage loss of initial body weight from D0 to D14 post bleomycin challenge. **(Q)** Hydroxyproline quantification from lung tissue (D14). **(R)** Percentage of lung Mo-AMs co-expressing CD206 or CD86. **(S)** Experimental set up for **(T-V).** Young recipient mice were transplanted with either Foxp3-DTR or Rosai26DTR bone marrow cells. Post cell reconstitution, mice were challenged with PBS or bleomycin and administered DT (i.p) at the shown timepoints between D0-D14 or D7-D14. **(T)** Absolute cell counts of Tregs in the lungs at D14 post bleomycin. **(U)** Body weight curve showing percentage loss of initial body weight from D0 to D14 post bleomycin challenge. **(V)** Percentage of Mo-AM in the lungs at D14, expressed as a percentage of total CD64+ MerTK+ cells. For (S10B, S10D-E, S10J-L, S10O) , Student's two tailed unpaired t test was used, (S10I) multiple unpaired t-tests, (S10M) Mann-Whitney test. (S10C, S10P, S10U) a two-way ANOVA with post-hoc Tukey's multiple comparison and (S10T, S10V) with post-hoc Šídák's multiple comparisons test was used. Error bars represent SEM.*P ≤ 0.05; **P < 0.01; ***P < 0.001; ns: not significant.

Fig. S11

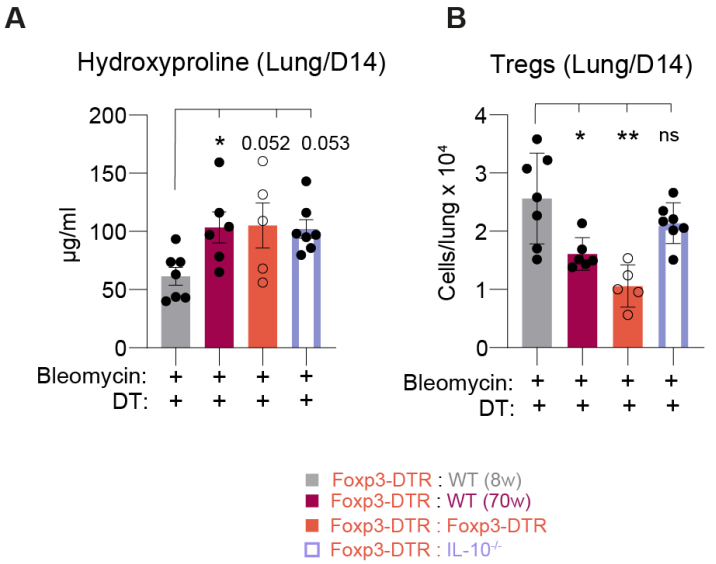

Fig. S11. Loss of IL-10 producing Tregs leads to Mo-AM accumulation.
Data from (Foxp3-DTR : WT (8w); (Foxp3-DTR : WT (70w); (Foxp3-DTR:Foxp3-DTR); (Foxp3-DTR: IL-10$^{-/-}$) chimeras at D14 post bleomycin. **(A)** Hydroxyproline quantification from lung tissue (D14). **(B)** Absolute cell numbers of lung Tregs. A one-way ANOVA with Dunnett's and Dunnett's T3 multiple comparisons to the Foxp3-DTR:WT (8w) group as the control was used. *P ≤ 0.05; **P < 0.01; ***P < 0.001; ns: not significant. Error bars represent SEM.

Table S1

Marker Name	Fluorophore (Color)	Company	Product ID	Clone	RRID	Dilution used for (1x10^6/100ul or similar ratio)
B220	PE	BioLegend	103208	RA3-6B2	AB_312993	1/200
CCR2	BV421	BioLegend	150605	SA203G11	AB_2571913	1/100
CD11b	Alexa Fluor 700	BioLegend	101222	M1/70	AB_493705	1/100
CD11b	BV605	BioLegend	101257	M1/70	AB_2565431	1/100
CD11c	PerCP/Cy5.5	BioLegend	117328	N418	AB_2129641	1/100
CD16/32	Pe-Cy7	BioLegend	101318	93	AB_2104156	1/100
CD16/32	NA	BioLegend	101320	93	AB_1574975	1/50
CD19	PE/Dazzle 594	BioLegend	115554	6D5	AB_2564001	1/200
CD19	PE	BioLegend	152408	1D3/CD19	AB_2629817	1/200
CD206	AF647	BioLegend	141712	C068C2	AB_10900420	1/100
CD25	FITC	BD Biosciences	558689	7D	AB_1645241	1/100
CD25	PE	BioLegend	102008	PC61	AB_312857	1/100
CD25	PerCP-Cy5.5	Thermo Fisher Scientific	45-0251-82	PC61	AB_914324	1/100
CD3	BV605	BioLegend	100237	17A2	AB_2562039	1/100
CD3	AF700	BioLegend	100216	17A2	AB_493697	1/100
CD3	PE/Dazzle 594	BioLegend	100246	17A2	AB_2565883	1/100
CD3	PE	BioLegend	100206	17A2	AB_312663	1/200
CD31	PE	BioLegend	160204	W18222B	AB_2876567	1/200
CD34	PerCP/Cy5.5	BioLegend	119328	MEC14.7	AB_2728137	1/100
CD4	PerCP-Cy5.5	BioLegend	100434	GK1.5	AB_893324	1/100
CD44	APC	BioLegend	103012	IM7	AB_312963	1/100
CD45	BV510	BioLegend	103138	30-F11	AB_2563061	1/100
CD45.1	APC	BioLegend	110714	A20	AB_313503	1/100
CD45.1	Pe-Cy7	BioLegend	110730	A20	AB_1134168	1/100
CD45.1	Pacific Blue	BioLegend	110722	A20	AB_492866	1/100
CD45.2	PE/Dazzle 594	BioLegend	109846	104	AB_2564177	1/200
CD49b	Pacific Blue	BioLegend	108918	DX5	AB_2265144	1/200
CD64	PE/Cy7	BioLegend	139314	X54-5/7.1	AB_2563904	1/100
CD64	PE/Dazzle 594	BioLegend	139320	X54-5/7.1	AB_2566559	1/100
CD86	PE-Cy7	Thermo Fisher Scientific	25-0862-82	GL1	AB_2573372	1/100
CD8a	BV605	BioLegend	100744	53-6.7	AB_2562609	1/100
CD8a	AF700	BioLegend	100730	53-6.7	AB_493703	1/100
CD90.2	Pe-Cy7	BioLegend	105326	30-H12	AB_2201290	1/100
c-kit	AF700	BioLegend	105846	2B8	AB_2783046	1/100
Epcam	PE	BioLegend	118206	G8.8	AB_1134172	1/200
F4/80	FITC	BioLegend	123108	BM8	AB_893502	1/100

F4/80	APC	BioLegend	123116	BM8	AB_893481	1/100
F4/80	PE	BioLegend	123110	BM8	AB_893486	1/200
Fixable Viability dye	eFluor 780	Invitrogen	65-0865-14	n/a	n/a	1/3000
Foxp3	APC	Thermo Fisher Scientific	17-5773-82	FJK-16s	AB_469457	1/100
Gata3	Pe-Cy7	BD Pharminge n	560405	L50-823	AB_1645544	1/100
GITR	Pe-Cy7	BioLegend	126318	DTA-1	AB_2563386	1/100
GR1	PE	BioLegend	108408	RB6-8C5	AB_313373	1/200
ICOS	PE	Thermo Fisher Scientific	12-9942-82	7E.17G9	AB_466274	1/100
IL-10	BV421	BioLegend	505021	JES5-16E3	AB_10900417	1/100
IL-10	PE/Dazzle 594	BioLegend	505033	JES5-16E3	AB_2566328	1/100
IL-7R	APC	BioLegend	135012	A7R34	AB_1937216	1/100
Lag3	BV605	BioLegend	125257	C9B7W	AB_3106205	1/100
Ly6C	BV605	BioLegend	128036	HK1.4	AB_2562353	1/200
Ly6C	PE	BioLegend	128008	HK1.4	AB_1186132	1/200
Ly6G	BV510	BioLegend	127633	1A8	AB_2562937	1/100
Ly6G	PE-Cy7	BioLegend	127617	1A8	AB_1877262	1/100
LyVE1	eFluor 660	Thermo Fisher Scientific	50-0443-82	ALY7	AB_10597449	1/100
MerTK	FITC	BioLegend	151504	2B10C42	AB_2617035	1/200
MerTK	APC	BioLegend	151507	2B10C42	AB_2650738	1/200
MHCII/I-A/I-E	AF700	BioLegend	107621	M5/114.15.1	AB_493726	1/200
MHCII/I-A/I-E	Pacific Blue	BioLegend	107620	M5/114.15.2	AB_493527	1/200
NK1.1	APC	BioLegend	108709	PK136	AB_313396	1/100
NK1.1	BV605	BioLegend	108739	PK136	AB_2562273	1/100
RorγT	PE/Dazzle 594	BD Biosciences	562684	Q31-378	AB_2651150	1/100
Sca-1	BV605	BioLegend	108134	D7	AB_2650926	1/100
Siglec-F	PE	BD Pharminge n	552126	E50-2440 (RUO)	AB_394341	1/100
Siglec-F	PerCP/Cy5.5	BD Pharminge n	565526	E50-2440 (RUO)	AB_2739281	1/100
ST2	APC	BioLegend	145306	DIH9	AB_2561917	1/100
T-bet	PE	BioLegend	644809	4B10	AB_2028583	1/100
TIGIT	PE/Dazzle 594	BioLegend	142110	1G9	AB_2566573	1/100

Table S1: List of antibodies used for flow cytometry and cell sorting.

Chapter 3

Extended Discussion

Over time and age, tightly regulated processes that maintain homeostasis, repair and resolution begin to deteriorate. A number of confounding factors right from the epigenetic to the macro-organ level drive this decline over time. Given the population and societal shifts we currently see, reducing disease burden that accompanies aging is a priority. Therefore, understanding the basic mechanisms that drive age-related disorders is essential (Budinger *et al*, 2017). Pulmonary fibrosis remains one of the most devastating chronic lung diseases with age being by far the most significant risk factor. The majority of cases occur in individuals over 60, yet the precise biological mechanisms linking aging to fibrosis remain incompletely understood (Raghu *et al.*, 2006). Despite a number of clinical trials and decades of research, lung transplant is the only current cure. Research on aging-related fibrosis has focused extensively on epithelial dysfunction, (Watanabe *et al.*, 2021), that impair epithelial regeneration and increase susceptibility to lung injury, contributing to fibrotic remodeling (Yao *et al.*, 2021). However, despite growing recognition of the immune system's role in orchestrating aberrant repair and fibrotic responses, it is unknown as how hematopoietic aging—specifically, the age of bone marrow-derived immune cells—shapes disease severity in lung fibrosis. Given that it is Mo-AMs that fuel lung fibrosis and seem to drive the fate of resolution or aberrant repair (Misharin *et al.*, 2017), their age-associated changes are poorly understood. The extent to which aging alters Mo-AM differentiation, persistence, and function in fibrosis has remained an open question in the field.

To address this, our study specifically examined the specific contribution of an aged bone marrow to the pathogenesis of lung fibrosis, independent of the aging lung epithelium. By employing heterochronic bone marrow transplant models, we investigated whether the age of hematopoietic-derived immune cells alone is sufficient to drive fibrotic exacerbation. This approach allowed us to distinguish the intrinsic impact of aged immune cells from the well-documented influence of an aging lung tissue. Our findings reveal that the age of the bone marrow plays a decisive role in shaping the fibrotic trajectory, not only by increasing Mo-AM influx but also by disrupting the regulatory networks that govern their transition to a homeostatic phenotype. The results presented in this study challenge the prevailing notion that lung fibrosis in aging is primarily an epithelial-driven process and instead highlight the critical role of the hematopoietic system in dictating disease outcome.

So far the field had assumed that the triggering events that led to an the development of lung fibrosis with increasing age was due to age-related changes or dysregulation in the non-immune compartment, which then led to increased immune infiltration and an altered immune and injury response downstream. Alterations in the lung tissue include dysregulation in collagen-producing fibroblast activation, in epithelial cell proteostasis or transition, increased permeability or leakiness of the epithelial barrier (Watanabe *et al.*, 2021). While these are indeed prime drivers of lung fibrosis and are altered with age, dysfunction of the immune system, another major player in the development of fibrosis (as described in Chapter 1), occurs simultaneously (McQuattie-Pimentel *et al.*, 2021; Strunz *et al.*, 2020; Watanabe *et al.*, 2021). Previous studies have largely utilized naturally aged mice to study the role of aging in fibrosis, where changes in both the non-immune and immune compartments are present, making it impossible to dissect the sole influence of immune aging on disease development. Here, we therefore, made use of a heterochronic mouse model, i.e we transplanted young or aged bone marrow into young mice. This way we were able to keep the lung tissue (structural cell compartment) of young origin and compare the impact young and aged hematopoietic stem cells and immune cells. A major finding in our study was that hematopoietic aging was enough to drive increased lung fibrosis independent of the age of the lung tissue. A recent study by Park et al 2024, observed a similar phenomenon. In their study they discovered that the age of the bone-marrow and hematopoietic stem cell niche also drove the susceptibility of lung cancer, despite the presence of young stromal cells which were previously also thought to be the primary drivers of tumor growth (Park *et al*, 2024). Our studies together present evidence that age-induced alterations stemming from the bone marrow, in the hematopoietic stem cells and subsequent immune cells can independently lead to disease in distance organs such as the lung.

Upon tissue injury, inflammatory immune cells such as neutrophils, monocytes and lymphocytes are recruited into the area of injury via chemokine gradients, where they clear debris, neutralize the acute pathogen and contribute to repair and restoring tissue architecture (Gieseck *et al.*, 2018; Pervizaj-Oruqaj *et al.*, 2024a). Studies using animal models often complicate this understanding by inducing simultaneous damage across all lung compartments, which hinders the ability to isolate the contributions of different lung niche components—stromal, immune, epithelial, and endothelial (McQuattie-Pimentel *et al.*, 2021). Severe damage, such as that caused by pneumonectomy, hyperoxia, bleomycin-injury affects all cellular compartments. Fibrosis, especially in experimental mouse-models such as the bleomycin model, is induced upon severe lung injury to the epithelia and the downstream dysregulation of the repair response leads to fibrosis (Misharin *et al.*, 2017). So, while a heterochronic transplant of hematopoietic cells neatly dissects pre-existing age-related effects

of the immune (bone-marrow derived) versus the lung tissue, it still could raise the question of whether the disease or repair response was determined by the nature of the recruited cells or by the extent of the initial damage to the tissue. At day 7 after treatment with bleomycin, which is when the inflammatory phase is at its peak, we saw that an aged bone-marrow led to increased inflammation: elevated pro-inflammatory cytokines, numbers of monocytes, neutrophils, Mo-AMs. This could potentially suggest that this was because the *early injury itself was heightened* in mice which were transplanted with aged immune cells, resulting in increased tissue fibrosis as a downstream consequence of this. To test this, we assessed bona-fide readouts of lung injury at this timepoint. This included measuring the amount of protein (albumin) present in the bronchoalveolar lavage and the number of apoptotic cells (TUNEL+), both quantitative indicators of lung injury (Matute-Bello *et al*, 2011). While bleomycin challenge, did cause a drastic increase in the protein levels and number of apoptotic cells compared to PBS-treated mice, this was comparable between mice which received young and aged bone marrow, showing the worsened age-dependent fibrosis that we see in our model, is unlikely to be caused by differences in the degree of initial lung injury. While it could be that markers of lung injury are different between the two groups prior to day 7, very early post initial injury, prior studies (Watanabe *et al.*, 2021; Weng *et al.*, 2022) do use day 7 after bleomycin administration to assess the damage to the lung tissue, supporting our choice of assessing the lung at this timepoint. Therefore, although a hypothesis aging immune cells alter the tissue's initial response to lung injury is an interesting plausibility, it does not seem to be the case, atleast with the readouts we assessed. A deeper characterization, especially one that looks into the epigenetic profile of the lung epithelial cells and fibroblasts that encountered aged immune cells (during reconstitution with aged bone marrow-derived immune cells) could reveal alterations in their imprinted memory and interactions that then influence their response to injury, adding yet another layer to the impact of aging on chronic disease onset.

As described in the introduction, advanced age brings with it marked alterations in the hematopoietic stem cell (HSC) compartment. There is a decline in overall stem cell function (de Haan *et al*, 1997) and a skewed distribution towards myeloid and platelet differentiation over lymphocyte production (Grover *et al*, 2016; Kowalczyk *et al*, 2015; Rossi *et al.*, 2005). This imbalance increases the risk of myeloid-based malignancies. In our model, we wanted to understand how these alterations could impact chronic disease in other organs, in our case lung fibrosis. We transplanted bone marrow cells from young or aged bone marrow into lethally irradiated young recipient mice. While this is an efficient system to dissect the role of the bone marrow vs the lung structural cells in lung fibrosis, it could be argued that irradiation induced inflammation can damage the HSC niche and induce a myeloid biased skewing of HSC differentiation. A previous study examined this and to discern the effect of an irradiated niche

on the efficacy of aged HSCs, Kuribayashi et al, 2020 (Kuribayashi *et al.*, 2021) transplanted an excess of aged HSCs into an intact young bone marrow niche and observed that despite successful engraftment of the aged HSCs, the dysfunctional regeneration and myeloid biased output persisted, indicating that was not a result of the myeloablative techniques used. They also showed that while a young niche was able to restore the transcriptional profile of aged HSCs, it had no impact on the DNA methylation and functional capacity of the aged HSCs, highlighting that cell intrinsic alterations with age persist independent of the bone marrow microenvironment. We observed that when mice were given bleomycin intratracheally, the numbers of myeloid progenitors in the bone marrow increased. Interestingly, this increase was much more pronounced in aged bone marrow recipients, whereas young recipients exhibited both myeloid and lymphoid progenitor expansion. It is important to note that our transplantation procedure involved the transfer of all bone marrow cells, including the existing distribution of hematopoietic stem cells (HSCs) in the donor mice. Consequently, the observed bias in expansion following bleomycin challenge could potentially be attributed to the initial disbalance of HSCs in the recipients. Previous work employing single-cell transplantation strategies of young and aged long-term HSCs (LT-HSCs) showed that the myeloid-lymphoid skewing persisted in these models, indicating that the observed effect was not solely influenced by the number of transplanted myeloid HSCs and that factors beyond the initial distribution of myeloid HSCs contribute to the observed bias (Kuribayashi *et al.*, 2021). Furthermore, our results also showed that in contrast to HSC compartment of naturally aged mice, which had significant differences in myeloid and lymphoid progenitor cell numbers at baseline, eight weeks post-transplant, these differences were not apparent in bone-marrow recipients. However, with bleomycin challenge, the skewing became significant, mirroring what we see in the bone-marrow of naturally young and aged mice. Recently, two studies have highlighted the critical role of an aging bone marrow and hematopoiesis in disease. Ross et al. demonstrated that depleting myeloid-biased HSCs in aged mice restores immune balance by reducing inflammation and enhancing lymphopoiesis, underscoring the active contribution of hematopoietic aging to immune dysfunction (Ross *et al*, 2024). Another study employed a similar heterochronic bone marrow transplant model in the context of lung cancer, showing that increased myelopoiesis led to an accumulation of monocyte-derived alveolar macrophages (Mo-AMs) that produced IL-1β, exacerbating tumor progression independently of stromal age—the traditionally assumed primary driver of age-associated cancer risk (Park *et al.*, 2024). Their findings reinforce the bone marrow-derived nature of pathogenic myeloid phenotypes and highlight its role as a conserved feature across disease models, with broad implications for aging-related pathologies. While Park et al. focused on clonal mutations as a key driver of these changes, we did not explore this aspect in our study. However, we hypothesize that intrinsic aging-associated alterations in the bone marrow are sufficient to

skew Mo-AM differentiation and function toward a pathogenic phenotype. Notably, similar to their findings in cancer, our study also showed that reconstitution with young bone marrow reduced disease severity in aged mice, further supporting the notion that age-associated hematopoietic changes are a key determinant of disease progression across diverse tissue pathologies.

In our study, we saw that after reconstitution with aged bone-marrow (at baseline), the numbers of tissue resident alveolar macrophages in bronchoalveolar lavage were reduced in mice given aged bone marrow cells. To first rule out if this was caused by changes in the localization of the AMs, we also looked at the lung tissue and found a similar reduction in lung TR-AMs in recipients of aged bone marrow. This is in line with findings in naturally aged mice, which have reduced numbers of TR-AMs in the lung that were transcriptionally distinct from young TR-AMs with cell-adhesion, cell cycle and proliferation genes downregulated thereby indicating a reduced potential of aged TR-AMs to efficiently fill or maintain the niche (McQuattie-Pimentel *et al.*, 2021). Interestingly, prior research suggests that aging alters the lung's extracellular matrix. McQuattie-Pimentel et al, 2021 found that aging lungs had increased hyaluronan deposition. When they cultured AMs derived from BMDMs with hyaluronan they found alterations in AM proliferation and response to GM-CSF (an important growth factor), and therefore concluded that the aged lung environment conferred this AM attrition (McQuattie-Pimentel *et al.*, 2021). However, this study did not directly compare the response of young and aged BMDMs cultured ex-vivo on hyaluronan to identify if any age-related effects persisted. (Park *et al.*, 2024)also found reduced numbers of AMs in aged mice, that had a lower proliferative capacity despite an increased baseline myeloid bias in the bone-marrow, corroborating our findings (Park *et al.*, 2024). While changes in the lung tissue could indeed impair AM proliferation, our observation where we see a similar AM reduction in our heterochronic model in which the age of the lung tissue was similar between recipients of young and aged bone marrow, indicates that the age of the immune environment and/or age of the AMs also played a role. In line with this, (Li *et al.*, 2022) also showed that when they transferred naïve AMs isolated from either young or aged mice into a neonatal mice lacking endogenous AMs (GMCSFR KO mice) young AMs proliferated adequately while aged AMs failed to do so, hinting at possible cell-intrinsic mechanisms at play that impacted their long-term survival. Taken together, our work in context with previous studies suggests that regardless of whether AMs are embryonically derived in a naturally aged lung or repopulated from aged bone marrow, they seem to ultimately fail to sustain their population over time, leading to a deficit in the lungs. Furthermore, a look into the tissue-resident macrophage landscape across tissues reveals that this loss of tissue-resident macrophages with age is not an exclusive feature of the lung AMs. In tissues such as the liver and skin where tissue-resident

macrophages (Kupffer cells and dermal macrophages respectively) share similar developmental origins as AMs, i.e embryonically derived and can self-sustain at steady-state (Hashimoto *et al.*, 2013), a similar loss occurs with age. In the liver, Kuppfer cell numbers were lower in older mice but with no obvious changes to their proliferation rate. This study attributed this depletion to the increase in low-grade inflammation that accompanies aging (Adé *et al*, 2022). In the skin, Dube et al found that there was a dramatic loss of dermal macrophages with age. These aged macrophages in the skin also had a pro-inflammatory phenotype with a reduced proliferative capacity, resembling features of aging lung AMs (Dube *et al*, 2022). These observations therefore reveal that there seems to be a systemically conserved feature of aging that impacts tissue-resident macrophages. If this is due to the lifespan, proliferation or turnover of the macrophages themselves, erosion of homeostatic 'youthful' macrophage niches or changes in inflammation and trophic factors over time is an important question that needs to be disentangled. The exact signals, whether AM-intrinsic or extrinsic from the lung microenvironment (and as our results indicate likely stemming from other immune cells) that AMs need to sustain themselves over a period of time are still unclear.

The availability of space in the macrophage niche is a primary determinant if circulating monocytes will engraft, differentiate into Mo-AMs and take up residence as TR-AMs (Guilliams *et al.*, 2020). Upon severe lung inflammation or injury, the alveolar macrophage niche undergoes dramatic remodeling, with the loss of tissue resident alveolar macrophages and their subsequent replacement by Mo-AMs from the bone marrow a common feature across a myriad of infections and injury model systems (Aegerter *et al.*, 2020; Li *et al.*, 2022; Machiels *et al.*, 2017). Given that aged mice had reduced TR-AMs and we found this to be recapitulated post reconstitution with an aged bone-marrow, we initially hypothesized that in line with the macrophage niche model, the increased numbers of infiltrating Mo-AMs that we saw from an aged bone-marrow could be due to this baseline space and deficit, I,e more monocytes were able to accumulate in the alveolar space To conclusively test this, we used a model where we shielded the thorax during irradiation. This protected the lung immune cells, allowing them to be of host origin. At baseline, we saw that the entire TR-AM compartment was of young origin. i.e host derived with no differences between recipients of young and aged bone-marrow and a similarly occupied TR-AM niche. Upon bleomycin, we however observed increased monocytes and Mo-AMs were still recruited from an aging bone marrow. This indicates that the output of the bone marrow progenitors or the differentiation and homing potential of aged monocytes and Mo-AMs is enhanced and is a major determinant of the number of infiltrating pro-fibrotic cells, independent of the initial niche space. Similarly, a prior study, attributed increased Mo-AM accumulation in aged mice upon bleomycin injury to increased epithelial barrier permeability (Watanabe *et al.*, 2021). While we did not specifically test barrier

permeability, the transplant of young bone marrow to aged mice, curbed the Mo-AM accumulation, once again pointing towards a role for bone marrow age in driving increased numbers.

The initial inflammatory/pro-fibrotic signature of Mo-AMs could be a result of their recent monocytic origin or due to their first imprinting event taking place in a highly inflamed lung post bleomycin injury. One hypothesis put forth in the field to explain the increased reactivity observed in Mo-AMs as opposed to TR-AMs of fetal origin is their recent monocytic past. While recruited monocytes differentiate into alveolar macrophages and join the pool of TR-AMs in the lung post injury or infection, studies have shown that when recruited Mo-AMs were analyzed even after 28 days post-infection with influenza (IVI) they still showed transcriptomic and chromatin signatures of their monocytic past. Aegerter et al, found that post IVI infection, upon stimulation with a second hit, bacterial infection, recruited AMs produced increased levels of IL6, with open chromatic signatures similar to that of blood monocytes and not present in resident AMs, highlighting the persistence of their monocyte 'legacy' (Aegerter *et al.*, 2020). We observed that Mo-AMs which were derived from an aged bone marrow had an enhanced profibrotic phenotype and over time in the lungs failed to mature and acquire a tissue-resident homeostatic phenotype at the same rate as young Mo-AMs. This could be due to either cell-intrinsic deficits or due to cell-extrinsic environmental differences. To determine the extent each factor contributed, we used a mixed bone-marrow chimera system where both young and aged Mo-AMs were exposed to the same lung environment and found that although aged Mo-AM numbers were increased, their phenotype was similar to young Mo-AMs and the impact on fibrosis exacerbation was reduced which showed that the l determinants of Mo-AM identity and function are driven by cell-extrinsic factors. Since in our model the extrinsic factors are also derived from the hematopoietic system, it shows that an aging immune system has a widespread role in driving lung fibrosis by increasing the number of profibrotic macrophages and also altering the lung immune microenvironment through dysregulated signaling such as restricted Treg-derived IL-10, which impair their return to homeostasis.

Chronic inflammation creates a pathologically non-permissive environment that disrupts tissue regeneration, impeding the transition of alveolar type 2 (AT2) to type 1 (AT1) cells, which are essential for restoring gas exchange in the lungs. The aberrant accumulation of damage-associated transitional progenitors (DATPs), characterized by markers such as KRT8 and CLDN4, is a hallmark of conditions like idiopathic pulmonary fibrosis (IPF) (Jiang *et al.*, 2020). These intermediary populations arise during the AT2-to-AT1 transition, a critical step in alveolar regeneration. However, persistent inflammation in diseases like IPF appears to stall this transition, leading to the accumulation of DATPs in fibrotic regions. Previous studies have shown that interstitial macrophages (IMs) and monocyte-derived alveolar macrophages (Mo-

AMs) play a key role in facilitating this differentiation process, with interstitial macrophage-derived IL-1β priming AT2 cells expressing Il1r1 for conversion into DATPs through a HIF1α-mediated glycolysis pathway (Choi *et al.*, 2020). Chronic IL-1β signaling, however, disrupts this progression, resulting in impaired alveolar repair. Building on this, our findings suggest that the persistence of inflammatory and profibrotic Mo-AMs, exacerbated by an aged bone marrow, results in a failure of Mo-AMs to transition into a resolving state. This could perpetuate a pro-inflammatory niche, further hindering AT2 to AT1 cell fate transitions and potentially contributing to failed epithelial regeneration. While we did not directly examine the molecular mechanisms underlying this interplay, we hypothesize that the dysregulated immune environment driven by aged Mo-AMs plays a central role in impairing the resolution of inflammation and epithelial repair. Targeting pathways that modulate Mo-AM phenotype or enhance pro-resolving signals, such as IL-10, may provide therapeutic avenues to restore epithelial regeneration and mitigate fibrosis progression.

Severe injury or infection can lead to either appropriate regeneration and repair or if not tightly regulated to uncontrolled fibrosis and scarring (Diegelmann & Evans, 2004). The initial inflammatory signals serve to kickstart efficient repair processes, however, post this there is a specific window of time during which the inflammatory signals should be removed or blocked, and failure to do so leads to a dysregulated fibrotic response with ongoing inflammation and beyond this point removal of the inflammatory signal does not seem to reverse fibrosis in most organs (Adler *et al.*, 2020). Hence, early control of the inflammatory response is crucial as the tissue maneuvers this fine balance between repair or fibrosis. In our study, we found that aged bone marrow recipients had an exaggerated inflammatory response during the early phase of bleomycin challenge in comparison with young bone marrow recipients, characterised by excessive neutrophil, monocyte, and Mo-AM infiltration as well as a heightened inflammatory milieu with significantly elevated IFN-y and IL-6 but decreased IL-10 available in the lung microenvironment. This reduced availability of a key anti-inflammatory mediator (Fiorentino *et al*, 1991) therefore could be responsible for failing to control the inflammation induced by bleomycin injury and controlling the switch between repair and fibrosis. IL-10 signaling has been previously implicated to be important in regulating bleomycin induced lung fibrosis with CD4+ T cell derived IL-10 limiting an IL-17A driven fibrotic pathology and reducing pro-fibrotic TGF-β activity. Furthermore IL-10 KO mice displayed exacerbated fibrosis driven by elevated IFN-y and IL-17A (Wilson *et al.*, 2010) . In our study we found that aged BM recipients as well as aged mice had decreased CD4+ T cell derived IL-10 upon bleomycin challenge, with young chimeric mice lacking T cell specific IL-10 mimicking the worsened fibrotic response we observed in aged bone marrow recipients. This therefore indicates that a key fibrotic limiting pathway, atleast in the context of a bleomycin injury model, is dysregulated in aged bone

marrow recipients. Conversely a recent study found that IL-10 propagated fibrosis by driving the polarisation of IL-10 receptor expressing Mo-AMs and inducing the expression of PDGFa, a profibrotic mediator, in these macrophages (Bhattacharyya *et al.*, 2022). In line with this study, we also observed IL-10 receptor expression to be specific to pro-fibrotic Mo-AMs within the macrophage clusters in the lung upon bleomycin challenge. However, we observed that IL-10 functioned to calm the initial inflammatory signature of Mo-AMs, in particular subduing their expression of IL-6, CCL17, CXCL1, that was particularly upregulated by aged Mo-AMs. We believe the contradictory results of the role of IL-10 during fibrosis can be attributed to the complex nature of fibrosis. In our study IL-10 seems to function as an early anti-inflammatory mediator working to negate the ongoing inflammatory signature of Mo-AMs and by doing so removing the inflammatory signal and propagating appropriate resolution and repair, the lack of which in aged bone marrow recipients leads to exacerbated fibrosis. However, in the absence of an immediate need to block an inflammatory signature, the presence of IL-10 can also push Mo-AMs into a state of repair overdrive by inducing an 'M2' state thus creating a dysregulated fibrosis response (Bhattacharyya *et al.*, 2022; Sica & Mantovani, 2012; Wynn & Vannella, 2016). Indeed, we observe that in young bone marrow-derived Mo-AMs, there is an initial heightened inflammatory profile that diminishes over time. This is accompanied by the early activation of IL-10-induced genes. In contrast, aged Mo-AMs exhibit a delayed induction of inflammatory genes and an increased pro-fibrotic profile over time, along with a late IL-10-induced signature, suggesting that although there is an eventual IL-10 induced signature seen in aged MoAMs, it may occur too late to effectively contain the inflammatory response and might even contribute to disease progression. However, taken together, the findings of our study of a pro-fibrotic Mo-AM specific IL-10R upregulation, in line with Bhattacharya et al, showing IL-10RA expression on pro-fibrotic macrophages in the lungs of IPF patients, highlights a key role for an IL-10 dependent modulation of macrophage function during fibrosis. Therefore, our data underscores the idea that a regulated IL-10 response serves as a critical decision point in the transition of an Mo-AM into an immunosedated TR-AM state (Kulikauskaite & Wack, 2020) by dampening its inflammatory signature and facilitating it to become responsive to signals in the environment that could drive the transition into long-lived homeostatic TR-AMs. This transition into an anti-inflammatory phenotype therefore functions to reign in excessive inflammation preventing further cell damage and chronic wounds or pathological fibrosis due to uncontrolled production of inflammatory mediators or a lack of resolving macrophages. Strategies aimed at reducing the accumulation of pro-inflammatory macrophages or promoting the shift towards reparative, anti-inflammatory phenotypes have shown potential for acerating tissue repair and might be useful to mitigate prolonged inflammation with age (Wynn & Vannella, 2016).

In our model, we found that the source of IL-10 that was reduced was derived from Tregs, with no detectable differences between any other young and aged immune cells. As described in the introduction, during homeostasis, TR-AMs also express IL-10R and need environmental IL-10 to maintain their immunosedated, low reactive state. Studies have shown that in this context, the lung epithelial cells are a source of IL-10 (Hussell & Bell, 2014a), with a reduction of epithelial cell derived IL-10 seen in conditions such as asthma. Upon epithelial injury, the loss or alteration of epithelial cell function raises the question of whether their IL-10 production is diminished. Although we did not explicitly investigate the differences in epithelial derived IL-10 through the time course, it is tempting to speculate that given that infiltrating Tregs are recruited in upon injury and expand consistently across lung injury models (Hawrylowicz & O'Garra, 2005; Proto *et al.*, 2018), they may serve as a transient compensatory source of a key anti-inflammatory factor IL-10, potentially bridging the gap during this critical window when homeostatic sources of IL-10 are possibly lost. In a model of acute peritonitis lipopolysaccharide-induced lung injury, Tregs were also shown to be integral for restraining inflammation. This study showed that Treg-derived IL-13, facilitated autocrine production of IL-10 by lung macrophages which then enhanced macrophage mediated efferocytosis and clearance of apoptotic cells to hasten resolution of injury (Proto *et al.*, 2018). Like this study, we also found a significant expansion of Tregs post bleomycin-induced lung injury, suggesting that an increase in Tregs as an injury response seemed to be a conserved feature across tissues. While we did not specifically test for Treg-derived IL-13, similar to decreased lung IL-10 we also observe a reduction of overall lung IL-13 availability, which could suggest a similar Treg-derived deficiency. However, in contrast to this study, while we saw that TR-AMs, IMs and Mo-AMs (lung macrophages) did indeed produce IL-10, we found no differences in IL-10 production between young and aged myeloid cells. Moreover, we saw that specific loss of IL-10-production by Tregs worsened fibrosis and caused Mo-AM accumulation, indicating that in our model it was Treg-derived IL-10 that promoted resolution of bleomycin-induced lung injury. Moreover, acute injury models in these studies focused on the role of Tregs in the early post-injury phase, where enhanced clearance of apoptotic cells might be key to limiting inflammation. In our model we found that Treg-mediated IL-10 curtailed the expansion of inflammatory Mo-AMs and promoted their homeostatic transition, post the acute stage as specific depletion of IL-10 or Tregs between D7-D14 alone was sufficient to exacerbate fibrosis and prevent Mo-AM maturation, whereas only early depletion while causing weightloss and inflammation did not impact the Mo-AM phenotype or numbers. This suggests that Tregs might contribute to different stages of resolution through distinct mechanisms. Adoptive transfer of young Tregs into aged mice at different stages of the disease might reveal the exact dynamics of Treg-Mo-AM interactions and the timepoint when IL-10 from Tregs is truly required by Mo-AMs to transition in concert with other mediators in the environment.

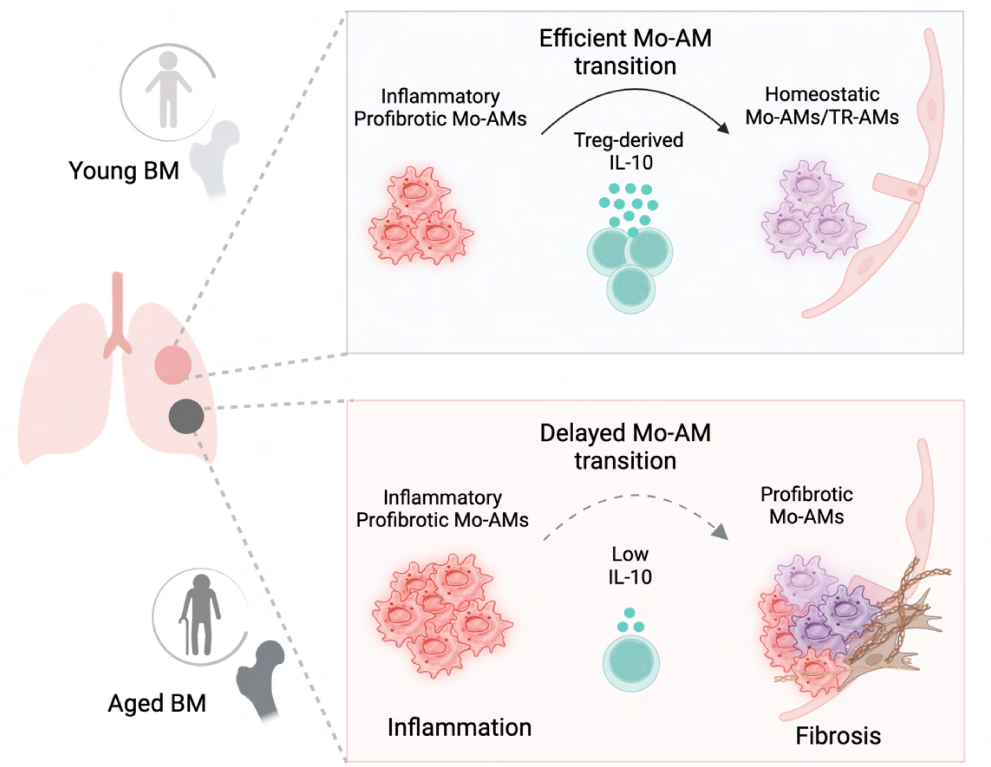

Thesis Figure 20: Graphical Abstract
An aged bone marrow exacerbates lung fibrosis by driving Mo-AM accumulation. In the lungs Mo-AMs have a delayed transition into a TR-AM phenotype due to less availability of Treg-derived IL-10.

Conclusions and outlook

Our study establishes hematopoietic aging as a key driver of lung fibrosis severity, demonstrating that the age of the bone marrow is a critical determinant of disease outcome. We show that an aged bone marrow fuels the accumulation of profibrotic Mo-AMs, which exhibit delayed maturation into a homeostatic state, perpetuating inflammation and fibrosis. Mechanistically, we identify that Treg-derived IL-10 as a key factor in promoting timely Mo-AM transition and as repair pathway that is disrupted with age. Our work highlights the systemic impact that aging has on tissue integrity and disease progression, emphasizing the need to look at interactions and contributions of both the tissue and immune system in repair, aging and disease.

The failure of aged Mo-AMs to efficiently transition not only sustains inflammation but likely impacts fibroblast activation, epithelial integrity, and overall tissue repair. Persistent Mo-AM-driven inflammation may influence fibroblast function and AT2-to-AT1 epithelial cell

differentiation, potentially impairing epithelial regeneration, and prolonging fibrosis. Future work will be needed to unravel the true impact that this delayed return to homeostasis and residency of macrophages has on tissue function and restoration of the injured lung. Early in life, in the first week, newly seeded AMs also transition from a highly inflammatory to a low-reactive phenotype, in parallel with alveologenesis. Whether parallels exist between development and the return to homeostasis in adult lung environments need to be further investigated. While insights from early life AM development may inform approaches to reprogram macrophages in aged lungs, tissue imprinting over a lifetime of exposure to inflammation needs to be considered. More broadly, with age, we need to adapt our understanding of what 'homeostasis' truly means. Homeostasis or homeostatic tissue-niches are not static states but evolve with age, inflammation, and repeated environmental exposures. Tissue niches, including the macrophage niche, adapt over time, and the concept of *returning to homeostasis* may not fully capture the reality and widespread impact of immune adaptation and inflammatory memory. Instead of resetting to a prior state, tissues may establish a new equilibrium that reflects accumulated challenges and cellular memory. Understanding these shifts is critical for refining therapeutic strategies that aim to restore function rather than merely suppress pathology. Identifying ways to modulate macrophage fate and their impact on tissue repair will be key to developing targeted strategies that mitigate fibrosis and promote tissue repair and regeneration in aging individuals.

Bibliography

Aberdein JD, Cole J, Bewley MA, Marriott HM, Dockrell DH (2013) Alveolar macrophages in pulmonary host defence – the unrecognized role of apoptosis as a mechanism of intracellular bacterial killing. *Clinical and Experimental Immunology* 174: 193-202

Abramson MJ, Murambadoro T, Alif SM, Benke GP, Dharmage SC, Glaspole I, Hopkins P, Hoy RF, Klebe S, Moodley Y *et al* (2020) Occupational and environmental risk factors for idiopathic pulmonary fibrosis in Australia: case–control study. *Thorax* 75: 864-869

Adé K, Coronilla JS, Obino D, Weinberger T, Kaiser C, Mella S, Chen C, Katsimpardi L, Werts C, Li H *et al*, 2022. Inflammation drives age-induced loss of tissue resident macrophages. Cold Spring Harbor Laboratory.

Adegunsoye A, Kropski JA, Behr J, Blackwell TS, Corte TJ, Cottin V, Glanville AR, Glassberg MK, Griese M, Hunninghake GM *et al* (2024) Genetics and Genomics of Pulmonary Fibrosis: Charting the Molecular Landscape and Shaping Precision Medicine. *American Journal of Respiratory and Critical Care Medicine* 210: 401-423

Adler M, Mayo A, Zhou X, Franklin RA, Meizlish ML, Medzhitov R, Kallenberger SM, Alon U (2020) Principles of Cell Circuits for Tissue Repair and Fibrosis. *iScience* 23: 100841

Aegerter H, Kulikauskaite J, Crotta S, Patel H, Kelly G, Hessel EM, Mack M, Beinke S, Wack A (2020) Influenza-induced monocyte-derived alveolar macrophages confer prolonged antibacterial protection. *Nat Immunol* 21: 145-157

Aegerter H, Lambrecht BN, Jakubzick CV (2022) Biology of lung macrophages in health and disease. *Immunity* 55: 1564-1580

Akashi K, Traver D, Miyamoto T, Weissman IL (2000) A clonogenic common myeloid progenitor that gives rise to all myeloid lineages. *Nature* 404: 193-197

Alder JK, Barkauskas CE, Limjunyawong N, Stanley SE, Kembou F, Tuder RM, Hogan BLM, Mitzner W, Armanios M (2015) Telomere dysfunction causes alveolar stem cell failure. *Proceedings of the National Academy of Sciences* 112: 5099-5104

Angelidis I, Simon LM, Fernandez IE, Strunz M, Mayr CH, Greiffo FR, Tsitsiridis G, Ansari M, Graf E, Strom T-M *et al* (2019) An atlas of the aging lung mapped by single cell transcriptomics and deep tissue proteomics. *Nat Commun* 10

Aran D, Looney AP, Liu L, Wu E, Fong V, Hsu A, Chak S, Naikawadi RP, Wolters PJ, Abate AR *et al* (2019) Reference-based analysis of lung single-cell sequencing reveals a transitional profibrotic macrophage. *Nat Immunol* 20: 163-172

Arpaia N, Green JA, Moltedo B, Arvey A, Hemmers S, Yuan S, Treuting PM, Rudensky AY (2015) A Distinct Function of Regulatory T Cells in Tissue Protection. *Cell* 162: 1078-1089

Atabai K, Jame S, Azhar N, Kuo A, Lam M, McKleroy W, Dehart G, Rahman S, Xia DD, Melton AC *et al* (2009) Mfge8 diminishes the severity of tissue fibrosis in mice by binding and targeting collagen for uptake by macrophages. *J Clin Invest* 119: 3713-3722

Auffray C, Fogg D, Garfa M, Elain G, Join-Lambert O, Kayal S, Sarnacki S, Cumano A, Lauvau G, Geissmann F (2007) Monitoring of Blood Vessels and Tissues by a Population of Monocytes with Patrolling Behavior. *Science* 317: 666-670

B. Moore B, Lawson WE, Oury TD, Sisson TH, Raghavendran K, Hogaboam CM (2013) Animal Models of Fibrotic Lung Disease. *Am J Respir Cell Mol Biol* 49: 167-179

Babb TG, Rodarte JR (2000) Mechanism of reduced maximal expiratory flow with aging. *Journal of Applied Physiology* 89: 505-511

Bailey JI, Puritz CH, Senkow KJ, Markov NS, Diaz E, Jonasson E, Yu Z, Swaminathan S, Lu Z, Fenske S *et al* (2024) Profibrotic monocyte-derived alveolar macrophages are expanded in patients with persistent respiratory symptoms and radiographic abnormalities after COVID-19. *Nat Immunol* 25: 2097-2109

Bain CC, Bravo-Blas A, Scott CL, Gomez Perdiguero E, Geissmann F, Henri S, Malissen B, Osborne LC, Artis D, Mowat AM (2014) Constant replenishment from circulating monocytes maintains the macrophage pool in the intestine of adult mice. *Nat Immunol* 15: 929-937

Bain CC, Macdonald AS (2022) The impact of the lung environment on macrophage development, activation and function: diversity in the face of adversity. *Mucosal Immunology* 15: 223-234

Barkauskas CE, Cronce MJ, Rackley CR, Bowie EJ, Keene DR, Stripp BR, Randell SH, Noble PW, Hogan BLM (2013) Type 2 alveolar cells are stem cells in adult lung. *Journal of Clinical Investigation* 123: 3025-3036

Barth MW, Hendrzak JA, Melnicoff MJ, Morahan PS (1995) Review of the macrophage disappearance reaction. *Journal of Leukocyte Biology* 57: 361-367

Basil MC, Katzen J, Engler AE, Guo M, Herriges MJ, Kathiriya JJ, Windmueller R, Ysasi AB, Zacharias WJ, Chapman HA *et al* (2020) The Cellular and Physiological Basis for Lung Repair and Regeneration: Past, Present, and Future. *Cell Stem Cell* 26: 482-502

Beerman I, Bock C, Brian, Zachary, Gu H, Meissner A, Derrick (2013) Proliferation-Dependent Alterations of the DNA Methylation Landscape Underlie Hematopoietic Stem Cell Aging. *Cell Stem Cell* 12: 413-425

Bertrand JY, Jalil A, Klaine ML, Jung S, Cumano A, Godin I (2005) Three pathways to mature macrophages in the early mouse yolk sac. *Blood* 106: 3004-3011

Bhandary YP, Shetty SK, Marudamuthu AS, Ji H-L, Neuenschwander PF, Boggaram V, Morris GF, Fu J, Idell S, Shetty S (2013) Regulation of Lung Injury and Fibrosis by p53-Mediated Changes in Urokinase and Plasminogen Activator Inhibitor-1. *The American Journal of Pathology* 183: 131-143

Bhattacharya M, Ramachandran P (2023) Immunology of human fibrosis. *Nat Immunol* 24: 1423-1433

Bhattacharyya A, Boostanpour K, Bouzidi M, Magee L, Chen TY, Wolters R, Torre P, Pillai SK, Bhattacharya M (2022) IL10 trains macrophage profibrotic function after lung injury. *Am J Physiol Lung Cell Mol Physiol* 322: L495-L502

Blasco MA (2005) Telomeres and human disease: ageing, cancer and beyond. *Nature Reviews Genetics* 6: 611-622

Boe DM, Hulsebus HJ, Najarro KM, Mullen JE, Kim H, Tan AC, McMahan RH, Kovacs EJ (2022) Advanced age is associated with changes in alveolar macrophages and their responses to the stress of traumatic injury. *Journal of Leukocyte Biology* 112: 1371-1386

Bogeska R, Mikecin A-M, Kaschutnig P, Fawaz M, Büchler-Schäff M, Le D, Ganuza M, Vollmer A, Paffenholz SV, Asada N *et al* (2022) Inflammatory exposure drives long-lived impairment of hematopoietic stem cell self-renewal activity and accelerated aging. *Cell Stem Cell* 29: 1273-1284.e1278

Boothby IC, Cohen JN, Rosenblum MD (2020) Regulatory T cells in skin injury: At the crossroads of tolerance and tissue repair. *Science Immunology* 5: eaaz9631

Borthwick LA, Barron L, Hart KM, Vannella KM, Thompson RW, Oland S, Cheever A, Sciurba J, Ramalingam TR, Fisher AJ *et al* (2016) Macrophages are critical to the maintenance of IL-13-dependent lung inflammation and fibrosis. *Mucosal Immunology* 9: 38-55

Bosurgi L, Cao YG, Cabeza-Cabrerizo M, Tucci A, Hughes LD, Kong Y, Weinstein JS, Licona-Limon P, Schmid ET, Pelorosso F *et al* (2017) Macrophage function in tissue repair and remodeling requires IL-4 or IL-13 with apoptotic cells. *Science* 356: 1072-1076

Branchett WJ, Cook J, Oliver RA, Bruno N, Walker SA, Stölting H, Mack M, O'Garra A, Saglani S, Lloyd CM (2021) Airway macrophage-intrinsic TGF-β1 regulates pulmonary immunity during early-life allergen exposure. *Journal of Allergy and Clinical Immunology* 147: 1892-1906

Branchett WJ, St€ H, Oliver RA, Walker SA, Puttur F, Gregory LG, Gabry Sov A L, Wilson MS, O'garra A, Lloyd CM *et al* (2020) A T cell-myeloid IL-10 axis regulates pathogenic IFN-g-dependent immunity in a mouse model of type 2-low asthma A T cell-myeloid IL-10 axis regulates pathogenic IFN-γ-dependent immunity in a mouse model of type 2-low asthma.

Brinkmann V, Reichard U, Goosmann C, Fauler B, Uhlemann Y, Weiss DS, Weinrauch Y, Zychlinsky A (2004) Neutrophil Extracellular Traps Kill Bacteria. *Science* 303: 1532-1535

Brown CC, Rudensky AY (2023) Spatiotemporal regulation of peripheral T cell tolerance. *Science* 380: 472-478

Brunkow ME, Jeffery EW, Hjerrild KA, Paeper B, Clark LB, Yasayko S-A, Wilkinson JE, Galas D, Ziegler SF, Ramsdell F (2001) Disruption of a new forkhead/winged-helix protein, scurfin, results in the fatal lymphoproliferative disorder of the scurfy mouse. *Nature Genetics* 27: 68-73

Bruunsgaard H, Andersen-Ranberg K, Hjelmborg JVB, Pedersen BK, Jeune B (2003) Elevated levels of tumor necrosis factor alpha and mortality in centenarians. *The American Journal of Medicine* 115: 278-283

Budinger GS, Kohanski RA, Gan W, Kobor MS, Amaral LA, Armanios M, Kelsey KT, Pardo A, Tuder R, Macian F *et al* (2017) The Intersection of Aging Biology and the Pathobiology of Lung Diseases: A Joint NHLBI/NIA Workshop. *The Journals of Gerontology: Series A* 72: 1492-1500

Burzyn D, Kuswanto W, Kolodin D, Jennifer, Cerletti M, Jang Y, Sefik E, Tze, Amy, Benoist C *et al* (2013) A Special Population of Regulatory T Cells Potentiates Muscle Repair. *Cell* 155: 1282-1295

Cakarova L, Marsh LM, Wilhelm J, Mayer K, Grimminger F, Seeger W, Lohmeyer J, Herold S (2009) Macrophage Tumor Necrosis Factor-α Induces Epithelial Expression of Granulocyte–Macrophage Colony-stimulating Factor. *American Journal of Respiratory and Critical Care Medicine* 180: 521-532

Campbell C, Dikiy S, Bhattarai SK, Chinen T, Matheis F, Calafiore M, Hoyos B, Hanash A, Mucida D, Bucci V *et al* (2018) Extrathymically Generated Regulatory T Cells Establish a Niche for Intestinal Border-Dwelling Bacteria and Affect Physiologic Metabolite Balance. *Immunity* 48: 1245-1257.e1249

Campisi J (2013) Aging, Cellular Senescence, and Cancer. *Annual Review of Physiology* 75: 685-705

Campisi J, D'Adda Di Fagagna F (2007) Cellular senescence: when bad things happen to good cells. *Nature Reviews Molecular Cell Biology* 8: 729-740

Campisi J, Kapahi P, Lithgow GJ, Melov S, Newman JC, Verdin E (2019) From discoveries in ageing research to therapeutics for healthy ageing. *Nature* 571: 183-192

Cesari M, Penninx BWJH, Pahor M, Lauretani F, Corsi AM, Williams GR, Guralnik JM, Ferrucci L (2004) Inflammatory Markers and Physical Performance in Older Persons: The InCHIANTI Study. *The Journals of Gerontology Series A: Biological Sciences and Medical Sciences* 59: M242-M248

Chaib S, Tchkonia T, Kirkland JL (2022) Cellular senescence and senolytics: the path to the clinic. *Nat Med* 28: 1556-1568

Chakarov S, Lim HY, Tan L, Lim SY, See P, Lum J, Zhang X-M, Foo S, Nakamizo S, Duan K *et al* (2019) Two distinct interstitial macrophage populations coexist across tissues in specific subtissular niches. *Science* 363: eaau0964

Chambers RC (2003) Role of coagulation cascade proteases in lung repair and fibrosis. *Eur Respir J* 22: 33s-35s

Chambers SM, Shaw CA, Gatza C, Fisk CJ, Donehower LA, Goodell MA (2007) Aging Hematopoietic Stem Cells Decline in Function and Exhibit Epigenetic Dysregulation. *PLoS Biology* 5: e201

Chaudhary NI, Schnapp A, Park JE (2006) Pharmacologic Differentiation of Inflammation and Fibrosis in the Rat Bleomycin Model. *American Journal of Respiratory and Critical Care Medicine* 173: 769-776

Chen F, El-Naccache DW, Ponessa JJ, Lemenze A, Espinosa V, Wu W, Lothstein K, Jin L, Antao O, Weinstein JS *et al* (2022a) Helminth resistance is mediated by differential activation of recruited monocyte-derived alveolar macrophages and arginine depletion. *Cell Reports* 38: 110215

Chen J, Stubbe J (2005) Bleomycins: towards better therapeutics. *Nature Reviews Cancer* 5: 102-112

Chen ST, Park MD, Del Valle DM, Buckup M, Tabachnikova A, Thompson RC, Simons NW, Mouskas K, Lee B, Geanon D *et al* (2022b) A shift in lung macrophage composition is associated with COVID-19 severity and recovery. *Science Translational Medicine* 14

Chen W, Jin W, Hardegen N, Lei K-J, Li L, Marinos N, McGrady G, Wahl SM (2003) Conversion of Peripheral CD4+CD25− Naive T Cells to CD4+CD25+ Regulatory T Cells by TGF-β Induction of Transcription Factor Foxp3 . *The Journal of Experimental Medicine* 198: 1875-1886

Chen X, Hyatt BA, Mucenski ML, Mason RJ, Shannon JM (2006) Identification and characterization of a lysophosphatidylcholine acyltransferase in alveolar type II cells. *Proceedings of the National Academy of Sciences* 103: 11724-11729

Chen Y, Pu Q, Ma Y, Zhang H, Ye T, Zhao C, Huang X, Ren Y, Qiao L, Liu H-M *et al* (2021) Aging Reprograms the Hematopoietic-Vascular Niche to Impede Regeneration and Promote Fibrosis. *Cell Metabolism* 33: 395-410.e394

Chiaramonte MG, Donaldson DD, Cheever AW, Wynn TA (1999) An IL-13 inhibitor blocks the development of hepatic fibrosis during a T-helper type 2–dominated inflammatory response. *Journal of Clinical Investigation* 104: 777-785

Chilosi M, Poletti V, Zamò A, Lestani M, Montagna L, Piccoli P, Pedron S, Bertaso M, Scarpa A, Murer B *et al* (2003) Aberrant Wnt/β-Catenin Pathway Activation in Idiopathic Pulmonary Fibrosis. *The American Journal of Pathology* 162: 1495-1502

Choi J, Park JE, Tsagkogeorga G, Yanagita M, Koo BK, Han N, Lee JH (2020) Inflammatory Signals Induce AT2 Cell-Derived Damage-Associated Transient Progenitors that Mediate Alveolar Regeneration. *Cell Stem Cell* 27: 366-382 e367

Chung EY, Liu J, Homma Y, Zhang Y, Brendolan A, Saggese M, Han J, Silverstein R, Selleri L, Ma X (2007) Interleukin-10 Expression in Macrophages during Phagocytosis of Apoptotic Cells Is Mediated by Homeodomain Proteins Pbx1 and Prep-1. *Immunity* 27: 952-964

Cialdai F, Risaliti C, Monici M (2022) Role of fibroblasts in wound healing and tissue remodeling on Earth and in space. *Frontiers in Bioengineering and Biotechnology* 10

Cohen HJ, Pieper CF, Harris T, Rao KMK, Currie MS (1997) The Association of Plasma IL-6 Levels With Functional Disability in Community-Dwelling Elderly. *The Journals of Gerontology Series A: Biological Sciences and Medical Sciences* 52A: M201-M208

Cohen M, Giladi A, Gorki AD, Solodkin DG, Zada M, Hladik A, Miklosi A, Salame TM, Halpern KB, David E *et al* (2018) Lung Single-Cell Signaling Interaction Map Reveals Basophil Role in Macrophage Imprinting. *Cell* 175: 1031-1044 e1018

Coker R, Laurent G, Shahzeidi S, Hernandez-Rodriguez N, Pantelidis P, Du Bois R, Jeffery P, McAnulty R (1996) Diverse cellular TGF-beta 1 and TGF-beta 3 gene expression in normal human and murine lung. *Eur Respir J* 9: 2501-2507

Connolly MK, Bedrosian AS, Mallen-St. Clair J, Mitchell AP, Ibrahim J, Stroud A, Pachter HL, Bar-Sagi D, Frey AB, Miller G (2009) In liver fibrosis, dendritic cells govern hepatic inflammation in mice via TNF-α. *Journal of Clinical Investigation*

Coppé J-P, Desprez P-Y, Krtolica A, Campisi J (2010) The Senescence-Associated Secretory Phenotype: The Dark Side of Tumor Suppression. *Annual Review of Pathology: Mechanisms of Disease* 5: 99-118

Correa-Gallegos D, Jiang D, Rinkevich Y (2021) Fibroblasts as confederates of the immune system. *Immunological Reviews* 302: 147-162

Cumano A, Godin I (2007) Ontogeny of the Hematopoietic System. *Annual Review of Immunology* 25: 745-785

D'Alessio FR, Tsushima K, Aggarwal NR, West EE, Willett MH, Britos MF, Pipeling MR, Brower RG, Tuder RM, McDyer JF *et al* (2009) CD4+CD25+Foxp3+ Tregs resolve

experimental lung injury in mice and are present in humans with acute lung injury. *Journal of Clinical Investigation* 119: 2898-2913

Dagher R, Copenhaver AM, Besnard V, Berlin A, Hamidi F, Maret M, Wang J, Qu X, Shrestha Y, Wu J *et al* (2020) IL-33-ST2 axis regulates myeloid cell differentiation and activation enabling effective club cell regeneration. *Nat Commun* 11

Daniel B, Czimmerer Z, Halasz L, Boto P, Kolostyak Z, Poliska S, Berger WK, Tzerpos P, Nagy G, Horvath A *et al* (2020) The transcription factor EGR2 is the molecular linchpin connecting STAT6 activation to the late, stable epigenomic program of alternative macrophage polarization. *Genes & Development* 34: 1474-1492

de Haan G, Nijhof W, Van Zant G (1997) Mouse strain-dependent changes in frequency and proliferation of hematopoietic stem cells during aging: correlation between lifespan and cycling activity. *Blood* 89: 1543-1550

De Sadeleer LJ, Verleden SE, De Dycker E, Yserbyt J, Verschakelen JA, Verbeken EK, Nemery B, Verleden GM, Hermans F, Vanaudenaerde BM *et al* (2018) Clinical behaviour of patients exposed to organic dust and diagnosed with idiopathic pulmonary fibrosis. *Respirology* 23: 1160-1165

Deaglio S, Dwyer KM, Gao W, Friedman D, Usheva A, Erat A, Chen J-F, Enjyoji K, Linden J, Oukka M *et al* (2007) Adenosine generation catalyzed by CD39 and CD73 expressed on regulatory T cells mediates immune suppression. *The Journal of Experimental Medicine* 204: 1257-1265

Della Latta V, Cecchettini A, Del Ry S, Morales MA, 2015. Bleomycin in the setting of lung fibrosis induction: From biological mechanisms to counteractions, Pharmacological Research. Academic Press, pp. 122-130.

Desai TJ, Brownfield DG, Krasnow MA (2014) Alveolar progenitor and stem cells in lung development, renewal and cancer. *Nature* 507: 190-194

Desmoulière A, Chaponnier C, Gabbiani G (2005) Perspective Article: Tissue repair, contraction, and the myofibroblast. *Wound Repair and Regeneration* 13: 7-12

Diegelmann RF, Evans MC (2004) Wound healing: an overview of acute, fibrotic and delayed healing. *Front Biosci* 9: 283-289

Dorshkind K, Hofer T, Montecino-Rodriguez E, Pioli PD, Rodewald HR (2020) Do haematopoietic stem cells age? *Nat Rev Immunol* 20: 196-202

Dube CT, Ong YHB, Wemyss K, Krishnan S, Tan TJ, Janela B, Grainger JR, Ronshaugen M, Mace KA, Lim CY (2022) Age-Related Alterations in Macrophage Distribution and Function Are Associated With Delayed Cutaneous Wound Healing. *Frontiers in Immunology* 13

Duffield JS, Forbes SJ, Constandinou CM, Clay S, Partolina M, Vuthoori S, Wu S, Lang R, Iredale JP (2005) Selective depletion of macrophages reveals distinct, opposing roles during liver injury and repair. *Journal of Clinical Investigation* 115: 56-65

Dugan B, Conway J, Duggal NA (2023) Inflammaging as a target for healthy ageing. *Age and Ageing* 52

Duong L, Radley H, Lee B, Dye D, Pixley F, Grounds M, Nelson D, Jackaman C (2021) Macrophage function in the elderly and impact on injury repair and cancer. *Immunity & Ageing* 18

Dykstra B, Olthof S, Schreuder J, Ritsema M, de Haan G (2011) Clonal analysis reveals multiple functional defects of aged murine hematopoietic stem cells. *J Exp Med* 208: 2691-2703

Dzau VJ, Inouye SK, Rowe JW, Finkelman E, Yamada T (2019) Enabling Healthful Aging for All — The National Academy of Medicine Grand Challenge in Healthy Longevity. *New England Journal of Medicine* 381: 1699-1701

Dzierzak E, Speck NA (2008) Of lineage and legacy: the development of mammalian hematopoietic stem cells. *Nat Immunol* 9: 129-136

Epelman S, Kory, Anna, Dorothy, Javier, Calderon B, Brija T, Emmanuel, Ivanov S, Ansuman *et al* (2014) Embryonic and Adult-Derived Resident Cardiac Macrophages Are Maintained through Distinct Mechanisms at Steady State and during Inflammation. *Immunity* 40: 91-104

Eric, Reynaud D, Kang Y-A, Carlin D, Fernando, Andrew, Joshua, Göttgens B, Passegué E (2015) Functionally Distinct Subsets of Lineage-Biased Multipotent Progenitors Control Blood Production in Normal and Regenerative Conditions. *Cell Stem Cell* 17: 35-46

Eric M. Pietras DR, Yoon-A. Kang, Daniel Carlin, Fernando J. Calero-Nieto, Andrew D. Leavitt, Joshua M. Stuart, Berthold Göttgens, Emmanuelle Passegué, (2015) Functionally Distinct Subsets of Lineage-Biased Multipotent Progenitors Control Blood Production in Normal and Regenerative Conditions. *Cell Stem Cell* 17: 35-46

Fabre T, Barron AMS, Christensen SM, Asano S, Bound K, Lech MP, Wadsworth MH, 2nd, Chen X, Wang C, Wang J *et al* (2023) Identification of a broadly fibrogenic macrophage subset induced by type 3 inflammation. *Sci Immunol* 8: eadd8945

Fadok VA, Bratton DL, Konowal A, Freed PW, Westcott JY, Henson PM (1998) Macrophages that have ingested apoptotic cells in vitro inhibit proinflammatory cytokine production through autocrine/paracrine mechanisms involving TGF-beta, PGE2, and PAF. *Journal of Clinical Investigation* 101: 890-898

Fan J-M, Huang X-R, Ng Y-Y, Nikolic-Paterson DJ, Mu W, Atkins RC, Lan HY (2001) Interleukin-1 induces tubular epithelial-myofibroblast transdifferentiation through a transforming growth factor-β1-dependent mechanism in vitro. *American Journal of Kidney Diseases* 37: 820-831

Fernandez Perez ER, Daniels CE, Schroeder DR, St Sauver J, Hartman TE, Bartholmai BJ, Yi ES, Ryu JH (2010) Incidence, prevalence, and clinical course of idiopathic pulmonary fibrosis: a population-based study. *Chest* 137: 129-137

Fernandez S, Jose P, Avdiushko MG, Kaplan AM, Cohen DA (2004) Inhibition of IL-10 Receptor Function in Alveolar Macrophages by Toll-Like Receptor Agonists. *J Immunol* 172: 2613-2620

Ferrucci L, Fabbri E (2018) Inflammageing: chronic inflammation in ageing, cardiovascular disease, and frailty. *Nature Reviews Cardiology* 15: 505-522

Ferrucci L, Semba RD, Guralnik JM, Ershler WB, Bandinelli S, Patel KV, Sun K, Woodman RC, Andrews NC, Cotter RJ *et al* (2010) Proinflammatory state, hepcidin, and anemia in older persons. *Blood* 115: 3810-3816

Fiorentino DF, Zlotnik A, Mosmann TR, Howard M, O'Garra A (1991) IL-10 inhibits cytokine production by activated macrophages. *J Immunol* 147: 3815-3822

Fogg DK, Sibon C, Miled C, Jung S, Aucouturier P, Littman DR, Cumano A, Geissmann F (2006) A Clonogenic Bone Marrow Progenitor Specific for Macrophages and Dendritic Cells. *Science* 311: 83-87

Fontenot JD, Gavin MA, Rudensky AY (2003) Foxp3 programs the development and function of CD4+CD25+ regulatory T cells. *Nat Immunol* 4: 330-336

Franceschi C, Bonafe M, Valensin S, Olivieri F, De Luca M, Ottaviani E, De Benedictis G (2000) Inflamm-aging. An evolutionary perspective on immunosenescence. *Ann N Y Acad Sci* 908: 244-254

Franceschi C, Campisi J (2014) Chronic Inflammation (Inflammaging) and Its Potential Contribution to Age-Associated Diseases. *The Journals of Gerontology Series A: Biological Sciences and Medical Sciences* 69: S4-S9

Franz B, Fritzsching B, Riehl A, Oberle N, Klemke CD, Sykora J, Quick S, Stumpf C, Hartmann M, Enk A *et al* (2007) Low number of regulatory T cells in skin lesions of patients with cutaneous lupus erythematosus. *Arthritis & Rheumatism* 56: 1910-1920

Frasca D, Blomberg BB (2009) Effects of aging on B cell function. *Current Opinion in Immunology* 21: 425-430

Fujii T, Fuchs BC, Yamada S, Lauwers GY, Kulu Y, Goodwin JM, Lanuti M, Tanabe KK (2010) Mouse model of carbon tetrachloride induced liver fibrosis: Histopathological changes and expression of CD133 and epidermal growth factor. *BMC Gastroenterology* 10: 79

Fujisaki J, Wu J, Carlson AL, Silberstein L, Putheti P, Larocca R, Gao W, Saito TI, Celso CL, Tsuyuzaki H *et al* (2011) In vivo imaging of Treg cells providing immune privilege to the haematopoietic stem-cell niche. *Nature* 474: 216-219

Fulop T, Larbi A, Dupuis G, Le Page A, Frost EH, Cohen AA, Witkowski JM, Franceschi C (2018) Immunosenescence and Inflamm-Aging As Two Sides of the Same Coin: Friends or Foes? *Frontiers in Immunology* 8

Furman D, Campisi J, Verdin E, Carrera-Bastos P, Targ S, Franceschi C, Ferrucci L, Gilroy DW, Fasano A, Miller GW *et al* (2019) Chronic inflammation in the etiology of disease across the life span. *Nat Med* 25: 1822-1832

Gambineri E, Torgerson TR, Ochs HD (2003) Immune dysregulation, polyendocrinopathy, enteropathy, and X-linked inheritance (IPEX), a syndrome of systemic autoimmunity caused by mutations of FOXP3, a critical regulator of T-cell homeostasis. *Current Opinion in Rheumatology* 15: 430-435

Gandhi SA, Min B, Fazio JC, Johannson KA, Steinmaus C, Reynolds CJ, Cummings KJ (2024) The Impact of Occupational Exposures on the Risk of Idiopathic Pulmonary Fibrosis: A Systematic Review and Meta-Analysis. *Annals of the American Thoracic Society* 21: 486-498

Gao X, Dong Y, Liu Z, Niu B (2013) Silencing of triggering receptor expressed on myeloid cells-2 enhances the inflammatory responses of alveolar macrophages to lipopolysaccharide. *Molecular Medicine Reports* 7: 921-926

Gardai SJ, Xiao Y-Q, Dickinson M, Nick JA, Voelker DR, Greene KE, Henson PM (2003) By Binding SIRPα or Calreticulin/CD91, Lung Collectins Act as Dual Function Surveillance Molecules to Suppress or Enhance Inflammation. *Cell* 115: 13-23

Gasse P, Mary C, Guenon I, Noulin N, Charron S, Schnyder-Candrian S, Schnyder B, Akira S, Quesniaux VFJ, Lagente V *et al* (2007) IL-1R1/MyD88 signaling and the inflammasome are essential in pulmonary inflammation and fibrosis in mice. *Journal of Clinical Investigation*

Geissmann F, Jung S, Littman DR (2003) Blood Monocytes Consist of Two Principal Subsets with Distinct Migratory Properties. *Immunity* 19: 71-82

Gerli R, Monti D, Bistoni O, M. Mazzone A, Peri G, Cossarizza A, Di Gioacchino M, E. F. Cesarotti M, Doni A, Mantovani A *et al* (2001) Chemokines, sTNF-Rs and sCD30 serum levels in healthy aged people and centenarians. *Mechanisms of Ageing and Development* 121: 37-46

Gheibi Hayat SM, Bianconi V, Pirro M, Sahebkar A (2019) Efferocytosis: molecular mechanisms and pathophysiological perspectives. *Immunology & Cell Biology* 97: 124-133

Ghosh S, Gregory D, Smith A, Kobzik L (2011) MARCO Regulates Early Inflammatory Responses against Influenza. *Am J Respir Cell Mol Biol* 45: 1036-1044

Gibbons MA, Mackinnon AC, Ramachandran P, Dhaliwal K, Duffin R, Phythian-Adams AT, Van Rooijen N, Haslett C, Howie SE, Simpson AJ *et al* (2011) Ly6C^{hi}Monocytes Direct Alternatively Activated Profibrotic Macrophage Regulation of Lung Fibrosis. *American Journal of Respiratory and Critical Care Medicine* 184: 569-581

Gieseck RL, Wilson MS, Wynn TA (2018) Type 2 immunity in tissue repair and fibrosis. *Nature Rev Immun* 18: 62-76

Ginhoux F (2014) Fate PPAR-titioning: PPAR-γ 'instructs' alveolar macrophage development. *Nat Immunol* 15: 1005-1007

Ginhoux F, Greter M, Leboeuf M, Nandi S, See P, Gokhan S, Mehler MF, Conway SJ, Ng LG, Stanley ER *et al* (2010) Fate Mapping Analysis Reveals That Adult Microglia Derive from Primitive Macrophages. *Science* 330: 841-845

Ginhoux F, Guilliams M (2016) Tissue-Resident Macrophage Ontogeny and Homeostasis. *Immunity* 44: 439-449

Ginhoux F, Jung S (2014) Monocytes and macrophages: developmental pathways and tissue homeostasis. *Nature Rev Immun* 14: 392-404

Ginhoux F, Schultze JL, Murray PJ, Ochando J, Biswas SK (2016) New insights into the multidimensional concept of macrophage ontogeny, activation and function. *Nat Immunol* 17: 34-40

Gomez Perdiguero E, Klapproth K, Schulz C, Busch K, Azzoni E, Crozet L, Garner H, Trouillet C, De Bruijn MF, Geissmann F *et al* (2015) Tissue-resident macrophages originate from yolk-sac-derived erythro-myeloid progenitors. *Nature* 518: 547-551

Gorgoulis V, Adams PD, Alimonti A, Bennett DC, Bischof O, Bishop C, Campisi J, Collado M, Evangelou K, Ferbeyre G *et al* (2019) Cellular Senescence: Defining a Path Forward. *Cell* 179: 813-827

Gorki AD, Symmank D, Zahalka S, Lakovits K, Hladik A, Langer B, Maurer B, Sexl V, Kain R, Knapp S (2022) Murine Ex Vivo Cultured Alveolar Macrophages Provide a Novel Tool to Study Tissue-Resident Macrophage Behavior and Function. *Am J Respir Cell Mol Biol* 66: 64-75

Grabiec AM, Hussell T (2016) The role of airway macrophages in apoptotic cell clearance following acute and chronic lung inflammation. *Seminars in Immunopathology* 38: 409-423

Grant RA, Morales-Nebreda L, Markov NS, Swaminathan S, Querrey M, Guzman ER, Abbott DA, Donnelly HK, Donayre A, Goldberg IA *et al* (2021) Circuits between infected macrophages and T cells in SARS-CoV-2 pneumonia. *Nature* 590: 635-641

Grover A, Sanjuan-Pla A, Thongjuea S, Carrelha J, Giustacchini A, Gambardella A, Macaulay I, Mancini E, Luis TC, Mead A *et al* (2016) Single-cell RNA sequencing reveals molecular and functional platelet bias of aged haematopoietic stem cells. *Nat Commun* 7: 11075

Gschwend J, Sherman SP, Ridder F, Feng X, Liang H-E, Locksley RM, Becher B, Schneider C (2021a) Alveolar macrophages rely on GM-CSF from alveolar epithelial type 2 cells before and after birth.

Gschwend J, Sherman SPM, Ridder F, Feng X, Liang H-E, Locksley RM, Becher B, Schneider C (2021b) Alveolar macrophages rely on GM-CSF from alveolar epithelial type 2 cells before and after birth. *J Exp Med* 218

Guilliams M, De Kleer I, Henri S, Post S, Vanhoutte L, De Prijck S, Deswarte K, Malissen B, Hammad H, Lambrecht BN (2013) Alveolar macrophages develop from fetal monocytes that differentiate into long-lived cells in the first week of life via GM-CSF. *J Exp Med* 210: 1977-1992

Guilliams M, Mildner A, Yona S (2018) Developmental and Functional Heterogeneity of Monocytes. *Immunity* 49: 595-613

Guilliams M, Thierry GR, Bonnardel J, Bajenoff M (2020) Establishment and Maintenance of the Macrophage Niche. *Immunity* 52: 434-451

Gulati S, Thannickal VJ (2019) The Aging Lung and Idiopathic Pulmonary Fibrosis. *Am J Med Sci* 357: 384-389

Gurujeyalakshmi G, Giri SN (1995) Molecular Mechanisms of Antifibrotic Effect of Interferon Gamma in Bleomycin-Mouse Model of Lung Fibrosis: Downregulation of TGF-β and Procollagen I and III Gene Expression. *Experimental Lung Research* 21: 791-808

Haczku A (2008) Protective role of the lung collectins surfactant protein A and surfactant protein D in airway inflammation. *Journal of Allergy and Clinical Immunology* 122: 861-879

Hams E, Armstrong ME, Barlow JL, Saunders SP, Schwartz C, Cooke G, Fahy RJ, Crotty TB, Hirani N, Flynn RJ *et al* (2014) IL-25 and type 2 innate lymphoid cells induce pulmonary fibrosis. *Proceedings of the National Academy of Sciences* 111: 367-372

Han S, Budinger GRS, Gottardi CJ (2023) Alveolar epithelial regeneration in the aging lung. *Journal of Clinical Investigation* 133

Hart KM, Fabre T, Sciurba JC, Gieseck RL, Borthwick LA, Vannella KM, Acciani TH, De Queiroz Prado R, Thompson RW, White S *et al* (2017) Type 2 immunity is protective in metabolic disease but exacerbates NAFLD collaboratively with TGF-β. *Science Translational Medicine* 9: eaal3694

Hashimoto D, Chow A, Noizat C, Teo P, Beasley MB, Leboeuf M, Becker CD, See P, Price J, Lucas D *et al* (2013) Tissue-resident macrophages self-maintain locally throughout adult life with minimal contribution from circulating monocytes. *Immunity* 38: 792-804

Hawrylowicz CM, O'Garra A (2005) Potential role of interleukin-10-secreting regulatory T cells in allergy and asthma. *Nature Rev Immun* 5: 271-283

Hazeldine J, Harris P, Chapple IL, Grant M, Greenwood H, Livesey A, Sapey E, Lord JM (2014) Impaired neutrophil extracellular trap formation: a novel defect in the innate immune system of aged individuals. *Aging Cell* 13: 690-698

Hecker L, Logsdon NJ, Kurundkar D, Kurundkar A, Bernard K, Hock T, Meldrum E, Sanders YY, Thannickal VJ (2014) Reversal of Persistent Fibrosis in Aging by Targeting Nox4-Nrf2 Redox Imbalance. *Science Translational Medicine* 6: 231ra247-231ra247

Henderson NC, Rieder F, Wynn TA (2020) Fibrosis: from mechanisms to medicines. *Nature* 587: 555-566

Hernández-Rodríguez NA, Cambrey AD, Chambers RC, Gray AJ, McAnulty RJ, Laurent GJ, Harrison NK, Southcott AM, Dubois RM, Black CM *et al* (1995) Role of thrombin in pulmonary fibrosis. *The Lancet* 346: 1071-1073

Herold S, Mayer K, Lohmeyer J (2011) Acute Lung Injury: How Macrophages Orchestrate Resolution of Inflammation and Tissue Repair. *Frontiers in Immunology* 2

Herold S, Steinmueller M, Von Wulffen W, Cakarova L, Pinto R, Pleschka S, Mack M, Kuziel WA, Corazza N, Brunner T *et al* (2008) Lung epithelial apoptosis in influenza virus pneumonia: the role of macrophage-expressed TNF-related apoptosis-inducing ligand. *The Journal of Experimental Medicine* 205: 3065-3077

Hirani N, Mackinnon AC, Nicol L, Ford P, Schambye H, Pedersen A, Nilsson UJ, Leffler H, Sethi T, Tantawi S *et al* (2021) Target inhibition of galectin-3 by inhaled TD139 in patients with idiopathic pulmonary fibrosis. *Eur Respir J* 57: 2002559

Hoeffel G, Chen J, Lavin Y, Low D, Francisca, See P, Anna, Lum J, Low I, E *et al* (2015) C-Myb+ Erythro-Myeloid Progenitor-Derived Fetal Monocytes Give Rise to Adult Tissue-Resident Macrophages. *Immunity* 42: 665-678

Hoeffel G, Ginhoux F (2018) Fetal monocytes and the origins of tissue-resident macrophages. *Cellular Immunology* 330: 5-15

Hoeffel G, Wang Y, Greter M, See P, Teo P, Malleret B, Leboeuf M, Low D, Oller G, Almeida F *et al* (2012) Adult Langerhans cells derive predominantly from embryonic fetal liver monocytes with a minor contribution of yolk sac–derived macrophages. *J Exp Med* 209: 1167-1181

Hori S, Nomura T, Sakaguchi S (2003) Control of Regulatory T Cell Development by the Transcription Factor Foxp3. *Science* 299: 1057-1061

Hotchkiss RS, Strasser A, McDunn JE, Swanson PE (2009) Cell Death. *New England Journal of Medicine* 361: 1570-1583

Hou Y, Chen M, Bian Y, Hu Y, Chuan J, Zhong L, Zhu Y, Tong R (2024) Insights into vaccines for elderly individuals: from the impacts of immunosenescence to delivery strategies. *npj Vaccines* 9

Hsia CCW, Hyde DM, Weibel ER (2016) Lung Structure and the Intrinsic Challenges of Gas Exchange. *Comprehensive Physiology*: 827-895

Humbles AA, Lloyd CM, McMillan SJ, Friend DS, Xanthou G, McKenna EE, Ghiran S, Gerard NP, Yu C, Orkin SH *et al* (2004) A Critical Role for Eosinophils in Allergic Airways Remodeling. *Science* 305: 1776-1779

Hussell T, Bell TJ, 2014a. Alveolar macrophages: Plasticity in a tissue-specific context, Nature Rev Immun. pp. 81-93.

Hussell T, Bell TJ (2014b) Alveolar macrophages: plasticity in a tissue-specific context. *Nature Rev Immun* 14: 81-93

Hutchinson J, Fogarty A, Hubbard R, McKeever T (2015) Global incidence and mortality of idiopathic pulmonary fibrosis: a systematic review. *Eur Respir J* 46: 795-806

Iredale JP (2007) Models of liver fibrosis: exploring the dynamic nature of inflammation and repair in a solid organ. *Journal of Clinical Investigation* 117: 539-548

Iredale JP, Benyon RC, Pickering J, McCullen M, Northrop M, Pawley S, Hovell C, Arthur MJ (1998) Mechanisms of spontaneous resolution of rat liver fibrosis. Hepatic stellate cell apoptosis and reduced hepatic expression of metalloproteinase inhibitors. *Journal of Clinical Investigation* 102: 538-549

Ivanov II, McKenzie BS, Zhou L, Tadokoro CE, Lepelley A, Lafaille JJ, Cua DJ, Littman DR (2006) The Orphan Nuclear Receptor RORγt Directs the Differentiation Program of Proinflammatory IL-17+ T Helper Cells. *Cell* 126: 1121-1133

Iwasaki H, Akashi K (2007) Myeloid Lineage Commitment from the Hematopoietic Stem Cell. *Immunity* 26: 726-740

Jain N, Nguyen H, Chambers C, Kang J (2010) Dual function of CTLA-4 in regulatory T cells and conventional T cells to prevent multiorgan autoimmunity. *Proceedings of the National Academy of Sciences* 107: 1524-1528

Jaiswal S, Ebert BL (2019) Clonal hematopoiesis in human aging and disease. *Science* 366: eaan4673

Jaiswal S, Natarajan P, Silver AJ, Gibson CJ, Bick AG, Shvartz E, McConkey M, Gupta N, Gabriel S, Ardissino D *et al* (2017) Clonal Hematopoiesis and Risk of Atherosclerotic Cardiovascular Disease. *New England Journal of Medicine* 377: 111-121

Janssen WJ, McPhillips KA, Dickinson MG, Linderman DJ, Morimoto K, Xiao YQ, Oldham KM, Vandivier RW, Henson PM, Gardai SJ (2008) Surfactant Proteins A and D Suppress Alveolar Macrophage Phagocytosis via Interaction with SIRPα. *American Journal of Respiratory and Critical Care Medicine* 178: 158-167

Jenkins SJ, Ruckerl D, Cook PC, Jones LH, Finkelman FD, Van Rooijen N, Macdonald AS, Allen JE (2011) Local Macrophage Proliferation, Rather than Recruitment from the Blood, Is a Signature of T _H 2 Inflammation. *Science* 332: 1284-1288

Jiang J, Fisher EM, Murasko DM (2011) CD8 T cell responses to influenza virus infection in aged mice. *Ageing Research Reviews*

Jiang P, Gil De Rubio R, Hrycaj SM, Gurczynski SJ, Riemondy KA, Moore BB, Omary MB, Ridge KM, Zemans RL (2020) Ineffectual Type 2–to–Type 1 Alveolar Epithelial Cell Differentiation in Idiopathic Pulmonary Fibrosis: Persistence of the KRT8^{hi} Transitional State. *American Journal of Respiratory and Critical Care Medicine* 201: 1443-1447

Joetham A, Takada K, Taube C, Miyahara N, Matsubara S, Koya T, Rha Y-H, Dakhama A, Gelfand EW (2007) Naturally Occurring Lung CD4+CD25+ T Cell Regulation of Airway Allergic Responses Depends on IL-10 Induction of TGF-β. *J Immunol* 178: 1433-1442

Johannson KA, Vittinghoff E, Lee K, Balmes JR, Ji W, Kaplan GG, Kim DS, Collard HR (2014) Acute exacerbation of idiopathic pulmonary fibrosis associated with air pollution exposure. *Eur Respir J* 43: 1124-1131

Johnson GR, Moore MAS (1975) Role of stem cell migration in initiation of mouse foetal liver haemopoiesis. *Nature* 258: 726-728

Johnston RJ, Poholek AC, Ditoro D, Yusuf I, Eto D, Barnett B, Dent AL, Craft J, Crotty S (2009) Bcl6 and Blimp-1 Are Reciprocal and Antagonistic Regulators of T Follicular Helper Cell Differentiation. *Science* 325: 1006-1010

Joshi N, Watanabe S, Verma R, Jablonski RP, Chen CI, Cheresh P, Markov NS, Reyfman PA, McQuattie-Pimentel AC, Sichizya L *et al* (2020) A spatially restricted fibrotic niche in pulmonary fibrosis is sustained by M-CSF/M-CSFR signalling in monocyte-derived alveolar macrophages. *Eur Respir J* 55: 1900646

Kalekar LA, Cohen JN, Prevel N, Sandoval PM, Mathur AN, Moreau JM, Lowe MM, Nosbaum A, Wolters PJ, Haemel A *et al* (2019) Regulatory T cells in skin are uniquely poised to suppress profibrotic immune responses. *Science Immunology* 4: eaaw2910

Kam M, Caliez J, Nunes H, Gille T (2022) The road to hell is paved with good intentions: a look back at the PANTHER-IPF trial. *Breathe* 18: 220074

Kapnadak SG, Raghu G (2021) Lung transplantation for interstitial lung disease. *European Respiratory Review* 30: 210017

Karsunky H, Inlay MA, Serwold T, Bhattacharya D, Weissman IL (2008) Flk2+ common lymphoid progenitors possess equivalent differentiation potential for the B and T lineages. *Blood* 111: 5562-5570

Kasbekar M, Mitchell CA, Proven MA, Passegué E (2023) Hematopoietic stem cells through the ages: A lifetime of adaptation to organismal demands. *Cell Stem Cell* 30: 1403-1420

Kato K, Logsdon NJ, Shin Y-J, Palumbo S, Knox A, Irish JD, Rounseville SP, Rummel SR, Mohamed M, Ahmad K *et al* (2020) Impaired Myofibroblast Dedifferentiation Contributes to Nonresolving Fibrosis in Aging. *Am J Respir Cell Mol Biol* 62: 633-644

Kearley J, Barker JE, Robinson DS, Lloyd CM (2005) Resolution of airway inflammation and hyperreactivity after in vivo transfer of CD4+CD25+ regulatory T cells is interleukin 10 dependent. *The Journal of Experimental Medicine* 202: 1539-1547

Kelsh R, You R, Horzempa C, Zheng M, McKeown-Longo PJ (2014) Regulation of the Innate Immune Response by Fibronectin: Synergism between the III-1 and EDA Domains. *PLoS ONE* 9: e102974

Kennedy BK, Berger SL, Brunet A, Campisi J, Cuervo AM, Epel ES, Franceschi C, Lithgow GJ, Morimoto RI, Pessin JE *et al* (2014) Geroscience: Linking Aging to Chronic Disease. *Cell* 159: 709-713

Keyes BE, Liu S, Asare A, Naik S, Levorse J, Polak L, Lu CP, Nikolova M, Pasolli HA, Fuchs E (2016) Impaired Epidermal to Dendritic T Cell Signaling Slows Wound Repair in Aged Skin. *Cell* 167: 1323-1338.e1314

Kierdorf K, Erny D, Goldmann T, Sander V, Schulz C, Perdiguero EG, Wieghofer P, Heinrich A, Riemke P, Hölscher C *et al* (2013) Microglia emerge from erythromyeloid precursors via Pu.1- and Irf8-dependent pathways. *Nature Neuroscience* 16: 273-280

Kim JM, Rasmussen JP, Rudensky AY (2007) Regulatory T cells prevent catastrophic autoimmunity throughout the lifespan of mice. *Nat Immunol* 8: 191-197

King TE, Jr., Bradford WZ, Castro-Bernardini S, Fagan EA, Glaspole I, Glassberg MK, Gorina E, Hopkins PM, Kardatzke D, Lancaster L *et al* (2014) A phase 3 trial of pirfenidone in patients with idiopathic pulmonary fibrosis. *N Engl J Med* 370: 2083-2092

King TE, Pardo A, Selman M (2011) Idiopathic pulmonary fibrosis. *The Lancet* 378: 1949-1961

Kinsey GR, Sharma R, Huang L, Li L, Vergis AL, Ye H, Ju S-T, Okusa MD (2009) Regulatory T Cells Suppress Innate Immunity in Kidney Ischemia-Reperfusion Injury. *Journal of the American Society of Nephrology* 20: 1744-1753

Kinzina ED, Podolskiy DI, Dmitriev SE, Gladyshev VN (2019) Patterns of Aging Biomarkers, Mortality, and Damaging Mutations Illuminate the Beginning of Aging and Causes of Early-Life Mortality. *Cell Reports* 29: 4276-4284.e4273

Kitani A, Fuss I, Nakamura K, Kumaki F, Usui T, Strober W (2003) Transforming Growth Factor (TGF)-β1–producing Regulatory T Cells Induce Smad-mediated Interleukin 10 Secretion That Facilitates Coordinated Immunoregulatory Activity and Amelioration of TGF-β1–mediated Fibrosis. *The Journal of Experimental Medicine* 198: 1179-1188

Knapp S, Leemans JC, Florquin S, Branger J, Maris NA, Pater J, Van Rooijen N, Van Der Poll T (2003) Alveolar Macrophages Have a Protective Antiinflammatory Role during Murine Pneumococcal Pneumonia. *American Journal of Respiratory and Critical Care Medicine* 167: 171-179

Knoedler S, Broichhausen S, Guo R, Dai R, Knoedler L, Kauke-Navarro M, Diatta F, Pomahac B, Machens H-G, Jiang D *et al* (2023) Fibroblasts – the cellular choreographers of wound healing. *Frontiers in Immunology* 14

Knudsen L, Ochs M (2018) The micromechanics of lung alveoli: structure and function of surfactant and tissue components. *Histochemistry and Cell Biology* 150: 661-676

Kobayashi Y, Tata A, Konkimalla A, Katsura H, Lee RF, Ou J, Banovich NE, Kropski JA, Tata PR (2020) Persistence of a regeneration-associated, transitional alveolar epithelial cell state in pulmonary fibrosis. *Nature Cell Biology* 22: 934-946

Kolaczkowska E, Kubes P (2013) Neutrophil recruitment and function in health and inflammation. *Nature Rev Immun* 13: 159-175

Kondo M, Weissman IL, Akashi K (1997) Identification of Clonogenic Common Lymphoid Progenitors in Mouse Bone Marrow. *Cell* 91: 661-672

Königshoff M, Kramer M, Balsara N, Wilhelm J, Amarie OV, Jahn A, Rose F, Fink L, Seeger W, Schaefer L *et al* (2009) WNT1-inducible signaling protein–1 mediates pulmonary fibrosis in mice and is upregulated in humans with idiopathic pulmonary fibrosis. *Journal of Clinical Investigation*

Kopf M, Schneider C, Nobs SP (2015) The development and function of lung-resident macrophages and dendritic cells. *Nat Immunol* 16: 36-44

Korfei M, Ruppert C, Mahavadi P, Henneke I, Markart P, Koch M, Lang G, Fink L, Bohle R-M, Seeger W *et al* (2008) Epithelial Endoplasmic Reticulum Stress and Apoptosis in Sporadic Idiopathic Pulmonary Fibrosis. *American Journal of Respiratory and Critical Care Medicine* 178: 838-846

Kotsianidis I, Nakou E, Bouchliou I, Tzouvelekis A, Spanoudakis E, Steiropoulos P, Sotiriou I, Aidinis V, Margaritis D, Tsatalas C *et al* (2009) Global Impairment of CD4⁺CD25⁺FOXP3⁺Regulatory T Cells in Idiopathic Pulmonary Fibrosis. *American Journal of Respiratory and Critical Care Medicine* 179: 1121-1130

Kovtonyuk LV, Fritsch K, Feng X, Manz MG, Takizawa H (2016) Inflamm-Aging of Hematopoiesis, Hematopoietic Stem Cells, and the Bone Marrow Microenvironment. *Frontiers in Immunology* 7

Kowalczyk MS, Tirosh I, Heckl D, Rao TN, Dixit A, Haas BJ, Schneider RK, Wagers AJ, Ebert BL, Regev A (2015) Single-cell RNA-seq reveals changes in cell cycle and differentiation programs upon aging of hematopoietic stem cells. *Genome Res* 25: 1860-1872

Krishnarajah S, Ingelfinger F, Friebel E, Cansever D, Amorim A, Andreadou M, Bamert D, Litscher G, Lutz M, Mayoux M *et al* (2021) Single-cell profiling of immune system alterations in lymphoid, barrier and solid tissues in aged mice. *Nature Aging* 2: 74-89

Kulikauskaite J, Wack A (2020) Teaching Old Dogs New Tricks? The Plasticity of Lung Alveolar Macrophage Subsets. *Trends Immunol* 41: 864-877

Kulkarni U, Zemans RL, Smith CA, Wood SC, Deng JC, Goldstein DR (2019) Excessive neutrophil levels in the lung underlie the age-associated increase in influenza mortality. *Mucosal Immunology* 12: 545-554

Kumagai Y, Takeuchi O, Kato H, Kumar H, Matsui K, Morii E, Aozasa K, Kawai T, Akira S (2007) Alveolar Macrophages Are the Primary Interferon-α Producer in Pulmonary Infection with RNA Viruses. *Immunity* 27: 240-252

Kuribayashi W, Oshima M, Itokawa N, Koide S, Nakajima-Takagi Y, Yamashita M, Yamazaki S, Rahmutulla B, Miura F, Ito T *et al* (2021) Limited rejuvenation of aged hematopoietic stem cells in young bone marrow niche. *J Exp Med* 218

Kuwano K, Hagimoto N, Kawasaki M, Yatomi T, Nakamura N, Nagata S, Suda T, Kunitake R, Maeyama T, Miyazaki H *et al* (1999) Essential roles of the Fas-Fas ligand pathway in the development of pulmonary fibrosis. *Journal of Clinical Investigation* 104: 13-19

Lahl K, Loddenkemper C, Drouin C, Freyer J, Arnason J, Eberl G, Hamann A, Wagner H, Huehn J, Sparwasser T (2007) Selective depletion of Foxp3+ regulatory T cells induces a scurfy-like disease. *J Exp Med* 204: 57-63

Latchney SE, Calvi LM (2017) The aging hematopoietic stem cell niche: Phenotypic and functional changes and mechanisms that contribute to hematopoietic aging. *Seminars in Hematology* 54: 25-32

Lechner AJ, Driver IH, Lee J, Conroy CM, Nagle A, Locksley RM, Rock JR (2017) Recruited Monocytes and Type 2 Immunity Promote Lung Regeneration following Pneumonectomy. *Cell Stem Cell* 21: 120-134 e127

Lendahl U, Muhl L, Betsholtz C (2022) Identification, discrimination and heterogeneity of fibroblasts. *Nat Commun* 13

Levick SP, McLarty JL, Murray DB, Freeman RM, Carver WE, Brower GL (2009) Cardiac Mast Cells Mediate Left Ventricular Fibrosis in the Hypertensive Rat Heart. *Hypertension* 53: 1041-1047

Ley B, Collard HR, King TE, Jr. (2011) Clinical course and prediction of survival in idiopathic pulmonary fibrosis. *Am J Respir Crit Care Med* 183: 431-440

Li D, Wu M (2021) Pattern recognition receptors in health and diseases. *Signal Transduction and Targeted Therapy* 6

Li F, Piattini F, Pohlmeier L, Feng Q, Rehrauer H, Kopf M (2022) Monocyte-derived alveolar macrophages autonomously determine severe outcome of respiratory viral infection. *Sci Immunol* 7: eabj5761

Liegeois M, Legrand C, Desmet CJ, Marichal T, Bureau F (2018) The interstitial macrophage: A long-neglected piece in the puzzle of lung immunity. *Cellular Immunology* 330: 91-96

Lim S, Caramori G, Tomita K, Jazrawi E, Oates T, Chung KF, Barnes PJ, Adcock IM (2004) Differential expression of IL-10 receptor by epithelial cells and alveolar macrophages. *Allergy* 59: 505-514

Lin KL, Suzuki Y, Nakano H, Ramsburg E, Gunn MD (2008) CCR2+ Monocyte-Derived Dendritic Cells and Exudate Macrophages Produce Influenza-Induced Pulmonary Immune Pathology and Mortality. *J Immunol* 180: 2562-2572

Liu Z, Gu Y, Chakarov S, Bleriot C, Kwok I, Chen X, Shin A, Huang W, Dress RJ, Dutertre CA *et al* (2019) Fate Mapping via Ms4a3-Expression History Traces Monocyte-Derived Cells. *Cell* 178: 1509-1525.e1519

Loffredo LF, Savage TM, Ringham OR, Arpaia N (2024) Treg–tissue cell interactions in repair and regeneration. *J Exp Med* 221

Loos P, Baiwir J, Maquet C, Javaux J, Sandor R, Lallemand F, Marichal T, Machiels B, Gillet L (2023) Dampening type 2 properties of group 2 innate lymphoid cells by a gammaherpesvirus infection reprograms alveolar macrophages. *Sci Immunol* 8: eabl9041

López-Otín C, Blasco MA, Partridge L, Serrano M, Kroemer G (2013) The Hallmarks of Aging. *Cell* 153: 1194-1217

López-Otín C, Blasco MA, Partridge L, Serrano M, Kroemer G (2023) Hallmarks of aging: An expanding universe. *Cell* 186: 243-278

Machiels B, Dourcy M, Xiao X, Javaux J, Mesnil C, Sabatel C, Desmecht D, Lallemand F, Martinive P, Hammad H *et al* (2017) A gammaherpesvirus provides protection against allergic asthma by inducing the replacement of resident alveolar macrophages with regulatory monocytes. *Nat Immunol* 18: 1310-1320

Malainou C, Abdin SM, Lachmann N, Matt U, Herold S (2023) Alveolar macrophages in tissue homeostasis, inflammation, and infection: evolving concepts of therapeutic targeting. *Journal of Clinical Investigation* 133

Martinon F, Mayor A, Tschopp J (2009) The Inflammasomes: Guardians of the Body. *Annual Review of Immunology* 27: 229-265

Mass E, Ballesteros I, Farlik M, Halbritter F, Günther P, Crozet L, Jacome-Galarza CE, Händler K, Klughammer J, Kobayashi Y *et al* (2016) Specification of tissue-resident macrophages during organogenesis. *Science* 353: aaf4238-aaf4238

Mass E, Nimmerjahn F, Kierdorf K, Schlitzer A (2023) Tissue-specific macrophages: how they develop and choreograph tissue biology. *Nature Rev Immun* 23: 563-579

Mathis D, Benoist C (2004) Back to Central Tolerance. *Immunity* 20: 509-516

Matute-Bello G, Downey G, Moore BB, Groshong SD, Matthay MA, Slutsky AS, Kuebler WM (2011) An Official American Thoracic Society Workshop Report: Features and Measurements of Experimental Acute Lung Injury in Animals. *Am J Respir Cell Mol Biol* 44: 725-738

Maul J, Loddenkemper C, Mundt P, Berg E, Giese T, Stallmach A, Zeitz M, Duchmann R (2005) Peripheral and Intestinal Regulatory CD4+CD25high T Cells in Inflammatory Bowel Disease. *Gastroenterology* 128: 1868-1878

Maus UA, Janzen S, Wall G, Srivastava M, Blackwell TS, Christman JW, Seeger W, Welte T, Lohmeyer J (2006) Resident Alveolar Macrophages Are Replaced by Recruited Monocytes in Response to Endotoxin-Induced Lung Inflammation. *Am J Respir Cell Mol Biol* 35: 227-235

McCowan J, Fercoq F, Kirkwood PM, T'Jonck W, Hegarty LM, Mawer CM, Cunningham R, Mirchandani AS, Hoy A, Humphries DC *et al* (2021) The transcription factor EGR2 is indispensable for tissue-specific imprinting of alveolar macrophages in health and tissue repair. *Science Immunology* 6

McKeown S, Richter AG, O'Kane C, McAuley DF, Thickett DR (2009) MMP expression and abnormal lung permeability are important determinants of outcome in IPF. *Eur Respir J* 33: 77-84

McKinley KL, Longaker MT, Naik S (2023) Emerging frontiers in regenerative medicine. *Science* 380: 796-798

McQuattie-Pimentel AC, Ren Z, Joshi N, Watanabe S, Stoeger T, Chi M, Lu Z, Sichizya L, Aillon RP, Chen CI *et al* (2021) The lung microenvironment shapes a dysfunctional response of alveolar macrophages in aging. *J Clin Invest* 131: e140299

Medvinsky A, Dzierzak E (1996) Definitive Hematopoiesis Is Autonomously Initiated by the AGM Region. *Cell* 86: 897-906

Mejia-Ramirez E, Florian MC (2020) Understanding intrinsic hematopoietic stem cell aging. *Haematologica* 105: 22-37

Meliopoulos VA, Van De Velde L-A, Van De Velde NC, Karlsson EA, Neale G, Vogel P, Guy C, Sharma S, Duan S, Surman SL *et al* (2016) An Epithelial Integrin Regulates the Amplitude of Protective Lung Interferon Responses against Multiple Respiratory Pathogens. *PLOS Pathogens* 12: e1005804

Meng C, Wang S, Wang X, Lv J, Zeng W, Chang R, Li Q, Wang X (2020) Amphiregulin inhibits TNF-α-induced alveolar epithelial cell death through EGFR signaling pathway. *Biomedicine & Pharmacotherapy* 125: 109995

Merad M, Manz MG, Karsunky H, Wagers A, Peters W, Charo I, Weissman IL, Cyster JG, Engleman EG (2002) Langerhans cells renew in the skin throughout life under steady-state conditions. *Nat Immunol* 3: 1135-1141

Messaoudi I, Lemaoult JL, Guevara-Patino JA, Metzner BM, Nikolich-ŽUgich J (2004) Age-related CD8 T Cell Clonal Expansions Constrict CD8 T Cell Repertoire and Have the Potential to Impair Immune Defense. *The Journal of Experimental Medicine* 200: 1347-1358

Miller KN, Victorelli SG, Salmonowicz H, Dasgupta N, Liu T, Passos JF, Adams PD (2021) Cytoplasmic DNA: sources, sensing, and role in aging and disease. *Cell* 184: 5506-5526

Miller M (2010) Structural and Physiological Age-Associated Changes in Aging Lungs. *Seminars in Respiratory and Critical Care Medicine* 31: 521-527

Minshall EM, Leung DYM, Martin RJ, Song YL, Cameron L, Ernst P, Hamid Q (1997) Eosinophil-associated TGF- β₁mRNA Expression and Airways Fibrosis in Bronchial Asthma. *Am J Respir Cell Mol Biol* 17: 326-333

Minutti CM, Jackson-Jones LH, García-Fojeda B, Knipper JA, Sutherland TE, Logan N, Ringqvist E, Guillamat-Prats R, Ferenbach DA, Artigas A *et al* (2017) Local amplifiers of IL-4Rα–mediated macrophage activation promote repair in lung and liver. *Science* 356: 1076-1080

Minutti CM, Modak RV, Macdonald F, Li F, Smyth DJ, Dorward DA, Blair N, Husovsky C, Muir A, Giampazolias E *et al* (2019) A Macrophage-Pericyte Axis Directs Tissue Restoration via Amphiregulin-Induced Transforming Growth Factor Beta Activation. *Immunity* 50: 645-654.e646

Miossec P, Korn T, Kuchroo VK (2009) Interleukin-17 and Type 17 Helper T Cells. *New England Journal of Medicine* 361: 888-898

Misharin AV, Morales-Nebreda L, Mutlu GM, Budinger GRS, Perlman H (2013) Flow Cytometric Analysis of Macrophages and Dendritic Cell Subsets in the Mouse Lung. *Am J Respir Cell Mol Biol* 49: 503-510

Misharin AV, Morales-Nebreda L, Reyfman PA, Cuda CM, Walter JM, McQuattie-Pimentel AC, Chen CI, Anekalla KR, Joshi N, Williams KJN *et al* (2017) Monocyte-derived alveolar macrophages drive lung fibrosis and persist in the lung over the life span. *J Exp Med* 214: 2387-2404

Mittelbrunn M, Kroemer G (2021) Hallmarks of T cell aging. *Nat Immunol* 22: 687-698

Miyazaki Y, Araki K, Vesin C, Garcia I, Kapanci Y, Whitsett JA, Piguet PF, Vassalli P (1995) Expression of a tumor necrosis factor-alpha transgene in murine lung causes lymphocytic and fibrosing alveolitis. A mouse model of progressive pulmonary fibrosis. *Journal of Clinical Investigation* 96: 250-259

Mogilenko DA, Shchukina I, Artyomov MN (2022) Immune ageing at single-cell resolution. *Nature Rev Immun* 22: 484-498

Mogilenko DA, Shpynov O, Andhey PS, Arthur L, Swain A, Esaulova E, Brioschi S, Shchukina I, Kerndl M, Bambouskova M *et al* (2021) Comprehensive Profiling of an Aging Immune System Reveals Clonal GZMK+ CD8+ T Cells as Conserved Hallmark of Inflammaging. *Immunity* 54: 99-115.e112

Montecino-Rodriguez E, Berent-Maoz B, Dorshkind K (2013) Causes, consequences, and reversal of immune system aging. *Journal of Clinical Investigation* 123: 958-965

Moore BB, Hogaboam CM (2008) Murine models of pulmonary fibrosis. *American Journal of Physiology-Lung Cellular and Molecular Physiology* 294: L152-L160

Moore MW, Herzog EL (2016) Regulatory T Cells in Idiopathic Pulmonary Fibrosis. *The American Journal of Pathology* 186: 1978-1981

Morales-Nebreda L, Misharin AV, Perlman H, Budinger GR (2015) The heterogeneity of lung macrophages in the susceptibility to disease. *Eur Respir Rev* 24: 505-509

Morita Y, Ema H, Nakauchi H (2010) Heterogeneity and hierarchy within the most primitive hematopoietic stem cell compartment. *J Exp Med* 207: 1173-1182

Morris DG, Huang X, Kaminski N, Wang Y, Shapiro SD, Dolganov G, Glick A, Sheppard D (2003) Loss of integrin αvβ6-mediated TGF-β activation causes Mmp12-dependent emphysema. *Nature* 422: 169-173

Morrison SJ, Weissman IL (1994) The long-term repopulating subset of hematopoietic stem cells is deterministic and isolatable by phenotype. *Immunity* 1: 661-673

Morse C, Tabib T, Sembrat J, Buschur KL, Bittar HT, Valenzi E, Jiang Y, Kass DJ, Gibson K, Chen W *et al* (2019) Proliferating SPP1/MERTK-expressing macrophages in idiopathic pulmonary fibrosis. *Eur Respir J* 54: 1802441

Movat HZ, Fernando NVP (1962) The fine structure of connective tissue. *Experimental and Molecular Pathology* 1: 509-534

Mu M, Gao P, Yang Q, He J, Wu F, Han X, Guo S, Qian Z, Song C (2020) Alveolar Epithelial Cells Promote IGF-1 Production by Alveolar Macrophages Through TGF-β to Suppress Endogenous Inflammatory Signals. *Frontiers in Immunology* 11

Muller-Sieburg CE, Cho RH, Karlsson L, Huang J-F, Sieburg HB (2004) Myeloid-biased hematopoietic stem cells have extensive self-renewal capacity but generate diminished lymphoid progeny with impaired IL-7 responsiveness. *Blood* 103: 4111-4118

Munger JS, Huang X, Kawakatsu H, Griffiths MJD, Dalton SL, Wu J, Pittet J-F, Kaminski N, Garat C, Matthay MA *et al* (1999) A Mechanism for Regulating Pulmonary Inflammation and Fibrosis: The Integrin αvβ6 Binds and Activates Latent TGF β1. *Cell* 96: 319-328

Muñoz-Rojas AR, Mathis D (2021) Tissue regulatory T cells: regulatory chameleons. *Nature Rev Immun* 21: 597-611

Murphy J, Summer R, Wilson AA, Kotton DN, Fine A (2008) The Prolonged Life-Span of Alveolar Macrophages. *Am J Respir Cell Mol Biol* 38: 380-385

Murray LA, Chen Q, Kramer MS, Hesson DP, Argentieri RL, Peng X, Gulati M, Homer RJ, Russell T, Van Rooijen N *et al* (2011) TGF-beta driven lung fibrosis is macrophage dependent and blocked by Serum amyloid P. *The International Journal of Biochemistry & Cell Biology* 43: 154-162

Murray P (2006) Understanding and exploiting the endogenous interleukin-10/STAT3-mediated anti-inflammatory response. *Current Opinion in Pharmacology* 6: 379-386

Murray PJ, Allen JE, Biswas SK, Fisher EA, Gilroy DW, Goerdt S, Gordon S, Hamilton JA, Ivashkiv LB, Lawrence T *et al*, 2014. Macrophage Activation and Polarization: Nomenclature and Experimental Guidelines, Immunity. Cell Press, pp. 14-20.

Murray PJ, Wynn TA (2011) Protective and pathogenic functions of macrophage subsets. *Nature Rev Immun* 11: 723-737

Nabhan AN, Brownfield DG, Harbury PB, Krasnow MA, Desai TJ (2018) Single-cell Wnt signaling niches maintain stemness of alveolar type 2 cells. *Science* 359: 1118-1123

Navaratnam V, Fleming KM, West J, Smith CJP, Jenkins RG, Fogarty A, Hubbard RB (2011) The rising incidence of idiopathic pulmonary fibrosis in the UK. *Thorax* 66: 462-467

Neupane AS, Willson M, Chojnacki AK, Vargas E Silva Castanheira F, Morehouse C, Carestia A, Keller AE, Peiseler M, Digiandomenico A, Kelly MM *et al* (2020) Patrolling Alveolar Macrophages Conceal Bacteria from the Immune System to Maintain Homeostasis. *Cell* 183: 110-125.e111

Newman AB, Sanders JL, Kizer JR, Boudreau RM, Odden MC, Zeki Al Hazzouri A, Arnold AM (2016) Trajectories of function and biomarkers with age: the CHS All Stars Study. *International Journal of Epidemiology*: dyw092

Ng B, Dong J, D'Agostino G, Viswanathan S, Widjaja AA, Lim W-W, Ko NSJ, Tan J, Chothani SP, Huang B *et al* (2019) Interleukin-11 is a therapeutic target in idiopathic pulmonary fibrosis. *Science Translational Medicine* 11: eaaw1237

Nishi K, Sakamaki T, Kao KS, Sadaoka K, Fujii M, Takaori-Kondo A, Miyanishi M (2019) Age-Associated Myeloid Biased Hematopoiesis Depends on Relative Decrease of Short-Term Hematopoietic Stem Cell. *Blood* 134: 2481-2481

Noble PW, Albera C, Bradford WZ, Costabel U, Glassberg MK, Kardatzke D, King TE, Lancaster L, Sahn SA, Szwarcberg J *et al* (2011) Pirfenidone in patients with idiopathic pulmonary fibrosis (CAPACITY): two randomised trials. *The Lancet* 377: 1760-1769

Nogalska A, Eerdeng J, Akre S, Vergel-Rodriguez M, Lee Y, Bramlett C, Chowdhury AY, Wang B, Cess CG, Finley SD *et al* (2024) Age-associated imbalance in immune cell regeneration varies across individuals and arises from a distinct subset of stem cells. *Cellular & Molecular Immunology* 21: 1459-1473

Nosbaum A, Prevel N, Truong H-A, Mehta P, Ettinger M, Scharschmidt TC, Ali NH, Pauli ML, Abbas AK, Rosenblum MD (2016) Cutting Edge: Regulatory T Cells Facilitate Cutaneous Wound Healing. *J Immunol* 196: 2010-2014

Ogger PP, Albers GJ, Hewitt RJ, O'Sullivan BJ, Powell JE, Calamita E, Ghai P, Walker SA, McErlean P, Saunders P *et al* (2020) Itaconate controls the severity of pulmonary fibrosis. *Sci Immunol* 5: eabc1884

Ogger PP, Byrne AJ (2021) Macrophage metabolic reprogramming during chronic lung disease. *Mucosal Immunology* 14: 282-295

Ohashi P (2003) Negative selection and autoimmunity. *Current Opinion in Immunology* 15: 668-676

Olajuyin AM, Zhang X, Ji H-L (2019) Alveolar type 2 progenitor cells for lung injury repair. *Cell Death Discovery* 5

Orkin SH (2000) Diversification of haematopoietic stem cells to specific lineages. *Nature Reviews Genetics* 1: 57-64

Orkin SH, Zon LI (2008) Hematopoiesis: An Evolving Paradigm for Stem Cell Biology. *Cell* 132: 631-644

Osawa M, Hanada K-I, Hamada H, Nakauchi H (1996) Long-Term Lymphohematopoietic Reconstitution by a Single CD34-Low/Negative Hematopoietic Stem Cell. *Science* 273: 242-245

Otogawa K, Kinoshita K, Fujii H, Sakabe M, Shiga R, Nakatani K, Ikeda K, Nakajima Y, Ikura Y, Ueda M *et al* (2007) Erythrophagocytosis by Liver Macrophages (Kupffer Cells) Promotes Oxidative Stress, Inflammation, and Fibrosis in a Rabbit Model of Steatohepatitis. *The American Journal of Pathology* 170: 967-980

Ovadya Y, Landsberger T, Leins H, Vadai E, Gal H, Biran A, Yosef R, Sagiv A, Agrawal A, Shapira A *et al* (2018) Impaired immune surveillance accelerates accumulation of senescent cells and aging. *Nat Commun* 9

Palis J, Robertson S, Kennedy M, Wall C, Keller G (1999) Development of erythroid and myeloid progenitors in the yolk sac and embryo proper of the mouse. *Development* 126: 5073-5084

Palis J, Yoder MC (2001) Yolk-sac hematopoiesis. *Experimental Hematology* 29: 927-936

Pang WW, Price EA, Sahoo D, Beerman I, Maloney WJ, Rossi DJ, Schrier SL, Weissman IL (2011) Human bone marrow hematopoietic stem cells are increased in frequency and myeloid-biased with age. *Proceedings of the National Academy of Sciences* 108: 20012-20017

Pardo A, Barrios R, Gaxiola M, Segura-Valdez L, Carrillo G, Estrada A, Mejía M, Selman M (2000) Increase of Lung Neutrophils in Hypersensitivity Pneumonitis Is Associated with Lung Fibrosis. *American Journal of Respiratory and Critical Care Medicine* 161: 1698-1704

Park MD, Le Berichel J, Hamon P, Wilk CM, Belabed M, Yatim N, Saffon A, Boumelha J, Falcomatà C, Tepper A *et al* (2024) Hematopoietic aging promotes cancer by fueling IL-1α–driven emergency myelopoiesis. *Science* 386

Peiser L, Mukhopadhyay S, Gordon S (2002) Scavenger receptors in innate immunity. *Current Opinion in Immunology* 14: 123-128

Pervizaj-Oruqaj L, Ferrero MR, Matt U, Herold S (2024a) The guardians of pulmonary harmony: alveolar macrophages orchestrating the symphony of lung inflammation and tissue homeostasis. *European Respiratory Review* 33: 230263

Pervizaj-Oruqaj L, Selvakumar B, Ferrero MR, Heiner M, Malainou C, Glaser RD, Wilhelm J, Bartkuhn M, Weiss A, Alexopoulos I *et al* (2024b) Alveolar macrophage-expressed Plet1 is a driver of lung epithelial repair after viral pneumonia. *Nat Commun* 15

Piguet PF, Collart MA, Grau GE, Kapanci Y, Vassalli P (1989) Tumor necrosis factor/cachectin plays a key role in bleomycin-induced pneumopathy and fibrosis. *The Journal of experimental medicine* 170: 655-663

Planer JD, Morrisey EE (2023) After the Storm: Regeneration, Repair, and Reestablishment of Homeostasis Between the Alveolar Epithelium and Innate Immune System Following Viral Lung Injury. *Annual Review of Pathology: Mechanisms of Disease* 18: 337-359

Plikus MV, Wang X, Sinha S, Forte E, Thompson SM, Herzog EL, Driskell RR, Rosenthal N, Biernaskie J, Horsley V (2021) Fibroblasts: Origins, definitions, and functions in health and disease. *Cell* 184: 3852-3872

Pooja, Hu Y, Yamamoto Y, Neo, Tay, Mu D, Sun Y, Lim, Dagher R, Elisabeth *et al* (2011) Distal Airway Stem Cells Yield Alveoli In Vitro and during Lung Regeneration following H1N1 Influenza Infection. *Cell* 147: 525-538

Proença De Oliveira-Maul J, Barbosa De Carvalho H, Goto DM, Maia RM, Fló C, Barnabé V, Franco DR, Benabou S, Perracini MR, Jacob-Filho W *et al* (2013) Aging, Diabetes, and Hypertension Are Associated With Decreased Nasal Mucociliary Clearance. *Chest* 143: 1091-1097

Proto JD, Doran AC, Gusarova G, Yurdagul A, Sozen E, Subramanian M, Islam MN, Rymond CC, Du J, Hook J *et al* (2018) Regulatory T Cells Promote Macrophage Efferocytosis during Inflammation Resolution. *Immunity* 49: 666-677.e666

Purton LE (2022) Adult murine hematopoietic stem cells and progenitors: an update on their identities, functions, and assays. *Experimental Hematology* 116: 1-14

Quirk JD, Sukstanskii AL, Woods JC, Lutey BA, Conradi MS, Gierada DS, Yusen RD, Castro M, Yablonskiy DA (2016) Experimental evidence of age-related adaptive changes in human acinar airways. *Journal of Applied Physiology* 120: 159-165

Raghu G, Remy-Jardin M, Myers JL, Richeldi L, Ryerson CJ, Lederer DJ, Behr J, Cottin V, Danoff SK, Morell F *et al* (2018) Diagnosis of Idiopathic Pulmonary Fibrosis. An Official ATS/ERS/JRS/ALAT Clinical Practice Guideline. *Am J Respir Crit Care Med* 198: e44-e68

Raghu G, Weycker D, Edelsberg J, Bradford WZ, Oster G (2006) Incidence and prevalence of idiopathic pulmonary fibrosis. *Am J Respir Crit Care Med* 174: 810-816

Ramachandran P, Dobie R, Wilson-Kanamori JR, Dora EF, Henderson BEP, Luu NT, Portman JR, Matchett KP, Brice M, Marwick JA *et al* (2019) Resolving the fibrotic niche of human liver cirrhosis at single-cell level. *Nature* 575: 512-518

Rauschmeier R, Gustafsson C, Reinhardt A, A-Gonzalez N, Tortola L, Cansever D, Subramanian S, Taneja R, Rossner MJ, Sieweke MH *et al* (2019) Bhlhe40 and Bhlhe41 transcription factors regulate alveolar macrophage self-renewal and identity. *The EMBO Journal* 38

Rawlins EL, Clark CP, Xue Y, Hogan BLM (2009) The Id2+ distal tip lung epithelium contains individual multipotent embryonic progenitor cells. *Development* 136: 3741-3745

Reilkoff RA, Peng H, Murray LA, Peng X, Russell T, Montgomery R, Feghali-Bostwick C, Shaw A, Homer RJ, Gulati M *et al* (2013) Semaphorin 7a⁺ Regulatory T Cells Are Associated with Progressive Idiopathic Pulmonary Fibrosis and Are Implicated in Transforming Growth Factor-β1–induced Pulmonary Fibrosis. *American Journal of Respiratory and Critical Care Medicine* 187: 180-188

Reyfman PA, Walter JM, Joshi N, Anekalla KR, McQuattie-Pimentel AC, Chiu S, Fernandez R, Akbarpour M, Chen C-I, Ren Z *et al* (2019) Single-Cell Transcriptomic Analysis of Human Lung Provides Insights into the Pathobiology of Pulmonary Fibrosis. *American Journal of Respiratory and Critical Care Medicine* 199: 1517-1536

Richard, Thirumalai, Kevin, Kevin, David, Lu W-Y, Ferreira-González S, Stuart, Vallier L, Thomas (2016) Interleukin-13 Activates Distinct Cellular Pathways Leading to Ductular Reaction, Steatosis, and Fibrosis. *Immunity* 45: 145-158

Richeldi L, Costabel U, Selman M, Kim DS, Hansell DM, Nicholson AG, Brown KK, Flaherty KR, Noble PW, Raghu G *et al* (2011) Efficacy of a Tyrosine Kinase Inhibitor in Idiopathic Pulmonary Fibrosis. *New England Journal of Medicine* 365: 1079-1087

Richeldi L, du Bois RM, Raghu G, Azuma A, Brown KK, Costabel U, Cottin V, Flaherty KR, Hansell DM, Inoue Y *et al* (2014) Efficacy and safety of nintedanib in idiopathic pulmonary fibrosis. *N Engl J Med* 370: 2071-2082

Rooijen V, Zetoune FS, Ward Riedemann PA, McClintock SD, Vidya Sarma J, Reuben N, Neff TA, Marco Hoesel L, Hongwei Gao NC, Guo R-F *et al* (2019) Stat3 Activation in Acute Lung Injury. *J Immunol References* 172: 7703-7712

Roquilly A, Jacqueline C, Davieau M, Mollé A, Sadek A, Fourgeux C, Rooze P, Broquet A, Misme-Aucouturier B, Chaumette T *et al* (2020) Alveolar macrophages are epigenetically altered after inflammation, leading to long-term lung immunoparalysis. *Nat Immunol* 21: 636-648

Ross JB, Myers LM, Noh JJ, Collins MM, Carmody AB, Messer RJ, Dhuey E, Hasenkrug KJ, Weissman IL (2024) Depleting myeloid-biased haematopoietic stem cells rejuvenates aged immunity. *Nature* 628: 162-170

Rossi DJ, Bryder D, Zahn JM, Ahlenius H, Sonu R, Wagers AJ, Weissman IL (2005) Cell intrinsic alterations underlie hematopoietic stem cell aging. *Proc Natl Acad Sci U S A* 102: 9194-9199

Rubtsov YP, Rasmussen JP, Chi EY, Fontenot J, Castelli L, Ye X, Treuting P, Siewe L, Roers A, Henderson WR *et al* (2008) Regulatory T Cell-Derived Interleukin-10 Limits Inflammation at Environmental Interfaces. *Immunity* 28: 546-558

Sabatel C, Radermecker C, Fievez L, Paulissen G, Chakarov S, Fernandes C, Olivier S, Toussaint M, Pirottin D, Xiao X *et al* (2017) Exposure to Bacterial CpG DNA Protects from

Airway Allergic Inflammation by Expanding Regulatory Lung Interstitial Macrophages. *Immunity* 46: 457-473

Sack C, Raghu G (2019) Idiopathic pulmonary fibrosis: unmasking cryptogenic environmental factors. *Eur Respir J* 53: 1801699

Sakaguchi S, Yamaguchi T, Nomura T, Ono M (2008) Regulatory T Cells and Immune Tolerance. *Cell* 133: 775-787

Sallusto F, Lanzavecchia A (1994) Efficient presentation of soluble antigen by cultured human dendritic cells is maintained by granulocyte/macrophage colony-stimulating factor plus interleukin 4 and downregulated by tumor necrosis factor alpha. *The Journal of experimental medicine* 179: 1109-1118

Saluzzo S, Gorki AD, Rana BMJ, Martins R, Scanlon S, Starkl P, Lakovits K, Hladik A, Korosec A, Sharif O *et al* (2017) First-Breath-Induced Type 2 Pathways Shape the Lung Immune Environment. *Cell Rep* 18: 1893-1905

Sanada C, Xavier-Ferrucio J, Lu Y-C, Min E, Zhang P-X, Zou S, Kang E, Zhang M, Zerafati G, Gallagher PG *et al* (2016) Adult human megakaryocyte-erythroid progenitors are in the CD34+CD38mid fraction. *Blood* 128: 923-933

Sanmiguel JM, Young K, Trowbridge JJ (2020) Hand in hand: intrinsic and extrinsic drivers of aging and clonal hematopoiesis. *Experimental Hematology* 91: 1-9

Satoh T, Nakagawa K, Sugihara F, Kuwahara R, Ashihara M, Yamane F, Minowa Y, Fukushima K, Ebina I, Yoshioka Y *et al* (2017) Identification of an atypical monocyte and committed progenitor involved in fibrosis. *Nature* 541: 96-101

Schafer S, Viswanathan S, Widjaja AA, Lim W-W, Moreno-Moral A, Delaughter DM, Ng B, Patone G, Chow K, Khin E *et al* (2017) IL-11 is a crucial determinant of cardiovascular fibrosis. *Nature* 552: 110-115

Schneider C, Nobs SP, Kurrer M, Rehrauer H, Thiele C, Kopf M (2014) Induction of the nuclear receptor PPAR-γ by the cytokine GM-CSF is critical for the differentiation of fetal monocytes into alveolar macrophages. *Nat Immunol* 15: 1026-1037

Schneider JL, Rowe JH, Garcia-De-Alba C, Kim CF, Sharpe AH, Haigis MC (2021) The aging lung: Physiology, disease, and immunity. *Cell* 184: 1990-2019

Seki E, Schwabe RF (2015) Hepatic inflammation and fibrosis: Functional links and key pathways. *Hepatology* 61: 1066-1079

Selmecki AM, Maruvka YE, Richmond PA, Guillet M, Shoresh N, Sorenson AL, De S, Kishony R, Michor F, Dowell R *et al* (2015) Polyploidy can drive rapid adaptation in yeast. *Nature* 519: 349-352

Selvarajah B, Platé M, Chambers RC (2023) Pulmonary fibrosis: Emerging diagnostic and therapeutic strategies. *Molecular Aspects of Medicine* 94: 101227

Sharma G, Goodwin J (2006) Effect of aging on respiratory system physiology and immunology. *Clinical Interventions in Aging* 1: 253-260

Shi C, Pamer EG (2011) Monocyte recruitment during infection and inflammation. *Nature Rev Immun* 11: 762-774

Shibata Y, Berclaz PY, Chroneos ZC, Yoshida M, Whitsett JA, Trapnell BC (2001) GM-CSF regulates alveolar macrophage differentiation and innate immunity in the lung through PU.1. *Immunity* 15: 557-567

Shiraishi K, Morley MP, Jones DL, Zhao G, Weiner AI, Basil MC, Cantu E, Ferguson LT, Oyster M, Babu A *et al* (2024) Airway epithelial cell identity and plasticity are constrained by Sox2 during lung homeostasis, tissue regeneration, and in human disease. *npj Regenerative Medicine* 9

Sica A, Mantovani A (2012) Macrophage plasticity and polarization: in vivo veritas. *Journal of Clinical Investigation* 122: 787-795

Simone D, Penkava F, Ridley A, Sansom S, Al-Mossawi MH, Bowness P (2021) Single cell analysis of spondyloarthritis regulatory T cells identifies distinct synovial gene expression patterns and clonal fates. *Communications Biology* 4

Singh A, Chakraborty S, Wong SW, Hefner NA, Stuart A, Qadir AS, Mukhopadhyay A, Bachmaier K, Shin J-W, Rehman J *et al* (2022) Nanoparticle targeting of de novo profibrotic macrophages mitigates lung fibrosis. *Proceedings of the National Academy of Sciences* 119

Singh B, Kasam RK, Sontake V, Wynn TA, Madala SK (2017) Repetitive intradermal bleomycin injections evoke T-helper cell 2 cytokine-driven pulmonary fibrosis. *American Journal of Physiology-Lung Cellular and Molecular Physiology* 313: L796-L806

Snelgrove RJ, Goulding J, Didierlaurent AM, Lyonga D, Vekaria S, Edwards L, Gwyer E, Sedgwick JD, Barclay AN, Hussell T (2008) A critical function for CD200 in lung immune homeostasis and the severity of influenza infection. *Nat Immunol* 9: 1074-1083

Somogyi V, Chaudhuri N, Torrisi SE, Kahn N, Müller V, Kreuter M (2019) The therapy of idiopathic pulmonary fibrosis: what is next? *European Respiratory Review* 28: 190021

Strunz M, Simon LM, Ansari M, Kathiriya JJ, Angelidis I, Mayr CH, Tsidiridis G, Lange M, Mattner LF, Yee M *et al* (2020) Alveolar regeneration through a Krt8+ transitional stem cell state that persists in human lung fibrosis. *Nat Commun* 11

Sun D, Luo M, Jeong M, Rodriguez B, Xia Z, Hannah R, Wang H, Le T, Kym, Chen R *et al* (2014) Epigenomic Profiling of Young and Aged HSCs Reveals Concerted Changes during Aging that Reinforce Self-Renewal. *Cell Stem Cell* 14: 673-688

Suryadevara V, Hudgins AD, Rajesh A, Pappalardo A, Karpova A, Dey AK, Hertzel A, Agudelo A, Rocha A, Soygur B *et al* (2024) SenNet recommendations for detecting senescent cells in different tissues. *Nature Reviews Molecular Cell Biology* 25: 1001-1023

Svedberg FR, Brown SL, Krauss MZ, Campbell L, Sharpe C, Clausen M, Howell GJ, Clark H, Madsen J, Evans CM *et al* (2019) The lung environment controls alveolar macrophage metabolism and responsiveness in type 2 inflammation. *Nat Immunol* 20: 571-580

Swann JW, Olson OC, Passegué E (2024) Made to order: emergency myelopoiesis and demand-adapted innate immune cell production. *Nature Rev Immun* 24: 596-613

Szabo SJ, Kim ST, Costa GL, Zhang X, Fathman CG, Glimcher LH (2000) A Novel Transcription Factor, T-bet, Directs Th1 Lineage Commitment. *Cell* 100: 655-669

Tang Q, Bluestone JA (2008) The Foxp3+ regulatory T cell: a jack of all trades, master of regulation. *Nat Immunol* 9: 239-244

Tarling JD, Coggle JE (1982) Evidence for the pulmonary origin of alveolar macrophages. *Cell Proliferation* 15: 577-584

Thulabandu V, Chen D, Atit RP (2018) Dermal fibroblast in cutaneous development and healing. *WIREs Developmental Biology* 7: e307

Trapnell BC, Whitsett JA (2002) GM-CSF Regulates Pulmonary Surfactant Homeostasis and Alveolar Macrophage-Mediated Innate Host Defense. *Annual Review of Physiology* 64: 775-802

Trapnell BC, Whitsett JA, Nakata K (2003) Pulmonary Alveolar Proteinosis. *New England Journal of Medicine* 349: 2527-2539

Travaglini KJ, Nabhan AN, Penland L, Sinha R, Gillich A, Sit RV, Chang S, Conley SD, Mori Y, Seita J *et al* (2020) A molecular cell atlas of the human lung from single-cell RNA sequencing. *Nature* 587: 619-625

Trujillo G, Hartigan AJ, Hogaboam CM (2010) T regulatory cells and attenuated bleomycin-induced fibrosis in lungs of CCR7-/- mice. *Fibrogenesis & Tissue Repair* 3: 18

Tsou C-L, Peters W, Si Y, Slaymaker S, Aslanian AM, Weisberg SP, Mack M, Charo IF (2007) Critical roles for CCR2 and MCP-3 in monocyte mobilization from bone marrow and recruitment to inflammatory sites. *Journal of Clinical Investigation* 117: 902-909

Ueno M, Maeno T, Nomura M, Aoyagi-Ikeda K, Matsui H, Hara K, Tanaka T, Iso T, Suga T, Kurabayashi M (2011) Hypoxia-inducible factor-1α mediates TGF-β-induced PAI-1 production in alveolar macrophages in pulmonary fibrosis. *American Journal of Physiology-Lung Cellular and Molecular Physiology* 300: L740-L752

Ulloa L, Doody J, Massagué J (1999) Inhibition of transforming growth factor-β/SMAD signalling by the interferon-γ/STAT pathway. *Nature* 397: 710-713

Umezawa H, Ishizuka M, Maeda K, Takeuchi T (1967) Studies on bleomycin. *Cancer* 20: 891-895

van de Laar L, Saelens W, De Prijck S, Martens L, Scott CL, Van Isterdael G, Hoffmann E, Beyaert R, Saeys Y, Lambrecht BN *et al* (2016) Yolk Sac Macrophages, Fetal Liver, and Adult Monocytes Can Colonize an Empty Niche and Develop into Functional Tissue-Resident Macrophages. *Immunity* 44: 755-768

Van Den Blink B, Dillingh MR, Ginns LC, Morrison LD, Moerland M, Wijsenbeek M, Trehu EG, Bartholmai BJ, Burggraaf J (2016) Recombinant human pentraxin-2 therapy in patients with idiopathic pulmonary fibrosis: safety, pharmacokinetics and exploratory efficacy. *Eur Respir J* 47: 889-897

Van Der Poll T, Opal SM (2009) Pathogenesis, treatment, and prevention of pneumococcal pneumonia. *The Lancet* 374: 1543-1556

Van Furth R, Cohn ZA (1968) THE ORIGIN AND KINETICS OF MONONUCLEAR PHAGOCYTES. *The Journal of Experimental Medicine* 128: 415-435

Vanderheiden A, Thomas J, Soung AL, Davis-Gardner ME, Floyd K, Jin F, Cowan DA, Pellegrini K, Creanga A, Pegu A *et al* (2021) CCR2 Signaling Restricts SARS-CoV-2 Infection. *mBio* 12

Vannella KM, Ramalingam TR, Borthwick LA, Barron L, Hart KM, Thompson RW, Kindrachuk KN, Cheever AW, White S, Budelsky AL *et al* (2016) Combinatorial targeting of TSLP, IL-25, and IL-33 in type 2 cytokine–driven inflammation and fibrosis. *Science Translational Medicine* 8: 337ra365-337ra365

Vanneste D, Bai Q, Hasan S, Peng W, Pirottin D, Schyns J, Maréchal P, Ruscitti C, Meunier M, Liu Z *et al* (2023) MafB-restricted local monocyte proliferation precedes lung interstitial macrophage differentiation. *Nat Immunol* 24: 827-840

Varol C, Mildner A, Jung S (2015) Macrophages: Development and Tissue Specialization. *Annual Review of Immunology* 33: 643-675

Velnar T, Bailey T, Smrkolj V (2009) The Wound Healing Process: An Overview of the Cellular and Molecular Mechanisms. *Journal of International Medical Research* 37: 1528-1542

Verheyden JM, Sun X (2020) A transitional stem cell state in the lung. *Nature Cell Biology* 22: 1025-1026

Vestweber D (2015) How leukocytes cross the vascular endothelium. *Nature Rev Immun* 15: 692-704

Vicente R, Mausset-Bonnefont A-L, Jorgensen C, Louis-Plence P, Brondello J-M (2016) Cellular senescence impact on immune cell fate and function. *Aging Cell* 15: 400-406

Vieira Braga FA, Kar G, Berg M, Carpaij OA, Polanski K, Simon LM, Brouwer S, Gomes T, Hesse L, Jiang J *et al* (2019) A cellular census of human lungs identifies novel cell states in health and in asthma. *Nat Med* 25: 1153-1163

Vignali DAA, Collison LW, Workman CJ (2008) How regulatory T cells work. *Nature Rev Immun* 8: 523-532

Walker JA, McKenzie ANJ (2018) TH2 cell development and function. *Nature Rev Immun* 18: 121-133

Walker LSK, Abbas AK (2002) The enemy within: keeping self-reactive T cells at bay in the periphery. *Nature Rev Immun* 2: 11-19

Wan YY, Flavell RA (2007) 'Yin–Yang' functions of transforming growth factor-β and T regulatory cells in immune regulation. *Immunological Reviews* 220: 199-213

Wang F, Xia H, Yao S (2020) Regulatory T cells are a double-edged sword in pulmonary fibrosis. *International Immunopharmacology* 84: 106443

Watanabe S, Markov NS, Lu Z, Piseaux Aillon R, Soberanes S, Runyan CE, Ren Z, Grant RA, Maciel M, Abdala-Valencia H *et al* (2021) Resetting proteostasis with ISRIB promotes epithelial differentiation to attenuate pulmonary fibrosis. *Proc Natl Acad Sci U S A* 118

Wculek SK, Heras-Murillo I, Mastrangelo A, Mañanes D, Galán M, Miguel V, Curtabbi A, Barbas C, Chandel NS, Enríquez JA *et al* (2023) Oxidative phosphorylation selectively orchestrates tissue macrophage homeostasis. *Immunity* 56: 516-530.e519

Weibel ER (2015) On the Tricks Alveolar Epithelial Cells Play to Make a Good Lung. *American Journal of Respiratory and Critical Care Medicine* 191: 504-513

Weissman IL (2000) Stem Cells. *Cell* 100: 157-168

Wendisch D, Dietrich O, Mari T, Von Stillfried S, Ibarra IL, Mittermaier M, Mache C, Chua RL, Knoll R, Timm S *et al* (2021) SARS-CoV-2 infection triggers profibrotic macrophage responses and lung fibrosis. *Cell* 184: 6243-6261.e6227

Weng A, Maciel Herrerias M, Watanabe S, Welch LC, Flozak AS, Grant RA, Aillon RP, Dada LA, Han SH, Hinchcliff M *et al* (2022) Lung Injury Induces Alveolar Type 2 Cell Hypertrophy and Polyploidy with Implications for Repair and Regeneration. *Am J Respir Cell Mol Biol* 66: 564-576

Westphalen K, Gusarova GA, Islam MN, Subramanian M, Cohen TS, Prince AS, Bhattacharya J (2014) Sessile alveolar macrophages communicate with alveolar epithelium to modulate immunity. *Nature* 506: 503-506

Wick G, Backovic A, Rabensteiner E, Plank N, Schwentner C, Sgonc R (2010) The immunology of fibrosis: innate and adaptive responses. *Trends Immunol* 31: 110-119

Wijsenbeek M, Suzuki A, Maher TM (2022) Interstitial lung diseases. *The Lancet* 400: 769-786

Wilkinson HN, Hardman MJ (2020) Wound healing: cellular mechanisms and pathological outcomes. *Open Biology* 10: 200223

Williams MC (2003) Alveolar Type I Cells: Molecular Phenotype and Development. *Annual Review of Physiology* 65: 669-695

Williamson EJ, Walker AJ, Bhaskaran K, Bacon S, Bates C, Morton CE, Curtis HJ, Mehrkar A, Evans D, Inglesby P *et al* (2020) Factors associated with COVID-19-related death using OpenSAFELY. *Nature* 584: 430-436

Wilson A, Laurenti E, Oser G, Van Der Wath RC, Blanco-Bose W, Jaworski M, Offner S, Dunant CF, Eshkind L, Bockamp E *et al* (2008) Hematopoietic Stem Cells Reversibly Switch from Dormancy to Self-Renewal during Homeostasis and Repair. *Cell* 135: 1118-1129

Wilson MS, Madala SK, Ramalingam TR, Gochuico BR, Rosas IO, Cheever AW, Wynn TA (2010) Bleomycin and IL-1beta-mediated pulmonary fibrosis is IL-17A dependent. *J Exp Med* 207: 535-552

Wilson MS, Wynn TA (2009) Pulmonary fibrosis: pathogenesis, etiology and regulation. *Mucosal Immunology* 2: 103-121

Winter C, Taut K, Srivastava M, LäNger F, Mack M, Briles DE, Paton JC, Maus R, Welte T, Gunn MD *et al* (2007) Lung-Specific Overexpression of CC Chemokine Ligand (CCL) 2 Enhances the Host Defense to Streptococcus pneumoniae Infection in Mice: Role of the CCL2-CCR2 Axis. *J Immunol* 178: 5828-5838

Winterbottom CJ, Shah RJ, Patterson KC, Kreider ME, Panettieri RA, Rivera-Lebron B, Miller WT, Litzky LA, Penning TM, Heinlen K *et al* (2018) Exposure to Ambient Particulate Matter Is Associated With Accelerated Functional Decline in Idiopathic Pulmonary Fibrosis. *Chest* 153: 1221-1228

Wong CK, Smith CA, Sakamoto K, Kaminski N, Koff JL, Goldstein DR (2017) Aging Impairs Alveolar Macrophage Phagocytosis and Increases Influenza-Induced Mortality in Mice. *J Immunol* 199: 1060-1068

Woods PS, Kimmig LM, Meliton AY, Sun KA, Tian Y, O'Leary EM, Gökalp GA, Hamanaka RB, Mutlu GM (2020) Tissue-Resident Alveolar Macrophages Do Not Rely on Glycolysis for LPS-induced Inflammation. *Am J Respir Cell Mol Biol* 62: 243-255

Wynn T (2008) Cellular and molecular mechanisms of fibrosis. *The Journal of Pathology* 214: 199-210

Wynn TA (2004) Fibrotic disease and the TH1/TH2 paradigm. *Nature Rev Immun* 4: 583-594

Wynn TA, Ramalingam TR (2012) Mechanisms of fibrosis: therapeutic translation for fibrotic disease. *Nat Med* 18: 1028-1040

Wynn TA, Vannella KM (2016) Macrophages in Tissue Repair, Regeneration, and Fibrosis. *Immunity* 44: 450-462

Xie T, Wang Y, Deng N, Huang G, Taghavifar F, Geng Y, Liu N, Kulur V, Yao C, Chen P *et al* (2018) Single-Cell Deconvolution of Fibroblast Heterogeneity in Mouse Pulmonary Fibrosis. *Cell Reports* 22: 3625-3640

Xing Y, Hogquist KA (2012) T-Cell Tolerance: Central and Peripheral. *Cold Spring Harbor Perspectives in Biology* 4: a006957-a006957

Xiong H, Carter RA, Leiner IM, Tang Y-W, Chen L, Kreiswirth BN, Pamer EG (2015) Distinct Contributions of Neutrophils and CCR2⁺Monocytes to Pulmonary Clearance of Different Klebsiella pneumoniae Strains. *Infection and Immunity* 83: 3418-3427

Xiong H, James, Dane, Rebecca, Ingrid, Eric (2016) Innate Lymphocyte/Ly6C hi Monocyte Crosstalk Promotes Klebsiella Pneumoniae Clearance. *Cell* 165: 679-689

Xu P, Wang M, Song W-M, Wang Q, Yuan G-C, Sudmant PH, Zare H, Tu Z, Orr ME, Zhang B (2022) The landscape of human tissue and cell type specific expression and co-regulation of senescence genes. *Molecular Neurodegeneration* 17

Yamada C, Sano H, Shimizu T, Mitsuzawa H, Nishitani C, Himi T, Kuroki Y (2006) Surfactant Protein A Directly Interacts with TLR4 and MD-2 and Regulates Inflammatory Cellular Response. *Journal of Biological Chemistry* 281: 21771-21780

Yamamoto R, Nakauchi H (2020) In vivo clonal analysis of aging hematopoietic stem cells. *Mechanisms of Ageing and Development* 192: 111378

Yamamoto R, Wilkinson AC, Ooehara J, Lan X, Lai C-Y, Nakauchi Y, Pritchard JK, Nakauchi H (2018) Large-Scale Clonal Analysis Resolves Aging of the Mouse Hematopoietic Stem Cell Compartment. *Cell Stem Cell* 22: 600-607.e604

Yang IV, Fingerlin TE, Evans CM, Schwarz MI, Schwartz DA (2015a) MUC5B and Idiopathic Pulmonary Fibrosis. *Annals of the American Thoracic Society* 12: S193-S199

Yang J, Hernandez BJ, Alanis DM, Narvaez O, Vila-Ellis L, Akiyama H, Evans SE, Ostrin EJ, Chen J (2015b) Development and plasticity of alveolar type 1 cells. *Development* 143: 54-65

Yang L, Bryder D, Adolfsson JR, Nygren J, MåNsson R, Sigvardsson M, Jacobsen SEW (2005) Identification of Lin–Sca1+kit+CD34+Flt3– short-term hematopoietic stem cells capable of rapidly reconstituting and rescuing myeloablated transplant recipients. *Blood* 105: 2717-2723

Yao C, Guan X, Carraro G, Parimon T, Liu X, Huang G, Mulay A, Soukiasian HJ, David G, Weigt SS *et al* (2021) Senescence of Alveolar Type 2 Cells Drives Progressive Pulmonary Fibrosis. *American Journal of Respiratory and Critical Care Medicine* 203: 707-717

Yin L, Zheng D, Limmon GV, Leung NH, Xu S, Rajapakse JC, Yu H, Chow VT, Chen J (2014) Aging exacerbates damage and delays repair of alveolar epithelia following influenza viral pneumonia. *Respiratory Research* 15

Yona S, Kim KW, Wolf Y, Mildner A, Varol D, Breker M, Strauss-Ayali D, Viukov S, Guilliams M, Misharin A *et al* (2013) Fate mapping reveals origins and dynamics of monocytes and tissue macrophages under homeostasis. *Immunity* 38: 79-91

Yu X, Buttgereit A, Lelios I, Utz SG, Cansever D, Becher B, Greter M (2017) The Cytokine TGF-β Promotes the Development and Homeostasis of Alveolar Macrophages. *Immunity* 47: 903-912.e904

Zacharias WJ, Frank DB, Zepp JA, Morley MP, Alkhaleel FA, Kong J, Zhou S, Cantu E, Morrisey EE (2018) Regeneration of the lung alveolus by an evolutionarily conserved epithelial progenitor. *Nature* 555: 251-255

Zahalka S, Starkl P, Watzenboeck ML, Farhat A, Radhouani M, Deckert F, Hladik A, Lakovits K, Oberndorfer F, Lassnig C *et al* (2022) Trained immunity of alveolar macrophages requires metabolic rewiring and type 1 interferon signaling. *Mucosal Immunology* 15: 896-907

Zaidi A, Green L (2019) Physiology of haemostasis. *Anaesthesia & Intensive Care Medicine* 20: 152-158

Zeisberg EM, Tarnavski O, Zeisberg M, Dorfman AL, McMullen JR, Gustafsson E, Chandraker A, Yuan X, Pu WT, Roberts AB *et al* (2007) Endothelial-to-mesenchymal transition contributes to cardiac fibrosis. *Nat Med* 13: 952-961

Zhang D, Tang Z, Huang H, Zhou G, Cui C, Weng Y, Liu W, Kim S, Lee S, Perez-Neut M *et al* (2019) Metabolic regulation of gene expression by histone lactylation. *Nature* 574: 575-580

Zhang F, Ayaub EA, Wang B, Puchulu-Campanella E, Li YH, Hettiarachchi SU, Lindeman SD, Luo Q, Rout S, Srinivasarao M *et al* (2020) Reprogramming of profibrotic macrophages for treatment of bleomycin-induced pulmonary fibrosis. *EMBO Molecular Medicine* 12

Zhang H, Cavazzoni CB, Podestà MA, Bechu ED, Ralli G, Chandrakar P, Lee J-M, Sayin I, Tullius SG, Abdi R *et al* (2023) IL-21–producing effector Tfh cells promote B cell alloimmunity in lymph nodes and kidney allografts. *JCI Insight* 8

Zhang Q, Raoof M, Chen Y, Sumi Y, Sursal T, Junger W, Brohi K, Itagaki K, Hauser CJ (2010) Circulating mitochondrial DAMPs cause inflammatory responses to injury. *Nature* 464: 104-107

Zhao J, Zhao J, Legge K, Perlman S (2011) Age-related increases in PGD2 expression impair respiratory DC migration, resulting in diminished T cell responses upon respiratory virus infection in mice. *Journal of Clinical Investigation* 121: 4921-4930

Zhao M, Wang L, Wang M, Zhou S, Lu Y, Cui H, Racanelli AC, Zhang L, Ye T, Ding B *et al* (2022) Targeting fibrosis: mechanisms and clinical trials. *Signal Transduction and Targeted Therapy* 7

Zheng W-P, Flavell RA (1997) The Transcription Factor GATA-3 Is Necessary and Sufficient for Th2 Cytokine Gene Expression in CD4 T Cells. *Cell* 89: 587-596

Zhou X, Franklin RA, Adler M, Jacox JB, Bailis W, Shyer JA, Flavell RA, Mayo A, Alon U, Medzhitov R (2018) Circuit Design Features of a Stable Two-Cell System. *Cell* 172: 744-757 e717

Ziegler-Heitbrock L (2007) The CD14+ CD16+ blood monocytes: their role in infection and inflammation. *Journal of Leukocyte Biology* 81: 584-592

Appendix

Licenses

Thesis Figures:

Figure 1: Order License ID 1581045-1 (Content publisher: American Association for the Advancement of Science)

Figure 2: Created in BioRender. Farhat, A. (2025) https://BioRender.com/z24x434

Figure 3: Order License ID 1581045-2 (Content publisher: CELL PRESS)

Figure 4: Order License ID 1578203-1 (Content publisher: Nature Research)

Figure 5: Order License ID 1581045-3 (Content publisher: Nature Research)

Figure 6: (A) Order License ID 1581045-4 (Content publisher: Lancet publishing group)

(C) Created in BioRender. Farhat, A. (2025) https://BioRender.com/n30r532

Figure 7: (Verheyden & Sun, 2020)

Figure 8: Created in BioRender. Farhat, A. (2025) https://BioRender.com/g61q409

Figure 9: Order License ID 1581045-5 (Content publisher: Nature Research)

Figure 10: Order License ID 1581045-7 (Content publisher: Nature Research)

Figure 11: Created in BioRender. Farhat, A. (2025) https://BioRender.com/x63c829

Figure 12: Created in BioRender. Farhat, A. (2025) https://BioRender.com/z19e086

Figurr 13: Created in BioRender. Farhat, A. (2025) https://BioRender.com/ m44w589

Figure 14: Order License ID 1581045-6 (Content publisher: Nature Research)

Figure 15: Order License ID 1581050-1 Content publisher: CELL PRESS)

Figure 16: Created in BioRender. Farhat, A. (2025) https://BioRender.com/e08o094

Figure 17: Created in BioRender. Farhat, A. (2025) https://BioRender.com/y66i192

Figure 18: Order License ID 1581066-1 Content publisher: CELL PRESS)

Figure 19: Created in BioRender. Farhat, A. (2025) https://BioRender.com/s82d285

Figure 20: Created in BioRender. Farhat, A. (2025) https://BioRender.com/g79e468

Curriculum Vitae

Asma Farhat

Pre-doctoral Fellow, Medical University of Vienna/CeMM

asma.farhat@meduniwien.ac.at | farhatasma17@gmail.com | linkedin.com/in/asma-farhat-b1b2a1151 | +43-1/40400-51400

Research Division of Infection Biology, Medical University of Vienna, Waehringer Guertel 18-20, 1090 Vienna, Austria.

CeMM, Research Center for Molecular Medicine of the Austrian Academy of Sciences, Lazarettgasse 14, 1090 Vienna, Austria.

Research interest

Innate immunity, tissue repair and regeneration, fibrosis, developmental immunity, aging

Education

Doctor of Philosophy (PhD) in Immunology
Jan 2019 – Present.

Medical University of Vienna
Research Center for Molecular Medicine of the Austrian Academy of Sciences Supervisor:
Prof. Sylvia Knapp, MD, PhD
Expected graduation date: 04/2025.

CeMM PhD Program Introductory Lectures
Sept 2018 – Dec 2018.
Lectures in immunology, molecular biology, cancer biology, systems biology, laboratory management

Master of Science (MSc) in Genomic Approaches to Drug Discovery
Sept 2017 – Sept 2018.
The University of Sheffield, Sheffield, United Kingdom
Functional Genomics, Drug Development and Discovery, 3D tissue culture and Genome Editing, Critical Analysis of Current Science, Ethics, Law and Public Awareness of Science.

Bachelor of Science (BSc) in Biomedical Science
Sept 2014 – Aug 2017.
The University of Sheffield, Sheffield, United Kingdom
Human Anatomy, Cancer Biology, Stem cell and tissue engineering, Developmental biology, Neuroscience, Cell and Molecular Biology, Cardiovascular Pharmacology, Forensic Anatomy, Modelling human disease.

A and AS levels (Cambridge International Examinations)
Aug 2011 – Aug 2013.
Inventure Academy, Bangalore, India

IGCSE, (Cambridge International Examinations)
Jun 2009 – Jan 2011.
Primus Public School, Bangalore, India

Scientific/Research Training

PhD Training
Jan 2019 – April 2024
Dissertation: '*An ageing bone marrow exacerbates lung fibrosis by fueling profibrotic macrophage persistence*'
Supervisor: Prof. Sylvia Knapp, MD, PhD Medical
University of Vienna
Inflammation, injury, and repair in the context of lung fibrosis using in-vivo mouse models.

Rotation project
Oct 2018 - Nov 2018
Christoph Bock Lab, CeMM

MSc Laboratory project
Oct 2017 - Sept 2018
Dissertation: Identifying components of the transcriptional regulatory network underlying stem cell fate in colorectal cancer.
Supervisor: Dr Stephen Brown
The University of Sheffield
Identifying enhancers regulating LGR5 activity in gut stem cells in colorectal cancer.

MSc Rotation project
Nov 2017 – Feb 2018
Project: Repurposing small molecule inhibitors of Notch signalling in inflammatory bowel disease.
High-throughput small molecule screening.

Undergraduate Laboratory Project
Oct 2016- Dec 2016
Dissertation: Does Telomere dysfunction impair phagocytosis in gut associated leukocytes?
Supervisor: Dr Catarina Henriques
The University of Sheffield
Macrophage function using zebrafish in-vivo models.

Summer Research Internship
Jun 2016 – Aug 2016
Project: Impact of telomere dysfunction and ageing on phagocytosis of gut associated macrophages.
Supervisor: Dr Catarina Henriques
The University of Sheffield

High School Internship
May 2012 – Jun 2012
Mitra Biotech Cancer Research, Bangalore

Awards

NIH/Keystone Conference Scholarship – *Keystone Symposium on Fibrosis Inflammation, Drivers, and Therapeutic Resolution*	2024
Austrian Society of Allergy and Immunology (ÖGAI) Travel Grant	2023
StV Postgrad Conference Grant – *Medical University of Vienna*	2023
Austrian Society of Allergy and Immunology (ÖGAI) Travel Grant	2023
Best Poster Award – *16th Young Scientists Association (YSA) Symposium*	2021
Cambridge Outstanding Learner Award – *Top in India (A Level Psychology)*	2013
Cambridge Outstanding Learner Award – *Top in India (IGCSE History)*	2010

Conference Participation

Selected short talk, Dec 2024
Keystone Symposium: Fibrosis: Inflammation, Drivers, and Therapeutic Resolution, Whistler, Canada

Poster Presentation + Organizer for Early Career Event, Nov 2024
European Macrophage and Dendritic Cell Society (EMDS), Vienna, Austria.

Poster Presentation, Nov 2023
European Macrophage and Dendritic Cell Society (EMDS), Ghent, Belgium.

Poster Presentation, Apr 2023
Keystone Symposium: From first breath: Lung development, infection, repair and aging, Snowbird, Utah, USA.

Selected short talk + Session Chair, Sept 2022
European Macrophage and Dendritic Cell Society (EMDS), Bonn, Germany.

Oral Workshop Presentation, Aug 2022
World Immune Regulation Meeting (WIRM), Davos, Switzerland.

Poster Presentation, Jun 2022
Keystone Symposium: Tissue Fibrosis and Repair: Mechanisms, Human Disease and Therapies Keystone, USA.

Video Talk, Nov 2021

Annual Meeting of the Austrian Society of Allergy and Immunology, Next Generation Immunology Symposium.

Poster Presentation, Sept 2021
European Congress of Immunology (ECI), Online.

Poster Presentation, Jun 2021
European Macrophage and Dendritic Cell Society (EMDS), Online.

Poster Presentation, Jun 2021
16th Young Scientists Association (YSA) Symposium, Vienna

Participant, Keystone Symposium: Fibrosis and Tissue Repair: From Molecules and Mechanics to Therapeutic Approaches (Q6), Victoria, Canada.

Poster Presentation, Feb 2019
CeMM Scientific Recess, Waidhofen, Austria

Publications

1. **Farhat, A**., Radhouani, M., Deckert, F., Zahalka, S., Pimenov, L., Fokina, A., Hakobyan, A., Oberndorfer, F., Brösamlen, J., Hladik, A., Lakovits, K., Meng, F., Quattrone, F., Boon, L., Vesely, C., Starkl, P., Boucheron, N., Menche, J., van der Veeken, J., Ellmeier, W., Gorki, A.D., Campbell, C., Gawish, R., Knapp, S. '*An aging bone marrow exacerbates lung fibrosis by fueling profibrotic macrophage persistence*'. (Accepted, *Science Immunology*).

2. Radhouani, M., **Farhat, A**., Hakobyan, A., Zahalka, S., Pimenov, L., Fokina, A., Hladik, A., Lakovits, K., Brösamlen, J., Dvorak, V., Nunes, N., Zech, A., Idzko, M., Krausgruber, T., Köhl, J., Uluckan, O., Kovarik, J., Hoehlig, K., Vater, A., Eckhard, M., Sombke, A., Fortelny, N., Menche, J., Knapp, S., Starkl, P. '*Bacterial skin infection imprints bone marrow eosinophils to promote allergic skin-lung crosstalk'.* (Accepted, *Science Immunology*).

3. Fortelny,N., Farlik,M., Fife,V.,Gorki,A-D.,Lassnig,C., Maurer,B., Meissl,K.., Dolezal,M., Boccuni,L., Geetha,A., Akagha,M-J., Karjalainen,A., Shoebridge,S., **Farhat,A.,** Mann,U., Jain,R., Tikoo,S., Zila,N., Esser-Skala,W., Krausgruber,T., Sitnik,K., Penz,T., Hladik,A., Suske,T., Zahalka,S., Martin,S., Barreca,D., Halbritter,F., Macho-Maschler,S., Weninger,W., Neubauer,H., Moriggl,R., Knapp,S., Sexl,V., Strobl,B., Decker,T., Müller,M., Bock,C. (2024). *JAK-STAT signaling maintains homeostasis in T cells and macrophages.* *Nature Immunology*, *25, 847–859 .* https://doi.org/10.1038/s41590-024-01804-1

4. Holter,D. B., Zahalka,S., Watzenboeck, M. L., Artner, T. J., Radhouani, M., **Farhat, A**., Gawish, R., Lakovits, K., Hladik, A., Quattrone, F., Krausgruber,T., Fortelny,N., Knapp, S., Starkl, P. *Activated mast cells can modulate macrophage polarization and antibacterial responses.* (Accepted, *Journal of Allergy and Clinical Immunology*).

5. Gawish, R., Maier, B., Obermayer, G., Watzenboeck, M. L., Gorki, A.-D., Quattrone, F., **Farhat, A**., Lakovits, K., Hladik, A., Korosec, A., Alimohammadi, A., Mesteri, I., Oberndorfer, F., Oakley, F., Brain, J., Boon, L., Lang, I., Binder, C. J., & Knapp, S. (2022). A neutrophil–B-cell axis impacts tissue damage control in a mouse model of intraabdominal bacterial infection via CXCR4. *eLife*, *11:e78291*. https://doi.org/10.7554/elife.78291

6. Zahalka, S., Starkl, P., Watzenboeck, M. L., **Farhat, A**., Radhouani, M., Deckert, F., Hladik, A., Lakovits, K., Oberndorfer, F., Lassnig, C., Strobl, B., Klavins, K., Matsushita, M., Sanin, D. E., Grzes, K. M., Pearce, E. J., Gorki, A.-D., & Knapp, S. (2022). Trained immunity of alveolar macrophages requires metabolic rewiring and type 1 interferon signaling. *Mucosal Immunology*, *15* (5*), 896–907*. https://doi.org/10.1038/s41385-022-00528-5

7. Ellis, P. S., Martins, R. R., Thompson, E. J., **Farhat, A**., Renshaw, S. A., & Henriques, C. M. (2022). A subset of gut leukocytes has telomerase-dependent "hyper-long" telomeres and require telomerase for function in zebrafish. *Immunity & Ageing*, *19* (1). https://doi.org/10.1186/s12979-022-00287-8

8. Watzenboeck, M. L., Drobits, B., Zahalka, S., Gorki, A.-D., **Farhat, A**., Quattrone, F., Hladik, A., Lakovits, K., Richard, G. M., Lederer, T., Strobl, B., Versteeg, G. A., Boon, L., Starkl, P., & Knapp, S. (2021). Lipocalin 2 modulates dendritic cell activity and shapes immunity to influenza in a microbiome dependent manner. *PLOS Pathogens*, *17* (4): *e1009487*. https://doi.org/10.1371/journal.ppat.1009487

Technical skills

In-vivo mouse and adult zebrafish techniques, Flow cytometry and cell sorting, Microscopy, NGS library preparation (RNA-seq, ATAC-seq, CHIP-seq), molecular and cell biology techniques.

Memberships in Societies and Research Groups:

Austrian Association for Allergy and Immunology (ÖGAI)
British Society for Immunology (BSI)
SFB JAK-STAT Monarchies, Vienna
Strategic Collaborative Program: Environmental & Multi-system Molecular Medicine, CeMM
Strategic Collaborative Program: Mechanisms of Aging, CeMM

Additional work experience

Copy Editor, Phenotype (Oxford, Berlin, Vienna)	2021–2023
Human Anatomy Peer Mentor for Level 2 Students, Sheffield, United Kingdom	2016–2017
Global Campus Ambassador, Sheffield, United Kingdom	2016–2017
Communications Intern, SECMOL, Ladakh, India	Feb 2014 – Apr 2014
Special Education Intern, Inventure Academy, Bangalore, India	Oct 2013 – Dec 2013
Research Intern, Centre for Public History, Bangalore, India	un 2013 – Aug 2013